UNIVERSITY OF SOUTHAMPTON

FACULTY OF ENGINEERING, SCIENCE AND MATHEMATICS

Institute of Sound and Vibration Research

MECHANISM OF NONLINEAR BIODYNAMIC RESPONSE OF THE HUMAN BODY EXPOSED TO WHOLE-BODY VIBRATION

by

Ya Huang

Thesis for the degree of Doctor of Philosophy

May 2008

UNIVERSITY OF SOUTHAMPTON

ABSTRACT

FACULTY OF ENGINEERING, SCIENCE AND MATHEMATICS

INSTITUTE OF SOUND AND VIBRATION RESEARCH

Doctor of Philosophy

MECHANISM OF NONLINEAR BIODYNAMIC RESPONSE OF THE HUMAN BODY EXPOSED TO WHOLE-BODY VIBRATION

by Ya Huang

When the human body is exposed to mechanical vibration, the resonance frequencies of the frequency response functions, such as apparent mass and transmissibility, decrease with increasing magnitude of excitation. For the past two decades, this biodynamic 'nonlinearity' has been reported with vertical and horizontal excitation of the body in a wide variety of static sitting and standing postures that require activity from muscles to maintain the stability of the body. There has been speculation, but no experimental evidence, as to the mechanism causing the non-linearity. A review of the literature suggested that either active muscular activity or passive thixotropy of soft tissues is the primary cause of the nonlinearity. The principal objective of this thesis is to identify, and provide experimental evidence of, the primary causal mechanism for the biodynamic nonlinearity.

With 0.5 to 20 Hz broadband random vertical vibration at 0.25 and 2.0 ms^{-2} r.m.s., the first experiment investigated the effect of voluntary periodic upper-body movement and vibration magnitude on the apparent masses of 14 seated subjects. Some movements of the body, such as 'back-abdomen bending', significantly reduced the difference in resonance frequency at the two vibration magnitudes compared with the difference during upright static sitting. Without voluntary periodic movement, the median apparent mass resonance frequency was 5.47 Hz at the low vibration magnitude and 4.39 Hz at the high vibration magnitude. With voluntary periodic movement (e.g. back-abdomen bending), the resonance frequency was 4.69 Hz at the low vibration magnitude and 4.59 Hz at the high vibration magnitude. It was concluded that voluntary or involuntary muscular activity, or passive thixotropy of soft tissues, or both muscle activity and thixotropy, could explain the reduction in nonlinearity evident during voluntary periodic movement.

The effect of shear history and vibration magnitude on the apparent mass was investigated using 12 subjects in a relaxed semi-supine posture assumed to involve less muscle activity than static sitting and standing. The semi-supine subjects were exposed to two types of vertical (in the *x*-axis of the semi-supine body) and longitudinal horizontal (*z*-axis) vibration: (i) continuous random vibration (0.25–20 Hz) at five magnitudes (0.125, 0.25, 0.5, 0.75, and 1.0 ms^{-2} r.m.s.); (ii) intermittent random vibration (0.25–20 Hz) alternating between 1.0 and 0.25 ms^{-2} r.m.s. With continuous random vibration, the dominant primary resonance frequency in the median normalised apparent mass decreased from 10.35 to 7.32 Hz as the magnitude of vertical vibration increased from 0.125 to 1.0 ms^{-2} r.m.s., and from 3.66 to 2.44 Hz as the magnitude of horizontal vibration increased from 0.125 to 1.0 ms^{-2} r.m.s. With the intermittent vibration, the resonance frequency was higher at the higher magnitude (1.0 ms^{-2} r.m.s.) and lower at the lower magnitude (0.25 ms^{-2} r.m.s.) than during continuous vibration at the same magnitudes. The response was typical of thixotropy being the primary cause of the nonlinearity.

Harmonic distortions in the dynamic force of semi-supine subjects exposed to sinusoidal excitation showed similar dependence on the frequency and magnitude of vibration as previously reported for seated subjects, again suggesting thixotropy as a primary cause of the nonlinearity.

In a group of 12 subjects, the apparent mass and transmissibility to the sternum, upper abdomen, and lower abdomen were measured in three supine postures (relaxed semi-supine, lying flat, and constrained semi-supine) during vertical random vibration (0.25 to 20 Hz) at seven vibration magnitudes (nominally 0.0313, 0.0625, 0.125, 0.25, 0.5, 0.75 and 1.0 ms^{-2} r.m.s.). The motion transmission path that included more soft tissues exhibited a greater nonlinear response. The substantial nonlinearities found in transmissibilities to both the sternum and the abdomen of supine subjects, and previously reported for the transmissibilities of seated and standing subjects, imply that soft tissues at the excitation-subject interface contribute to the nonlinearity.

It is concluded that the thixotropy of soft tissues, rather than voluntary or involuntary muscular activity, is the primary cause of the biodynamic nonlinearity seen with varying magnitudes of excitation.

Contents

DECLARATION OF AUTHORSHIP

I, Ya Huang, declare that the thesis entitled

MECHANISM OF NONLINEAR BIODYNAMIC RESPONSE OF THE HUMAN BODY EXPOSED TO WHOLE-BODY VIBRATION

and the work presented in the thesis are both my own, and have been generated by me as the result of my own original research. I confirm that:

- this work was done wholly or mainly while in candidature for a research degree at this University;
- where any part of this thesis has previously been submitted for a degree or any other qualification at this University or any other institute, this has been clearly stated;
- where I have consulted the published work of others, this is always clearly attributed;
- where I have quoted from the work of others, the source is always given. With the exception of such quotations, this thesis is entirely my own work;
- I have acknowledged all main sources of help;
- Where the thesis is based on work done by myself jointly with others. I have made clear exactly what was done by others and what I have contributed myself;
- Parts of this work have been published as:

Huang Y and Griffin MJ (2006). Effect of voluntary periodic muscular activity on nonlinearity in the apparent mass of the seated human body during vertical random whole-body vibration. Journal of Sound and Vibration 298 (2006), 824 – 840.

Huang Y and Griffin MJ (2008a). Non-linear dual-axis biodynamic response of the semi-supine human body during vertical whole-body vibration. Journal of Sound and Vibration 312 (2008) 296 – 315.

Huang Y and Griffin MJ (2008b). Non-linear dual-axis biodynamic response of the semi-supine human body during longitudinal horizontal whole-body vibration. Journal of Sound and Vibration 312 (2008) 273 – 295.

Signed: ……

Date: ……

Acknowledgments

Thank you to Mike, my supervisor, for his highly experienced supervision, long-suffering patience and sustaining encouragement and support. Thank you to Dr Neil Ferguson, my internal reviewer and examiner, who provided constructive advice on nonlinearity and modelling.

Further thanks goes to all previous and current members of the Human Factors Research Unit for the friendly environment and consistent support they provided. Special thanks goes to Dr Tom Gunston for his skilful mentoring and advice on both experimental testing and computing. Thank you to Dr Chris Lewis for his advice on signal processing software and hardware. Thank you to Mr Peter Russell and Mr Gary Parker for their technical support in the lab. Thank you to Dr Miyuki Morioka, Mr Martin Toward, Mr Ian Wyllie and Dr Naser Nawayseh for their help and advice on running experiments. Thank you to Mr Cheng Gu and Mr Keith Walton for the time and assistance they gave me, especially when my trials and test sessions overran.

My appreciation also goes to all subjects that took part in my experiments. Without their time and patience I would not have been able to finish my studies on time.

Thank you to my friends, Jiguang for keeping me physically fit and mentally healthy, Matthieu for your visit to Southampton on a hard time, Kate and Nick for the many memorable holidays and constant support…

My gratitude goes to my mother, Xinya, and my father, Songnian, not just for giving me eyes to see and ears to hear, but also for bringing me up as a man with everlasting faith and hope.

Thank you to Xin, my wife and unique friend, for her constant and unconditional support to my life and career…

To my parents,

wife

and grandmothers

Chapter 1

Introduction

We are exposed to whole-body vibration throughout our lives. A baby travels in a pram, commuters by car, train, or bicycle, rescue crews by helicopters, boats, and earthmoving machineries. These environments expose the human body to vibration with different waveforms, durations, and magnitudes. An understanding of how vibration is transmitted to and through the human body (i.e. biodynamics) is a prerequisite to understanding how vibration affects health, safety, performance, and comfort.

A key to understanding the biodynamic responses of the body is the fact that the human body has resonance frequencies that decrease with increasing vibration magnitude. For over two decades, this biodynamic 'nonlinearity' has been reported in sitting and standing postures with all directions of excitation, and no study has found a condition that greatly changes the nonlinearity. There have been various speculations, but no experimental evidence, as to the mechanisms causing the nonlinearity. Current standards for the evaluation of human exposure to whole-body vibration assume a linear model of the response of the human body (e.g. ISO 5981, 1987; BS 6841, 1987; ISO 2631, 1997).

Knowledge of the mechanisms causing the nonlinearity will advance understanding of the mechanisms controlling body movement at resonance, and assist the evolution of biodynamic models of the human body in response to vibration over a range of magnitudes. For example, the mechanism may partially explain the nonlinearity in discomfort around the major resonance of the body during vibration. Such changes in discomfort may also reflect changes to the risk of injury during whole-body vibration.

The research undertaken for this PhD thesis was designed to discover the principal mechanism causing the biodynamic nonlinearity of the human body during whole-body vibration.

The thesis consists of ten chapters including this introductory chapter:

Chapter 2 reviews the biodynamic responses of the seated, standing, and supine human body using measures of apparent mass and transmissibility. Studies investigating the effect of excitation magnitude are discussed in detail. The main hypotheses and objectives for each experimental study reported in the thesis are established at the end of the review.

Chapter 3 describes the main experimental equipment and the methods employed for data analysis.

Chapter 4 investigates the effect of voluntary periodic upper-body movement and vibration magnitude on the apparent masses of 14 seated subjects.

Chapter 5 studies the effect of different shear histories on the nonlinearity of 12 relaxed semi-supine subjects by using continuous and intermittent vertical random vibration at a low and a high magnitude.

Chapter 6 reports a similar study as Chapter 5 but with longitudinal horizontal excitation of the same group of 12 semi-supine subjects.

Chapter 7 analyses the frequency-dependence and magnitude-dependence of the distortion in dynamic force harmonic for the same group of 12 relaxed semi-supine subjects exposed to vertical and horizontal sinusoidal excitation.

Chapter 8 examines the effect of vibration magnitude on the apparent mass and the transmissibilities to the sternum and the abdomen of 12 subjects in different supine postures.

Chapter 9 presents a general discussion of the findings reported in the thesis.

Chapter 10 provides the main conclusions from each study in the thesis and offers recommendations for future work.

Chapter 2

Literature review

2.1 Introduction

Since the 1960s, the biodynamic responses of the seated and standing human body exposed to whole-body vibration have been found to be dependent on a variety of variables. These may include: posture (e.g. kyphotic and erect), muscle activity (e.g. tensed and relaxed), seating condition (e.g. body constraints and increased pressure at buttocks), body characteristics (e.g. age and gender), vibration waveform (e.g. sinusoids, narrowband random stimuli, and broadband random stimuli), and vibration magnitude etc. A linear system will have the same dynamic behaviour (i.e. resonance frequency, and magnitude of response) with different vibration inputs.

In the past two decades, the biodynamic responses of the human body have been found to be nonlinear: the resonance frequencies in frequency response functions (e.g. apparent mass and transmissibility) decrease with increasing vibration magnitude. This nonlinearity has been observed in the vertical and the fore-and-aft responses of the seated human body exposed to vertical whole-body vibration (e.g. Hinz and Seidel, 1987; Fairley and Griffin, 1989; Mansfield and Griffin, 2000; Mansfield and Griffin, 2002; Matsumoto and Griffin, 2002a; Nawayseh and Griffin, 2003), in the fore-and-aft and the vertical responses of the seated human body exposed to fore-and-aft whole-body vibration (e.g. Fairley and Griffin, 1990; Mansfield and Lundström, 1999a; Holmlund and Lundström, 2001; Nawayseh and Griffin, 2005a; Abdul Jalil, 2005), and in the vertical and the fore-and-aft responses of the standing human body exposed to vertical whole-body vibration (e.g. Matsumoto and Griffin, 1998a; Subashi *et al*., 2006).

To identify factors influencing the nonlinearity, the effects of various steady-state sitting conditions have been studied with different vibration magnitudes. The nonlinearity has been found in all sitting and standing conditions investigated. These conditions included: different upper-body postures of seated subjects (e.g. Fairley and Griffin, 1989; Mansfield and Griffin, 2002), different postures of standing subjects (e.g. Matsumoto and Griffin, 1998a; Subashi *et al*., 2006), different muscle tensions at different locations of the body (e.g. Mansfield and Griffin, 2002; Matsumoto and Griffin, 2002b), and different contact pressures on the buttocks of seated subjects (e.g. Mansfield and Griffin, 2002; Nawayseh and Griffin, 2003; Nawayseh and Griffin, 2005a).

The objective of this chapter is to identify all possible causes that may primarily contribute to the biodynamic nonlinearity.

Section 2.2 reviews the measures used to represent the biodynamic responses of the human body. Section 2.3 and Section 2.4 discuss the factors that influence the biodynamic responses of the human body in terms of driving-point mechanical impedance (including apparent mass) and transmissibility. Section 2.5 outlines lumped parameter dynamic models used to represent the biodynamic responses of the human body. Having established the scope of the nonlinearity, Section 2.6 discusses the major causes of the nonlinearity. Finally Section 2.7 summarizes the review and concludes on principal factors that may have caused of the nonlinearity.

2.2 Measures of the biodynamic responses of the human body

The driving-point frequency response functions are used to describe the relationship between the input signal and the ensuing output signals at the same point, usually at the interface between the subject and the vibration source. This interface is often called seat-subject interface (also known as 'subject-excitation interface'), with 'seat' referring to the contact surface between the subject and the vibration source. For example, the seat-subject interface could be the seat surface or backrest for the seated subjects, the foot platform for the standing subjects or the recumbent back support for the supine subjects. If the acceleration is used as input at the interface and the dynamic force is output, the frequency response function represents the 'apparent mass' of the body. If the velocity is used as input, the frequency response function represents the 'mechanical impedance'.

The apparent mass (also known as 'driving-point apparent mass' or 'effective mass') at a frequency f, $M(f)$, is defined as the complex ratio of the output (or driving) force, $F(f)$, to the input acceleration, $a(f)$, measured at the seat-subject interface:

$$M(f) = \frac{F(f)}{a(f)} \tag{2.1}$$

The mechanical impedance (also known as 'driving-point mechanical impedance') at a frequency f, $Z(f)$, is defined as the complex ratio of the output (or driving) force, $F(f)$, to the input velocity, $v(f)$, measured at the seat-subject interface:

$$Z(f) = \frac{F(f)}{v(f)} \tag{2.2}$$

There are more studies using apparent mass than mechanical impedance. One reason is that the apparent mass can be directly obtained from measured

acceleration and force transducers. At low frequencies, the human body has the behaviour of a rigid mass, i.e. the apparent mass represents the static weight of the body (Griffin, 1990). Another important difference between the two measures of impedance is that the primary resonance frequency in the mechanical impedance is either the same or higher than the primary resonance frequency in the apparent mass. Mansfield (2005) showed this difference by transforming the transfer function of a single-degree-of-freedom mass-spring-damper system: the resonance frequency was 5.50 Hz in the mechanical impedance, while 4.25 Hz in the apparent mass with the same mass-spring-damper parameters. Furthermore, the resonance frequency in the transmissibility between the base and moving mass of the single-degree-of-freedom system is the same as that in the apparent mass. Therefore, the apparent mass gives a more direct representation of the biodynamic response than the mechanical impedance.

Normally the term 'apparent mass' is used when the output force is in-line with the input acceleration. The term 'cross-axis apparent mass' is used when the output force is perpendicular to the input acceleration. For example, with an upright seated subject, the fore-and-aft cross-axis apparent mass is calculated by taking the output force in the direction perpendicular to the vertical input acceleration in the mid-sagittal plane.

'Transmissibility' represents the amount of motion transmitted between two locations. Normally the acceleration is used for convenience of measurement. The transmissibility is defined as the complex ratios of the motion measured at the output location to the motion measured at the input reference location. The input reference motion is usually measured at the seat-subject interface. For example:

$$T(f) = \frac{a_{L5}(f)}{a_B(f)} \tag{2.3}$$

where $T(f)$ is the transmissibility between the vertical acceleration at the seat base, $a_B(f)$, and the vertical acceleration at the fifth vertebra of lumbar spine, $a_{L5}(f)$.

The apparent mass (or mechanical impedance) is a measure of the overall dynamic response of the human body above the force sensing platform. It takes into account all movements, vibration transmission paths and mechanisms above the seat-subject interface. On the other hand, the transmissibilities at different body locations can be used to identify modes contributing to resonances of the human body.

Subjects have different static weights. When comparing effects of independent variables, such as the posture and vibration magnitude, or comparing different studies with different subject groups, the 'normalised apparent mass' is used to

reduce such variability among subjects (so called inter-subject variability) due to the difference in static weight (Fairley, 1986). The normalised apparent mass is the apparent mass divided by the static mass of the body above the force sensing elements in the frequency domain.

'Absorbed power' of the human body during exposure to vibration is another measure of dynamic responses of the human body (Lundström and Holmlund 1998, Mansfield and Griffin 1998, Mansfield *et al*. 2001). The absorbed power is defined as the product of the force and the velocity at the seat-subject interface. The absorbed power can be a measure of the vibration severity as its magnitude increases with vibration magnitude and duration (velocity is the integral of acceleration by time).

The apparent mass and transmissibility are used in this thesis.

2.3 Mechanical impedance and apparent mass of the human body

2.3.1 Vertical excitation

Studies measuring apparent mass and mechanical impedance during vertical whole-body vibration showed a primary resonance frequency of the seated body at around 5 Hz (Fairley and Griffin, 1989; Kitazaki and Griffin, 1998; Mansfield and Griffin, 2000; Mansfield and Griffin, 2002; Matsumoto and Griffin, 2002a; Matsumoto and Griffin, 2002b). A minor secondary resonance has been reported between about 8 and 12 Hz (Fairley and Griffin, 1989; Mansfield and Griffin, 2000; Mansfield and Griffin 2002).

The majority of reported biodynamic studies used male subjects, therefore the subjects in the reviewed literature were males unless otherwise stated.

The inter-subject variability of the apparent mass (Figure 2.1) has been found to be related to various factors. The primary apparent mass resonance frequencies of 60 subjects (24 men, 24 women, and 12 children) showed significant negative correlations with the total body weight and the ratio of sitting weight to sitting height (Fairley and Griffin, 1989). The normalised apparent masses at resonance of the 60 subjects were positively correlated to the total body weight and the height of the lower legs. The authors also found the effect of the inter-subject variability was greater than the effect of posture or vibration magnitude. However, for individual subjects, the upper-body posture and vibration magnitude tended to have a greater effect on the apparent mass than the gender or age.

The human biodynamic response to vibration can be simplified to a single-degree-of-freedom mass-spring-damper system so as to represent the dominant resonance characteristics of the apparent mass or mechanical impedance (Griffin, 1990). The resonance frequency and the magnitude of the apparent mass or impedance at resonance indicate the equivalent stiffness and the equivalent damping of the human body.

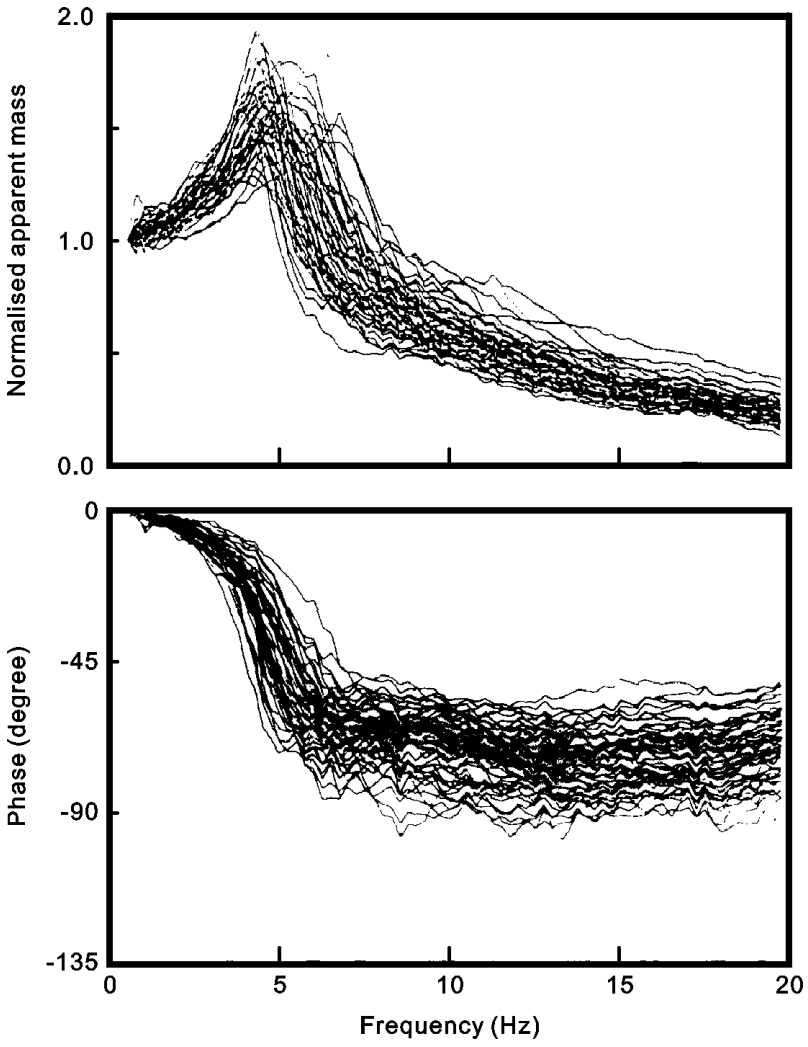

Figure 2.1 Normalised (at 0.5 Hz) apparent mass modulus and phases of the 60 upright seated human subjects exposed to broadband (0.25 to 20 Hz) random vertical whole-body vibration at 1.0 ms^{-2} r.m.s. (Fairley and Griffin, 1989).

2.3.1.1 Effect of posture and muscle tension

Different apparent mass resonance frequencies of seated subjects have been reported with different upper-body postures. During 0.25–20 Hz broadband random vibration at 1.0 ms^{-2} r.m.s., eight subjects showed higher resonance frequencies with 'erect' and 'tensed' sitting postures than a 'normal' upright posture (Fairley and Griffin, 1989). The authors found the resonance frequency increased by about 1.5 Hz when the posture changed from 'slouched' to 'very erect' in five steps. The apparent mass at resonance was higher as the posture became more erect. The resonance frequency of the mean normalised apparent mass of eight subjects increased from 4.4 to 5.2 Hz when their posture changed from 'slouched' to 'erect' (Figure 2.2, Kitazaki and Griffin, 1998). The mean normalised apparent mass at resonance was found to be higher with more erect postures. With 30 upright seated subjects exposed to 2 to 100 Hz sinusoidal vibration, Holmlund *et al*. (2000) also found the mechanical impedance at peak was higher with an 'erect' posture than a 'relaxed' posture. Mansfield and Griffin (2002) studied the effect of nine sitting postures on apparent mass (Figure 2.3). Comparing with the resonance frequency of the normal upright sitting posture (median 5.27 Hz), the resonance frequencies of the kyphotic (median 6.25 Hz) and the anterior lean (median 6.06 Hz) postures were found to be higher but only at 0.2 ms^{-2} r.m.s. – no significant difference was found between the three postures at higher vibration magnitudes (i.e. 1.0 and 2.0 ms^{-2} r.m.s., Figure 2.4). A 'kyphotic' posture in this study, similar to the previously reported 'slouched' posture, showed the lowest normalised apparent mass at resonance among the nine postures. This was consistent with previous studies suggesting a higher degree of damping with the more relaxed, or slouched, postures.

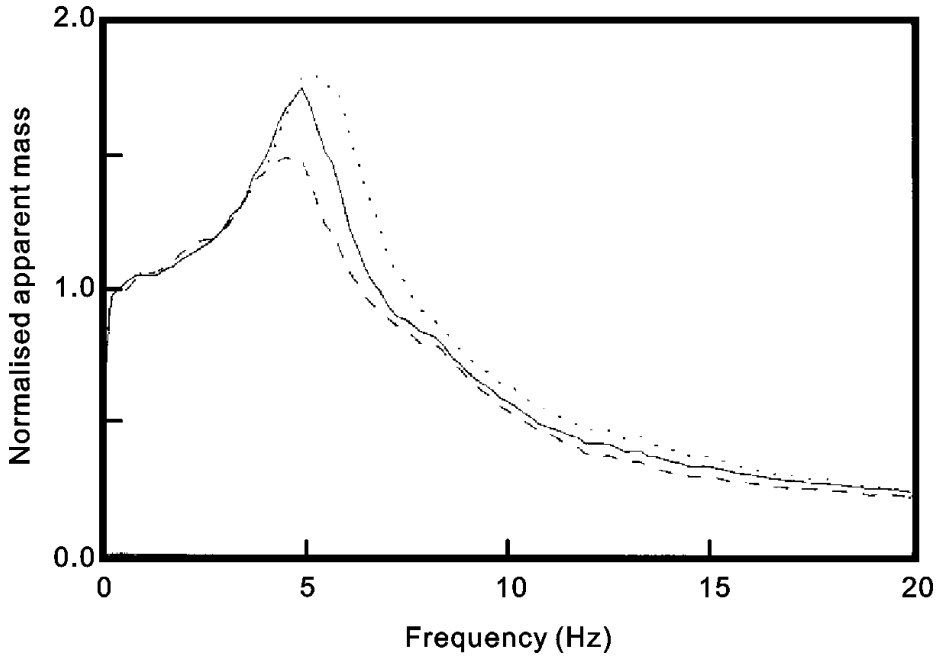

Figure 2.2 Mean normalised apparent masses of the eight upright seated subjects in the erect posture (· · · · · ·), normal posture (———), and the slouched posture (— — —) during broadband (0.5 to 35 Hz) random vertical vibration at 1.7 ms^{-2} r.m.s. (Kitazaki and Griffin, 1998).

Most studies with different sitting postures agree that a more erect or tensed posture results in a higher resonance frequency, i.e. higher effective stiffness of the human body. However, some studies found that the effect of sitting posture was insignificant (e.g. Mansfield and Griffin, 2002). Inter-subject variability could be one reason for this inconsistency. Mansfield and Griffin (2002) noticed that the 'anterior lean' was one of the postures that exhibited the most variability at all three magnitudes investigated (i.e. 0.2, 1.0, and 2.0 ms^{-2} r.m.s.). In the study conducted by Fairley and Griffin (1989), two of the eight subjects (Subject 6 and Subject 8) showed a very small effect of the 'tense' posture on the resonance frequency compared with the normal upright posture, while another two (Subject 3 and Subject 5) exhibited a significant increase in resonance frequencies when changing from 'normal' to 'erect', and to 'tense' (Figure 2.5). Such variability may arise from different abilities in maintaining a posture, or different muscular control capabilities and strategies.

By exposing twelve seated subjects to broadband 1–20 Hz random vertical whole-body vibration at 0.4 ms^{-2} r.m.s., Mansfield and Maeda (2005) compared sitting conditions featuring an upper-body 'twist' and a left-to-right voluntary periodic 'move' with the normal upright ('back-off') sitting posture. The apparent mass resonance frequency of the 'twist' was higher than the 'back-off' posture, while no significant

difference in resonance frequency was found between the ‘move’ and the ‘back-off’ posture. The ‘move’ condition showed the lowest normalised apparent mass at resonance, and there was no significant difference in the normalised apparent mass at resonance between the ‘twist’ and the ‘back-off’ posture. The voluntary ‘move’ condition tended to increase the damping of the body; however, it did not alter the equivalent stiffness. The ‘move’ condition was designed to mimic the body movement of agricultural truck drivers. It was anticipated that the voluntary movement condition would alter the muscular activity in response to vibration so that the equivalent stiffness, or resonance frequency, of the body would be changed. The insignificant effect of the voluntary movement on the resonance frequency might be because either: (i) the change in stiffness of the body was not primarily caused by a change in the muscular activity, or, (ii) the voluntary movement employed was not sufficient to influence the muscular activity that could change the body stiffness.

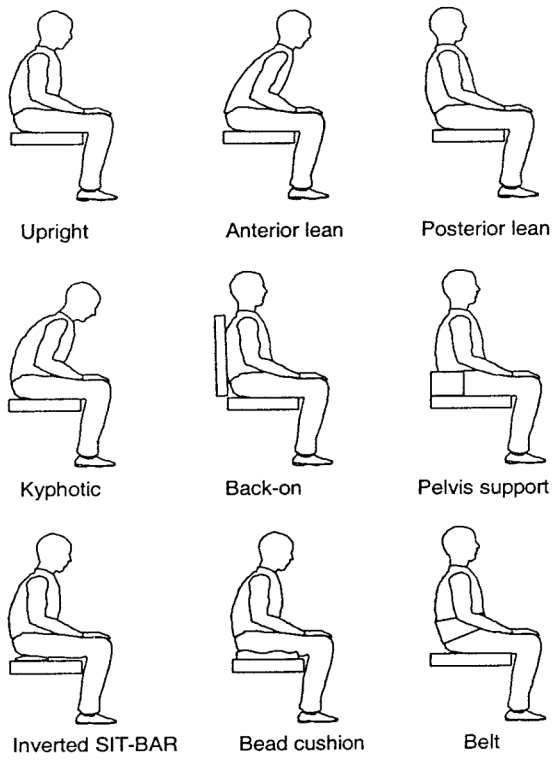

Figure 2.3 Diagrammatic representation of the nine sitting postures (Mansfield and Griffin, 2002).

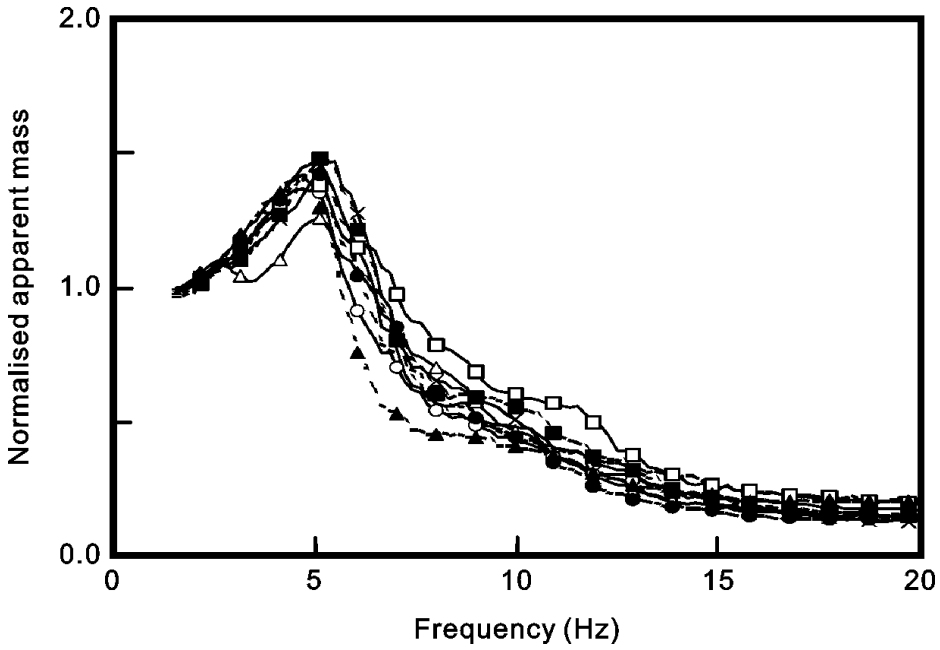

Figure 2.4 Median normalised apparent mass for 12 seated subjects exposed to broadband 1–20 Hz random vertical vibration at 1.0 ms^{-2} r.m.s.: ———, upright; —x—, anterior lean; —o—, posterior lean; —Δ—, kyphotic; —□—, back-on; - - - -, pelvis support; —●—, inverted SIT-BAR; —▲—, cushion; —■—, belt (Mansfield and Griffin, 2002).

An increase in steady-state muscle tension at the buttocks and abdomen caused the apparent mass resonance frequency of upright seated subjects to increase (Matsumoto and Griffin 2002b). This trend was evident in the apparent mass of a single subject (Figure 2.6) and the median normalised apparent mass of a group of eight subjects.

Multifidus, and other deep spinal muscles, play an important role in stabilizing the body (Valencia and Munro, 1985). This is consistent with the electromyography (EMG) measured at the lumbar multifidus without vibration (Blüthner *et al*., 2002): the averaged EMG was higher with an 'erect' than a 'relaxed' sitting posture, and higher with a 'bent-forward' posture than an 'erect' posture. By exposing 38 subjects to narrowband whole-body vibration, Blüthner *et al*. (2002) found that the timing and the magnitude of the frequency response functions of the EMG activities of different back muscles varied with three different sitting postures (i.e., 'relaxed', 'erect', and 'bent-forward'). The transfer function from the seat input acceleration to the multifidus EMG showed that the muscular activity increased as the posture changed from 'relaxed' to 'erect', and from 'erect' to 'bent-forward' (Figure 2.7). This was most apparent at the peak in the transfer function between 5 to 9 Hz. A change in muscle tension resulting from a change in the upper-body posture during vibration would influence the magnitude of the muscular activity in response to vibration. The greatest time lag of the multifidus in all three postures occurred at around 2 to 3 Hz

with a gradual reduction in the lag at higher frequencies (Figure 2.7). Fast and slow muscle fibres were found to respond to different frequencies of whole-body vibration (Blüthner *et al*. 1997). At frequencies around 1 to 2 Hz, the relaxed posture exhibited less time lag than the erect and bent-forward postures (Figure 2.7), suggesting that increased steady-state muscle tension during vibration might have delayed the response of the slow fibres.

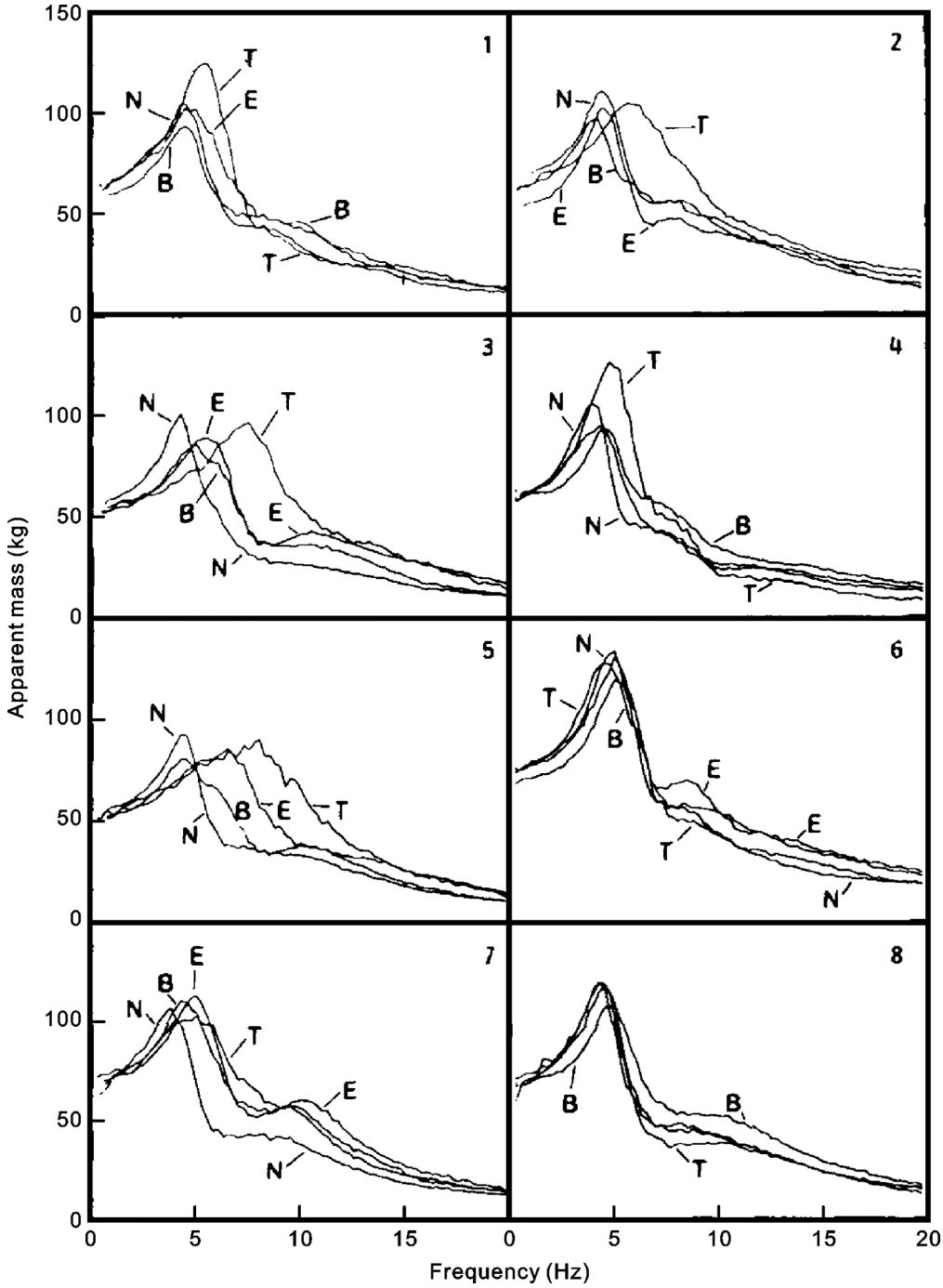

Figure 2.5 Effect of posture and muscle tension (N=normal; E=erect; B=backrest; T=tense) on the apparent masses of eight seated subjects exposed to broadband 0.25–20 Hz random vertical whole-body vibration at 1.0 ms^{-2} r.m.s. (Fairley and Griffin, 1989).

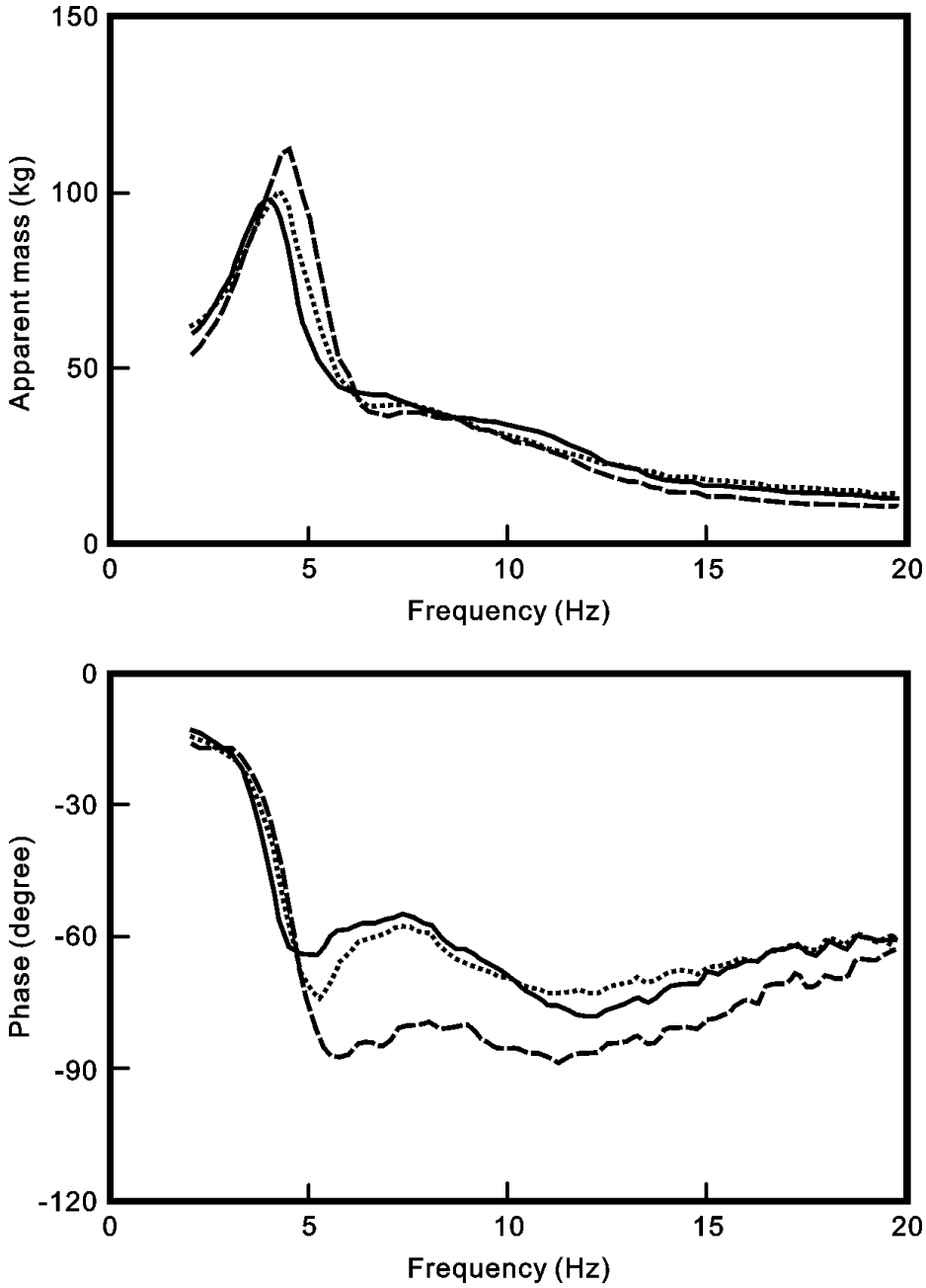

Figure 2.6 Apparent masses and phases of a single upright seated subject exposed to broadband (2.0 to 20 Hz) random vertical whole-body vibration at 1.4 ms^{-2} r.m.s.: ——— , normal upright; — — — , buttocks tensed; ····· , abdomen minimized (adapted from Matsumoto and Griffin, 2002b).

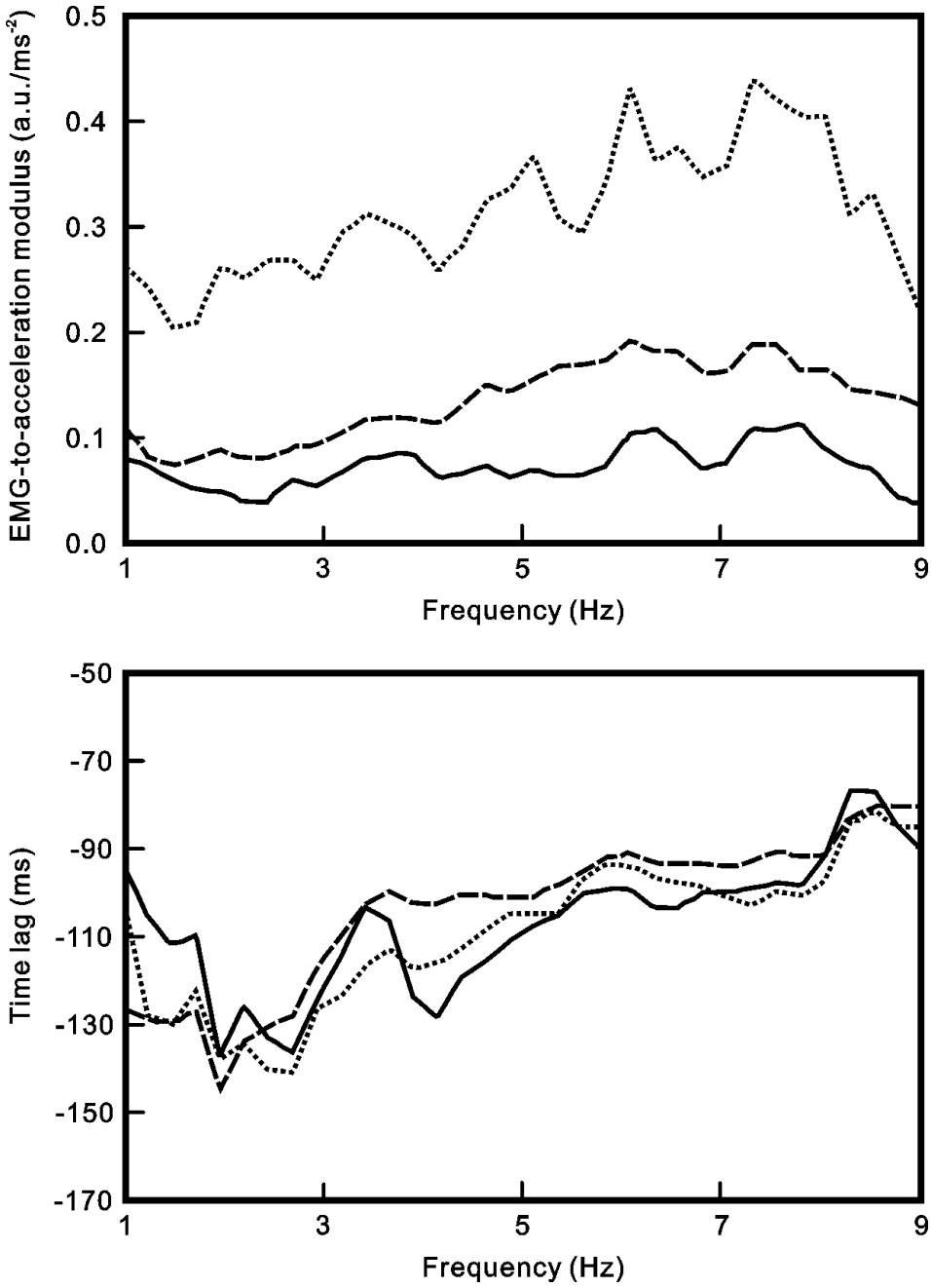

Figure 2.7 Transfer function modulus (upper) and time lag (lower) between the input acceleration at the seat and the mean processed EMG measured at the lumbar multifidus in arbitrary unit (a.u.) with three sitting postures: ——— , relaxed; — — — , erect; ····· , bent-forward. Results were obtained by averaging the measurements from 38 seated subjects exposed to narrowband (1 to 9 Hz, with a maximum at 3 Hz) random vibration at 1.4 ms^{-2} r.m.s. (adapted from, Blüthner *et al*. 2002).

The apparent mass resonance frequency of a 'normal' standing posture was slightly higher than that of a 'normal' sitting posture, but both were in the range from 5 to 6 Hz (Matsumoto and Griffin, 2000). The authors speculated that the small difference in resonance frequencies of the two postures was due to some 'common dynamic

mechanisms' in the upper body. The standing posture showed lower apparent mass at resonance than the sitting posture. But the apparent mass was higher with the standing posture at frequencies above 10 Hz. The researchers attributed the difference in resonance apparent mass, characteristic of damping, between the two postures to changes in contact tissues (i.e. buttocks for seated and sole for standing subjects) and the dynamics of legs.

With three standing postures, Matsumoto and Griffin (1998a) found the apparent mass resonance frequency was higher with the normal standing posture (median 5.5 Hz) than a one-leg posture (median 3.75 Hz), and higher with the one-leg posture than a legs bent posture (median 2.75 Hz; Figure 2.8). Subashi *et al*. (2006) reported that the leg posture had more influence on the resonance of the body than the upper-body posture, and this was consistent in both studies (Figure 2.8). Subashi *et al*. (2006) attributed the minor change in upper body posture to an increase in damping due to increased muscle activities in the upper body of the lordotic and anterior lean postures compared to the upright posture. Bending the knees had a significant effect on softening the response in both studies.

Two apparent resonances were found in the fore-and-aft cross-axis apparent mass of the standing subjects exposed to vertical vibration (Figure 2.9, Subashi *et al*., 2006). Bending of the spine had a greater effect on the fore-and-aft cross-axis apparent mass than the apparent mass: the lordotic (with bent spine) standing posture increased both resonance peaks in the cross-axis response. It was possible that the rotational mechanism of the pelvis, which contributed to the cross-axis response, was locked by increased muscle activity at pelvis and the geometry of the curved spinal column. Therefore, the fore-and-aft force at the floor could have been increased. The cross-axis response was less with the anterior lean posture than the upright posture. This might be caused by increased inertial forces from the leaning upper body acting out of phase with the forces in the lower body. A similar effect was found in upright seated subjects with arms horizontally 'extended' (Mansfield and Maeda, 2005), and an 'automotive' sitting posture with backrest contact and arms holding a steering wheel (Rakheja *et al*., 2002).

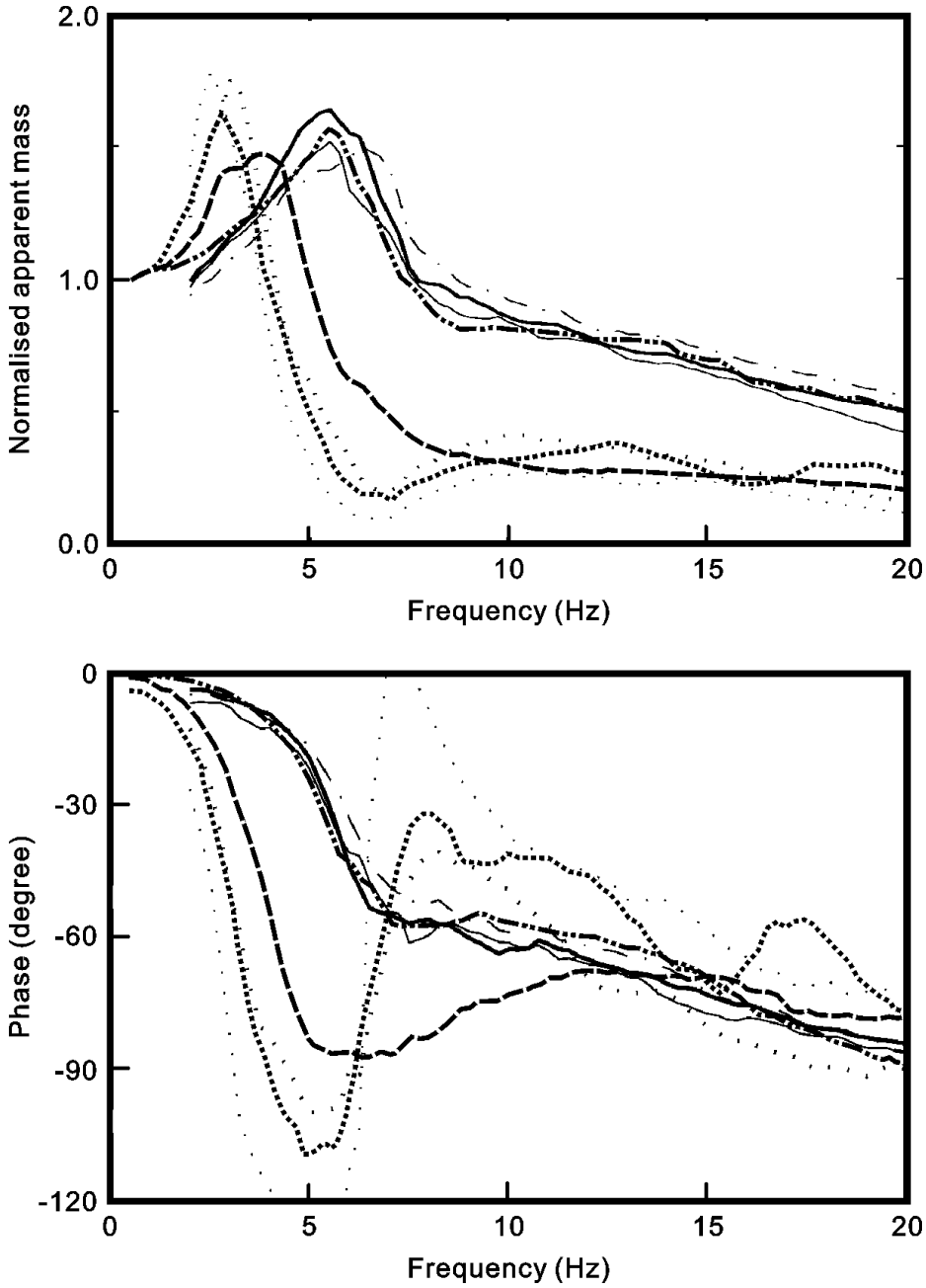

Figure 2.8 Median normalised apparent masses and phases of 12 standing subjects exposed to broadband (0.5 to 30 Hz) random vertical whole-body vibration at 1.0 ms^{-2} r.m.s.: —··—··— , normal standing posture; — — — , one leg posture; ····· , leg bent posture (0.5 to 20 Hz data adapted from Matsumoto and Griffin, 1998a). Median normalised apparent masses and phases of another group of 12 standing subjects exposed to broadband (2 to 20 Hz) random vertical whole-body vibration at 0.5 ms^{-2} r.m.s.: ——— , upright; ——— , lordotic; — · — · — , anterior lean; . . . . . , knees bent; . . . . . , knees more bent (adapted from Subashi *et al.*, 2006).

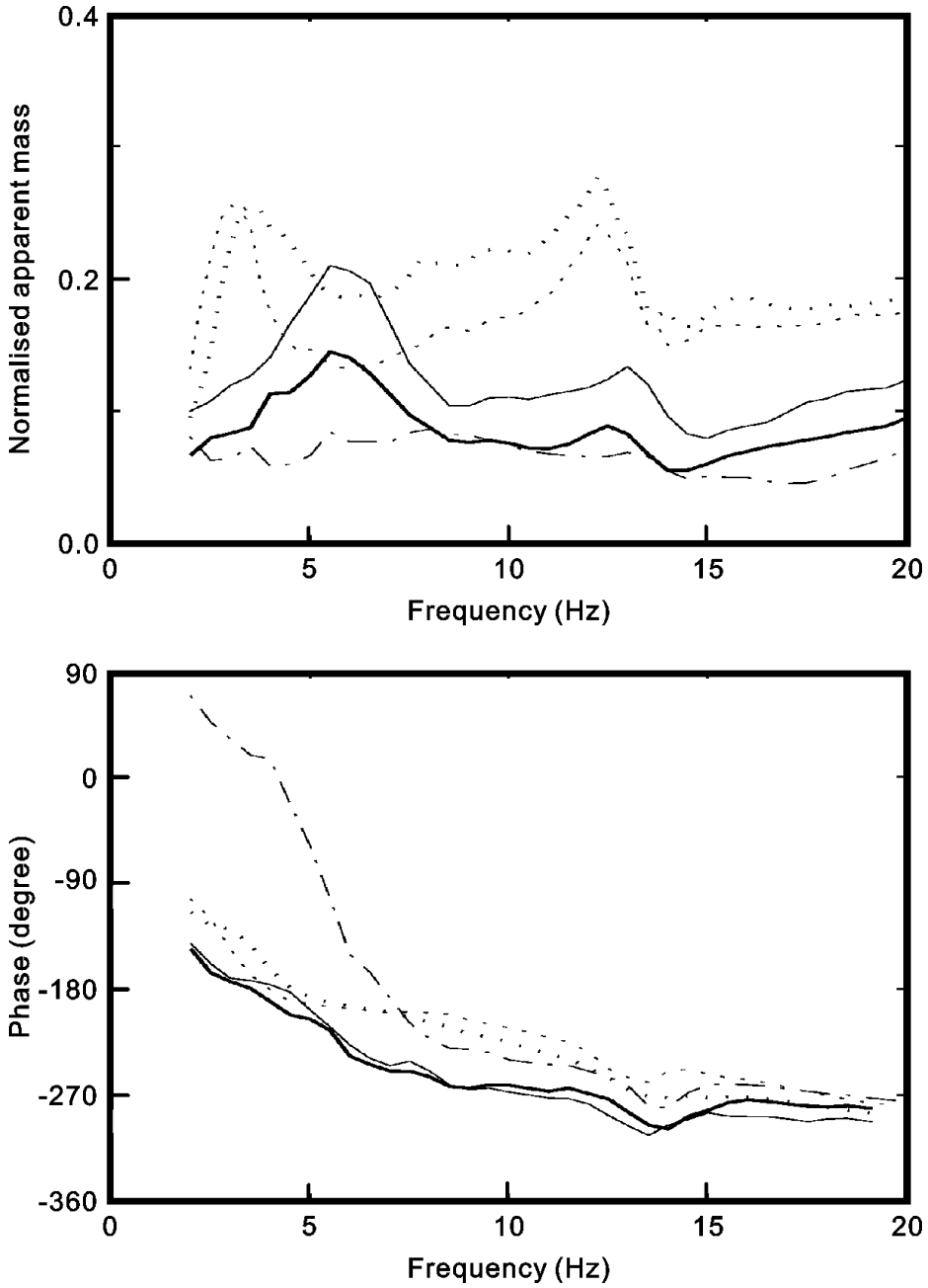

Figure 2.9 Median normalised fore-and-aft cross-axis apparent masses and phases of 12 standing subjects exposed to broadband (2 to 20 Hz) random vertical whole-body vibration at 0.5 ms^{-2} r.m.s.: ——— , upright; ——— , lordotic; — · — · — , anterior lean; . . . . . , knees bent; . . . . . , knees more bent (adapted from Subashi *et al*., 2006).

Very few studies have measured the mechanical impedance of the supine human body (Vogt *et al*., 1973; Vogt *et al*., 1978; Vykukal, 1968). The primary resonance frequency was found to be around 6 Hz in the mechanical impedance of the supine subjects with 2 to 20 Hz sinusoidal vibration at 3.5 ms^{-2} r.m.s. (Vogt *et al*., 1973), or with 1 to 20 Hz sinusoidal vibration at 2.1 ms^{-2} r.m.s. (Vogt *et al*., 1978). The primary resonance frequency occurred between 7 and 11 Hz in the mechanical impedance of 'semi-supine' space crew with 1 to 70 Hz sinusoidal vibration at 2.8 ms^{-2} r.m.s. (Vykukal, 1968). The difference between the first two studies and the third study might be due to different postures and different vibration magnitudes, as well as different sustained acceleration levels. For example, Vykukal (1968) used restraints with the semi-supine seat as a configuration of existing spacecraft. The primary resonance frequency of an upright seated human body was around 5 Hz in mechanical impedance with 2 to 200 Hz sinusoidal vibration at between 0.5 and 1.4 ms^{-2} r.m.s. (Holmlund *et al*., 2000). As will be shown later in this chapter, the sustained acceleration was found to stiffen the body (or increase the resonance frequency). The simultaneous sustained acceleration used by Vykukal (1968) and Vogt *et al*. (1973) could have increased the resonance frequency of the body.

2.3.1.2 Effect of seating condition – buttocks pressure, constraints, and backrest

Increasing the pressure on the buttocks (or tissues beneath the ischial tuberosities) has been reported to increase the resonance frequency of the seated human body (Sandover, 1978; Kitazaki, 1994). However, Mansfield and Griffin (2002) reported an insignificant change in the apparent mass resonance frequency when a normal upright posture was changed to an 'inverted SIT-BAR' or a 'bead cushion' condition (Figure 2.4). Decreasing the thigh contact area, with increased pressure on the buttocks, on a flat rigid seat by raising the footrest, Nawayseh and Griffin (2003) found neither the apparent mass resonance frequency (Figure 2.10), nor the fore-and-aft cross-axis apparent mass resonance frequency (Figure 2.11) was affected. The inconsistent effect of changing buttocks pressure in these studies might be due to some other seating conditions. For instance, Mansfield and Griffin (2002) and Nawayseh and Griffin (2003) used a footrest moving in phase with the seat; however, the feet were resting on a stationary footrest in Kitazaki's study. Near zero Hz, the apparent mass measured at the seat when the feet were supported on a footrest moving in phase with the seat was about the static sitting weight of the subject. However, when supporting the feet on a stationary footrest, the apparent mass near zero Hz was much lower than the static sitting weight (Fairley and Griffin, 1989). The authors attributed this effect to the relative motion between the seat and

the stationary footrest – at low frequencies, the thighs could apply force against the inertial forces of the moving body. In Sandover's study, subjects were seated with a backrest, which was not used by Mansfield and Griffin (2002) or Nawayseh and Griffin (2003). Sandover (1978) used a footrest moving in phase with the seat. The effect of a backrest on the dynamic response of the body to vibration will be discussed later in this section.

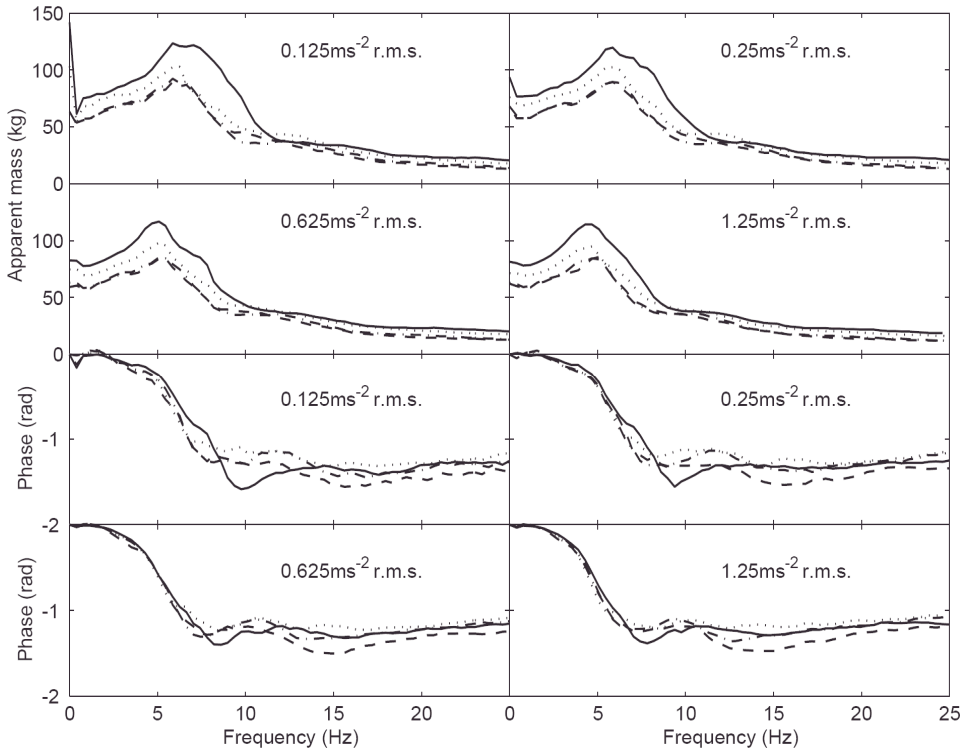

Figure 2.10 Median apparent masses and phases of 12 upright seated subject exposed to broadband (0.25 to 25 Hz) random vertical whole-body vibration at 0.125, 0.25, 0.625, and 1.25 ms^{-2} r.m.s. with four postures: ——— , feet hanging; . . . . . , maximum thigh contact; — · — · — , average thigh contact; - - - - - - , minimum thigh contact (Nawayseh and Griffin, 2003).

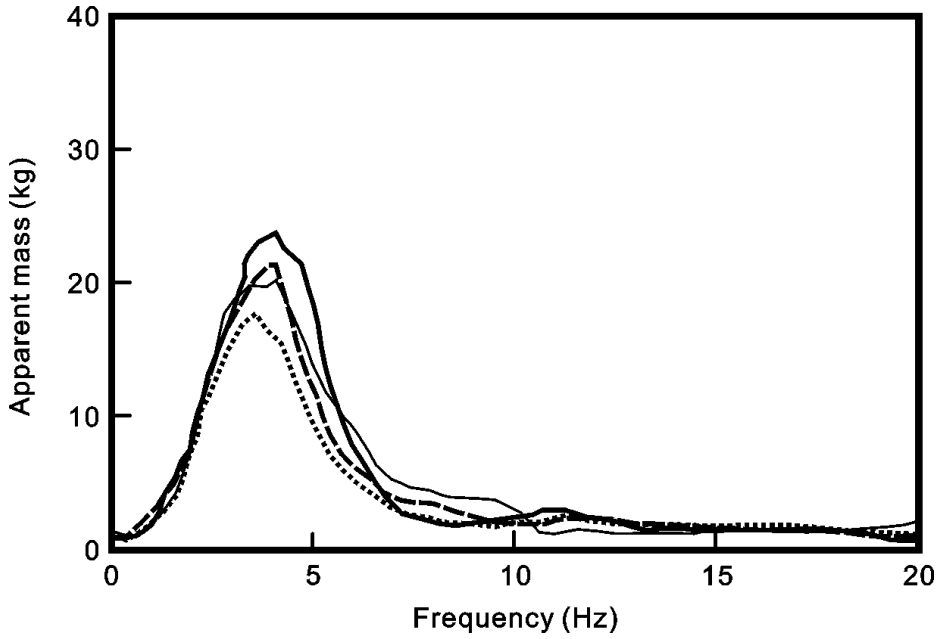

Figure 2.11 Median fore-and-aft cross-axis apparent masses of 12 upright seated subjects exposed to broadband (0.25 to 25 Hz) random vertical whole-body vibration at 1.25 ms^{-2} r.m.s.: ——— , feet hanging; — — — , maximum thigh contact; ..... , average thigh contact; ——— , minimum thigh contact (adapted from Nawayseh and Griffin, 2003).

The effect of body-constraining devices on the apparent mass has been investigated. Constraining the movement of viscera by using a wide webbing belt resulted in a mode between 7 and 8 Hz occurring in the apparent mass of a seated subject (Sandover, 1978). Kitazaki (1994) found an increase in apparent mass resonance frequency when the movement of the viscera was constrained by a wide abdominal belt. The apparent mass resonance frequency of 12 upright seated subjects exposed to random vibration at 0.2 and 2.0 ms^{-2} r.m.s. was increased by wearing an elastic abdominal belt (Figure 2.3, Mansfield and Griffin, 2002). Although the tightness and location of the body-constraining conditions may vary, all these conditions appear to reduce the local movement of soft tissues and the viscera. The stiffness of the body might be increased by constraining but the effect was small.

Adding an upright rigid backrest increased the apparent mass resonance frequency of an upright seated subject exposed to vertical random vibration (e.g. Toward, 2003; Nawayseh and Griffin, 2004). The increase in resonance frequency was also found in the fore-and-aft cross-axis apparent mass at seat (Figure 2.12, Nawayseh and Griffin, 2004). The apparent mass resonance frequencies measured with and without the backrest were significantly correlated. Assuming there was small postural change when adding an upright backrest, and considering the seated human body to be a multi-degree-of-freedom model, contact with the backrest could

constrain the movement of upper parts of the model, and therefore introduce additional stiffness and damping at the back.

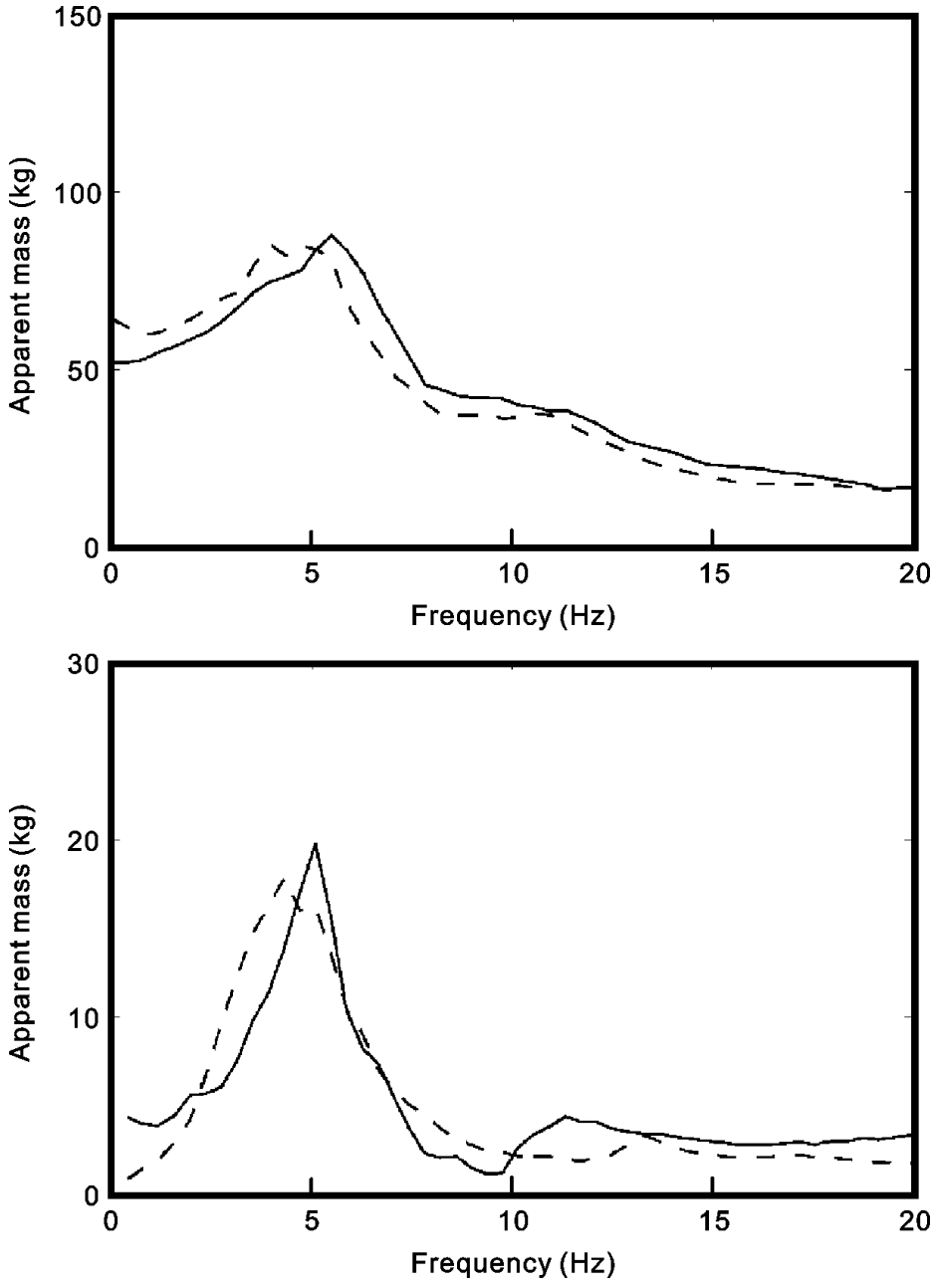

Figure 2.12 Median vertical apparent mass (upper) and median fore-and-aft cross-axis apparent mass (lower) of 11 upright seated subjects measured on the seat with broadband (0.25 to 25 Hz) random vertical whole-body vibration at 1.25 ms^{-2} r.m.s. in the average thigh contact posture: ——— , with an upright backrest; — — — , without the backrest (Nawayseh and Griffin, 2004).

Gradually inclining the upright backrest caused the apparent mass at resonance to decrease and the resonance frequency to increase. The resonance frequency of the median apparent mass increased from 5.27 to 6.44 when the backrest was inclined by 30 degrees (Figure 2.13, Toward, 2003). The reduction in apparent mass below 8 Hz might be due to more body weight being supported by the backrest as the backrest was inclined.

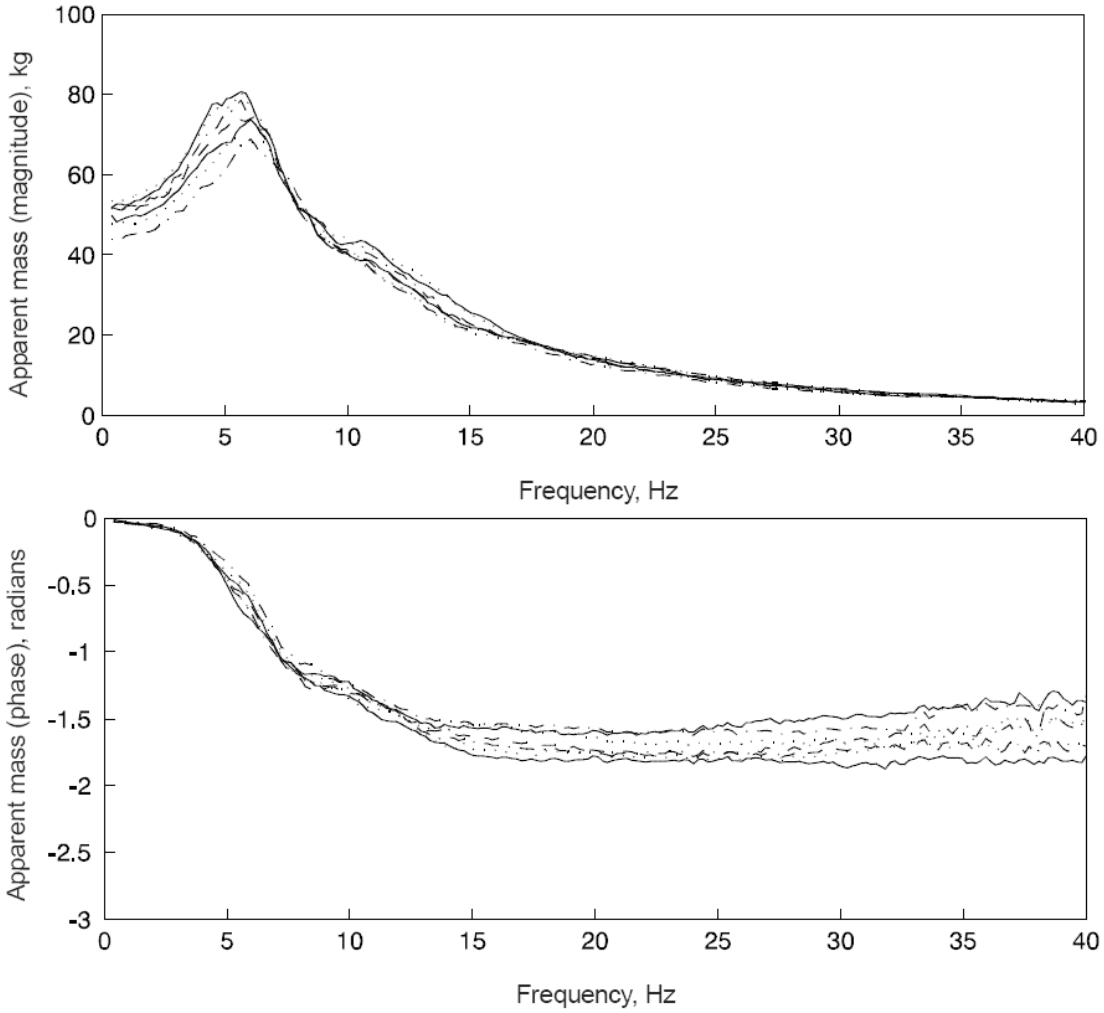

Figure 2.13 Median apparent mass modulus and phases at the seat surface for 12 seated subjects exposed to broadband (0.125 to 40 Hz) random vertical vibration at 1.0 ms^{-2} r.m.s. using rigid backrest inclined to 0^o (———), 5^o (.....), 10^o (— · — · —), 15^o (— — —), 20^o (**———**), 25^o (**.....**), and 30^o (**— · — · —**). The resonance frequency increased as the backrest inclined (Toward, 2003).

2.3.1.3 Effect of vibration magnitude – the biodynamic nonlinearity

In the past two decades, it has been consistently reported that the resonance frequency of the impedance (e.g. apparent mass) of the human body decreases with increasing magnitude of random vibration (e.g. Fairley and Griffin, 1989; Mansfield and Griffin, 2000; Matsumoto and Griffin 2002a; Matsumoto and Griffin, 1998a; Subashi *et al.*, 2006) and sinusoidal vibration (e.g. Hinz and Seidel, 1987; Mansfield, 1998; Matsumoto and Griffin, 2002b) vibration. This systematic change in the dynamic responses of the human body to different vibration magnitudes has been referred as the biodynamic 'nonlinearity' (Figure 2.14).

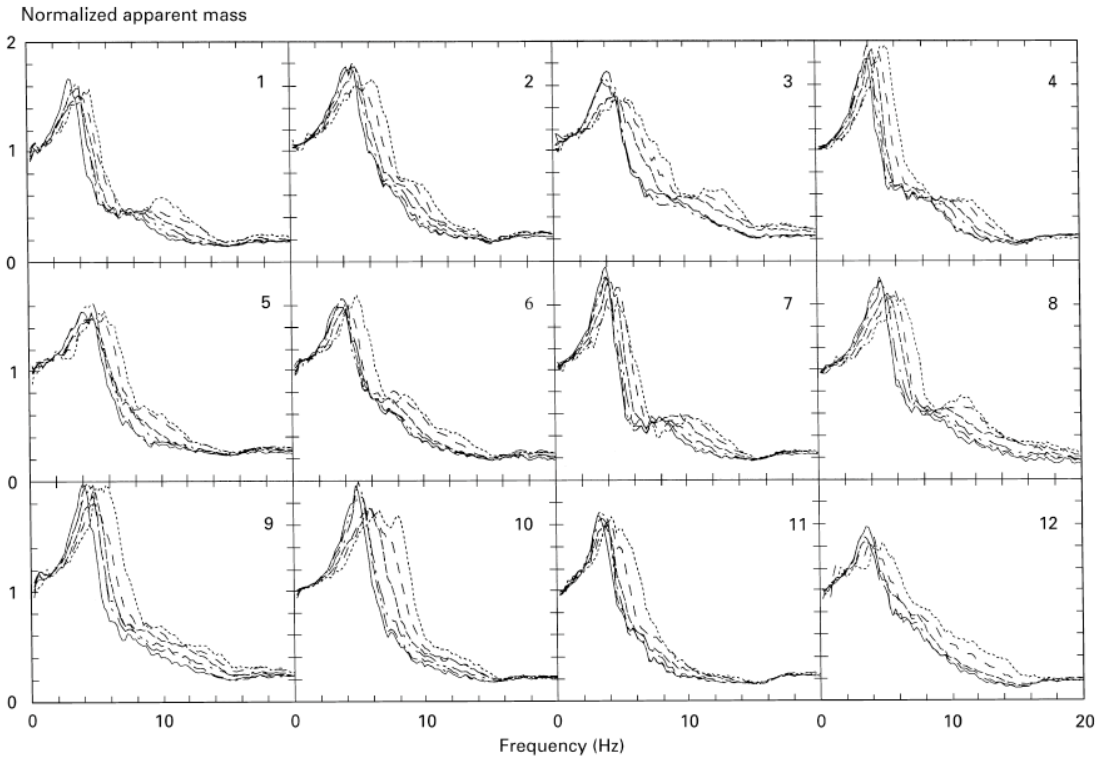

Figure 2.14 Normalised apparent masses of 12 upright seated subjects exposed to broadband (0.2 to 20 Hz) random vertical vibration at 0.25 (·····), 0.5 (— — —), 1.0 (— — —), 1.5 (— · — · —), 2.0 (- - ·· - - ·· - -), and 2.5 (———) ms^{-2} r.m.s. The resonance frequency decreased with increasing vibration magnitude (Mansfield and Griffin, 2000).

Seated subjects

With broadband random vibration, a number of steady-state sitting conditions have been used to investigate the effect of vibration magnitude (e.g., Fairley and Griffin, 1989; Mansfield and Griffin, 2000; Matsumoto and Griffin, 2002a; Matsumoto and Griffin, 2002b; Mansfield and Griffin, 2002; Nawayseh and Griffin, 2003). Table 2.1

shows the postures and seating conditions of the six most relevant biodynamic studies concerning the effect of vibration magnitude. The resonance frequencies of apparent masses measured at different vibration magnitudes in the six studies are compared in Table 2.2. The nonlinearity has been found in all steady-state sitting postures and conditions investigated. Nevertheless, the body tended to be less nonlinear while constant muscle tension of the buttocks and the abdomen was increased (Matsumoto and Griffin, 2002b). There was insignificant reduction in the nonlinearity when increasing the contact pressure on the buttocks by raising the footrest (Nawayseh and Griffin, 2003; Nawayseh and Griffin, 2004). The apparent masses measured at the footrest (Nawayseh and Griffin, 2003; Kitazaki, 1997) and at the upright backrest (Nawayseh and Griffin, 2004) during vertical vibration were also found to be nonlinear.

Some studies show that the nonlinear change in resonance frequency due to vibration magnitude is greater at lower magnitudes of vibration (e.g. Mansfield and Griffin, 2000; Matsumoto and Griffin, 2002a; see Figure 2.15 and Figure 2.16). This tends to support the idea that the human body is either more 'nonlinear' at lower magnitudes of vibration or that the 'nonlinear' mechanism(s) is more effective in stiffening the body at lower vibration magnitudes where there are lower inertial forces. However, some other studies report insignificant differences between the absolute change in the resonance frequency between two lower magnitudes and between two higher magnitudes of vibration (e.g. Matsumoto and Griffin, 2002b; Nawayseh and Griffin 2003; Nawayseh and Griffin 2004). This inconsistency might be due to some inter-subject variability. Mansfield and Griffin (2002) found most inter-subject variability at the lowest (0.2 ms^{-2} r.m.s.) of three vibration magnitudes (0.2, 1.0 and 2.0 ms^{-2} r.m.s.) for all nine postures investigated.

The apparent mass (or normalised apparent mass) at resonance has been reported to not depend on the vibration magnitude (Fairley and Griffin, 1989; Mansfield and Griffin, 2002; Matsumoto and Griffin, 2002a; Toward, 2002). However, Mansfield and Griffin (2000) reported that the individual apparent mass, as well as the median apparent mass of 12 subjects at resonance 'tended' to increase with increasing vibration magnitude when subjects adopted a normal upright sitting posture. In contrast, Nawayseh and Griffin (2003) found the median apparent mass at resonance of 12 subjects decreased with increased vibration magnitude with four different footrest heights. The apparent mass at resonance indicates the damping characteristic of the body. The inconsistent findings may be caused by inter-subject variability.

Table 2.1 Experimental conditions used in the six most relevant biodynamic studies of vibration magnitude and sitting posture.

Authors	Subjects	Stimuli	Conditions and measures
TEF-MJG 1989	60 subjects from public, 12 children, 24 women, 24 men	Random vertical 0.25 – 20 Hz	No backrest. Footrest moved with platform. Rigid seat. Comfortable upright sitting posture with normal muscle tension. Mean resonance frequency of apparent mass was used.
NJM-MJG 2000	12 subjects	Random vertical 0.2 – 20 Hz	No backrest. Footrest moved with platform. Rigid seat. Comfortable upright sitting posture. Resonance frequency of median normalised apparent mass was used.
YM-MJG 2002a	8 male subjects	Random vertical 0.5 – 20 Hz	No backrest. No footrest. Rigid seat. Comfortable upright sitting posture. Resonance frequency of median normalised apparent mass was used.
YM-MJG 2002b	8 male subjects	Random vertical 2.0 – 20 Hz	No backrest. Stationary footrest. Rigid seat. Comfortable upright sitting posture with: 1. Normal muscle tension. 2. Buttocks muscle tensed. 3. Abdominal muscle tensed. Resonance frequency of median normalised apparent mass was used.
NJM-MJG 2002	12 male subjects	Random vertical 1.0 – 20 Hz	No backrest. Footrest moved with platform. Rigid seat. Nine sitting postures and muscle tension conditions: 1. Comfortable upright. 2. Anterior lean bending at pelvis. 3. Posterior lean bending at pelvis. 4. Kyphotic slouched upper spine. 5. Back-on. 6. Pelvis support. 7. Inverted SIT-BAR increased pressure under ischial tuberosities. 8. Bead cushion. 9. Belt on. Median resonance frequency of normalised apparent mass was used (NOT resonance frequency of median normalised apparent mass).
NN-MJG 2003	12 male subjects	Random vertical 0.25 – 25 Hz	No backrest. Footrest moved with platform. Rigid seat. Four foot heights: 1. Foot hanging 2. Maximum thigh contact 3. Average thigh contact 4. Minimum thigh contact Median resonance frequency of apparent mass was used (NOT resonance frequency of median apparent mass).

TEF-MJG1989 = Fairley, T.E. and Griffin, M.J. (1989); NJM-MJG2000 = Mansfield, N.J. and Griffin, M.J. (2000); YM-MJG2002a = Matsumoto, Y. and Griffin, M.J. (2002a); YM-MJG2002b = Matsumoto, Y. and Griffin, M.J. (2002b); NJM-MJG2002 = Mansfield, N.J. and Griffin, M.J. (2002); NN-MJG2003 = Nawayseh, N. and Griffin, M.J. (2003).

Table 2.2 Apparent mass resonance frequencies (in Hz) of the six most relevant biodynamic studies of vibration magnitude and sitting posture.

Authors	Conditions	Vibration magnitude (ms^{-2}r.m.s.)												
		0.125	0.200	0.250	0.350	0.500	0.625	0.700	1.000	1.250	1.400	1.500	2.000	2.500
TEF-MJG 1989	Upright normal	-	-	6.00	-	n.a.	-	-	n.a.	-	-	-	4.00	-
NJM-MJG 2000	Upright normal	-	-	5.40	-	5.00	-	-	4.70	-	-	4.60	4.40	4.20
YM-MJG 2002a	Upright normal	6.40	-	6.16*	-	5.61*	-	-	5.36*	-	-	-	4.75	-
YM-MJG 2002b	Upright normal	-	-	-	5.25	5.17*	-	5.03*	4.82*	-	4.25	-	-	-
	Buttocks	-	-	-	5.00	4.89*	-	4.67*	4.48*	-	4.38	-	-	-
	Abdomen	-	-	-	5.13	5.03*	-	4.69*	4.36*	-	4.50	-	-	-
NJM-MJG 2002	Upright normal	-	5.27	-	-	-	-	-	5.08	-	-	-	4.69	-
	Anterior	-	6.06	-	-	-	-	-	5.18	-	-	-	4.79	-
	Posterior	-	5.47	-	-	-	-	-	4.59	-	-	-	4.39	-
	Kyphotic	-	6.25	-	-	-	-	-	5.08	-	-	-	4.49	-
	Back-on	-	5.47	-	-	-	-	-	5.08	-	-	-	4.69	-
	Pelvis support	-	5.86	-	-	-	-	-	5.08	-	-	-	4.69	-
	SIT-BAR	-	5.76	-	-	-	-	-	4.79	-	-	-	4.59	-
	Cushion	-	5.37	-	-	-	-	-	4.49	-	-	-	4.10	-
	Belt	-	6.45	-	-	-	-	-	5.08	-	-	-	4.88	-
NN-MJG 2003	Feet hanging	5.85	-	5.85	-	-	5.07	-	-	4.68	-	-	-	-
	Max. thigh contact	6.24	-	5.85	-	-	5.07	-	-	4.68	-	-	-	-
	Average thigh contact	5.85	-	5.85	-	-	5.46	-	-	4.68	-	-	-	-
	Min. thigh contact	5.85	-	5.85	-	-	5.07	-	-	5.07	-	-	-	-

- n.a.: tested but not available.
- *: resonance frequencies were estimated from graphic results.
- 'Authors' and 'Conditions': refer to Table 2.1.

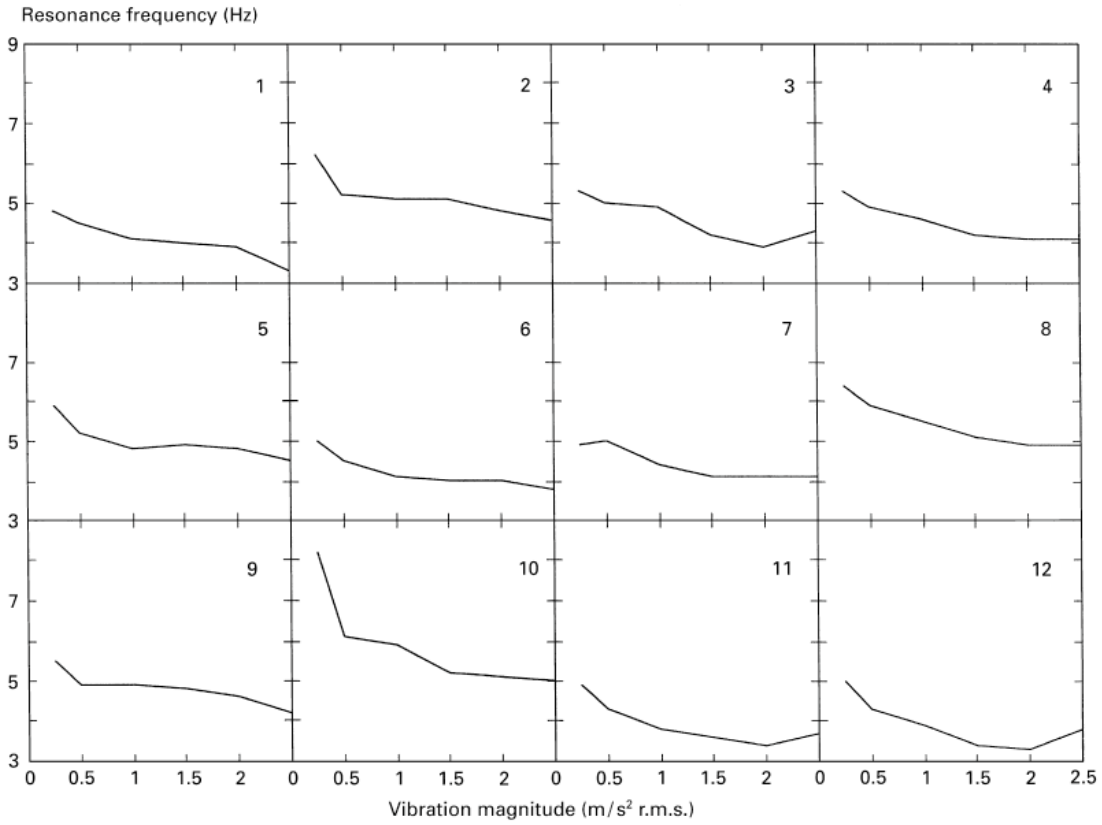

Figure 2.15 The effect of vibration magnitude on the apparent mass resonance frequencies of 12 upright seated subjects exposed to broadband 0.2–20 Hz random vertical vibration at 0.25, 0.5, 1.0, 1.5, 2.0, 2.5 ms^{-2} r.m.s.: the resonance frequency decrease with increasing vibration magnitude (Mansfield and Griffin, 2000).

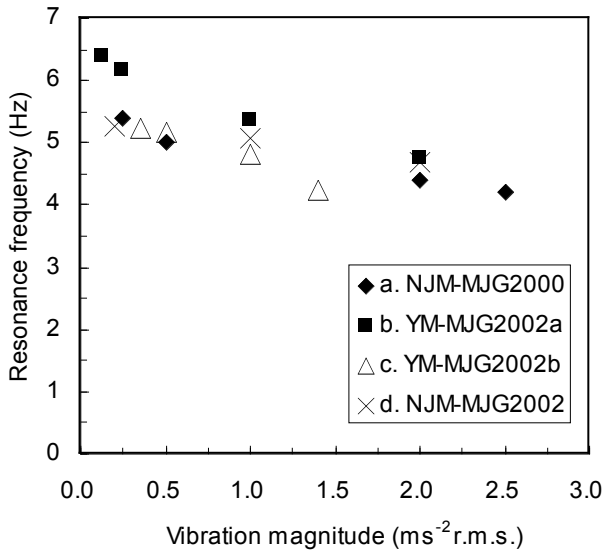

Figure 2.16 The effect of vibration magnitude on the median apparent mass resonance frequency of seated subjects exposed to broadband random vertical vibration: some studies showed greater change in resonance frequencies at lower magnitudes of vibration (♦, ■), while others (△, x) not consistent so (refer to Table 2.1 for notations of authors and experimental conditions).

With upright seated subjects but no backrest, the cross-axis apparent mass in the fore-and-aft direction was up to 60% of the static sitting weight of a subject (Nawayseh and Griffin, 2003). The cross-axis resonance frequency was correlated to the apparent mass resonance frequency at around 5 Hz. The authors attributed the two-dimensional response to some bending and pitching modes of the upper thoracic and cervical spine and the head around the resonance frequency in the vertical direction. The fore-and-aft cross-axis apparent mass was found to be nonlinear (Matsumoto and Griffin, 2002b; Nawayseh and Griffin, 2003, Figure 2.16).

Using an upright backrest, Nawayseh and Griffin (2004) reported the nonlinearity in the fore-and-aft cross-axis apparent mass on the seat (Figure 2.17) and at the backrest (Figure 2.18). The nonlinearity in the cross-axis direction was less with average buttocks pressure ('average thigh contact', Nawayseh and Griffin, 2003). However, in the vertical direction (the direction of excitation), the nonlinearity tended to decrease, though insignificantly, with increased buttocks pressure ('minimum thigh contact', Nawayseh and Griffin, 2003). So the authors speculated that the mechanism causing the nonlinearity in the fore-and-aft cross-axis direction was different from that in the vertical direction.

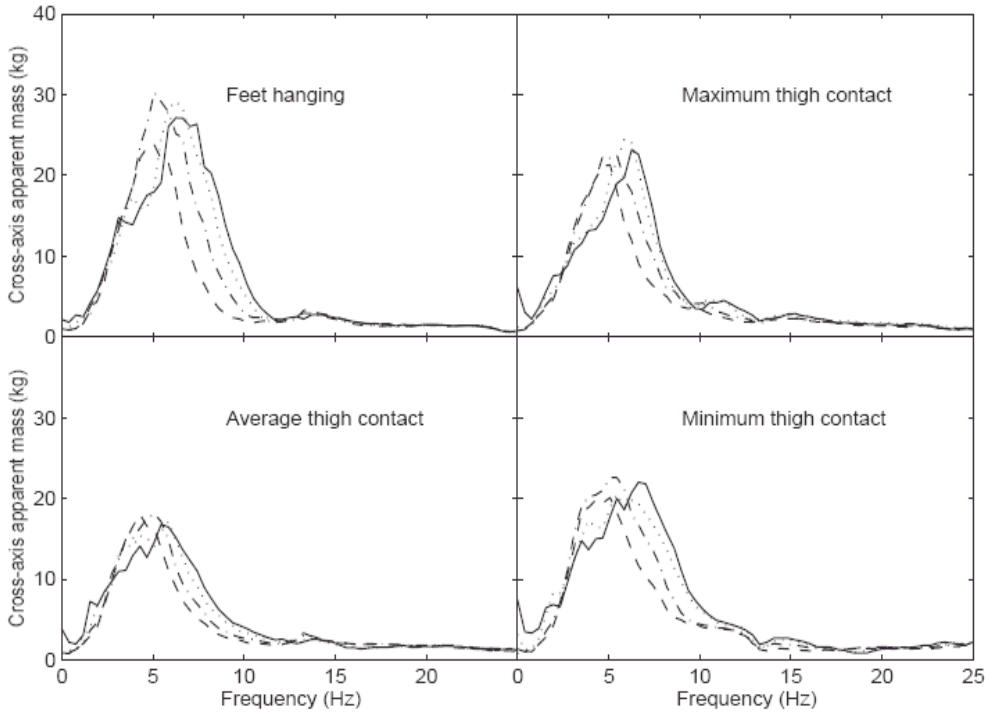

Figure 2.16 Median fore-and-aft cross-axis apparent masses of 12 upright seated subjects exposed to broadband (0.25 to 25 Hz) random vertical whole-body vibration at 0.125 (———), 0.25 (. . . . . .), 0.625 (— · — · —), and 1.25 (- - - - -) ms^{-2} r.m.s. with the four postures (Nawayseh and Griffin, 2003).

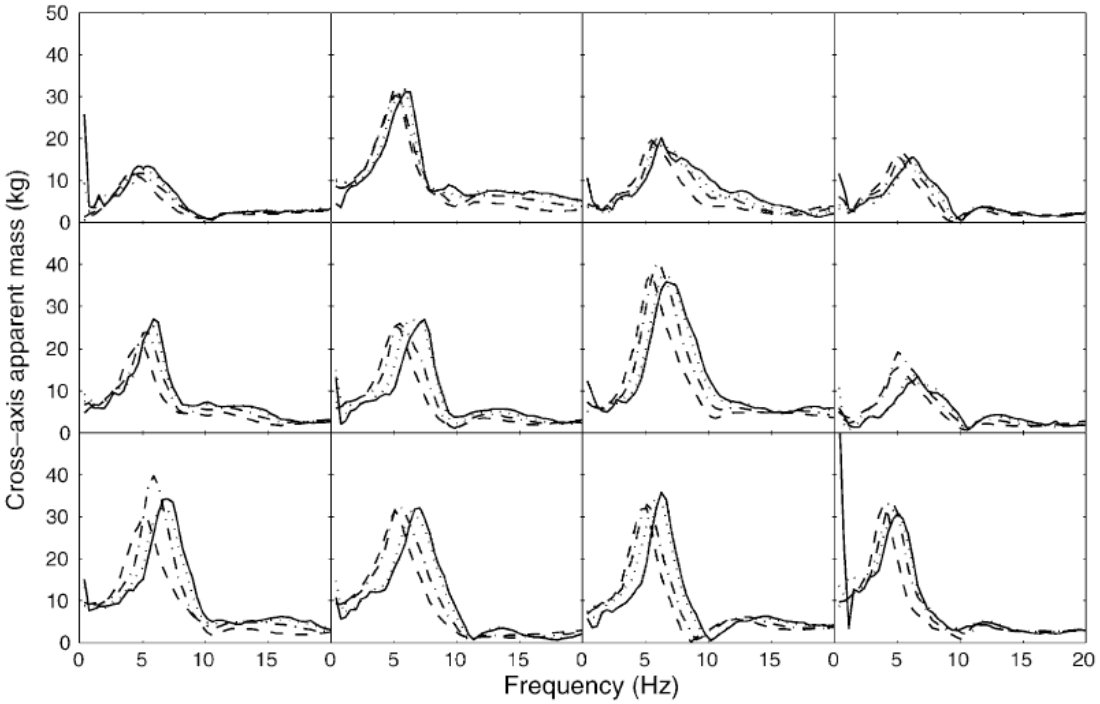

Figure 2.17 Fore-and-aft cross-axis apparent masses measured on the seat of 12 upright seated subjects exposed to broadband (0.25 to 25 Hz) random vertical whole-body vibration at 0.125 (———), 0.25 (. . . . . .), 0.625 (— · — · —), and 1.25 (- - - - - -) ms^{-2} r.m.s. with the minimum thigh contact posture and with a rigid upright backrest (Nawayseh and Griffin, 2004).

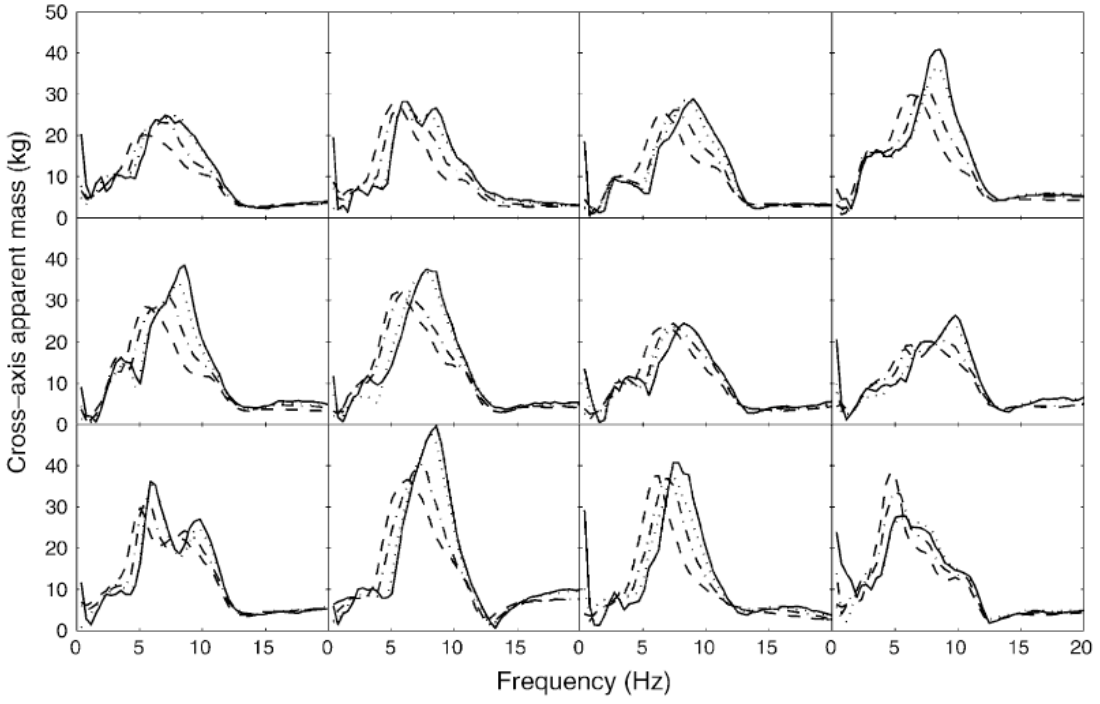

Figure 2.18 Fore-and-aft cross-axis apparent masses measured at the back of 12 upright seated subjects exposed to broadband (0.25 to 25 Hz) random vertical whole-body vibration at 0.125 (———), 0.25 (. . . . . .), 0.625 (— · — · —), and 1.25 (- - - - - -) ms^{-2} r.m.s. with the minimum thigh contact posture and with a rigid upright backrest (Nawayseh and Griffin, 2004).

With sinusoidal vibration at discrete frequencies, the apparent mass can be calculated by the ratio of the r.m.s. output (driving) force to the r.m.s. input acceleration. The nonlinearity has been reported with the seated human body exposed to vertical sinusoidal whole-body vibration (e.g. Hinz and Seidel, 1987; Mansfield, 1995; Matsumoto and Griffin, 2002b, Figure 2.19). To quantify the changes in the shape of the sinusoidal waveforms, harmonic distortions of the acceleration at different locations on the body and the driving force at the seat were calculated at each frequency (Griffin, 1990; Mansfield, 1995).

The harmonic distortions during sinusoidal excitation may be related to the nonlinearity due to vibration magnitude observed with random excitation. With 'erect' seated subjects exposed to vertical sinusoidal vibration, Wittman and Phillips (1969) found that the magnitude of the force time history in the positive loading phase (lowermost displacement) was higher than that in the negative unloading phase (uppermost displacement). The duration of the negative unloading (up) phase was longer than the positive loading phase. Hinz and Seidel (1987) found that the averaged time histories of accelerations at T5 and at the head of the seated subjects deviated from the sinusoidal input waveform at seat. During sinusoidal vertical whole-body vibration, the greatest harmonic distortion at the pelvis of the seated human body was observed at the resonance frequency around 5 Hz (see Figure 2.20, Mansfield, 1995). The distortion at the pelvis and the distortion of the driving force on the seat increased with increasing vibration magnitude (from 0.5 to 1.5 ms^{-2} r.m.s.) over the frequency range 4.0 to 12.5 Hz.

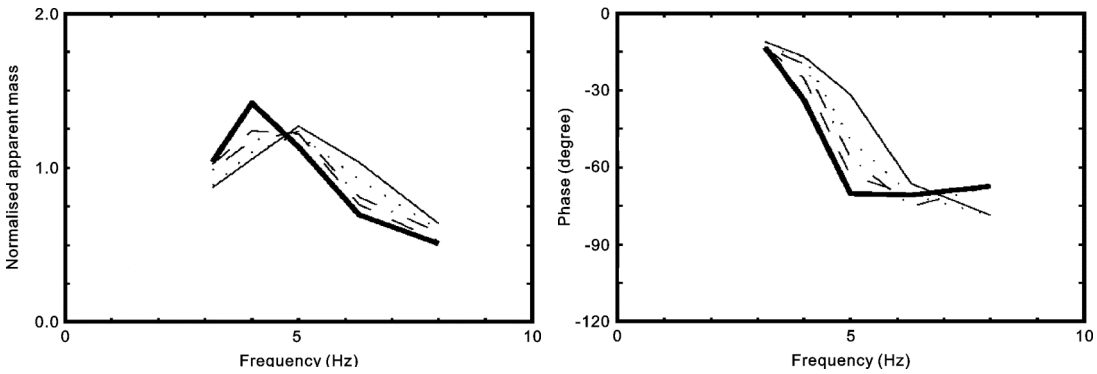

Figure 2.19 Median normalised apparent mass and phases of eight 'normal' upright seated subjects exposed to vertical sinusoidal vibration at five frequencies (3.15, 4.0, 5.0, 6.3 and 8.0 Hz) at 0.35 (———), 0.5 (. . . . .), 0.7 (— · — · —), 1.0 (— — —), and 1.4 (———) ms^{-2} r.m.s. (Matsumoto and Griffin, 2002b).

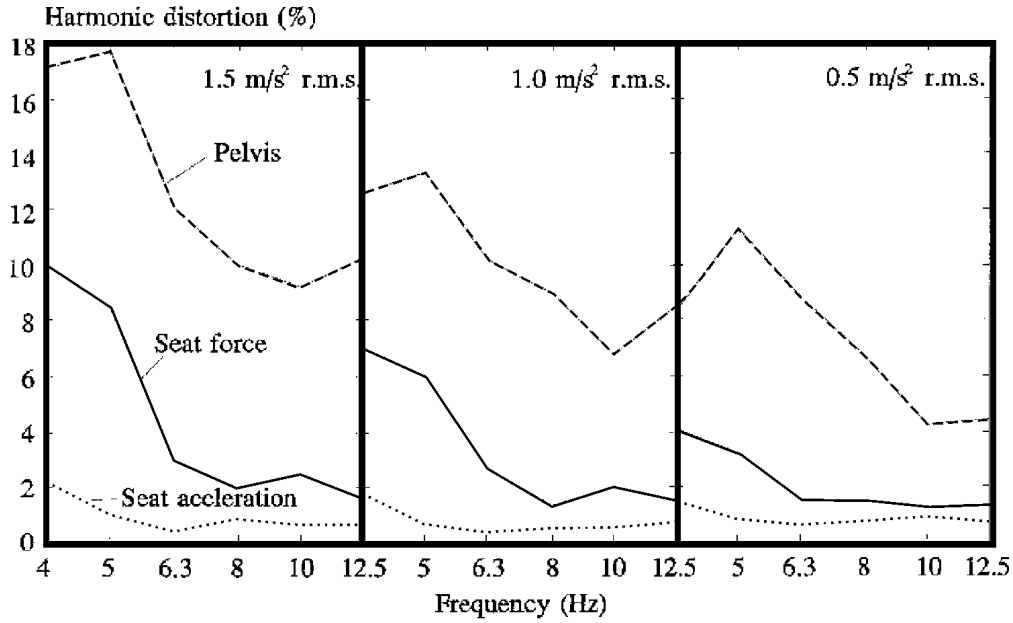

Figure 2.20 Median harmonic distortion of ten 'comfortable' upright seated subjects exposed to vertical sinusoidal vibration at six frequencies (4.0, 5.0, 6.3, 8.0, 10.0, and 12.5 Hz) and three vibration magnitudes (0.5, 1.0, and 1.5 ms^{-2} r.m.s.): ·····, seat acceleration; ——, seat force; - - -, pelvis acceleration (Mansfield, 1995).

Standing subjects

With a 'normal' upright standing posture Matsumoto and Griffin (1998a) reported that the median apparent mass resonance frequency decreased from 6.75 to 5.25 Hz while the vibration magnitude was increased from 0.125 to 2.0 ms^{-2} r.m.s. (Figure 2.21). With a 'legs bent' posture, the resonance frequency decreased from 3.0 to 2.5 Hz with increasing vibration magnitude from 0.125 to 2.0 ms^{-2} r.m.s. – but significant difference in the resonance frequency was only found between 0.25 and 0.5 ms^{-2} r.m.s. The nonlinearity was not found with a 'one leg' posture. Subashi *et al*. (2006) found the resonance frequency decreased from 6.39 to 5.63 Hz with increasing vibration magnitude from 0.125 to 0.5 ms^{-2} r.m.s. by using an upright standing posture similar to that used by Matsumoto and Griffin (1998a). Subashi *et al*. (2006) found the nonlinear change in resonance frequency to be significant between the three vibration magnitudes (0.125, 0.25 and 0.5 ms^{-2} r.m.s.) with the upright posture, but insignificant between 0.25 and 0.5 ms^{-2} r.m.s. when a lordotic, a knee bent, or a knee more bent posture was adopted by subjects. The authors speculated that the change in the nonlinearity with different standing postures was caused by modified voluntary and involuntary muscle activity – a reduction in the nonlinearity was reported associated with increased muscle tension when seated (Matsumoto and Griffin, 2002b).

The median fore-and-aft cross-axis apparent mass resonance frequency of the standing subjects tended to decrease with increasing vibration magnitude from 0.125 to 0.5 ms^{-2} r.m.s. (Figure 2.22, Subashi *et al*., 2006). However, this nonlinear response was not significantly different between any of the five standing postures (see Figure 2.9). The authors reckoned that the mechanism causing the nonlinearity in the direction of excitation might be different from that in the fore-and-aft cross-axis direction.

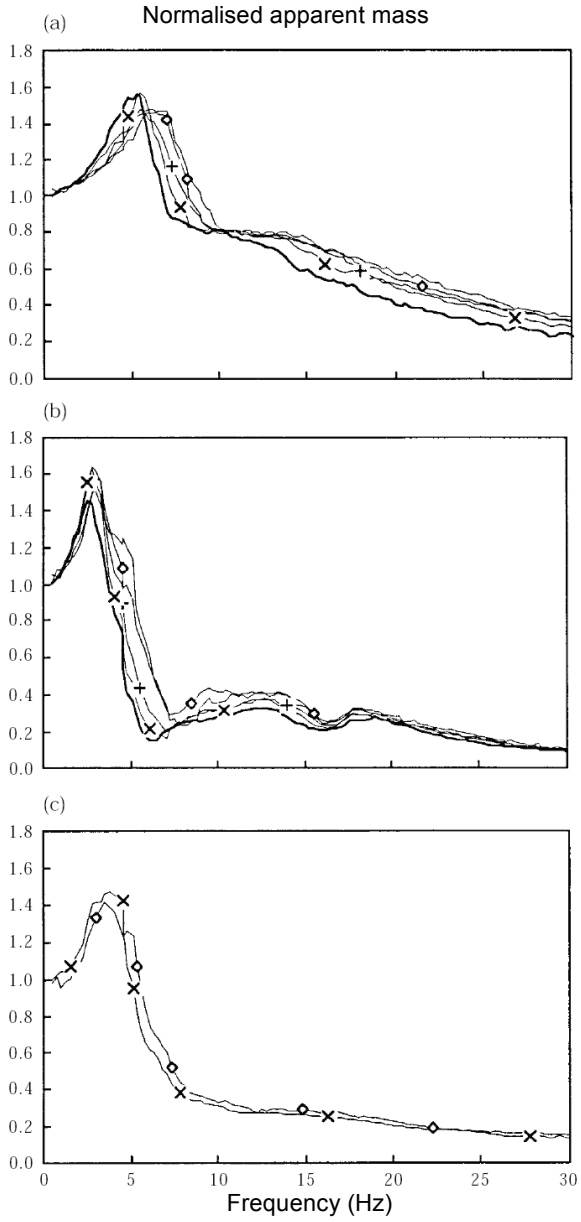

Figure 2.21 Median normalised apparent mass of 12 standing subjects exposed to vertical broadband (0.25 to 30 Hz) random vibration at 0.125 (———), 0.25 (—◊—), 0.5 (—+—), 1.0 (—x—x—), and 2.0 (———) ms^{-2} r.m.s. with (a) normal upright posture, (b) legs bent posture, and (c) one leg posture (Matsumoto and Griffin, 1998a).

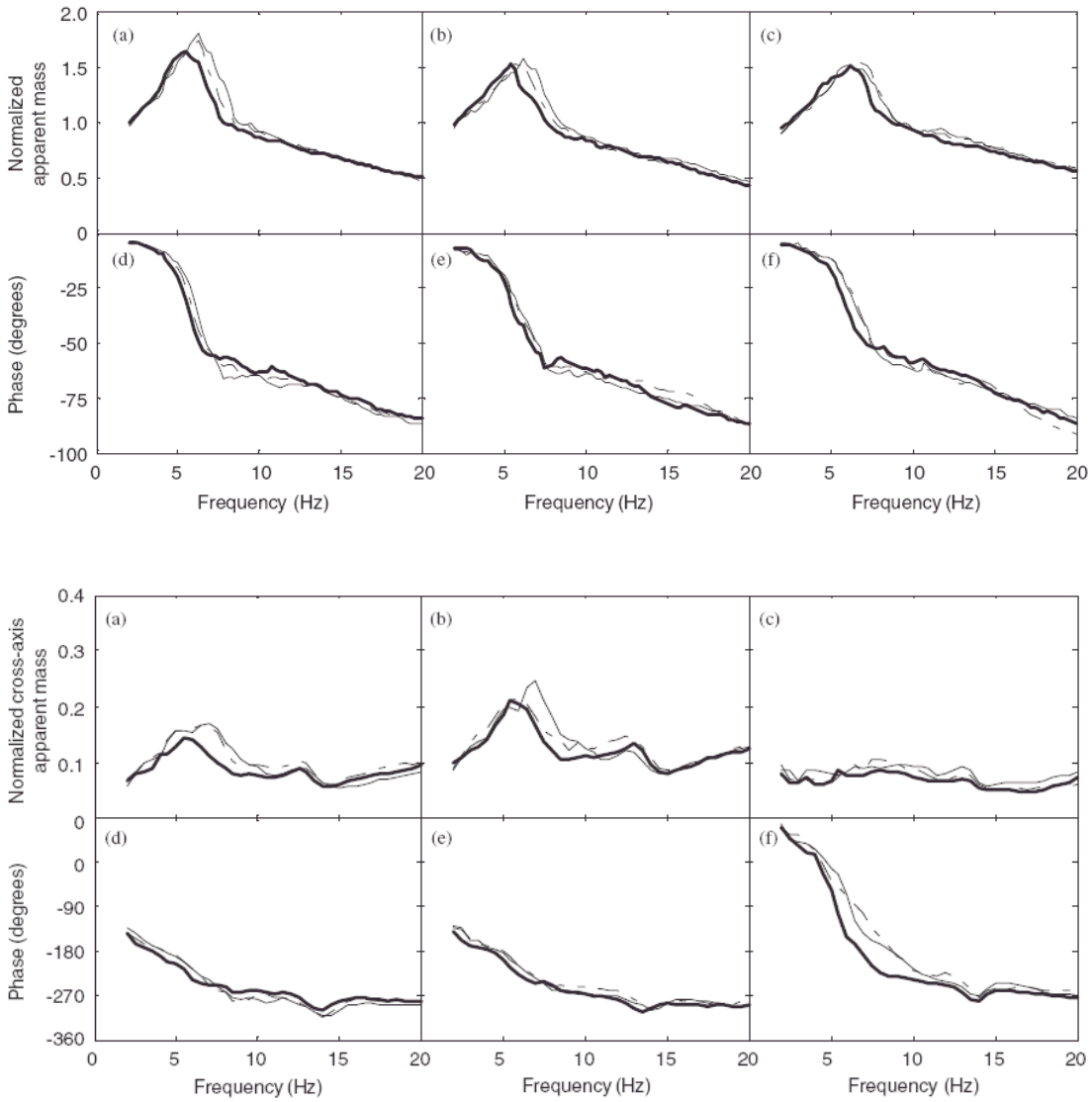

Figure 2.22 Median normalised apparent masses and phases (upper), and median normalised fore-and-aft cross-axis apparent masses and phases (lower) of 12 standing subjects exposed to broadband (2 to 20 Hz) random vertical whole-body vibration at 0.125 (———), 0.25 (— · — · —), and 0.5 (▬▬▬) ms^{-2} r.m.s. with three upper-body postures: upright (a, d), lordotic (b, e), and anterior lean (c, f) (Subashi *et al*., 2006).

Supine subjects

No study has measured the mechanical impedance or apparent mass of the supine human body with different magnitudes of vibration. A few studies have measured the mechanical impedance of the supine subjects exposed to single magnitude of sinusoidal vibration but under different magnitudes of lateral sustained acceleration produced by a centrifuge (Vogt *et al*., 1973; Vykukal, 1968). These studies found that the resonance frequency and the impedance at resonance both increased with increasing magnitude of the sustained acceleration. The increased stiffness of the body might be due to subjects increasing muscle tension to maintain their position and to avoid body parts to collapse while the acceleration level was increased. With

single magnitude of sinusoidal vibration but without sustained acceleration, Vogt *et al*. (1978) found that adding a rigid mass of 4.54 kg above the chest, abdomen and thighs increased the mechanical impedance measured at these locations and slightly increased the frequency of the peaks. The increase in the peak frequency was more apparent at the abdomen and the thighs with more soft tissues in the transmission path than the chest.

2.3.1.4 Effect of vibration spectrum

In the previous sections, broadband random vibration with equal energy at all frequencies was used to investigate the effect of posture, seating condition, and vibration magnitude. By superimposing single frequency sinusoids on broadband random vibration, Fairley (1986) found that the apparent mass around resonance could be affected by increased input energy at frequencies other than resonance frequencies. It has been shown in previous sections that the characteristic nonlinearity is most apparent around resonance. Studies have been conducted to investigate a range of narrowband stimuli with different frequency content and different magnitudes so as to examine the effect of the frequency composition of input spectra on the nonlinearity.

Mansfield (1998) measured the apparent mass of 10 subjects with four different frequency components at three different vibration magnitudes. The stimuli consisted of a broadband random vibration at 0.25 ms^{-2} r.m.s. with equal energy between 0.5 and 20 Hz with added vibration in four frequency bands of 0.5 to 2.0 Hz, 2.0 to 6.0 Hz, 6.0 to 10.0 Hz, and 10.0 to 20.0 Hz. The four frequency components were added at three vibration magnitudes to give the overall vibration of 0.5, 0.75 and 1.0 ms^{-2} r.m.s. The results showed that adding narrowband components at frequencies below 10 Hz did not affect the nonlinearity due to vibration magnitude. The vibration magnitude tended to have smaller effect on the resonance frequency while narrowband components were added at above 10 Hz.

Toward (2002) exposed 12 subjects to broadband random (0.125 to 25 Hz) vibration at 0.25 ms^{-2} r.m.s. superposed with nine narrowband components at ½-octave intervals (from 1 to 16 Hz) at four magnitudes (0.25, 0.4, 0.63, and 1.0 ms^{-2} r.m.s.). The apparent mass at resonance tended to decrease with increasing input magnitude while the narrowband components were added at frequencies below 4 Hz (Figure 2.23). At frequencies above 4 Hz this trend was reversed but the apparent mass at resonance was less affected by the input magnitude. The nonlinearity presented with broadband stimuli was also found with all nine narrowband inputs; however, the vibration magnitude had the greatest effect on the

resonance frequency when the narrowband components were added near the resonance frequencies (Figure 2.24).

The results of both studies (i.e. Mansfield, 1998 and Toward, 2002) are consistent in that the nonlinearity due to input vibration magnitude is most apparent with added narrowband input components at frequencies near resonance. The resonance indicates the greatest dynamic forces and movement of the body. These results suggest that the nonlinearity occurs when there is adequate input energy at frequencies around resonance.

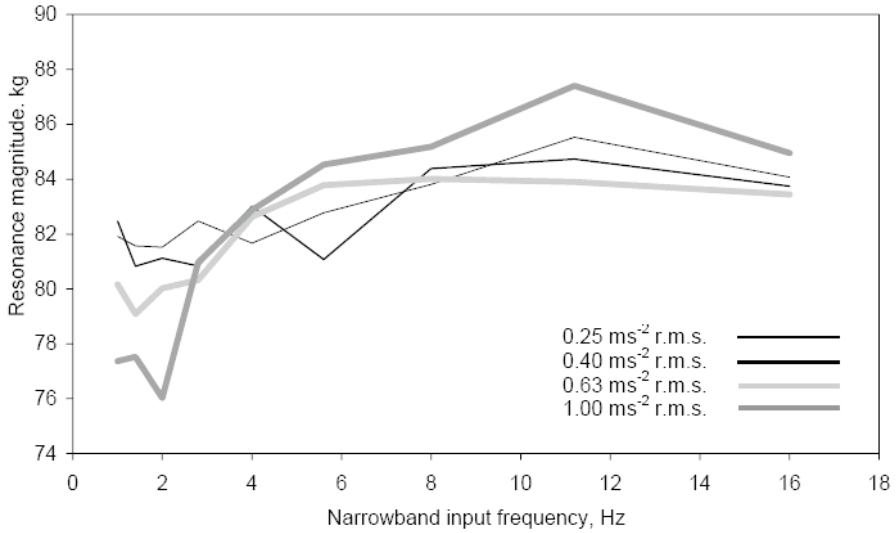

Figure 2.23 Median apparent mass at resonance measured with narrowband inputs at nine ½-octave input frequencies (centred at: 1.0, 1.4, 2.0, 2.8, 4.0, 5.6, 8.0, 11.2, 16.0 Hz) and four input magnitudes superimposed on 0.25 ms^{-2} r.m.s. broadband 0.125–25 Hz vibration (Toward, 2002).

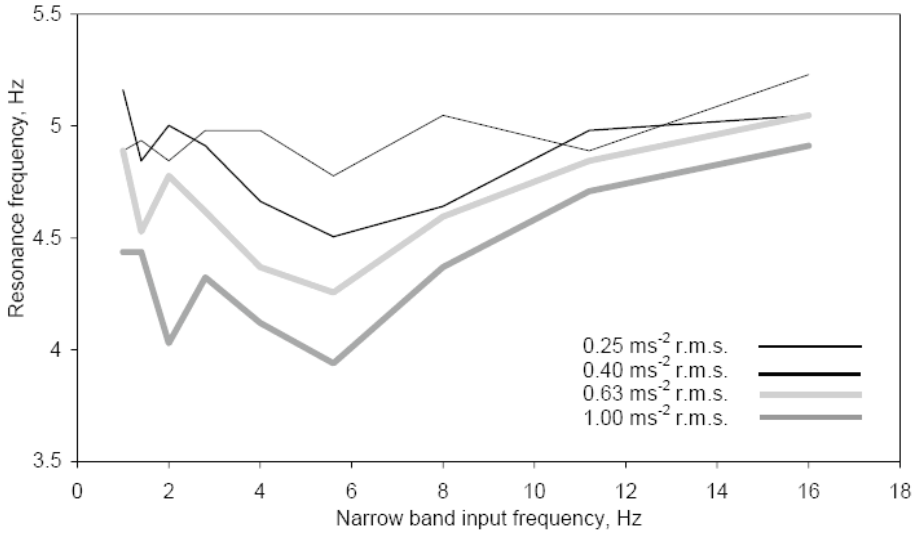

Figure 2.24 Median apparent mass resonance frequency measured with narrowband inputs at nine ½-octave input frequencies (centred at: 1.0, 1.4, 2.0, 2.8, 4.0, 5.6, 8.0, 11.2, 16.0 Hz) and four input magnitudes superimposed on 0.25 ms^{-2} r.m.s. broadband 0.125–25 Hz vibration (Toward, 2002).

2.3.2 Horizontal excitations

Substantial vibration has been found in the horizontal directions of off-road vehicles (e.g. Lundström and Lindberg, 1983). With seated subjects, studies have been conducted to measure the apparent masses when the body was excited in the fore-and-aft or lateral direction (e.g. Fairley and Griffin, 1990; Mansfield and Lundström, 1999a; Hinz *et al.*, 2006), and solely in the fore-and-aft direction (e.g. Nawayseh and Griffin, 2005a; Nawayseh and Griffin, 2005b; Abdul Jalil, 2005) at different magnitudes of vibration. The mechanical impedance was also measured while seated subjects were exposed to fore-and-aft or lateral excitation (e.g. Holmlund and Lundström, 1998; Holmlund and Lundström, 2001). The nonlinearity seen in the resonance frequency due to vibration magnitude reported with vertical excitation was consistently found with horizontal excitations.

2.3.2.1 Fore-and-aft excitation

With fore-and-aft random excitation, Fairley and Griffin (1990) found that the fore-and-aft apparent mass of the upright seated subject with no backrest had two resonances – one was around 0.7 Hz and another around 2.5 Hz. Nawayseh and Griffin (2005a) found three modes: the first was at around 1 Hz, the second between 1 and 3 Hz, and the third between 3 and 5 Hz. With excitation only at frequencies higher than 1 Hz, Mansfield and Lundström (1999a) found two modes – one from 2 to 3 Hz and another from 5 to 6 Hz – similar to the second and the third modes reported by Nawayseh and Griffin (2005a). Hinz *et al.* (2006) reported a major resonance between about 2 and 3 Hz and a minor peak around 1 Hz.

The difference in the apparent mass resonances of the above four studies might be due to different vibration magnitudes and sitting postures including feet and arm positions. The third mode above 3 Hz reported by Nawayseh and Griffin (2005a) was clearer at lower vibration magnitudes (the lowest being 0.125 ms^{-2} r.m.s.). The lowest vibration magnitude was 0.25 ms^{-2} r.m.s. in the studies conducted by Mansfield and Lundström (1999a) and by Hinz *et al.* (2006). However, the lowest magnitude was 0.5 ms^{-2} r.m.s. in the study conducted by Fairley and Griffin (1990). In terms of posture, Nawayseh and Griffin (2005a) used a height-adjustable footrest moving in phase with the seat to ensure the thigh contact areas of different subjects to be similar, while each of the other two studies (i.e. Mansfield and Lundström, 1999a and Hinz *et al.*, 2006) used identical seat and footrest height for all subjects. With high inter-subject variability in subject height, the fixed footrest height in the three studies – Fairley and Griffin, 1990; Mansfield and Lundström, 1999a; Hinz *et al.*, 2006 – meant subjects might sit in a combination of the 'minimum thigh contact',

'average thigh contact', and 'maximum thigh contact' postures used by Nawayseh and Griffin (2005a). These three sitting conditions were found to affect the apparent mass. Mansfield and Lundström (1999a) used a stationary footrest. A stationary footrest gave different apparent mass at low frequencies comparing with a moving footrest (see Section 2.3.1.2, Fairley and Griffin, 1989). Arm posture could be another factor causing difference numbers of resonances. Mansfield and Lundström (1999a) used an arm 'folded' posture. Hinz *et al*. (2006) instructed the subjects to put their hands on a forward handle about 10 cm above their knees, while most other studies used the hands-in-laps posture. Folding arms might have amplified the third mode, while stretching arms to the handle might have the effect of a vibration absorber increasing the damping and resulting in a less apparent third mode.

Both the fore-and-aft apparent mass (Figure 2.25) and the vertical cross-axis apparent mass (Figure 2.26) during fore-and-aft excitation were found to be nonlinear. To quantify the nonlinearity, Nawayseh and Griffin (2005a) compared the apparent masses at discrete frequencies in the range of the three resonance peaks (i.e., around 1 Hz, between 1 and 3 Hz, and between 3 and 5 Hz) at four vibration magnitudes from 0.125 to 1.25 ms^{-2} r.m.s. The authors found that the effect of vibration magnitude on apparent mass was more apparent at frequencies higher than 2.15 Hz in all four postures. Fairley and Griffin (1990) reported that the resonance frequency around 2.5 Hz decreased by about 1 to 2 Hz when the vibration magnitude increased from 0.5 to 2.0 ms^{-2} r.m.s., while the first mode at around 0.7 Hz was not affected by vibration magnitude. Mansfield and Lundström (1999a) showed that the dominant peak frequency around 2 to 3 Hz decreased as the vibration magnitude increased from 0.25 to 1.0 ms^{-2} r.m.s. Similarly in the study conducted by Hinz *et al.* (2006), the 'main peak frequency' of the normalised mean apparent mass decreased from 2.94 to 2.18 Hz with vibration magnitude increasing from 0.25 to 1.5 ms^{-2} r.m.s..

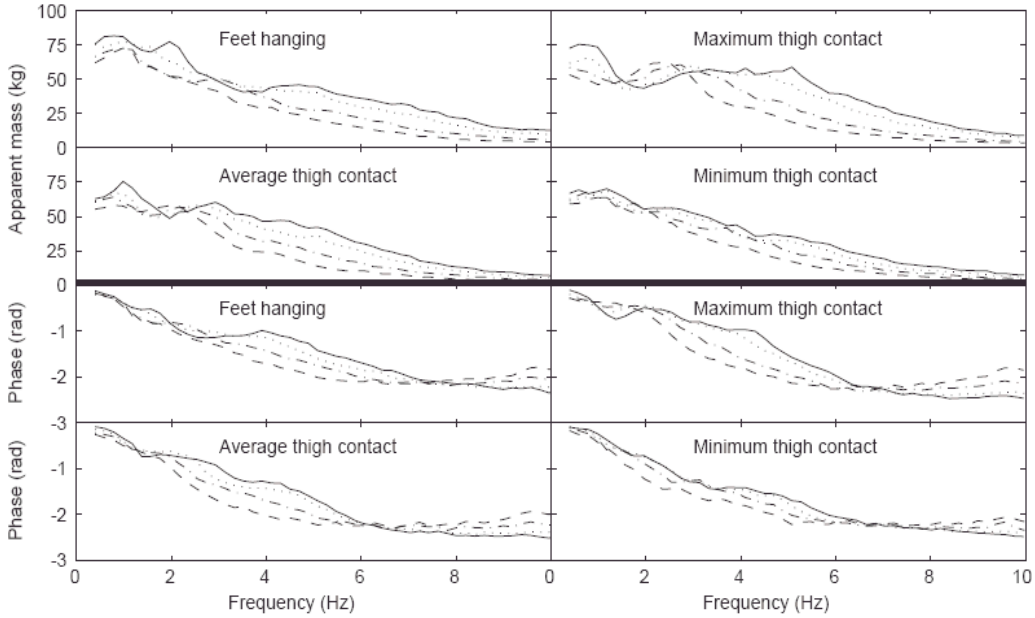

Figure 2.25 Median fore-and-aft apparent masses and phases of 12 upright seated subjects at the seat exposed to broadband (0.25 to 20 Hz) random fore-and-aft whole-body vibration at 0.125 (———), 0.25 (. . . . . .), 0.625 (— · — · —), and 1.25 (— — —) ms^{-2} r.m.s. with four postures (Nawayseh and Griffin, 2005a).

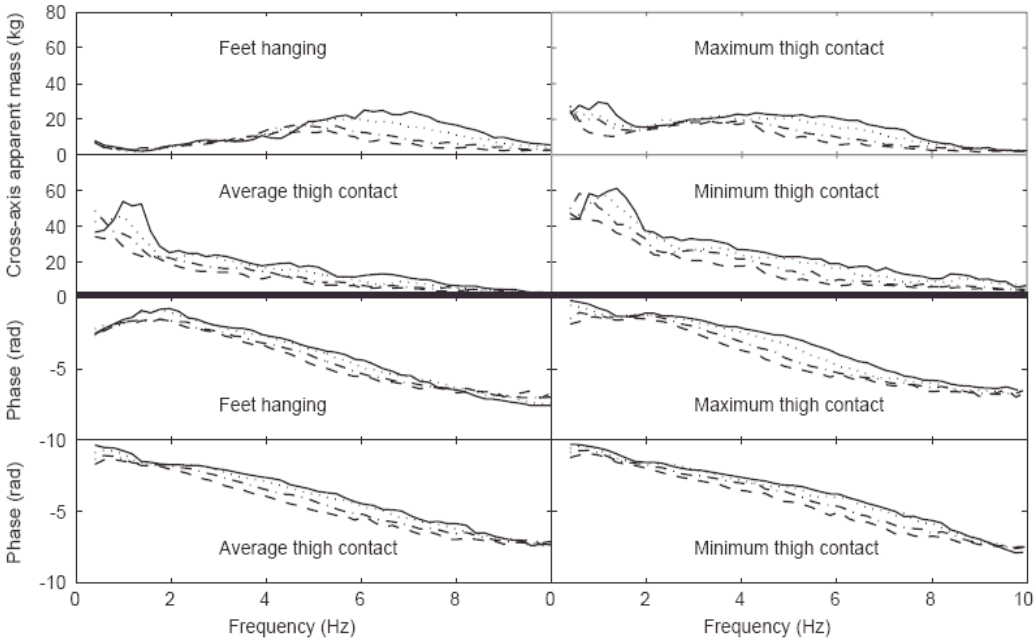

Figure 2.26 Median vertical cross-axis apparent masses and phases of 12 upright seated subjects at the seat exposed to broadband (0.25 to 20 Hz) random fore-and-aft whole-body vibration at 0.125 (———), 0.25 (. . . . . .), 0.625 (— · — · —), and 1.25 (— — —) ms^{-2} r.m.s. with four postures (Nawayseh and Griffin, 2005a).

With a backrest and fore-and-aft excitation, Nawayseh and Griffin (2005b) found the nonlinearity in the fore-and-aft apparent masses on the seat (Figure 2.27) and at the back (Figure 2.28), and the vertical cross-axis apparent masses on the seat (Figure 2.29) and at the back (Figure 2.30) of the upright seated subjects. The authors attributed the main resonance of the fore-and-aft apparent mass on the seat in the region of 4 Hz to a shearing mode of the buttocks tissue beneath the pelvis, which was associated with bending of the spine and pitching of the pelvis in the mid-sagittal plane. These rotational modes of the spine, the pelvis and the head could also have contributed to the vertical cross-axis resonance on the seat between 5 and 8 Hz.

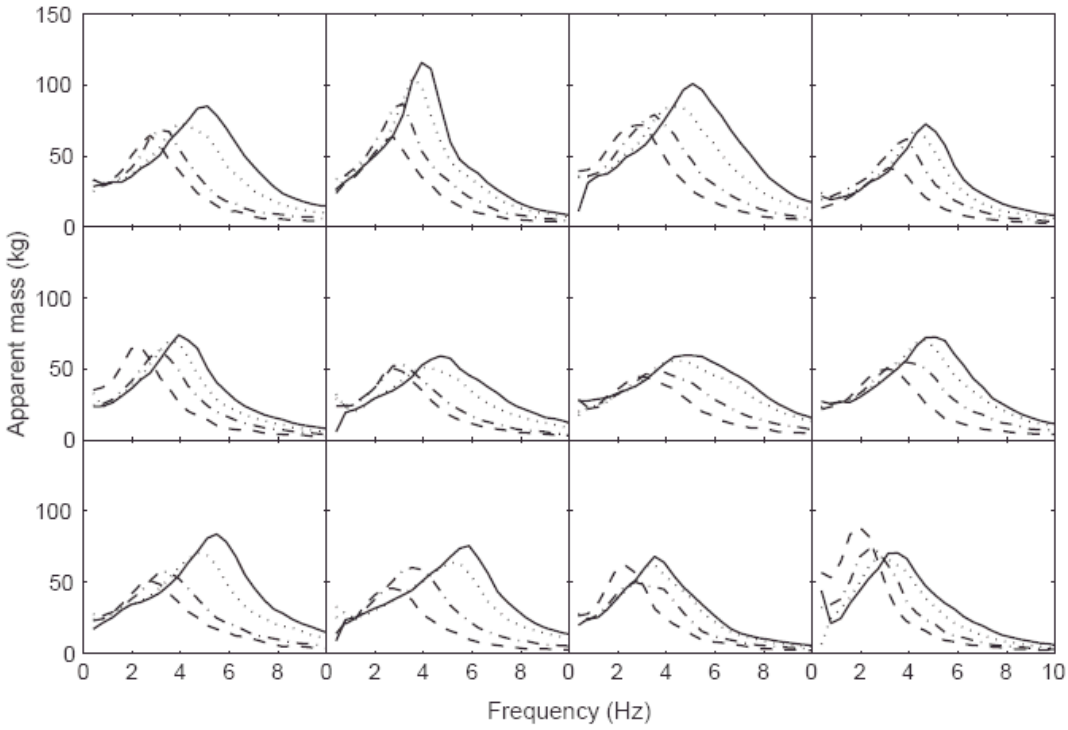

Figure 2.27 Fore-and-aft apparent masses measured on the seat of 12 upright seated subjects exposed to broadband (0.25 to 20 Hz) random fore-and-aft whole-body vibration at 0.125 (———), 0.25 (. . . . . .), 0.625 (— · — · —), and 1.25 (— — —) ms^{-2} r.m.s. with the average thigh contact posture and with a rigid upright backrest (Nawayseh and Griffin, 2005b).

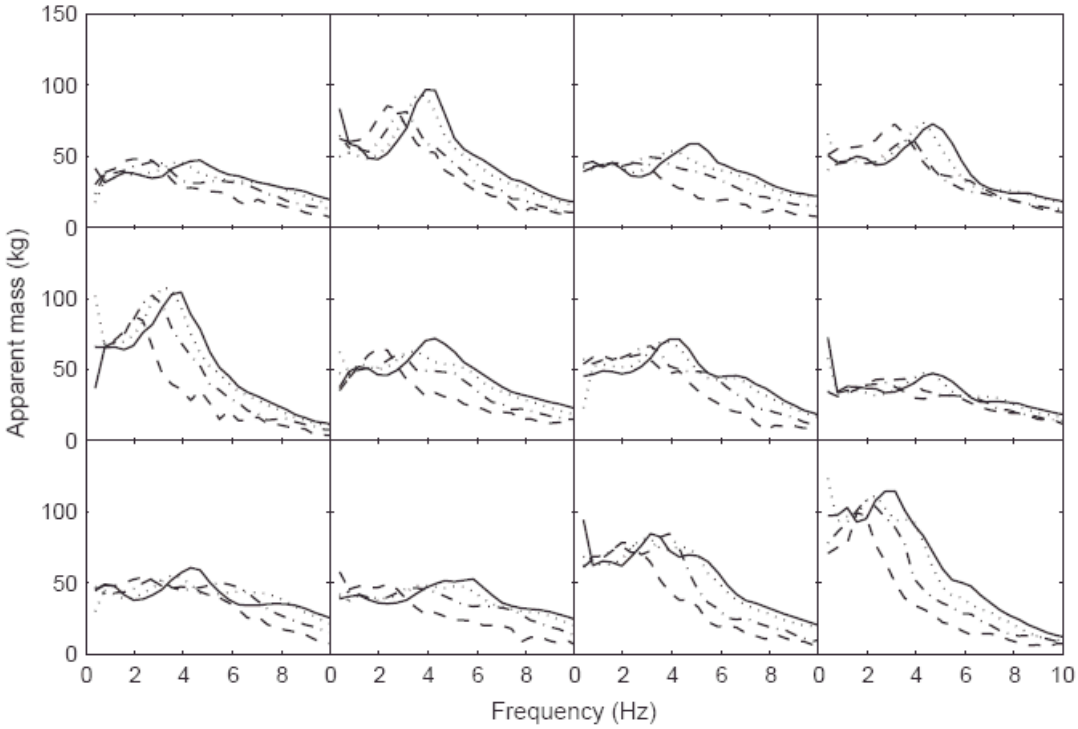

Figure 2.28 Fore-and-aft apparent masses measured at the back of 12 upright seated subjects exposed to broadband (0.25 to 20 Hz) random fore-and-aft whole-body vibration at 0.125 (———), 0.25 (. . . . . .), 0.625 (— · — · —), and 1.25 (— — —) ms^{-2} r.m.s. with the average thigh contact posture and with a rigid upright backrest (Nawayseh and Griffin, 2005b).

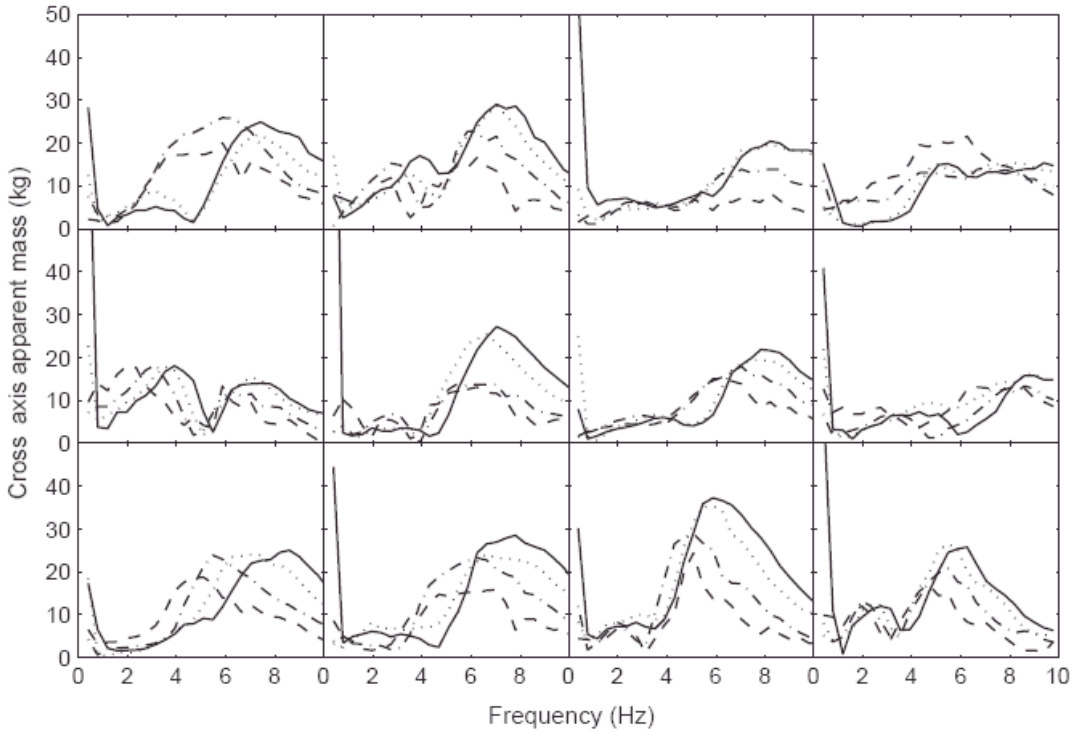

Figure 2.29 Vertical cross-axis apparent masses measured on the seat of 12 upright seated subjects exposed to broadband (0.25 to 20 Hz) random fore-and-aft whole-body vibration at 0.125 (———), 0.25 (. . . . . .), 0.625 (— · — · —), and 1.25 (— — —) ms^{-2} r.m.s. with the average thigh contact posture and with a rigid upright backrest (Nawayseh and Griffin, 2005b).

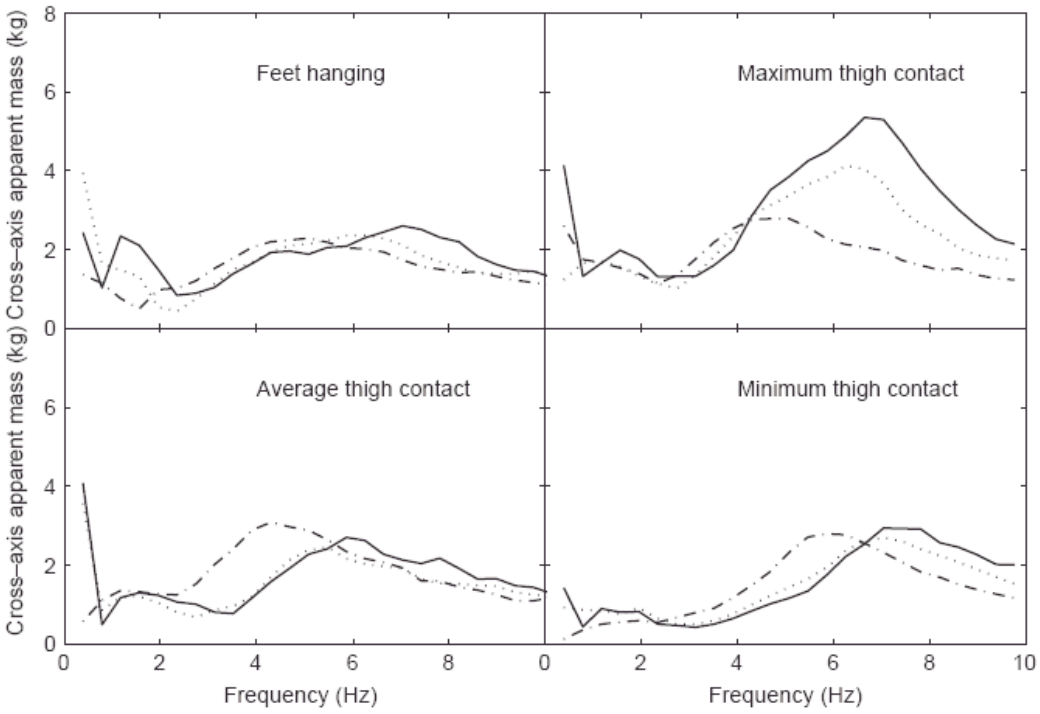

Figure 2.30 Vertical cross-axis apparent masses measured at the back of one upright seated subject exposed to broadband (0.25 to 20 Hz) random fore-and-aft whole-body vibration at 0.125 (———), 0.25 (. . . . . .), and 0.625 (— · — · —) ms^{-2} r.m.s. with four thigh contact postures and with a rigid upright backrest (Nawayseh and Griffin, 2005b).

Abdul Jalil (2005) measured the fore-and-aft apparent masses at five equally spaced locations on the back within the mid-sagittal plane (Figure 2.31, Location 1 and 5 were the lowest and the highest points on the back respectively). When measuring one location the other four locations on the back of the subject were not in contact with the backrest. The five locations were used to represent a different 'interface point' between the back and the rigid upright backrest. For example, the pivoting point of the back against the backrest when pitching would be different due to inter-subject variability such as the sitting height and body mass. The frequency of the first peak in apparent mass at around 2 Hz tended to increase as the location changed from the lower back to the upper back. However, the frequency of the second peak (around 4 to 8 Hz) decreased as the location changed from the lower to the upper back. By examining the difference in apparent mass modulus between different vibration magnitudes at discrete frequencies, the nonlinearity has been found in all five locations: at the lowest location (Location 1) on the back the nonlinearity occurred at frequencies above 5 Hz, at the middle back (Location 3) above 2.5 Hz, at the highest location (Location 5) above 1.25 Hz. The apparent masses at the five locations also showed that the effect of vibration magnitude was more apparent at the lowest location on the back, implying a more nonlinear response at this location (Figure 2.31). The median apparent masses of the entire

back have shown very similar envelop to those reported by Nawayseh and Griffin (2005b) with the average thigh contact posture. Abdul Jalil (2005) adjusted the footrest height for each subjects so that the lower legs and the thighs were normal and parallel to the horizontal flat rigid seat surface – similar to the average thigh contact posture used by Nawayseh and Griffin (2005b). At frequencies lower than 7 Hz, Abdul Jalil (2005) noticed that the apparent mass of the entire back had similar trends to that of the middle back (Location 3); at frequencies higher than 7 Hz, the apparent mass of the entire back was closest to that of the lower back (Location 2).

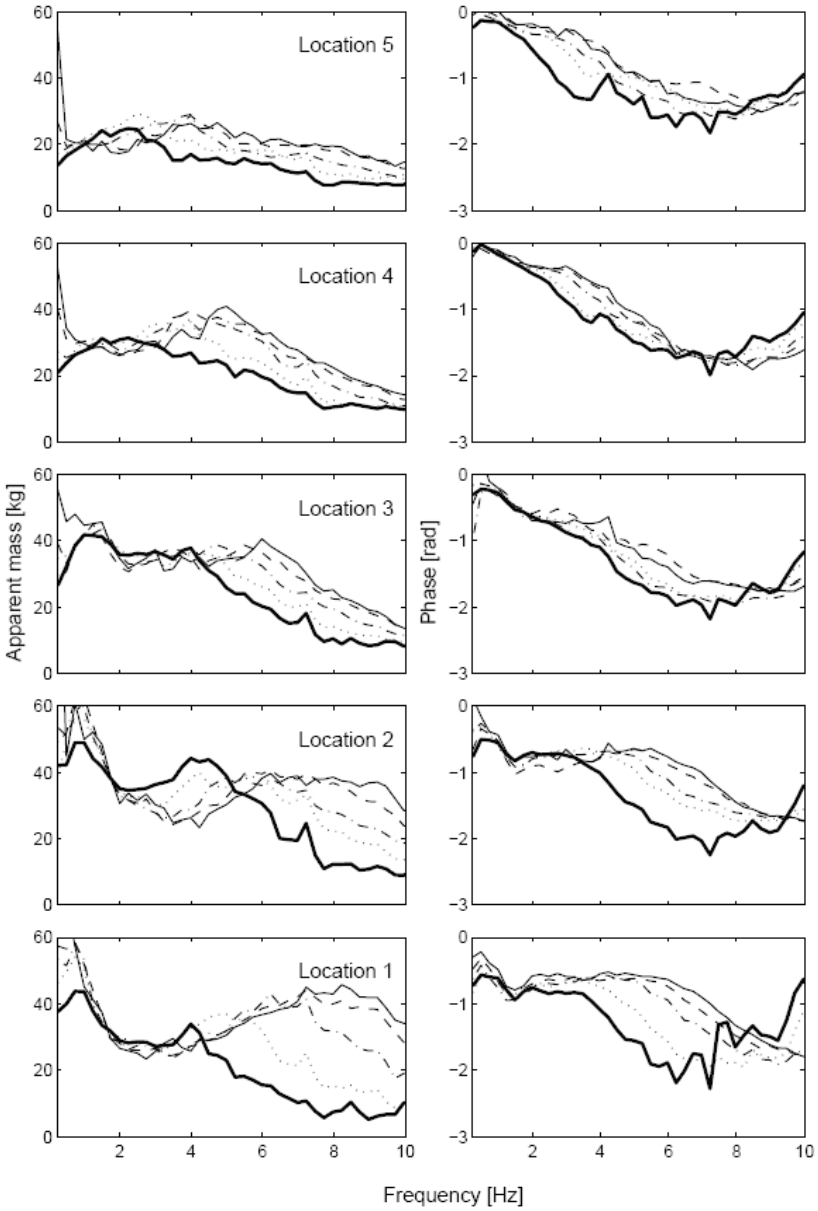

Figure 2.31 Median fore-and-aft apparent masses and phases measured at the five locations on the back (Location 1 was the lowest, 5 the highest) of 12 upright seated subjects exposed to broadband (0.25 to 10 Hz) random fore-and-aft whole-body vibration at 0.1 (———), 0.2 (— — —), 0.4 (— · — · —), 0.8 (. . . . . .), and 1.6 (━━━) ms^{-2} r.m.s. with a rigid upright backrest (Abdul Jalil, 2005).

2.3.2.2 Lateral excitation

During lateral random excitation, the lateral apparent mass or mechanical impedance of the human body has been found to be nonlinear: the frequencies of the peaks in the lateral apparent mass decreased as vibration magnitude increased. Fairley and Griffin (1990) showed the nonlinear response with the dominant peak in the lateral apparent mass at around 1 to 2 Hz – a similar range to the first resonance in the fore-and-aft apparent mass during fore-and-aft excitation. Similarly, Hinz *et al.* (2006) found that the peak frequency of the normalised mean apparent mass decreased from 2.04 to 1.37 Hz in the lateral direction when vibration magnitude increased from 0.25 to 1.5 ms^{-2} r.m.s. (Figure 2.32). A minor peak at frequencies lower than 1 Hz was also observed, but the peak frequency was not affected by vibration magnitude. With horizontal excitations at frequencies higher than 1.5 Hz, Mansfield and Lundström (1999a) found the characteristic nonlinearity with the horizontal apparent mass measured in all directions of excitation from the fore-and-aft (0 degree) to the lateral (90 degrees) direction (see Figure 2.33).

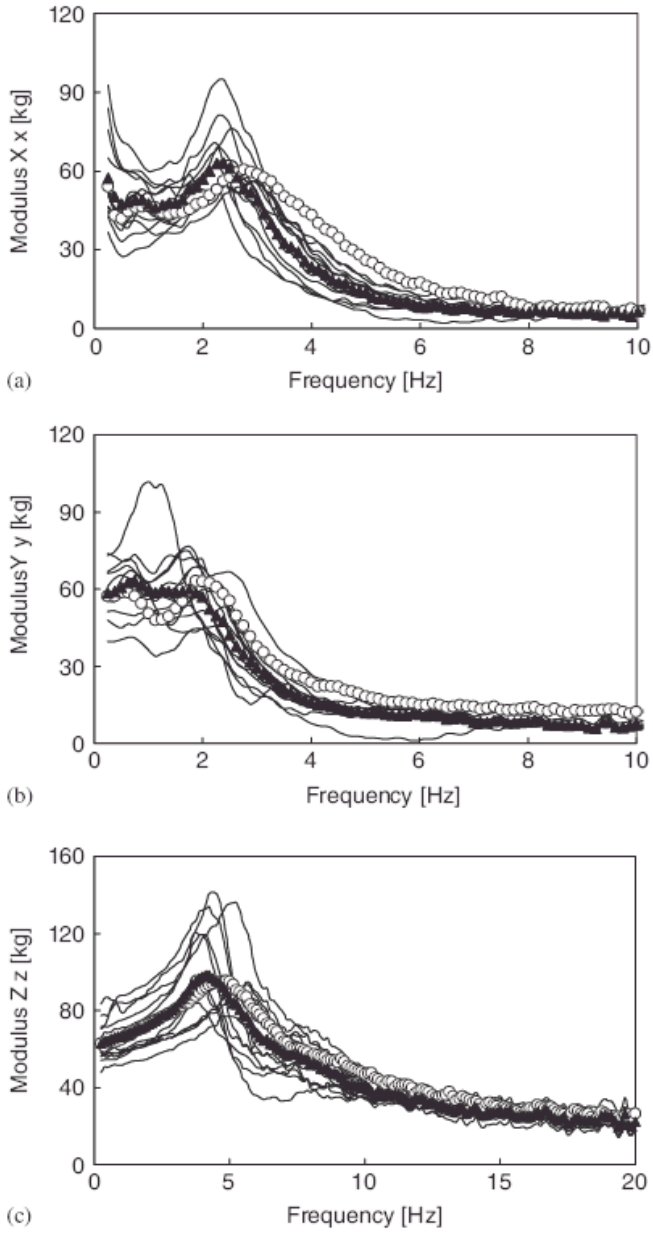

Figure 2.32 Mean apparent masses of 13 upright seated subjects exposed to fore-and-aft (a), lateral (b), and vertical (c) broadband (0.25 to 30 Hz) random whole-body vibration at 0.25 (○) and 1.0 (▲) ms^{-2} r.m.s. Individual data were shown: ——— (Hinz *et al.*, 2006).

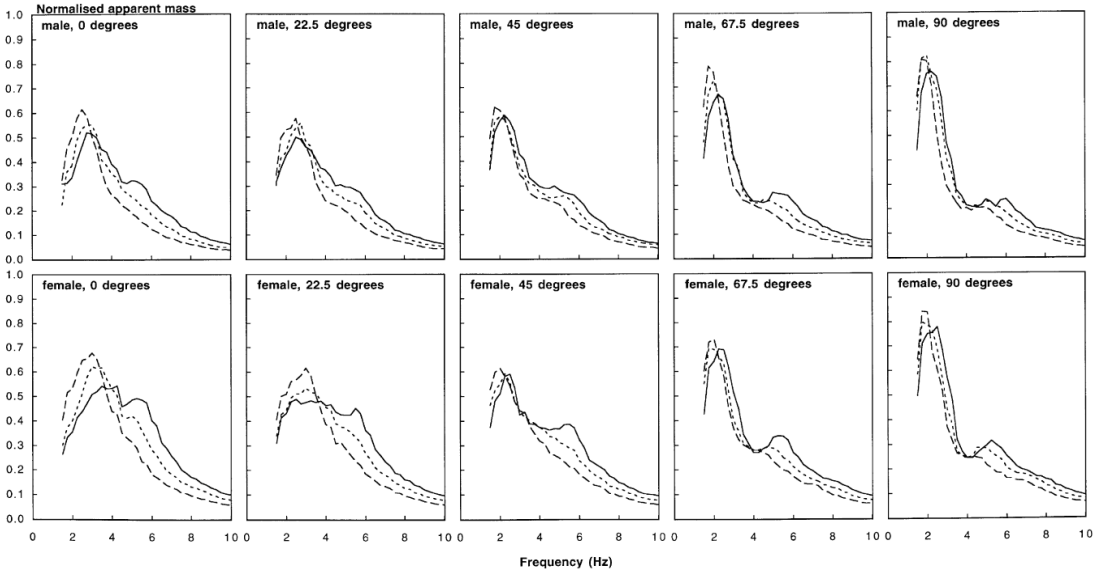

Figure 2.33 Median normalised apparent masses of 15 males and 15 females exposed to horizontal broadband (1.5 to 20 Hz) random vibration at 0 (fore-and-aft), 22.5, 45, 67.5, and 90 (lateral) degrees to the mid-sagittal plane at three vibration magnitudes: 0.25 (———), 0.5 (- - - - -) and 1.0 (— — —) ms^{-2} r.m.s. with a stationary footrest (Mansfield and Lundström, 1999a).

2.4 Transmissibility of the human body

Transmissibilities measured at different locations on the human body have been widely reported in the past two decades. With upright seated subjects these locations included: head (e.g. Hinz and Seidel, 1987; Paddan and Griffin, 1988), thoracic and lumbar spine (Hinz and Seidel, 1987; Kitazaki and Griffin, 1998; Matsumoto and Griffin, 1998b; Mansfield and Griffin, 2000; Matsumoto and Griffin, 2002a), and pelvis (Mansfield and Griffin, 2000; Mansfield and Griffin, 2002; Matsumoto and Griffin, 2002a). The transmissibilities to the head, spine and pelvis were also measured with standing subjects (e.g. Hagena *et al*., 1985; Pope *et al*., 1989; Herterich and Schnauber, 1992; Paddan and Griffin, 1993; Matsumoto and Griffin, 1998a). The anatomy of the spine and pelvis is shown in Figure 2.34.

Transmissibility has been measured to understand the transmission of vibration through and to the body so as to study the disturbances at the head (Griffin and Lewis, 1978) during manual control (Lewis and Griffin, 1978), or to help explain incidences of low back pain (Seidel and Heide, 1986). Measurement of vibration transmitted to different parts of the body could also help identify dynamic modes contributing to resonances seen in apparent mass and mechanical impedance. It has been shown in Section 2.3.1.3 that the cause of the apparent mass resonance is closely related to the cause of the nonlinearity. The objectives of this section are to identify the modes that have primarily contributed to the resonance in apparent mass and the effect of vibration magnitude on these modes.

Most studies measuring the transmissibilities to the spine and pelvis used vertical excitations with resultant motion measured in the vertical, fore-and-aft, and rotational directions. The accelerations on the body could be measured either with an invasive method or a non-invasive method. The 'invasive method' inserts one side of a Kirschner wire into the spinous processes and attaches the other side to an accelerometer. In the 'non-invasive method', the accelerations are measured on the skin and corrected by an impulse response function representing the response of the local tissue-accelerometer system (Kitazaki and Griffin, 1995; Kitazaki and Griffin, 1998). Some parts of the body surfaces might not be ideally align with the direction of excitation (e.g. the first thoracic vertebra, T1). This inclination of body surface could be reduced by taking into account the static angle between the surface and the vertical axis while calculating the transmissibility (Matsumoto and Griffin, 1998b). The 'non-invasive method' has been preferred in many previous studies for convenience and ethical reasons.

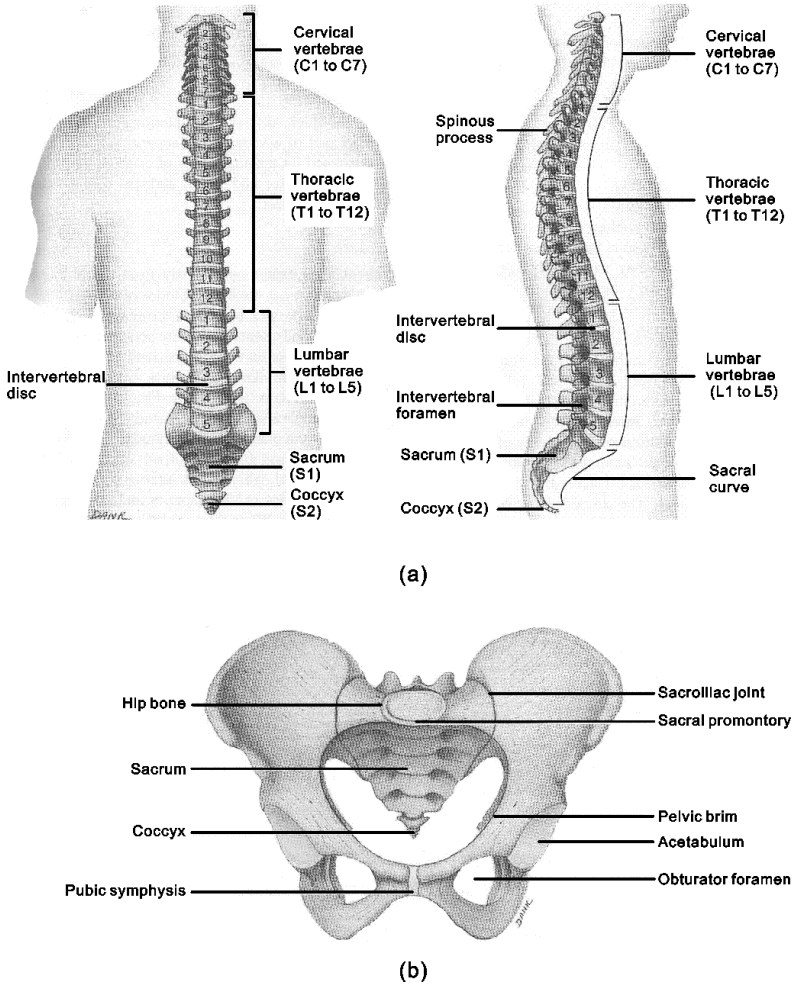

Figure 2.34 Anatomy of the human spine (a) and pelvis (b) (graphics were adapted from Tortora and Grabowski, 2003).

2.4.1 The seated human body

The transmissibilities in the vertical and fore-and-aft directions to T1, T6, T11, L3, and S2 of the upright seated subject showed eight mode shapes below 10 Hz during 0.5 to 35 Hz random vibration (Figure 2.35, Kitazaki and Griffin, 1998). The authors attributed the fourth mode at 4.9 Hz to the principal resonance observed in apparent mss at around 5 Hz. This mode consisted of 'an entire body mode in which the head, spinal column and the pelvis moved vertically due to axial and shear deformations of the buttocks tissue'. The fifth mode at 5.6 Hz contained a bending mode of the lumbar and the lower thoracic spine. The sixth mode at 8.1 and the seventh at 8.7 Hz were caused by pitching modes of the pelvis with varying pivoting points. The eighth mode at 9.3 Hz was due to a visceral movement. The sixth, seventh and eighth modes were considered to be related to the secondary resonance in apparent mass at around 8 Hz.

Using the Kirschner-wires invasive method and vertical 3 to 40-Hz sinusoidal vibration at 0.2 g, Hagena *et al*. (1985) observed a primary peak at around 4 Hz in the vertical transmissibilities to the C7, T6, L1, L4 and L5 of seated subjects. These transmissibilities also showed a secondary peak at around 8 Hz. The authors attributed the peak at around 4 Hz to the entire body rocking mode. The peak at 8 Hz could be due to a mode of the spine or some pitching modes of the pelvis similar to the modes at 8.1 and 8.7 Hz of seated subjects reported by Kitazaki and Griffin (1998) using non-invasive method.

Matsumoto and Griffin (1998b) measured the vertical, fore-and-aft, and pitch transmissibilities to the head, six locations along the spine (T1, T5, T10, L1, L3, L5) and the pelvis. The vertical transmissibilities to the spine and pelvis showed a peak in the vicinity of the apparent mass resonance frequency for each subject, i.e. 4.75 to 5.75 Hz (Figure 2.36). The authors also noticed that the vertical spinal and pelvic transmissibilities at peak tended to be higher with lower locations, but except for T1 – its movement might be amplified by the head. The fore-and-aft transmissibilities were much smaller than those in the vertical direction and occurred at a higher frequency range than the resonance frequency in apparent mass (Figure 2.36). Over the frequency range of the apparent mass resonance, the pitch transmissibilities to the head and T1 were found to be greater than those to the other locations. These results showed that relative motions of rocking and bending over the spine might have contributed to the resonance in the apparent mass at around 5 Hz (Figure 2.37). The authors commented that the primary resonance in the apparent mass was caused by a combination of translational and rotational modes in the mid-sagittal plane: a bending mode of the spine, a rocking mode of the

thoracic spine, a pitch mode of the pelvis, and axial and shear deformations of the tissue beneath the pelvis. The authors also pointed out that high damping property of the body made it difficult to determine the degree of contribution of each mode to the resonance.

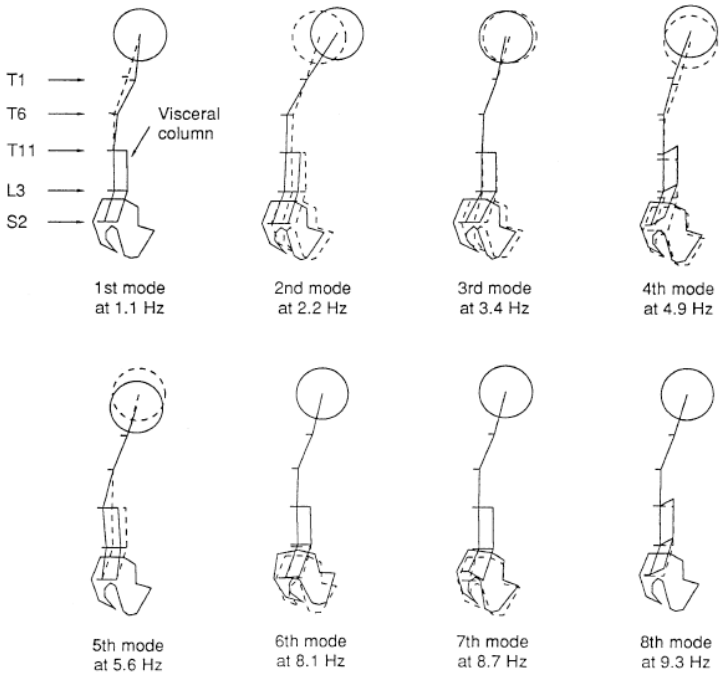

Figure 2.35 Vibration mode shapes extracted below 10 Hz from the mean transfer functions of eight normal upright seated subjects exposed to vertical broadband (0.5 to 35 Hz) random vibration at 1.7 ms^{-2} r.m.s.: - - - - - - (with initial position, ———). The extracted mode shapes consisted of various combinations of bending deformations of the spine, vertical motion of the viscera, axial and shear deformations of the buttocks tissue, pitching motion of the pelvis and pitching motion of the head (Kitazaki and Griffin, 1998).

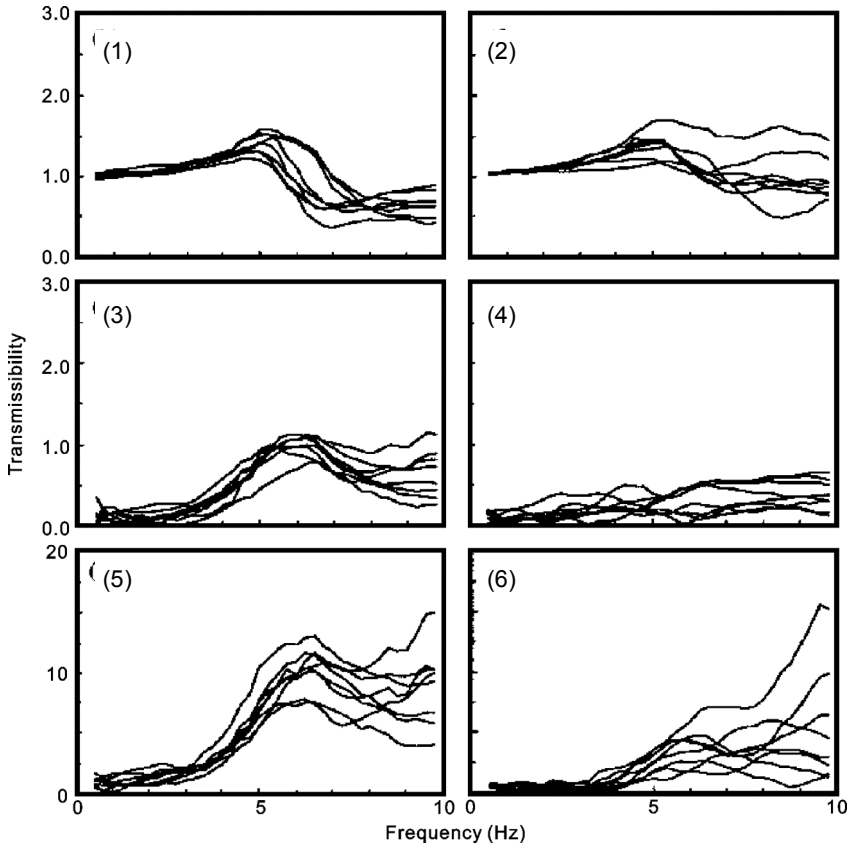

Figure 2.36 Transmissibilities from vertical seat to T1 (1, 3, 5) and L3 (2, 4, 6) in the vertical (1, 2), fore-and-aft (3, 4), and pitching (5, 6) axes of eight upright seated subjects exposed to vertical broadband (0.5 to 20 Hz) random vibration at 1.0 ms^{-2} r.m.s. (Matsumoto and Griffin, 1998b).

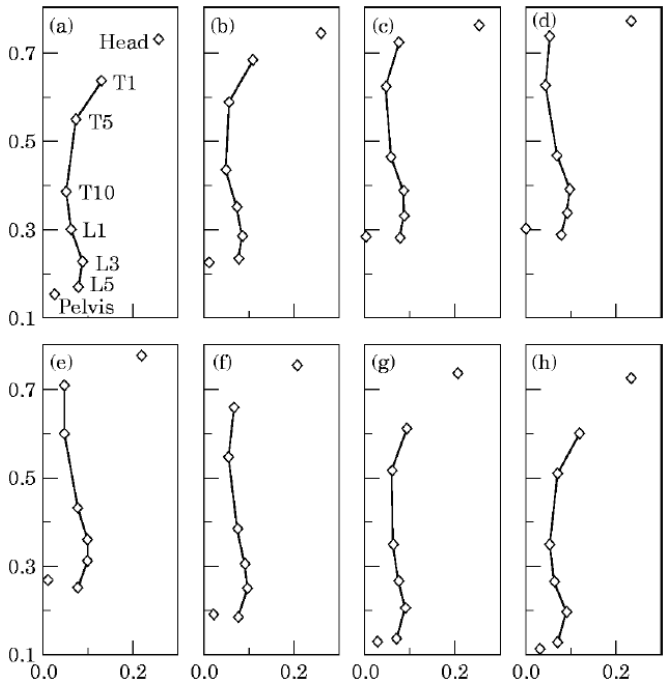

Figure 2.37 Movement of the upper body at the principal resonance frequency of the apparent mass of a single subject at 5 Hz when the seat moved upward and returned downward to the initial position. The units for both axes are metres, and the scale of the movement is exaggerated for clarity (Matsumoto and Griffin, 1998b).

With six magnitudes of vertical random vibration from 0.25 to 2.5 ms^{-2} r.m.s., the transmissibilities from the seat to the lumbar spine (L3), pelvis (posterior-superior iliac spine and iliac crest) and abdominal wall of twelve subjects were found to be nonlinear (Figure 2.38, Mansfield and Griffin, 2000). The authors found that the primary peak frequencies of the transmissibilities to the pelvis and the lumbar spine were in the same range as the resonance frequency in apparent mass (around 4 Hz). A degree of nonlinearity in the spine vertical to abdomen vertical transmissibility was found with individual subjects. But this nonlinearity was less apparent comparing with the nonlinearity found in the seat-to-spine and seat-to-abdomen transmissibilities. Since the spine-to-abdomen transmissibility reflected the dynamic response of the viscera, the authors concluded that the viscera alone could not account for the primary resonance in apparent mass, and that the nonlinearity might have been caused via a transmission path common to the spine and the abdomen. The authors speculated the cause of the nonlinearity to be a combination of factors such as that the spinal muscular activity did not increase proportionally with increasing vibration magnitude, and that the passive property of buttocks tissues had a softening effect with increasing vibration magnitude.

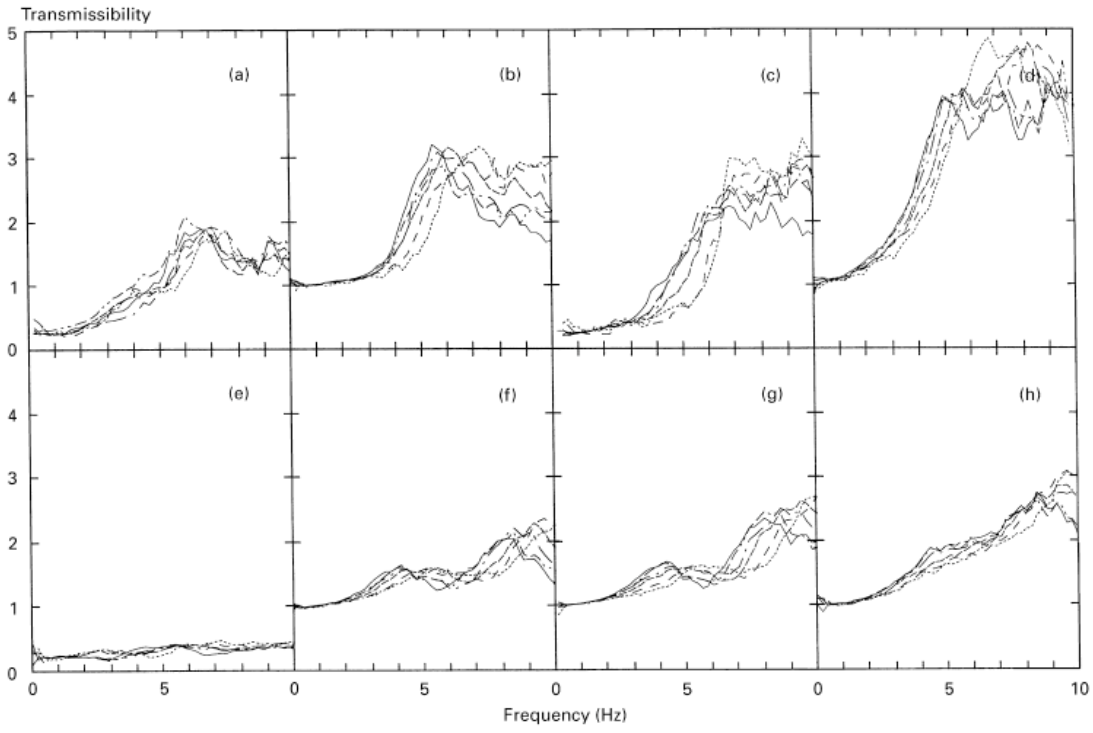

Figure 2.38 Median transmissibilities from vertical seat to lower abdominal wall: (a) fore-and-aft, (b) vertical; vertical seat to upper abdominal wall: (c) fore-and-aft, (d) vertical; vertical seat to lumbar spine (L3): (e) fore-and-aft, (f) vertical, (g) posterior-superior iliac spine, (h) iliac crest. Twelve upright seated subjects were exposed to vertical broadband (0.2 to 20 Hz) random vibration at 0.25 (·····), 0.5 (— — —), 1.0 (— — —), 1.5 (— · — · —), 2.0 (—··—··—), 2.5 (———) ms^{-2} r.m.s. (Mansfield and Griffin, 2000).

The nonlinearity has also been reported in the vertical, fore-and-aft and pitch transmissibilities to the head, spine (T1, T5, T10, L1, L3, L5) and pelvis (posterior-superior iliac spine) during vertical random vibration at five magnitudes from 0.125 to 2.0 ms^{-2} r.m.s. (Figure 2.39, Figure 2.40, and Figure 2.41, Matsumoto and Griffin, 2002a). The peak frequency of the vertical transmissibility to the L3 decreased from 6.27 to 4.75 Hz while the vibration magnitude was increased from 0.125 to 2.0 ms^{-2} r.m.s. The authors pointed out that the transmissibilities showing the relative motions at locations above L5 (Figure 2.42) exhibited less degree of nonlinearity comparing with that in the transmissibilities between the seat and various body locations. This is consistent with the less nonlinear relative motion measured with spine-to-abdomen transmissibility by Mansfield and Griffin (2000). Matsumoto and Griffin (2002a) attributed the nonlinear responses above L5 to the coupling between the spinal column and its surrounding tissues and structures, such as postural muscles and intra-abdominal pressure.

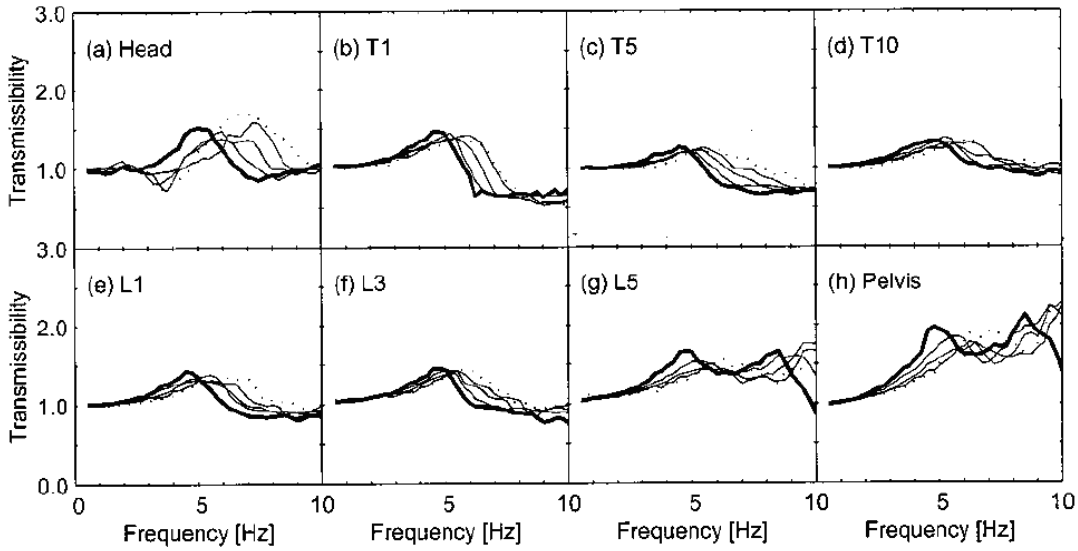

Figure 2.39 Median transmissibilities from vertical seat vibration to vertical vibration at each measurement location of eight upright seated subjects exposed to vertical broadband (0.5 to 20 Hz) random vibration at five magnitudes: 0.125 (· · · ·), 0.25, 0.5, 1.0, and 2.0 (———) ms^{-2} r.m.s. (Matsumoto and Griffin, 2002a).

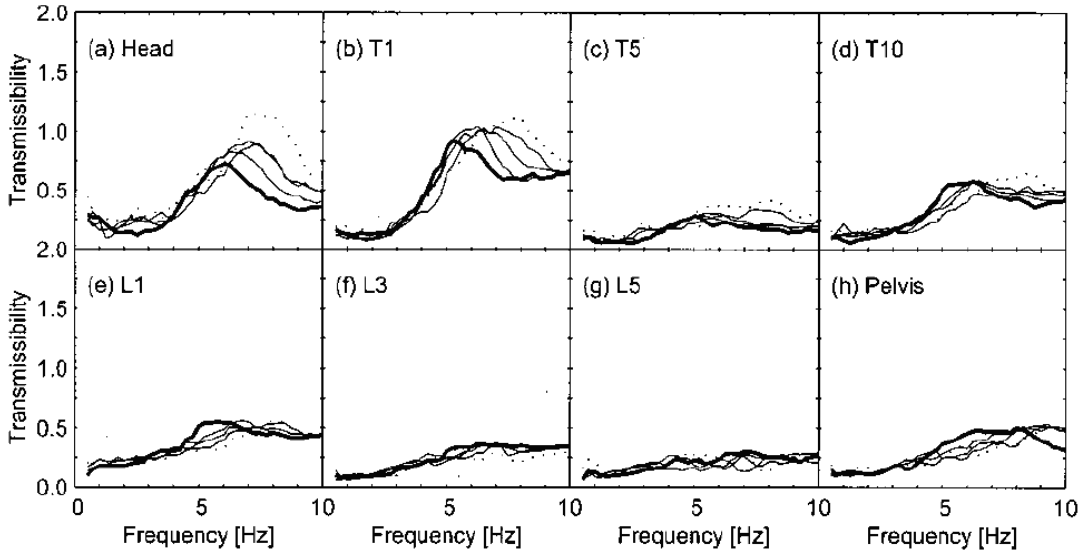

Figure 2.40 Median transmissibilities from vertical seat vibration to fore-and-aft vibration at each measurement location of eight upright seated subjects exposed to vertical broadband (0.5 to 20 Hz) random vibration at five magnitudes: 0.125 (· · · · ·), 0.25, 0.5, 1.0, and 2.0 (———) ms^{-2} r.m.s. (Matsumoto and Griffin, 2002a).

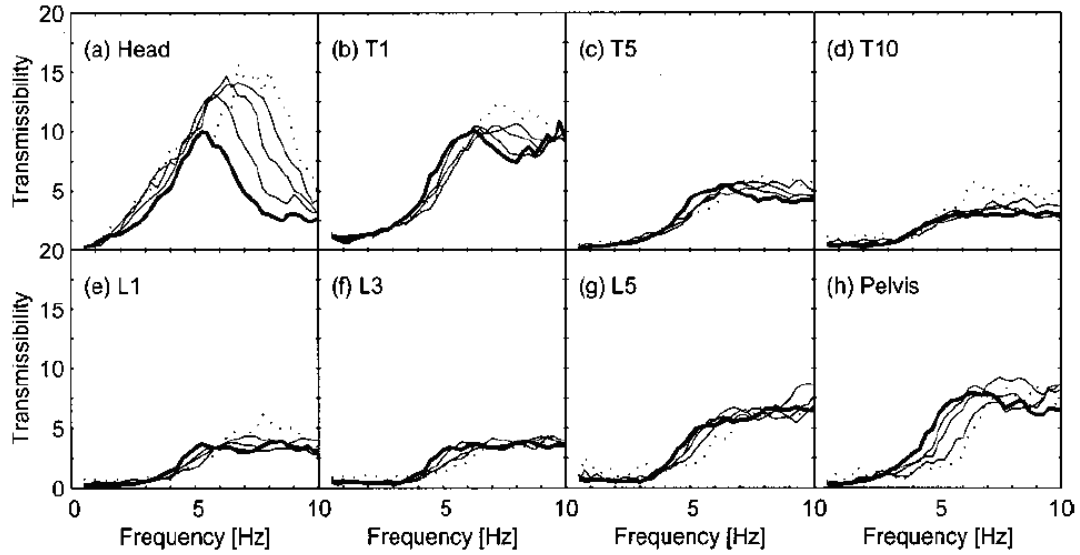

Figure 2.41 Median transmissibilities from vertical seat vibration to pitch vibration at each measurement location of eight upright seated subjects exposed to vertical broadband (0.5 to 20 Hz) random vibration at five magnitudes: 0.125 (· · · · ·), 0.25, 0.5, 1.0, and 2.0 (———) ms^{-2} r.m.s. The unit for the transmissibilities is [$rads^{-2}/ms^{-2}$] (Matsumoto and Griffin, 2002a).

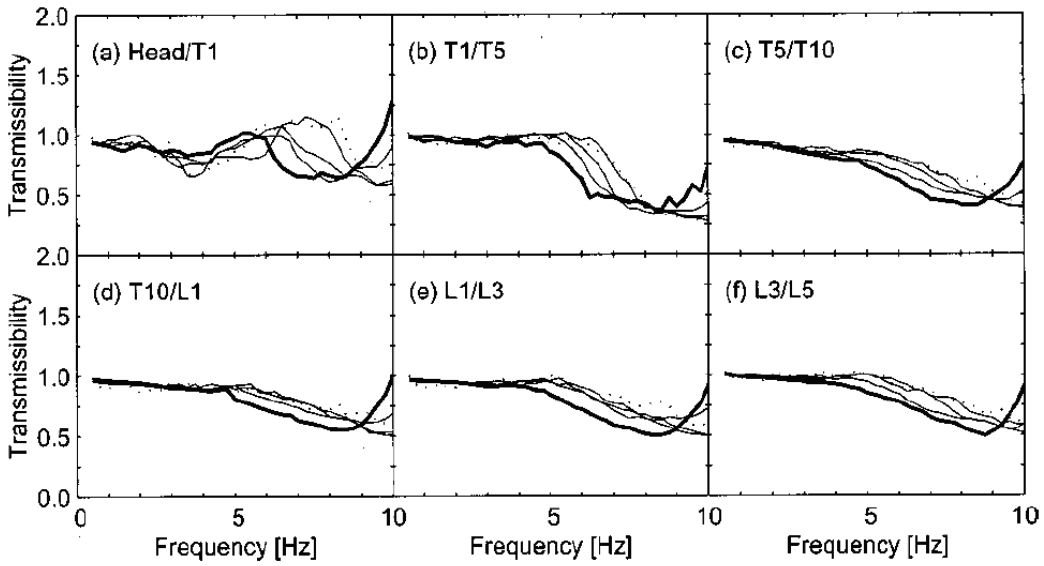

Figure 2.42 Median transmissibilities between vertical vibration at L5 and vertical vibration at each location above L5 of eight upright seated subjects exposed to vertical broadband (0.5 to 20 Hz) random vibration at five magnitudes: 0.125 (· · · · ·), 0.25, 0.5, 1.0, and 2.0 (———) ms^{-2} r.m.s. (Matsumoto and Griffin, 2002a).

The vertical transmissibility to the L3 reported by Mansfield and Griffin (2000) exhibited a peak at around 4 to 5 Hz and a more apparent peak at around 8 to 10 Hz (Figure 2.38 f). While the vertical transmissibility to L3 reported by Matsumoto and Griffin (2002a) showed a single peak in the region of 5 Hz (Figure 2.39 f). Although both studies used a similar 'upright normal' sitting posture with a horizontally flat rigid seat without backrest, different thigh contact conditions in the two studies might have caused the difference. In Matsumoto and Griffin's study, the subjects were asked to hang their lower legs freely when seated. In Mansfield and Griffin's study the footrest was fixed to 470 mm below the seat surface – subjects with different height might have different buttocks pressure and therefore different responses when seated on the same seat (see Nawayseh and Griffin, 2003). The standard deviation of the subject height in the Mansfield and Griffin's study was 70 mm, which was about 15% of the seating height (470 mm). Despite this difference in peak frequency range, the two studies have agreed on the nonlinear responses at various locations along the spine and the pelvis.

Both of the studies (i.e. Mansfield and Griffin, 2000 and Matsumoto and Griffin, 2002a) have shown less nonlinearity in the relative motions between the locations above the pelvis. This might suggest that the 'common transmission path' – the tissues beneath the pelvis – primarily caused the nonlinear responses to various body locations. Pelvis rotational transmissibility was found to be less nonlinear while a 'pelvis support' was used to constrain the movement of the pelvis during vertical

random vibration from 0.2 to 2.0 ms^{-2} r.m.s. (Mansfield and Griffin, 2002). But the nonlinearity in the apparent mass resonance frequency was not affected by the 'pelvis support' condition, possibly pelvic rotational motions did not primarily contribute to the nonlinearity in apparent mass.

2.4.2 The standing human body

With twelve subjects standing in a 'normal' upright posture, the vertical transmissibilities to the T1, T8, L4 and iliac crest and the fore-and-aft transmissibilities to the T1 and iliac crest exhibited a peak over the range 5 to 7 Hz, similar to the median resonance of the apparent mass (5.5 Hz) at the same vibration magnitude of 1.0 ms^{-2} r.m.s. (Figure 2.43, Matsumoto and Griffin, 1998a). The transmissibilities to the lower lumbar spine and the pelvis region were found to be greater than those to the upper lumbar and thoracic spine – consistent with larger relative motions occurring in the lower spine than in the upper spine. This evidence implies that dynamic mechanisms around the lower lumbar and pelvis regions may contribute to the resonance of the standing body. Similarly, with seated subjects, the vertical spinal and pelvic transmissibilities at peak (around the resonance frequency of the apparent mass) tended to be higher at lower locations (Matsumoto and Griffin, 1998b). The transmissibilities of the standing subjects showed greater inter-subject variability than the seated subjects (see Figure 2.36), possibly due to greater movement of the body and more voluntary control of posture.

With the normal standing posture, the vertical transmissibilities to L4 and to the knee were found to be nonlinear: the primary peak frequencies decreased with increasing vibration magnitude from 0.125 to 2.0 ms^{-2} r.m.s. (Figure 2.44, Matsumoto and Griffin, 1998a). This may suggest that the nonlinear responses could be caused along a transmission path common to L4 and the knee. For example, the dynamics of the foot sole and the dynamics of the lower legs might have contributed to the nonlinearity both found at L4 and the knee. Since the peak frequency of the knee (around 15 to 20 Hz) was markedly higher than that of the apparent mass (4 to 6 Hz), the resonance in apparent mass might not be primarily caused by the knee.

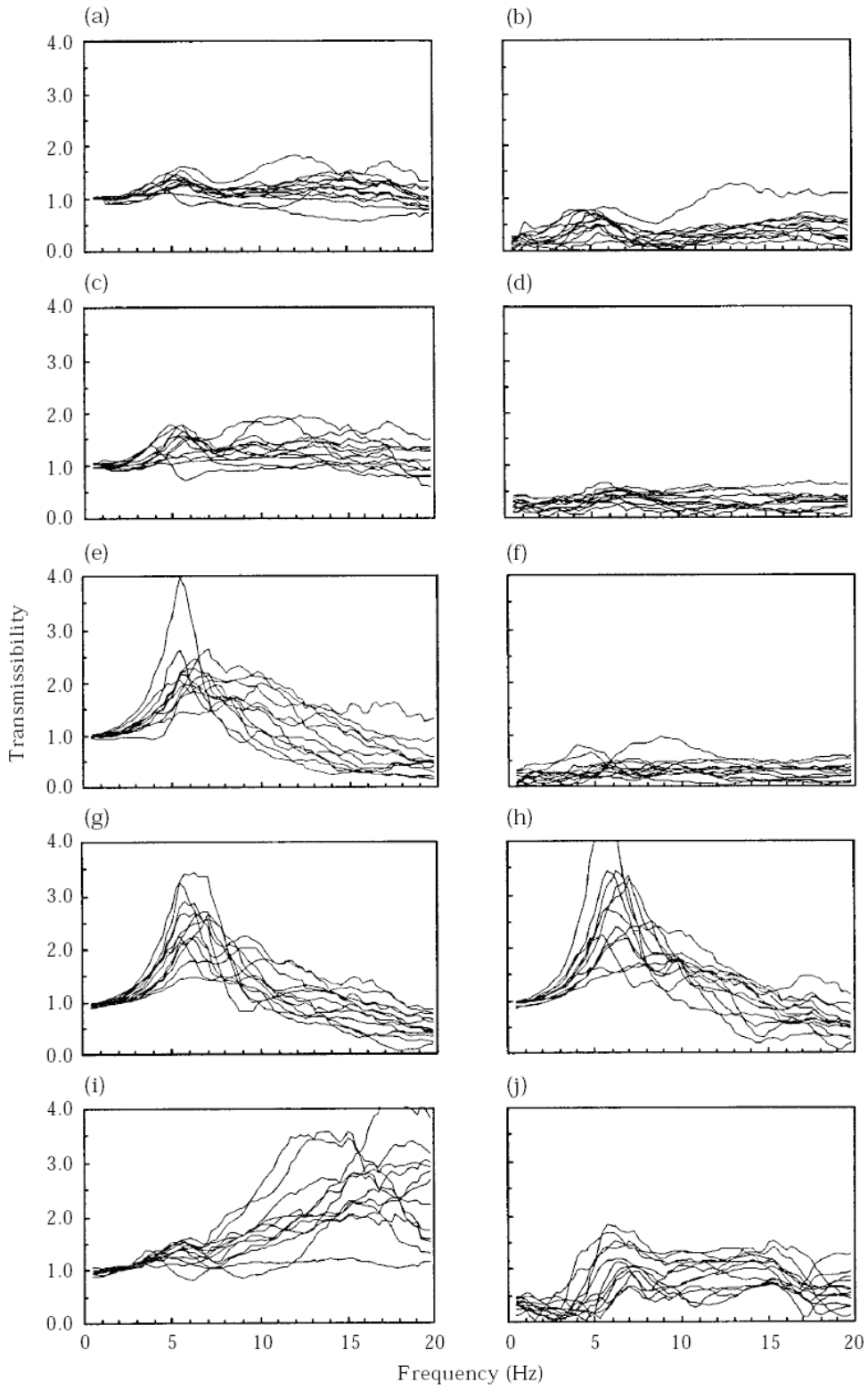

Figure 2.43 Transmissibilities of twelve subjects in the normal standing posture exposed to vertical broadband (0.5 to 30 Hz) random vibration at 1.0 ms^{-2} r.m.s. (a) T1 vertical; (b) T1 fore-and-aft; (c) T8 vertical; (d) T8 fore-and-aft; (e) L4 vertical; (f) L4 fore-and-aft; (g) left iliac crest vertical; (h) right iliac crest vertical; (i) knee vertical; (j) knee fore-and-aft (Matsumoto and Griffin, 1998a).

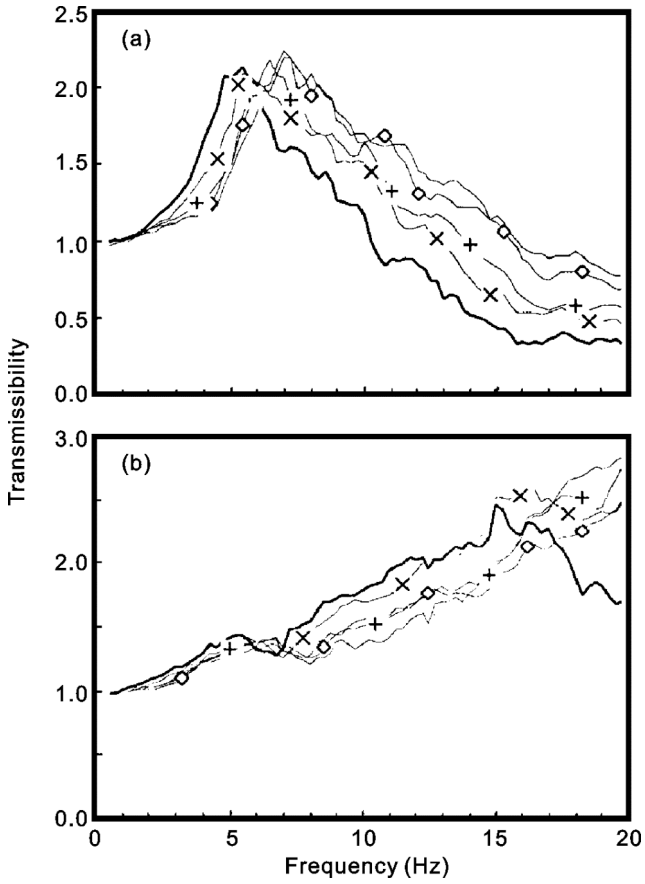

Figure 2.44 Median vertical transmissibilities to the L4 (a) and to the knee (b) of twelve subjects in the normal standing posture exposed to vertical broadband (0.5 to 30 Hz) random vibration at 0.125 (———), 0.25 (—◊—), 0.5 (—+—), 1.0 (—x—), and 2.0 (———) ms^{-2} r.m.s. (Matsumoto and Griffin, 1998a).

2.4.3 The supine human body

Few studies have measured the transmissibility of supine subjects, and none of these has used more than one vibration magnitude (e.g. Vogt *et al*., 1978; Liu *et al*., 1996). With a horizontally flat supine subject exposed to vertical sinusoidal vibration from 1 to 20 Hz at 2.1 ms^{-2} r.m.s., Vogt *et al*. (1978) found the frequency (and magnitude) of the primary resonance peak of the vertical transmissibilities to the chest to be around 6 Hz (1.7), to the abdomen around 5 Hz (2.7), and to the thigh around 5 Hz (2.1). The authors also found that adding a rigid mass of 4.54 kg to these three body locations separately resulted in increased peak frequency of the transmissibility to the abdomen and the thigh, but with the peak frequency at the chest roughly unchanged. Exposing five supine subjects to 0.69 ms^{-2} peak-to-peak sinusoidal vibration from 2 to 20 Hz, the peak frequency of the vertical transmissibility to the chest (at the sternum area) was around 5 Hz (Figure 2.45, Liu *et al*., 1996). The vertical transmissibility to the abdomen and the thigh exhibited two

peaks – the dominant primary peak was at around 5 Hz while the minor secondary peak at around 11 Hz. The median magnitude of the transmissibility at peak was about 1.4 at the abdomen and the chest, while about 1.8 at the thigh. The inter-subject variability of the transmissibility was greater at peak frequencies than other frequencies, and greater to the thigh and the abdomen than the chest. Assuming the transmission paths to the thigh and the abdomen involved more soft tissues than that the chest, the greater variability could be caused by greater movement and greater variability of dynamic characteristics of soft tissues comparing with boney skeletal structures (i.e. the chest).

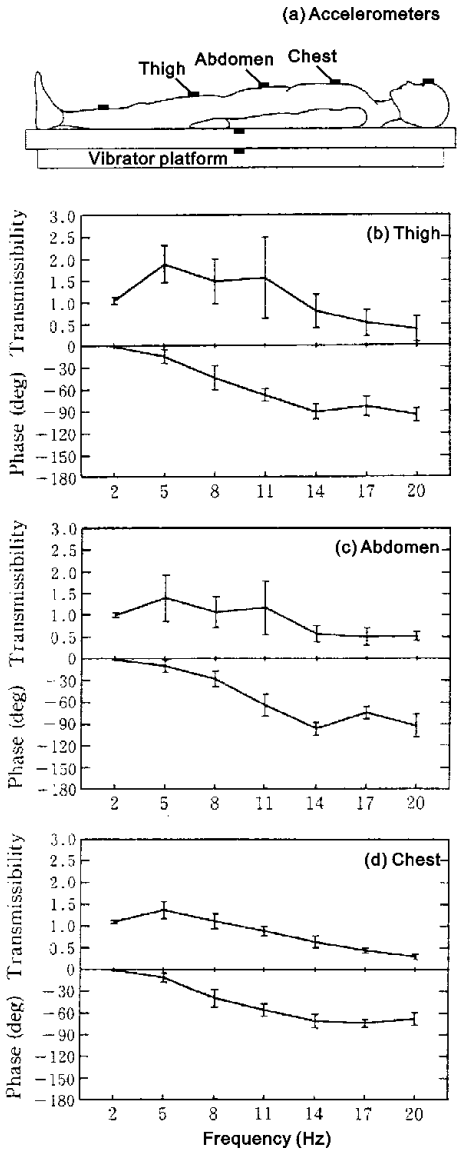

Figure 2.45 Median and ranges of the vertical transmissibilities to the thigh (b), the abdomen (c), and the chest (d) of five subjects in the horizontally flat supine posture (a) exposed to vertical sinusoidal (2 to 20 Hz) vibration at 0.69 ms^{-2} peak-to-peak. Locations of the accelerometers are shown in (a) (Liu *et al.*, 1996).

2.5 Biodynamic models of the human body

Measures of the biodynamic responses to vibration, such as the apparent mass and transmissibility, have been used to develop biodynamic models of the human body in response to whole-body vibration. Such models are used to predict the forces and movements in the body for a number of purposes (see Table 2.3). For example, models were constructed to predict the seat transmissibility, or the forces acting on the spine. The seat transmissibility can be defined as the amount of vibration transmitted through the seat to the body, usually in the form of a transfer function between the input vibration stimuli at the floor and the output acceleration at the seat-subject contact interface (Griffin, 1990). Forces acting on the spine have been considered to reflect the risk of injury during whole-body vibration. Therefore such forces were derived from the biodynamic models to predict the 'risk-zones' (e.g. Fritz, 2000; Seidel *et al*., 2001). Based on what information the biodynamic models try to predict or represent, these models can be summarized into three general categories: i) mechanistic models, which represent the qualitative mechanisms govern the body movement; ii) quantitative models, which describe the input-output relationships between input stimuli (e.g. acceleration at the floor) and the resultant biodynamic responses (e.g. apparent mass); iii) effect models, which reflect human discomfort, risk of injury, or performance for specific input stimuli (Griffin, 2001).

Each part of a mechanistic model usually represents an anatomical section of the human body. A mechanistic model can be defined by a suitable model form with a group of lumped parameters (i.e. discrete masses, springs and dampers) so as to represent the apparent mass and/or transmissibilities to more than one locations and in more than one directions (e.g. Mertens and Vogt, 1978; Matsumoto and Griffin, 2001; Nawayseh, 2003). Alternatively, more complex finite element models can be used to describe the forces transmitted to and through the spine by comparing the modal parameters of the model with the modal analysis of experimental data (e.g. Belytschko and Privitzer, 1978; Kitazaki and Griffin, 1997; Pankoke *et al*., 1998).

Table 2.3 Some applications of biodynamic models (Griffin, 1990).

To predict movement or forces caused by situations too hazardous for an experimental determination
To predict movement or forces caused by situations too numerous and varied for experimental determination
To understand the nature of body movements
To provide information necessary for the optimization of isolation systems and the dynamics of other systems coupled to the body
To determine standard impedance conditions for the vibration testing of systems used by man
To provide a convenient method of summarizing average experimental biodynamic data
To predict the influence of variables affecting biodynamic response

Quantitative models can be used to characterise the apparent mass (e.g. Fairley and Griffin, 1989; Mansfield, 1998; Wei and Griffin, 1998a; Matsumoto and Griffin, 2003) and mechanical impedance (e.g. Wittmann and Phillips, 1969; Vogt et al., 1973; Vogt et al., 1978; Smith, 1994), or to reproduce typical apparent masses or mechanical impedances so as to predict the seat transmissibility (e.g. Suggs *et al*., 1969; Wei and Griffin, 1998b). The forms of the models, however, do not necessarily have any anatomical representation of the body.

The lumped parameter method has been adopted in both mechanistic models and quantitative models. Lumped parameter models have the advantages to simplify and to quantify complex biodynamic responses of the human body in terms of a relatively small number of parameters comparing with complex finite element modal analysis. The number of parameters, or the degrees of freedom, is usually dependent on the purposes and applications of models. For example, the two-degree-of-freedom model developed by Wei and Griffin (1998a) and the five-degree-of-freedom model by Matsumoto and Griffin (2001) could both produce close fit to the measured apparent masses. Wei and Griffin's model was employed as a mathematical representation of the human response in order to predict the seat transmissibility. While with an anatomical model form, Matsumoto and Griffin's model was designed to represent the transmissibilities to various locations along the spine in the vertical and the cross-axis fore-and-aft directions during vertical whole-body vibration.

In the present thesis quantitative lumped parameter models, similar to those used by Wei and Griffin (1998a), will be used to quantify the nonlinearity. Models will be fitted to apparent mass at each vibration magnitude and each experimental condition to obtain resonance frequencies and parameters (see Chapter 3). Comprehensive reviews of the biodynamic models are available elsewhere (Griffin, 1990; Kitazaki, 1994; Boileau and Rakheja, 1998; Wei, 1998; Matsumoto, 1999; Seidel and Griffin, 2001). This section focuses on the lumped parameter models that are designed to represent the resonances in the apparent mass or transmissibility, with various vibration magnitudes where applicable. The following sections commence with some single- and two-degree-of-freedom models.

2.5.1 Lumped parameter models in the vertical direction

2.5.1.1 Models of the seated human body

Linear models

A single-degree-of-freedom mass-spring-damper model is the simplest form to represent the apparent mass of the seated human body in the vertical direction. Fairley and Griffin (1989) developed a single-degree-of-freedom model to describe the mean apparent mass and phase of 60 subjects with feet moving with the seat (Figure 2.46 a). The sprung mass m_1 represented the body mass moving relative to the platform; the unsprung mass m_2 represented the body mass and the legs that did not move relative to the platform. An additional degree of freedom represented the effect of the stationary footrest (m_3). The model was not calibrated to represent the effect of increased muscle tension, contact with backrest, or vibration magnitude.

A parallel two-degree-of-freedom model, in which the two sprung masses were coupled separately to the unsprung frame, was developed for vehicle seat testing by Suggs *et al*., (1969, Figure 2 46 b). Using sinusoidal vibration from 1.75 to 10 Hz with 0.5 Hz steps, the model parameters were determined by minimising the difference between the average mechanical impedance modulus of eleven subjects and the model response. A primary resonance at around 4.5 Hz was produced by the larger lower sprung mass representing the 'pelvis and abdomen'. A minor secondary resonance at around 8 Hz was produced by the smaller upper sprung mass representing the 'head and chest'. The unsprung frame was presumed to be the spine. The model was then implemented in a seat testing dummy to predict the seat transmissibility of a tractor seat. The authors considered the model to be sufficient to reproduce the mechanical impedance of the seated human body below 10 Hz.

Wei and Griffin (1998a) derived single- and parallel two-degree-of-freedom models to reproduce the apparent mass so as to predict the seat transmissibility (Figure 2.46 c and d). The model parameters were determined by comparing the model response with the measured (individual and mean) apparent mass modulus and phase of sixty subjects. The apparent masses were obtained by exposing the sixty subjects to 0.25 to 20 Hz broadband random vibration at 1.0 ms^{-2} r.m.s. by Fairley and Griffin (1989, Figure 2.1). Though of a similar form as Suggs *et al*.'s model, Wei and Griffin's model was designed to be a mathematical tool to represent the apparent mass modulus and phase without any anatomical representation of any parts of the body. The authors found that including the frame mass (i.e. m in the two degree-of-freedom model; m_1 in the single degree-of-freedom model) could improve the fitting results. The single-degree-of-freedom model was able to represent the individual apparent mass modulus over the frequency range 0 to 20 Hz. The two-degree-of-freedom model improved the fit in phase at frequencies higher than 8 Hz and resulted in better fit in modulus at around 5 Hz. The optimised parallel two-

degree-of-freedom model gave close fit to the primary resonance at about 5 Hz and the secondary resonance between 8 and 12 Hz. The authors pointed out that to provide an optimal model at different vibration magnitudes, different sets of parameters would be needed (e.g. Lewis, 2001) or, the model parameters had to be nonlinear. Their study also showed that greater degrees of freedom than two might not be necessary to represent the average response of a subject group to a certain input stimulus.

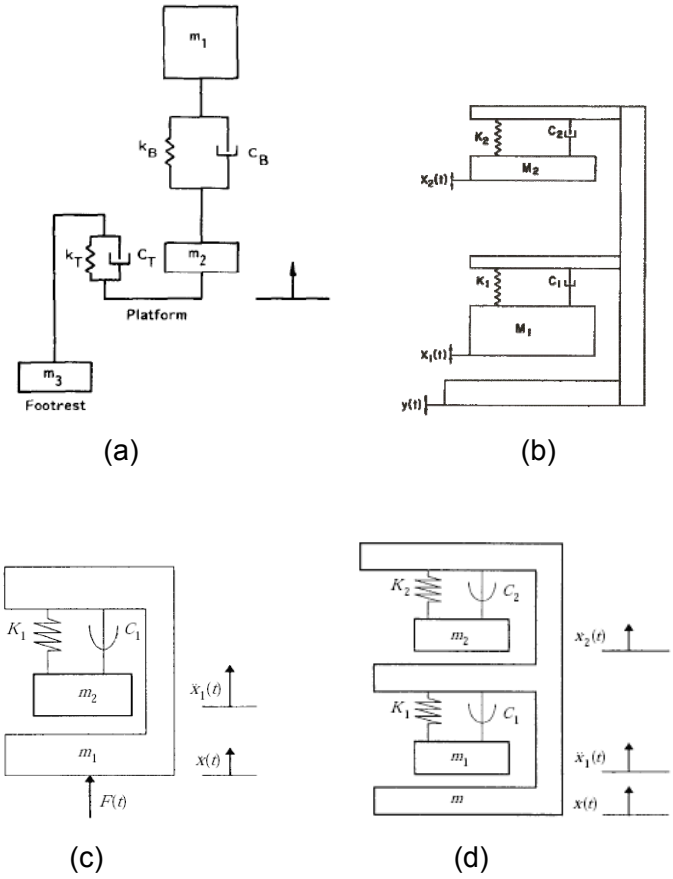

Figure 2.46 The simple lumped parameter models developed by Fairley and Griffin (1989) to represent the mean apparent mass and phase of 60 seated subjects (a), and by Wei and Griffin (1998a) to represent the individual and mean apparent mass modulus and phase (c). The parallel two-degree-of-freedom lumped parameter models proposed by Suggs *et al.* (1969) to represent the average mechanical impedance modulus (b), and by Wei and Griffin (1998a) to represent the individual and mean apparent mass modulus and phase (d).

Compared with the two-degree-of-freedom models, a more anatomically detailed five-degree-of-freedom model was developed to represent the human response to shocks concerning risk of injuries (Mertens and Vogt, 1978). The legs, buttocks, abdominal components, chest and head were expressed by *m1*, *m2*, *m4*, *m6*, and *m7* respectively (Figure 2.47). The spinal column was represented by the serial springs (*k3*, *k5*, and *k7*) and dampers (*c3*, *c5*, and *c7*). The segmental masses were

determined by previous anthropometric measurements from literature. The stiffness and damping parameters were determined by comparing the mechanical impedance and the transmissibility to the head between the model and the measurement by Mertens (1978). The resonance peak frequencies of the measured mechanical impedance and transmissibility to the head of the seated subjects increased with increasing sustained acceleration levels from 1 to 4 G. Different sets of stiffness and damping parameters were obtained to represent this 'nonlinear' response.

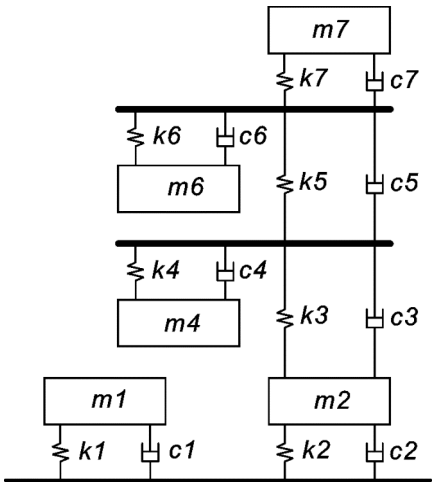

Figure 2.47 The five-degree-of-freedom model developed by Mertens and Vogt (1978) to represent the modulus and phase of the mechanical impedance and transmissibility to the head.

With anatomical representations of the legs, pelvis, spine, lower and upper torso, a five-degree-of-freedom model took into account the change in mechanical impedance (modulus and phase) with varying vibration magnitude (Figure 2.48 a, Smith, 1994). The impedance data were obtained by exposing four subjects to discrete sinusoidal excitation from 3 to 20 Hz at 0.347, 0.694, and 1.734 ms^{-2} r.m.s. Four peak regions were identified, and they were from 5 to 8 Hz, 7 to 9 Hz, 12 to 14 Hz, and 15 to 18 Hz. But as the vibration magnitude increased, the second, third and fourth peak tended to be less clear. The frequency of the first primary peak decreased from 6.8 to 5.9 and 5.2 Hz while the vibration magnitude increased from 0.347 to 0.694 and 1.734 ms^{-2} r.m.s. The largest change due to vibration magnitude was found in mass elements M_3, in spring elements K_2, and in damper elements C_2 and C_5 (Figure 2.49). These changes imply that the nonlinearity with vibration magnitude arises from a combination of different modes of the body.

The model proposed by Smith (1994) was modified to fit the 'major resonances' in the mechanical impedance modulus and transmissibility modulus to the chest, spine (C7), and thigh with a female (56 kg) and a male (75 kg) subject (Figure 2.48 b,

Smith, 2000). The model was also used to evaluate the effect of selected seat cushions. In order to accommodate the fittings to the transmissibilities, the model parameters were redistributed. The added degree of freedom representing the unsupported legs improved the prediction of effect of cushions. The author found that the goodness of fit differed significantly between the two subjects.

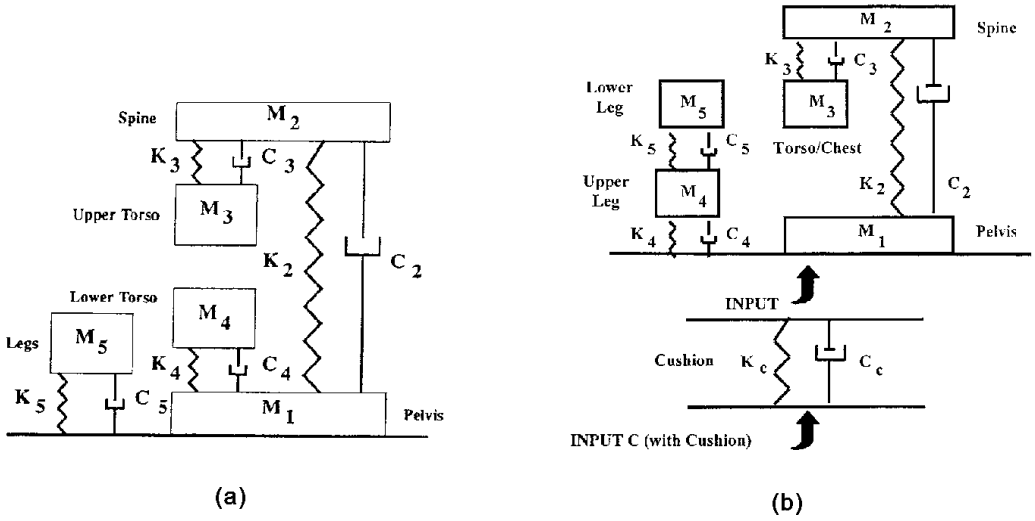

Figure 2.48 The five-degree-of-freedom models developed by: (a) Smith (1994) to represent the mechanical impedance modulus and phases at three magnitudes (0.347, 0.694, and 1.734 ms^{-2} r.m.s.) of sinusoidal excitation from 3 to 20 Hz; (b) Smith (2000) to simulate the major resonances in the mechanical impedance and transmissibilities to the chest, spine (C7) and thighs with and without cushions.

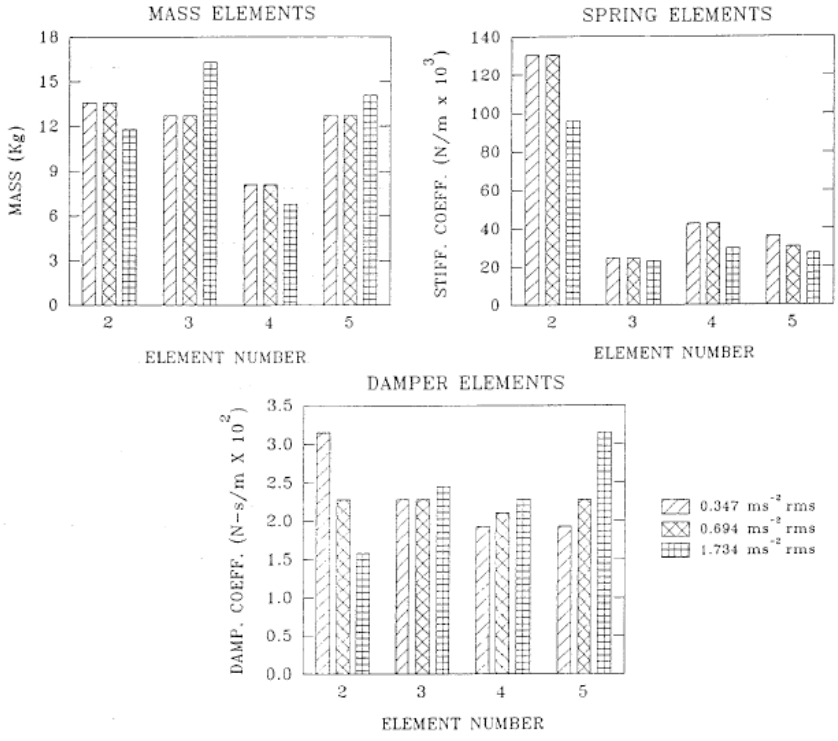

Figure 2.49 Parameters (masses, springs, and dampers) of the optimized five-degree-of-freedom model fitted to the mechanical impedance modulus and phases

at three magnitudes (0.347, 0.694, and 1.734 ms^{-2} r.m.s.) of sinusoidal excitation from 3 to 20 Hz (Smith, 1994).

The International Organisation for Standardization (ISO 5982, 2001) introduced a three-degree-of-freedom quantitative model to represent the apparent mass, mechanical impedance and seat-to-head transmissibility (Figure 2.50). The range of idealized parameters were defined for seated subjects with feet supported on the vibration platform and back unsupported. The stimuli were sinusoidal or broadband (0.5 to 20 Hz) random vertical vibration with unweighted acceleration equal or lower than 5 ms^{-2} r.m.s. As discussed in Section 2.3.1.3 and Section 2.4.1, there could be a difference of up to 2 Hz in resonance frequencies of the apparent mass, mechanical impedance and transmissibility when the excitation magnitude changes from 0.125 to 2.5 ms^{-2} r.m.s. Most occupational exposures to whole-body vibration have magnitudes of between 0.25 and 2.5 ms^{-2} r.m.s. This means the proposed idealized model parameter ranges (in ISO 5982, 2001) is inadequate to represent the change in biodynamic responses due to the magnitude of excitation.

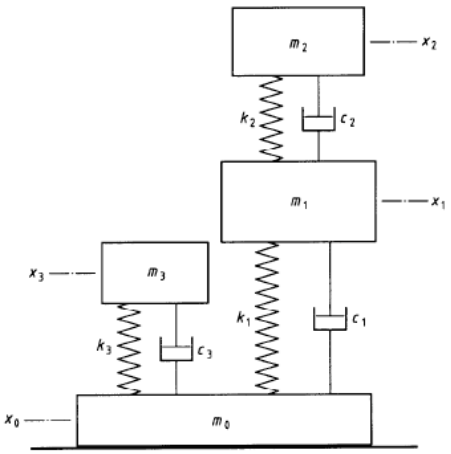

Figure 2.50 The three-degree-of-freedom model defined by the International Organisation for Standardization (ISO 5982, 2001) to represent the apparent mass, mechanical impedance and seat-to-head transmissibility of a seated person.

To study the mechanisms associated with the principle resonance in apparent mass at around 5 Hz, Matsumoto and Griffin (2001) developed four- and five-degree-of-freedom models with translational and rotational degrees of freedom representing the two-dimensional movement of the upper body in the mid-sagittal plane (Figure 2.51). The four-degree-of-freedom model (Model 1) consisted of four segmental masses corresponding to the legs (1), the pelvis (2), the viscera (4), and the upper body (3). The five-degree-of-freedom model (Model 2) had the similar form to the

Model 1 except that the upper body was represented by two masses, i.e. 3 and 5. For simplicity, the nonlinearity due to vibration magnitude was neglected. The mass and geometric parameters of the models were determined from previous literature (e.g. National Aeronautics and Space Administration, 1978; Kitazaki and Griffin, 1997). The translational spring and damper beneath mass 1 was to represent the buttocks tissues. The pitching of the pelvis and the bending of the spine were described by the rotational springs and dampers between mass 1 and 2, and between mass 2 and 3 respectively. The stiffness and damping parameters were optimized by minimizing the difference between the model response and the modulus and phases of the frequency response functions (i.e. apparent mass, vertical and fore-and-aft transmissibilities to locations along the spine). The study suggested that vertical motions due to deformation at the buttocks and viscera made a dominant contribution to the apparent mass resonance, but the contribution of the spinal bending motion was small. This modelling study conforms to the transmissibilities measured at a series of locations on the spine column (Matsumoto and Griffin, 1998b). The cross-axis model form was found to be effective representing the mechanisms around the resonance but only at single magnitudes.

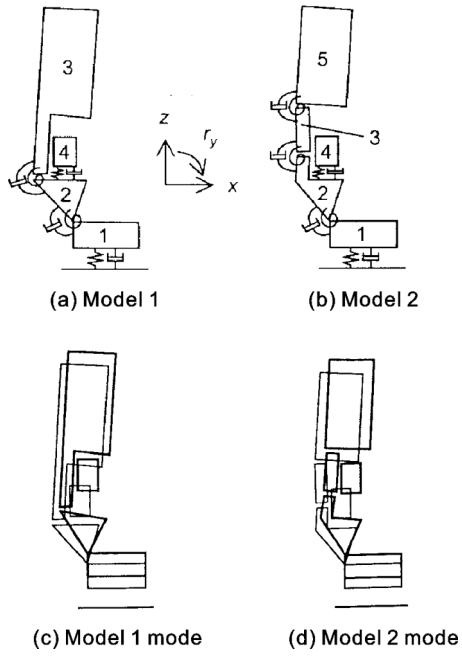

Figure 2.51 The four-degree-of-freedom model (a) and the five-degree-of-freedom model (b), and their mode shapes (c, d) corresponding to the principle resonance in the apparent mass at around 5 Hz (Matsumoto and Griffin, 2001)

Adopting similar rotational spring and damper mechanisms that used by Matsumoto and Griffin (2001), Nawayseh (2003) constructed a group of quantitative models to represent the vertical and cross-axis fore-and-aft forces at the seat during vertical

random excitation (Figure 2.52). In Model 1, mass 1 and mass 2 described the mass of the thighs carried by the seat and the mass of the upper body (including pelvis) respectively. The vertical translational spring and damper represented the stiffness and damping of the thighs and buttocks. The rotational degree of freedom reflected the pitching of the pelvis and bending of the spine. The geometry and mass 1 of the model were determined by referring to available anthropometric measurements (e.g. National Aeronautics and Space Administration, 1978). All other parameters (mass 2 and the translational and rotational springs and dampers) were optimized by minimizing the squared error of modulus and phase between the (vertical and fore-and-aft cross-axis) apparent mass and the model response. Modifying Model 1 to Model 2 showed that adding a vertical translational degree of freedom (i.e. mass 3) to mass 2 improved the fittings in the phases of both the vertical and the fore-and-aft cross-axis apparent mass as shown in Figure 2.53. Changing Model 1 to Model 3 showed improved fittings in the phase of vertical apparent mass. Combining Model 2 and Model 3 into Model 4, the author found improved fittings in the fore-and-aft cross-axis apparent mass. Optimizing Model 5 from Model 4 showed that mass 1 was not needed to produce the resonance behaviours of the seated body in both axes. The author pointed out that the fore-and-aft movement of the seated body on the seat surface during vertical excitation indicated marked shear deformations of tissues beneath the ischial tuberosities. By fitting Model 1 to the vertical and fore-and-aft cross-axis apparent mass obtained at four vibration magnitudes from 0.125 to 1.25 ms^{-2} r.m.s. (Nawayseh and Griffin, 2003), the stiffness of the vertical translation spring decreased with increasing vibration magnitude showing the greatest effect caused by vibration magnitude. This implies that the tissues beneath the ischial tuberosities primarily contribute to the nonlinearity, which is consistent with the findings by Matsumoto and Griffin (2002b) in which a buttocks tensed sitting condition was found to slightly affect the nonlinearity.

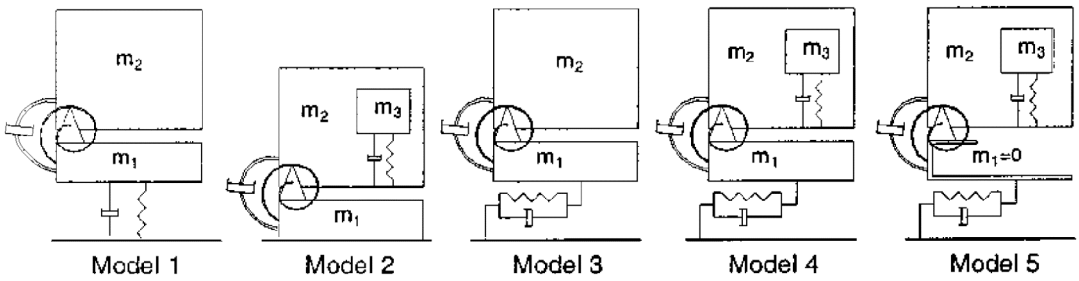

Figure 2.52 Models containing translational and rotational degrees of freedom used to represent in-line vertical and cross-axis fore-and-aft apparent mass at seat during vertical random excitation. The mass 3 in Model 2, 4 and 5 moved only in the vertical direction (Nawayseh, 2003)

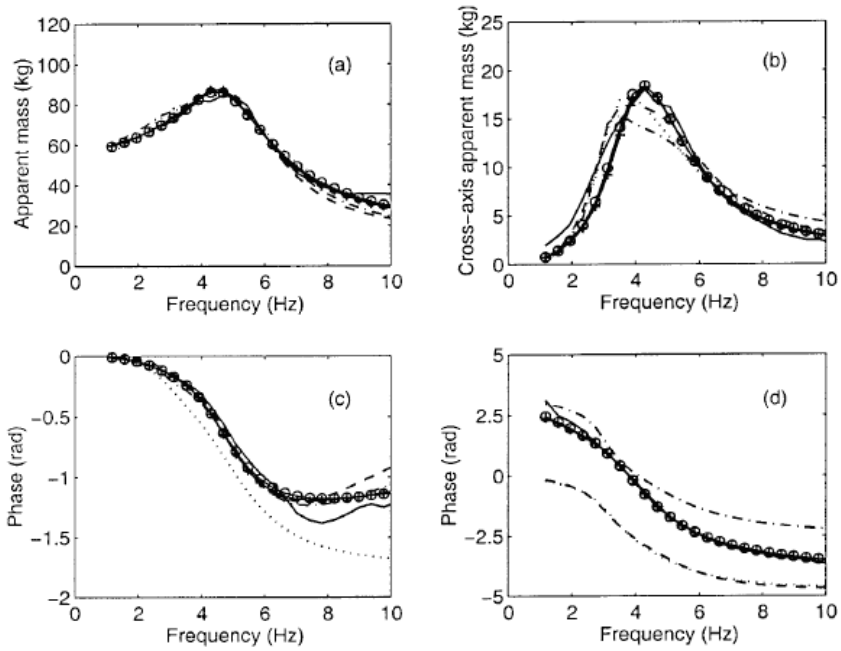

Figure 2.53 Median responses obtained experimentally and calculated using the five models in the 'average thigh contact posture' during vertical vibration. (a) and (b), vertical apparent mass and phase; (b) and (d) fore-and-aft cross-axis apparent mass and phase: ———, experimental measurement; ·····, Model 1; —·—·—, Model 2; — — —, Model 3; —+—+—, Model 4; —o—o—, Model 5 (Nawayseh, 2003)

Nonlinear models

Models with embedded 'nonlinear' components or 'nonlinear' geometric arrangements have been employed to represent particular 'nonlinear' behaviours of the body. 'Nonlinear' refers to the behaviour of a system that does not obey the superposition principle. For example, a linear spring will maintain the same stiffness at different ranges of displacement. But the stiffness of a nonlinear spring can be dependent on the magnitude of displacement, velocity or acceleration, or alternatively, dependent on some function that is not proportional to the displacement (e.g. a cubic spring). Nonlinear geometric arrangements of a dynamic system can also result in 'nonlinear' responses. In such systems, the effective stiffness, damping, or sprung mass varies when exposed to different magnitudes or waveforms of excitation. The characteristic nonlinearity of the resonance frequency of the frequency response functions due to vibration magnitude is one form of 'nonlinear' behaviour. The review of 'nonlinear' models containing 'nonlinear' components, or 'nonlinear' geometric arrangements, is to identify any possible representative mechanisms that could represent the characteristic nonlinearity.

Muksian and Nash (1974) used a multi-degree-of-freedom model to simulate the anatomical path from the pelvis to the head to describe the 'nonlinearities' of the body (Figure 2.54 a). The authors referred the nonlinearities to a number of nonlinear phenomena that had been observed in the human body: a sinusoidal input acceleration resulted in a non-sinusoidal output force of the seated body at the seat (Wittmann and Phillips, 1969); '… joint stiffness increase with deformation…' (Markolf and Steidel, 1970). A nonlinear cubic spring and damper were used between the back (m_2) and torso (m_3) to represent the ligaments attaching the ribs to the vertebrae. Coulomb friction forces were used to represent the sliding surfaces between the back and torso. The 'ballistocardiographic' muscle forces were modelled as a frequency dependent function acting on the thorax (m_4). The diaphragm (m_5) muscle forces were derived from half of the heartbeat rate. The model was calibrated to produce the transmissibilities to the head, back, torso, thorax, diaphragm, and abdomen during vertical sinusoidal vibration. The fittings from 1 to 7 Hz were better than those from 7 to 30 Hz. The authors did not establish and quantify the relationship between the 'nonlinear' behaviours and the transmissibilities. But this information is necessary if the model is to represent the frequency response function of the human body.

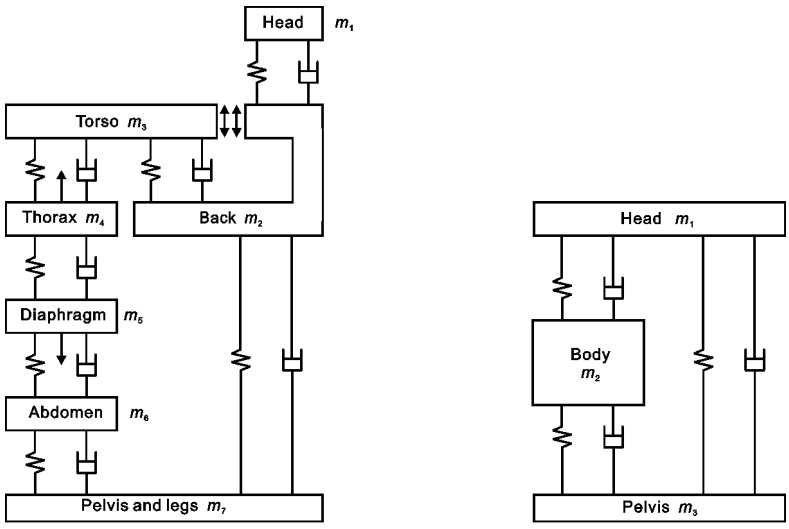

Figure 2.54 The multi-degree-of-freedom model (a) incorporating the nonlinear cubic spring and damper between the back and torso, and forces acting on the thorax, the diaphragm and between the back and torso (Muksian and Nash, 1974). The three-degree-of-freedom model (b) incorporating a frequency dependent nonlinear 'parabolic' damper between the pelvis and the body (Muksian and Nash, 1976).

Muksian and Nash (1976) modified the nonlinear model discussed above into a three-degree-of-freedom model with a dual transmission path from the pelvis to the head (Figure 2.54 b). The modified model was used to simulate the seat-to-shoulder (body) transmissibility and the seat-to-head transmissibility, both of which had a resonance peak at about 5 Hz. The model incorporated linear stiffness and damping parameters at frequencies lower than 10 Hz, but nonlinear 'parabolic' damping between the pelvis (m_3) and the body (m_2) was used at frequencies higher than 10 Hz. The authors concluded that frequency-dependent active components (e.g. muscles) of the body should be included in the biodynamic models. However, this argument was based on the fact that the proposed passive linear model could not represent the responses of the human body at the full range of frequencies from 1 to 30 Hz which might not be the case in other studies.

Based on a single-degree-of-freedom model form, Mansfield (1998) used a linear quasi-static variable parameter procedure and a nonlinear quasi-static variable parameter procedure to predict the median apparent mass modulus at six magnitudes (0.25, 0.5, 1.0, 1.5, 2.0, 2.5 ms^{-2} r.m.s.) of broadband (0.5 to 20 Hz) random vibration. In the linear procedure, a set of mass, stiffness, and damping parameters was obtained by minimizing the error between the median apparent mass and the predicted apparent mass at all six magnitudes. Then the optimized parameters were fixed and one parameter at a time was allowed to vary to minimize the error at each magnitude. The researcher found that optimizing the stiffness and mass had greater effect of reducing the error than changing the damping. When optimizing all parameters, the error was further reduced – the stiffness and damping decreased with increasing vibration magnitude but the change in the sprung mass did not show a clear trend. The nonlinear procedure started with the optimized parameters determined by the linear procedure. Then one of the nonlinear parameters (a softening cubic spring, a nonlinear friction damper, a nonlinear sprung mass) at a time was allowed to change to minimize the error at each magnitude (Figure 2.55). The error was reduced by varying the stiffness or the sprung mass, but not the damping parameter. These simulation results suggested that the change in the apparent mass resonance frequency due to vibration magnitude could be caused by variations in the effective stiffness or in the effective sprung mass of the body, or both.

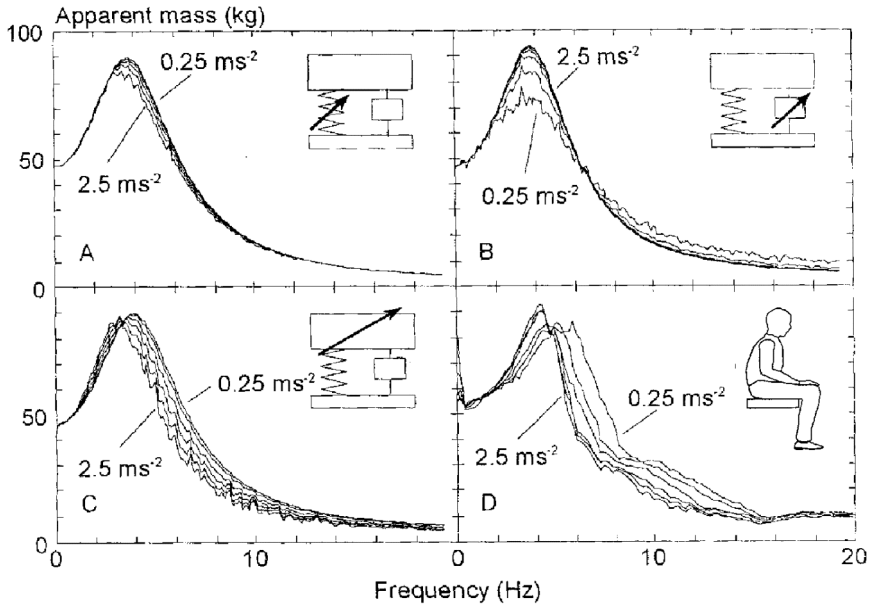

Figure 2.55 The predicted apparent masses at six magnitudes of vibration (0.25, 0.5, 1.0, 1.5, 2.0, 2.5 ms^{-2} r.m.s.) using the single-degree-of-freedom model by (A) varying the nonlinear stiffness only; (B) varying the nonlinear damping only; (C) varying the sprung mass; and (D) measured median apparent mass of twelve upright seated subjects. The nonlinear cubic spring force: $F_s = k\,x + K\,x^3$, where x is the relative displacement, k is the linear stiffness and K is the nonlinear component. The nonlinear friction damping force: $F_d = \pm\,(c\,|\,\dot{x}\,|\,+\,C)$, where c is the damping constant, C is the friction component, the sign of the force is always opposes the motion. The nonlinear inertial force exerted by nonlinear mass: $F_m = (m\ +\,|\,x\,|\,q\,M)\,\ddot{x}$, where m is the linear component, M is the nonlinear component of the mass proportional to displacement, q is a non-linear constant (Mansfield, 1998).

Modelling studies have been conducted using nonlinear geometric arrangements to incorporate nonlinear characteristics of the body. Hopkins (1971) modelled the nonlinear motion due to the geometry of the visceral mass by a non-rigidly attached visceral mass (Figure 2.56 a), and the nonlinear mechanisms of the lungs by a piston in a cylinder with an orifice (Figure 2.56 b). The two three-degree-of-freedom models had a similar 'dual' transmission path to that used by Muksian and Nash (1976). The models were used as mathematical tools to simulate the mechanical impedance and phase angle of the body measured with sinusoidal vibration of 1/2 to 1/4 G at frequencies 0 to 15 Hz. The author intended to include some nonlinear characteristics of the strain at the abdomen and the colon pressure when simulating of the mechanical impedance. But the effect of these nonlinearities was not defined or quantified in the mechanical impedance as the target fitting criteria.

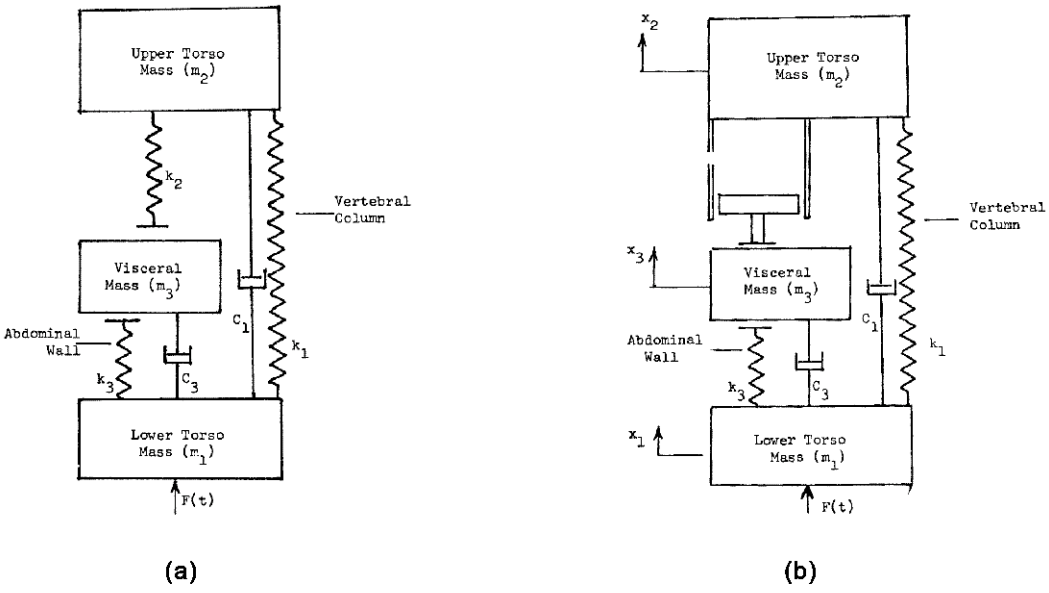

Figure 2.56 The nonlinear geometry models of the seated human body to incorporate: (a) nonlinear visceral mass motion reflected by the strain of the upper and lower abdomen; (b) nonlinear mechanism of the lungs reflected by the colon pressure (Hopkins, 1971).

The single-degree-of-freedom nonlinear model discussed above (Figure 2.55, Mansfield, 1998) showed that the characteristic nonlinearity in apparent mass due to vibration magnitude could be represented by a non-liner sprung mass. Mansfield (1998) developed the nonlinear mass concept into a physical inverted pendulum (Figure 2.57). The illustrative model was of a smaller scale comparing to the sitting weight of a human with a sprung mass of 2.7 kg, a stiffness of 160 N/m and an inclination of 20 degrees to the vertical. The apparent mass resonance frequency of the model decreased from 2.5 to 1.4 Hz while the vibration magnitude increased from 0.7 to 1.7 ms^{-2} r.m.s. The range of the model resonance frequency was different from that of the human subjects, whose median resonance frequency decreased from 5.4 to 4.2 Hz as the magnitude increased from 0.25 to 2.5 ms^{-2} r.m.s. The apparent masses of the model and the human subjects were compared based on a frequency ratio – the frequency was divided by the apparent mass resonance frequency at the lowest magnitude (Figure 2.58). The author noticed that the change in resonance frequency was larger for the model than for the subjects even a smaller range of magnitudes was used with the model. The author attributed this difference to the absence of dampers in the model to influence the angle of the pivoting arm. With damping, the sprung mass would move through smaller angles than without damping. Smaller angles would have narrower range of change in the stiffness and therefore narrower range of the resonance frequency of the model. Mansfield (1998) showed that the characteristic nonlinearity could be represented by

a nonlinear geometry of the sprung mass, but this could not testify that the inverted pendulum was the principal mechanism causing the nonlinearity in the human body. The nonlinearity observed between vertical vibration at L5 and vertical vibration at each location above L5 (Figure 2.42) suggested that the nonlinearity presented not only in the overall driving force (or apparent mass) but also at local sections of the body. The inverted pendulum might be suitable to simulate the effect of the nonlinearity on the apparent mass, but inadequate to explain the nature of the nonlinear responses found at different body locations.

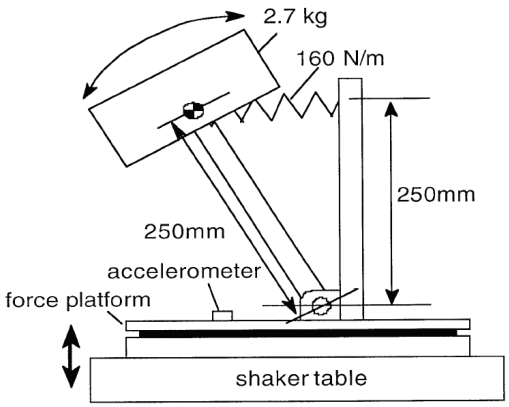

Figure 2.57 The single-degree-of-freedom inverted pendulum model to represent the nonlinearity in apparent mass resonance frequency due to vibration magnitude (Mansfield, 1998).

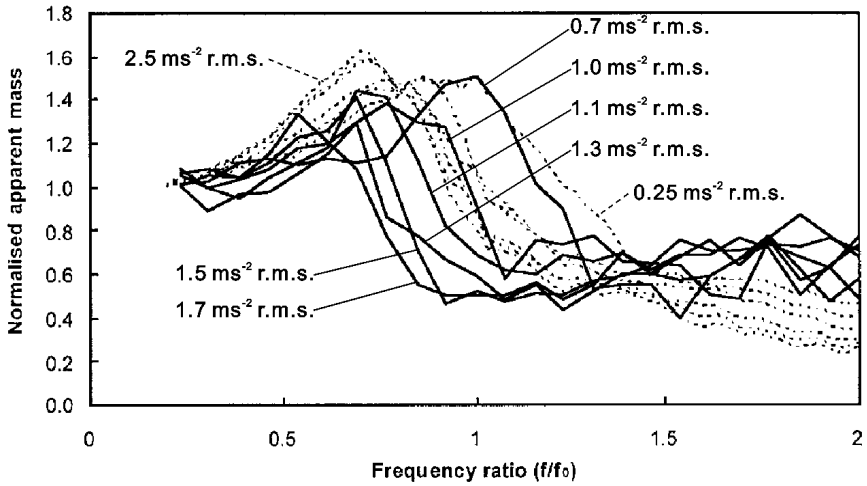

Figure 2.58 Comparison of the median normalised apparent mass of 12 upright seated subjects (- - -) exposed to 0.2 to 20 Hz random vibration at six magnitudes (0.25, 0.5, 1.0, 1.5, 2.0 and 2.5 ms^{-2} r.m.s.) with the responses of the inverted pendulum model (——) exposed to 0.5 to 20 Hz random vibration at six magnitudes: 0.7, 1.0, 1.1, 1.3, 1.5 and 1.7 ms^{-2} r.m.s. f is the frequency, f_0 is the apparent mass resonance frequency at the lowest magnitude, i.e. 0.7 ms^{-2} r.m.s. (Mansfield, 1998).

2.5.1.2 Models of the standing human body

Single- and two-degree-of-freedom quantitative models were developed to represent the apparent mass of standing subjects (Matsumoto and Griffin, 2003). The authors found that the two two-degree-of-freedom models, one with a serial form (Model 2a) and another with a parallel form (Model 2c), gave the best fit to the mean apparent mass and phase (Figure 2.59 c, e). Fittings of the data were better without the frame mass (m_0) especially in the phase – this was contrary to the parallel two degree-of-freedom model proposed for seated subjects by Wei and Griffin (1998a). The serial and the parallel two-degree-of-freedom models (Model 2a and Model 2c) showed equally good fits to the apparent masses and phases of twelve individual subjects. With increasing vibration magnitude from 0.25 to 2.0 ms^{-2} r.m.s., the serial model showed systematic decrease in both k_1 and k_2, while in the parallel model only k_2 decreased with each increase in vibration magnitude. In the parallel model k_2 corresponded to the primary resonance at around 5 Hz and k_2 corresponded to the secondary resonance at around 12 Hz. In the serial model, both k_1 and k_2 contributed to the primary resonance. The authors pointed out that the vibration magnitude had an effect mainly on the vibration mode responsible for the primary resonance.

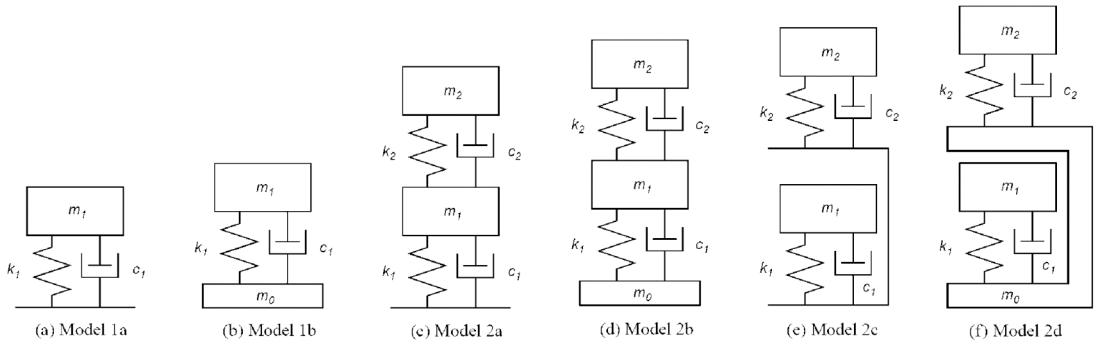

Figure 2.59 The single- (a, b) and two-degree-of-freedom (c, d, e, f) serial (c, d) and parallel (e, f) models used to represent the apparent mass of standing subjects with different postures and vibration magnitudes (Matsumoto and Griffin, 2003)

2.5.1.3 Models of the supine human body

A three-degree-of-freedom model of the horizontally flat supine subjects was developed to simulate the mechanical impedance and phase measured with vertical 2 to 20 Hz sinusoidal vibration at 0.5 G under five levels of lateral sustained acceleration (Figure 2.60, Vogt *et al.*, 1973). While increasing the sustained acceleration from 1 to 5 G, the optimized stiffness k_{211} and k_{11} increased

exponentially; the damping c_{211} and c_{11} increased linearly; the mass m_{211} and m_1 showed small increases.

Vogt *et al*. (1978) developed a multi-degree-of-freedom model based on the supine posture exposed to vertical 1 to 20 Hz sinusoidal vibration at 0.3 G with rigid mass attached to the top of the supine body (Figure 2.61). The model parameters were optimized by comparing the modulus and phases of the mechanical impedances and transmissibilities at the chest, abdomen and legs. The stiffness representing the abdomen and legs increased while adding the 4.54 kg rigid mass to the top of each part. But adding the rigid mass did not affect the stiffness of the chest. The author attributed this different response to the rib cage's greater ability to bear load with little change in the dynamic responses of the organs inside.

International Standard 5982 (1981) proposed a parallel three-degree-of-freedom model to represent the supine human body (Figure 2.62). The model parameters were obtained by comparing the mechanical impedance and phase of twelve supine subjects (62.2 to 104 kg) exposed to 0.5 to 31.5 Hz sinusoidal vibration at 1 to 2.5 ms^{-2} r.m.s.

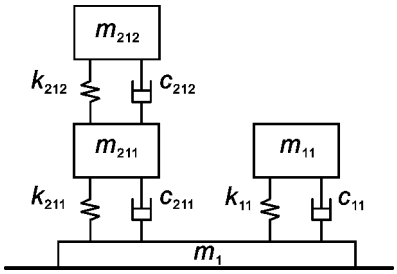

Figure 2.60 The three-degree-of-freedom model for the supine human body exposed to vertical 2 to 20 Hz sinusoidal vibration at 0.5 G under different levels (1 to 5 G) of sustained lateral acceleration produced by a centrifuge (Vogt *et al*., 1973).

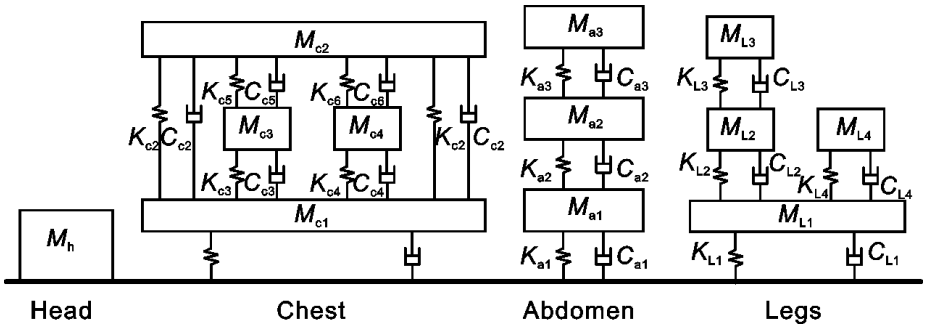

Figure 2.61 The multi-degree-of-freedom model for the supine human body exposed to vertical 1 to 20 Hz sinusoidal vibration at 0.3 G with and without a rigid mass attached on top of the body (Vogt *et al*., 1978).

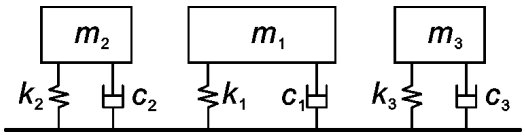

Figure 2.62 The three-degree-of-freedom model for the supine human body exposed to vertical 0.5 to 31.5 Hz sinusoidal vibration from 1 to 2.5 ms^{-2} r.m.s. (International Standard 5982, 1981).

2.5.2 Lumped parameter models in the horizontal direction

Quantitative models in the horizontal directions were proposed by Mansfield and Lundström (1999b) to represent the apparent masses and phases during fore-and-aft or lateral random vibration at 0.5 and 1.0 ms^{-2} r.m.s. (Figure 2.63). The model parameters were optimized by fitting the model responses to the experimental data reported by Mansfield and Lundström (1999a, Figure 2.33) and Fairley and Griffin (1990). The authors found the models with rigid support mass (m_0) gave better fitting results than those without. The model consisted of three parallel single degree-of-freedom systems with a rigid support mass (model 6) produced the best fit in both the fore-and-aft and lateral directions. The apparent mass modulus calculated by the model was in good agreement with measurement up to 10 Hz. But the calculated phase was in agreement with the measured phase only up to 4 Hz.

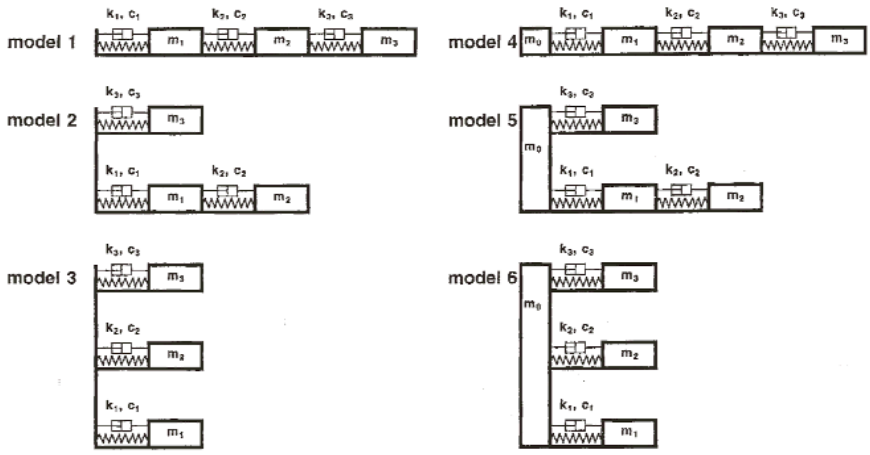

Figure 2.63 The three-degree-of-freedom models proposed to represent the apparent masses and phases of seated subjects exposed to fore-and-aft and lateral random vibration at 0.5 and 1.0 ms^{-2} r.m.s. (Mansfield Lundström, 1999b).

To quantify the fore-and-aft apparent mass and vertical cross-axis apparent mass and phase measured on the seat during fore-and-aft vibration, Nawayseh (2003) developed a three-degree-of-freedom model (Figure 2.64). The researcher found the final vertical model (Model 5 as shown in Figure 2.52) could not produce good

agreement with the measurements with fore-and-aft vibration especially the vertical cross-axis phase. The best fit was found by placing the vertical translational degree of freedom connecting with m_3 to the base.

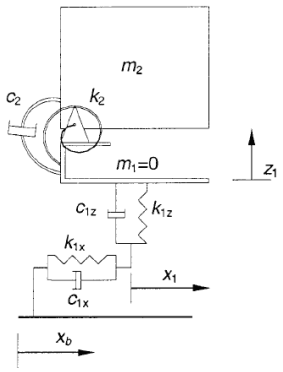

Figure 2.64 The three-degree-of-freedom model used to predict fore-and-aft apparent mass and vertical cross-axis apparent mass on the seat during fore-and-aft random vibration (Nawayseh, 2003).

A number of models incorporating fore-and-aft translational and rotational mechanisms were proposed by Abdul Jalil (2005) to represent the modulus and phase of the fore-and-aft apparent mass at the back (Figure 2.65). The experimental data were obtained by exposing twelve upright seated subjects to 0.25 to 10 Hz random fore-and-aft backrest vibration at 0.4 ms^{-2} r.m.s. After the model parameters were optimized by comparing the model responses with the experimental data, the models were used to estimate the fore-and-aft backrest transmissibility of car seat cushions with different pre-loads (50 to 200 N). With forces from the backrest applied to the segmental masses that could rotate, Model 3a and 4a exhibited better predictions of the backrest transmissibility than Model 1a and 2a.

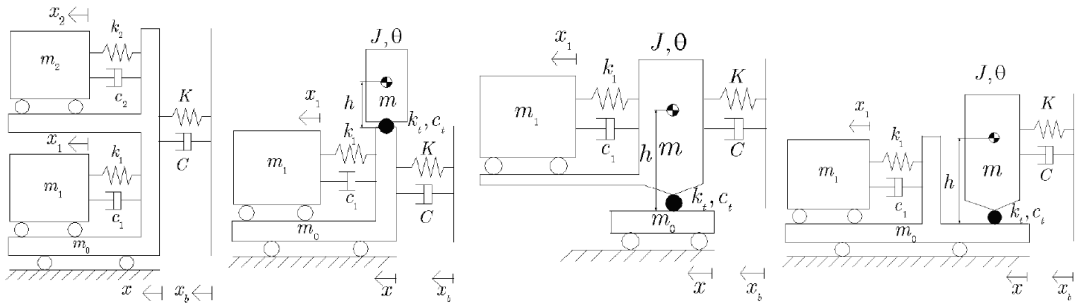

Figure 2.65 The models used to estimate the fore-and-aft apparent mass and backrest transmissibility during fore-and-aft vibration with the cushion model represented by *K* and *C* (Abdul Jalil, 2005).

2.6 Causes of the biodynamic nonlinearity

2.6.1 Summary of the most relevant biodynamic studies

It has been established that the resonance frequency in the frequency response functions (e.g. apparent mass and transmissibility) decreases with increasing vibration magnitude. This biodynamic nonlinearity has been found in the vertical and the fore-and-aft responses of the seated human body exposed to vertical whole-body vibration (e.g., Fairley and Griffin, 1989; Mansfield and Griffin, 2000; Matsumoto and Griffin, 2002a; Nawayseh and Griffin, 2003; Mansfield, 2006), in the fore-and-aft and the vertical responses of the seated human body exposed to fore-and-aft whole-body vibration (e.g. Fairley and Griffin, 1990; Mansfield and Lundström, 1999a; Holmlund and Lundström, 2001; Nawayseh and Griffin, 2005a; Abdul Jalil, 2005), and in the vertical and the fore-and-aft responses of the standing human body exposed to vertical whole-body vibration (e.g. Matsumoto and Griffin, 1998a; Subashi *et al*., 2006).

To identify the variables causing the nonlinearity, the effects of various steady-state sitting and standing conditions were studied, but the nonlinearity was found in all the conditions investigated.

The most relevant eight studies investigating the nonlinearity due to vibration magnitude are reviewed in this section. The first six studies using seated subjects and vertical vibration have been compared in terms of experimental conditions in Table 2.1 and resonance frequencies at various vibration magnitudes in Table 2.2. The last two of the eight studies used standing subjects. The review of each paper commences with a summary of the hypothesis and/or the hypothetical explanation of the characteristic nonlinearity.

1. Fairley and Griffin (1989)

The authors reported a softening effect with increasing vibration magnitude and suggested that a greater movement with high magnitudes of vibration may reduce the stiffness of the musculo-skeletal structure. A lesser change in the resonance frequency was observed at higher vibration magnitudes and it was suggested that subjects may involuntarily increase muscle tension to reduce the motion, or there may be limited ability to vary body stiffness.

The nonlinearity was found in apparent masses of all individual subjects with the primary resonance frequency decreasing from about 6 to 4 Hz as the vibration magnitude increased from 0.25 to 2.0 ms^{-2} r.m.s. The authors hypothesised that the reasons may be some combination of muscle activity or the dynamic properties of the human skeletal structure – similar to the nonlinear softening effect with

thixotropy, in which the stiffness of relaxed human tissues reduces during excitation (Lakie, *et al.*, 1979).

2. Mansfield and Griffin (2000)

The nonlinearity was observed along a transmission path common to the spine and the abdomen and the nonlinearity was suggested to be caused by a combination of factors: a) softening response of the buttocks tissue; b) bending or buckling response of the spine (i.e. a geometric nonlinearity – physically an inverted pendulum, see Figures 2.57 and 2.58); c) different muscular forces at different magnitude of vibration – a doubling of vibration magnitude did not result in a doubling of the muscle activity.

The principal resonance frequency in the apparent mass decreased from 5.4 to 4.2 Hz as the vibration magnitude increased from 0.25 to 2.5 ms^{-2} r.m.s. The nonlinearity in apparent mass was observed in the frequency range 3 to 16 Hz. The transmissibilities from the seat to the lower and upper abdomen wall were measured to investigate the cause of the primary apparent mass resonance frequency (Figure 2.38). It was concluded that the primary resonance of the human body consisted of several highly coupled modes (e.g. bending and buckling of the spine, pitching of the pelvis, and rocking of the abdomen). The authors attributed the nonlinearity to dynamics of buttocks tissue, geometric nonlinearity, and muscle activity, giving rise to 'a transmission path common to the spine and the abdomen'. They extended the causes of the characteristic nonlinearity from a previous study (Mansfield, 1998), which had rejected all other factors except geometric nonlinearity.

The fact that the lumbar spine vertical to abdomen vertical transmissibility was nonlinear might have suggested that the geometric nonlinearity was not the primary cause of the nonlinearity.

3. Matsumoto and Griffin (2002a)

It was concluded that the nonlinearity in apparent mass was not solely caused by the nonlinear geometric arrangements of the body. Softening characteristics in the passive soft tissues (i.e. thixotropy) and (voluntary and/or involuntary) muscle activity could primarily contribute to the nonlinearity.

The resonance frequency decreased from 6.4 to 4.75 Hz as the vibration magnitude increased from 0.125 to 2.0 ms^{-2} r.m.s. (Table 2.2). The transmissibilities of vertical seat to the vertical, fore-and-aft, and pitch axes along the spine, and to the pelvis, suggested that the bending or buckling of the spine and/or the softening effect of soft tissues along the spine might all contribute to the nonlinearity (see Figure 2.39 to 2.42).

4. Mansfield and Griffin (2002)

Insignificant changes in the nonlinearity were found over nine sitting conditions (Table 2.1 and Figure 2.3) of various postures (e.g. kyphotic, anterior and posterior lean), external constraints (e.g. abdominal belt), and contact conditions with the vibration source (e.g. pelvis support, backrest, inverted SIT-BAR and bead cushion).

The nine sitting conditions were designed to investigate the cause of the nonlinearity in the apparent mass (Figure 2.66). A similar nonlinearity was found in the seat-vertical-to-pelvis-rotation transmissibility. With the vibration magnitude at 0.2 and 1.0 ms^{-2} r.m.s. no significant difference in apparent mass resonance frequency was observed in the condition that controlled the rotation of the pelvis (pelvis support condition). Significantly higher resonance frequencies were reported in a condition with the visceral movement restricted ('belt' condition) at 0.2 and 2.0 ms^{-2} r.m.s. The anterior lean and the posterior lean conditions showed no significant change in apparent mass resonance frequency comparing with an upright posture, except for the anterior lean condition at 0.2 ms^{-2} r.m.s. Decreasing the contact area (increasing the pressure) at the buttocks tissue, by reducing the area of the seat surface (i.e. inverted SIT-BAR), decreased the apparent mass resonance frequencies at 1.0 and 2.0 ms^{-2} r.m.s. Differences in the nonlinearity were found in some of the postures, however, they were mainly small and inconsistent, and therefore difficult to interpret.

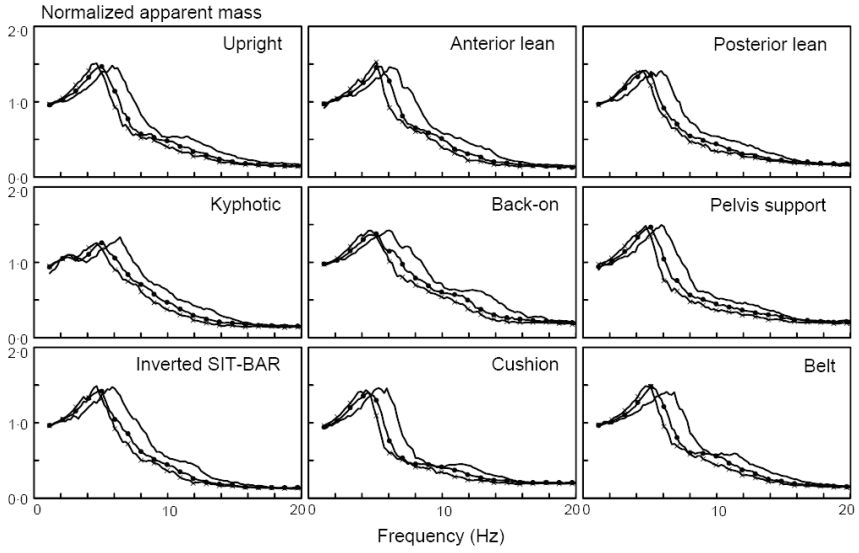

Figure 2.66 Median normalized apparent masses for 12 subjects in nine sitting conditions (see Figure 2.3) exposed to 1.0 to 20 Hz random vertical vibration at 0.2 (——), 1.0 (—●—), and 2.0 (—x—) ms^{-2} r.m.s. (Mansfield and Griffin, 2002).

5. Matsumoto and Griffin (2002b)

With broadband random vertical vibration, a slightly reduced degree of nonlinearity was found with increased muscle tension in the buttocks and abdomen (Figure 2.67). The subjects were instructed only to tense the buttocks or to minimize the abdomen with an upright sitting posture. The increased muscle tension was designed to decrease the involuntary changes in muscle activity during vibration. This small change in the nonlinearity might suggest that involuntary changes in muscle activity could alter the nonlinearity. However, the nonlinearity in the fore-and-aft cross-axis apparent mass was not affected by changes in muscle tension.

With sinusoidal excitations in this study, the changes in the nonlinearity were compared by testing the statistical difference between the magnitudes of the apparent mass modulus and phase at different vibration magnitudes and discrete frequencies. Increasing muscle tension at the buttocks showed slightly less degree of nonlinearity during the sinusoidal vibration.

The small effect of muscle tension has been confirmed by Mansfield *et al*. (2006) with 2.0 to 20 Hz random vertical vibration at 0.5, 1.0, and 1.5 ms^{-2} r.m.s.

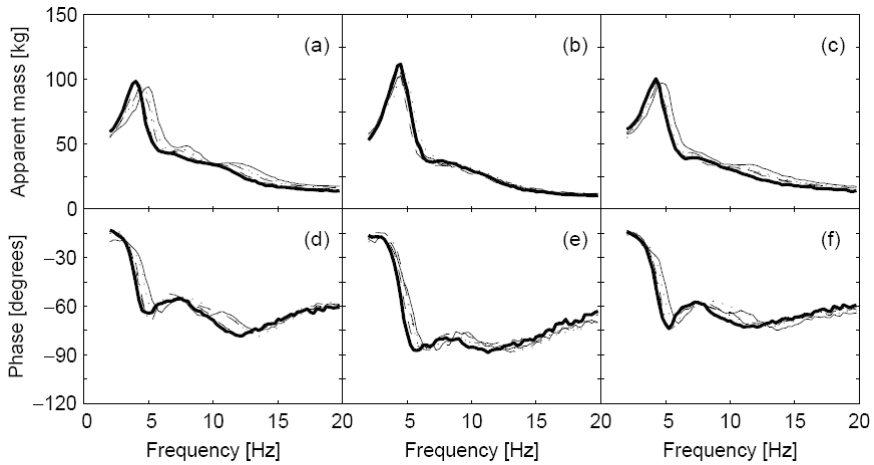

Figure 2.67 Apparent masses and phases of a subject in normal upright (a and d), buttocks tensed (b and e) and abdomen minimized (c and f) sitting conditions exposed to 2.0 to 20 Hz random vertical vibration at five magnitudes: 0.35 (——), 0.5 (· · · ·), 0.7 (— · —), 1.0 (— —), and 1.4 (**——**) ms^{-2} r.m.s. (Matsumoto and Griffin, 2002b).

6. Nawayseh and Griffin (2003)

During vertical random vibration, the nonlinearity was found to be slightly reduced when there was increased pressure in the buttocks tissues. This suggested that the dynamics of the buttocks tissues contributed to the nonlinearity.

The authors found the minimum thigh contact posture gave less degrees of nonlinearity than the maximum thigh contact and the feet hanging postures at the two highest magnitudes (0.625 and 1.25 ms^{-2} r.m.s., Figure 2.68). The pressure of the tissues beneath the ischial tuberosities was controlled by varying the thigh contact area (raising or lowering the feet).

The nonlinearity was also found in the cross-axis apparent mass in the fore-and-aft direction. However, changing the pressure in the buttocks did not affect the nonlinearity in the cross-axis apparent mass resonance frequency, consistent with the findings of Matsumoto and Griffin (2002b).

With the same thigh contact postures but fore-and-aft vibration, Nawayseh and Griffin (2005a) found the fore-and-aft apparent mass at the seat to be less nonlinear with the average thigh contact or minimum thigh contact condition than the feet hanging or maximum thigh contact condition (Figure 2.25). The changes in the nonlinearity were compared by testing the statistical difference between the fore-and-aft apparent mass magnitudes at different magnitudes and discrete frequencies.

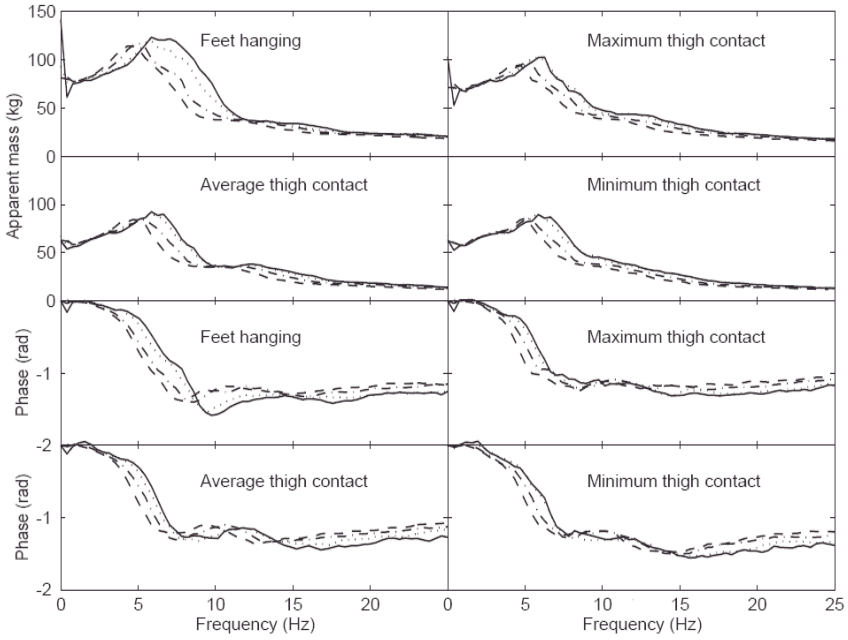

Figure 2.68 Median apparent mass and phase of 12 subjects in four feet height sitting conditions exposed to 0.25 to 25 Hz random vertical vibration at four magnitudes: 0.125 (——), 0.25 (· · · ·), 0.625 (— · —), and 1.25 (— —) ms^{-2} r.m.s. (Nawayseh and Griffin, 2003).

7. Matsumoto and Griffin (1998a)

The nonlinearity found in the apparent mass and transmissibilities to the spine, pelvis and knee of standing subjects suggested that these nonlinear responses could be caused through a transmission path common to the spine and the knee. For example, the dynamics of the tissues beneath the foot and the dynamics of the lower legs might have contributed to the nonlinearity found at the spine and the knee.

The nonlinearity was found in the apparent mass and transmissibilities to the spine, the pelvis and the knee with the normal upright standing and the legs bent posture (Figure 2.21 and 2.44). With legs bent, the effect of vibration magnitude on apparent mass resonance frequency was slightly smaller than that with normal upright standing. The fore-and-aft transmissibility at the knee was nonlinear and exhibited a similar peak frequency range as the apparent mass. With one leg standing, the nonlinearity was found in the pelvis transmissibility but not clear in the apparent mass. The small change in the nonlinearity might be caused by the different leg postures involving activities of different muscle groups and/or the altered dynamic property of the soft tissues along the vibration transmission paths.

8. Subashi et al. (2006)

Compared with an upright standing posture, lordotic, anterior lean, and legs bent postures exhibited slightly less nonlinearity in apparent mass (Figure 2.22). The authors attributed the insignificant change in the nonlinearity to some modified muscle activity similar to that found by Matsumoto and Griffin (2002b) using upright seated subjects. The lordotic and anterior lean postures might have increased the muscle tension at the abdomen. The legs bent posture might have modified the muscle groups which stabilize the posture by some voluntary or involuntary muscle activity.

The primary resonance frequency of the fore-and-aft cross-axis apparent mass was found to be close to that of the apparent mass. With different standing postures, the cross-axis apparent mass was nonlinear but the nonlinearity was less clear than that of the apparent mass. The nonlinearity in the cross-axis apparent mass was not affected by any of the standing postures. The nonlinear responses in the vertical and the fore-and-aft cross axes might have different causes.

9. Summary

From the studies reviewed above, three explanations have been proposed as the causes of the nonlinearity: the geometric nonlinearity of the body, the voluntary and/or involuntary muscle activity, and the passive thixotropy of tissues.

If the nonlinearity is caused by the nonlinear geometric characteristics of the human body, it should be possible to model the nonlinearity in the apparent mass and the transmissibilities to various body locations along the spine and pelvis. But such a model has not been found.

During vibration, voluntary and/or involuntary muscle activity is required to stabilize the body and to maintain the sitting or standing posture. Different vibration magnitudes would produce different inertial forces in the body. The muscle activities could vary with these different inertial forces resulting in different stiffness of the body at different magnitudes.

Thixotropy of soft tissues, in which the stiffness of tissues reduces during, or immediately after, excitation could have caused the nonlinear responses at various body locations and with different sitting and standing postures. It has been suggested that the buttocks tissues are associated with the vertical and fore-and-aft cross-axis mode of the body at the primary resonance. A softening thixotropic behaviour in the buttocks could have contributed to the nonlinearity found in both vertical and fore-and-aft cross-axis responses of seated persons.

The following sections discuss the two most probable causes of the nonlinearity: voluntary and/or involuntary muscle activity, and the passive thixotropy of body tissues.

2.6.2 Voluntary and involuntary muscle activity

Voluntary and involuntary muscle activity may both be activated during vibration, and are related to ‘tonic’ and ‘phasic’ responses of muscles. ‘Voluntary’ refers to conscious contractions of muscles by some central mechanism, while ‘involuntary’ describes the unconscious contractions. Postural muscles are involved in supporting the body with ‘tonic’ activity (i.e. a state of continuous contraction) during static sitting and static standing. During vibration, in order to stabilize the body in the presence of the externally applied motion, muscle activity varies with a ‘phasic’ response (i.e. muscles try to react and synchronize the inertial forces due to the oscillatory motions). Both voluntary and involuntary muscular activity can produce the phasic response; however, voluntary phasic contractions may only be effective

at low frequencies (i.e. below about 1 to 2 Hz). The tonic muscle activity is mainly provided by voluntary contractions.

A disproportionate change in the overall magnitude of the phasic activity of muscles with increasing vibration magnitude could cause the nonlinearity. The phasic muscular activity measured by electromyography (EMG) increases with increasing vibration magnitude (Robertson and Griffin 1989). But this increase in phasic muscular activity was not proportional to the increase in vibration magnitude (see Figure 2.69). Increased vibration magnitude will require increased tonic and phasic muscle activity to stabilize the body. Phasic muscular activity could have an upper limit in generating the dynamic force governing the stiffness of the body. As the vibration magnitude increases, the increase in muscular activity will become closer to its upper limit and disproportional to the increase in vibration magnitude. Increased tonic activity by voluntary increases in constant muscle tension did not affect the nonlinearity much (e.g. Matsumoto and Griffin, 2002b), possibly because the phasic activity was not changed.

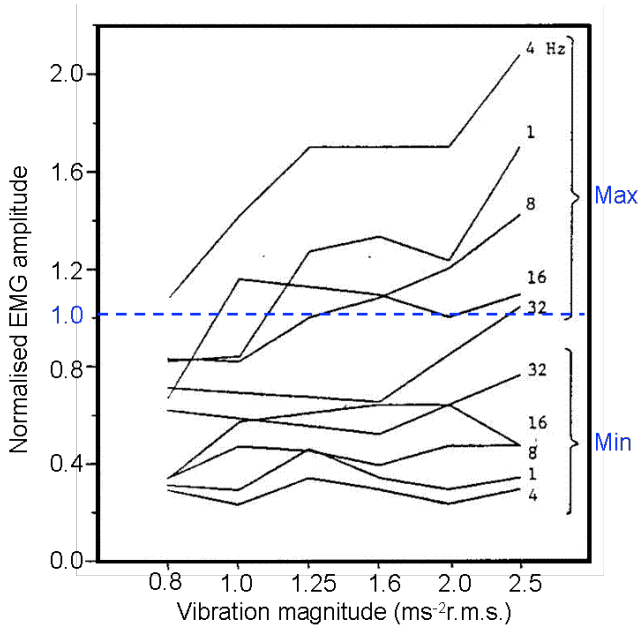

Figure 2.69 Mean normalised electromyographic (EMG) amplitudes (Max: peaks; Min: troughs) of four seated subjects exposed to 1, 4, 8, 16, and 32 Hz sinusoidal vertical whole-body vibration at 0.8, 1.0, 1.25, 1.6, 2.0 and 2.5 ms^{-2} r.m.s. (Robertson and Griffin, 1989).

Increased time lag of the phasic muscle activity due to increased vibration magnitude could also cause the nonlinearity with a 'reversal effect' such that the peak phasic muscle force could occur at the trough of the input acceleration. Blüthner *et al*. (2002) measured the EMG activities of the lumbar multifidus and the long lumbar spinae muscles, which were thought to influence the biodynamic responses of the body. The authors found the time lags shorter with lower magnitudes of vibration (Figure 2.70). The increased reversal effect with increased vibration magnitude could cause the dynamic force generated by muscles controlling the body movement disproportional to the increase in vibration magnitude, resulting in a decrease in dynamic stiffness of the body.

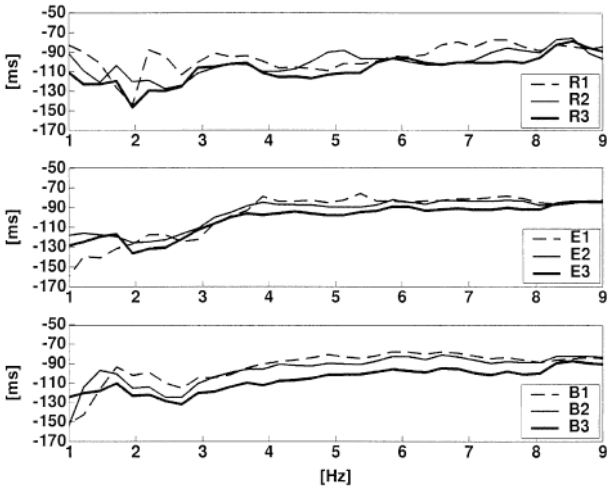

(a)

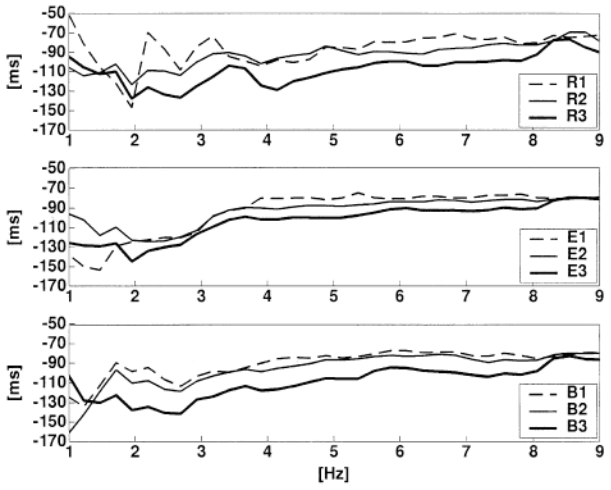

(b)

Figure 2.70 Time lags of the transfer function from the seat to the mean processed EMG measured at the m. longissimus thoracis pars lumborum (a) and the m. multifidus (b) with three sitting postures (R – relaxed; E – erect; B – bent-forward) during three levels of ISO (2631, 1985) weighted vertical vibration at 0.7 (— —: 1), 1.0 (——: 2) and 1.4 (▬▬: 3) ms^{-2} r.m.s. (Blüthner *et al*., 2002).

2.6.3 Passive thixotropy of body tissues

A thixotropic behaviour of the musculo-skeletal structure has been speculated to be a cause of the nonlinear change in the dynamic stiffness of the body during whole-body vibration by Fairley and Griffin (1989). However, no experimental evidence has been provided.

The origin of 'thixotropy' refers to some recovery behaviour of colloidal materials after some breakdown of structural linkages (Tanner, 1985). Perturbations break down structures but after a period of stillness the structures reform. Some human body tissues (protoplasm, mucus, etc.) have a similar thixotropic behaviour (Fung, 1981). Lakie (1986) found that the resonance frequency of the relaxed human finger was about 11.7 Hz after 1 second of a prior impulse tap excitation and 13.7 Hz after 5 seconds of the excitation (Figure 2.71) – a typical softening behaviour consistent with the nonlinear change in dynamic stiffness of the body in response to increased magnitudes of vibration. Since then the thixotropy has been used to describe as passive dynamic property of human tissues. The nature of thixotropy is such that the stiffness of the relaxed body tissues reduces during and immediately after prior high magnitudes of excitation, while the stiffness increases during and immediate after prior low magnitudes of excitation. In other words, the dynamic stiffness of tissues depends on the 'shear history' (i.e. velocity) of the excitation. Lakie (1986) has suggested that the vibration had the effect of immediately reducing the stiffness, and the degree of the reduction was dependent on the size of the movement. This coincides with the fact that the nonlinearity is always clearer at the principal resonance frequencies of the body, where the greatest body movement occurs. Although the responses of relaxed human muscles have been reported to be typical of thixotropy, different tonic or phasic muscle activity may affect the degree of the thixotropic effect. Almost all previous biodynamic studies of whole-body vibration at different vibration magnitudes used seated or standing postures which involve a degree of muscular activity for stabilization and postural control. This type of posture made the examination of the thixotropy effect during whole-body vibration difficult. Whereas thixotropy could present in activated muscles, there is always a doubt that muscular activity may have contributed to the biodynamic response of the body.

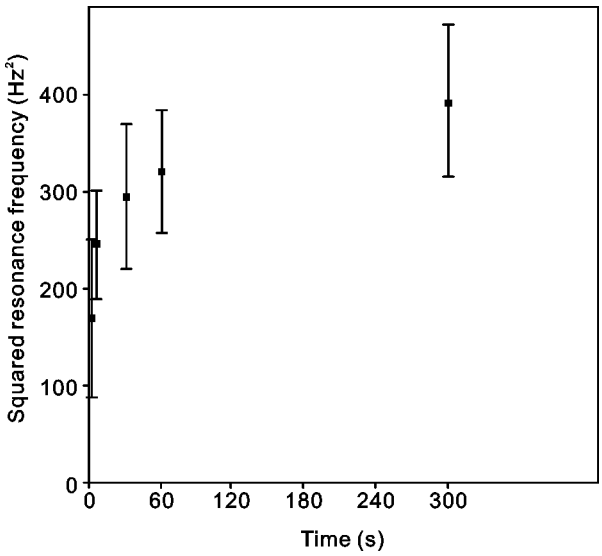

Figure 2.71 Finger stiffness: mean and standard deviations of the squared resonance frequencies (proportional to stiffness) of 11 subjects measured after a prior tap impulse excitation with a resting time of 1, 5, 30, 60, 300, and 600 seconds. The stiffness increased rapidly in the first 30 seconds. Individual results showed parallel patterns (Lakie, 1986).

An intermittent stimulus alternately at a high magnitude and a low magnitude allows the dynamic stiffness of the body to be measured after an immediately preceding low magnitude and after an immediately preceding high magnitude excitation. This would show whether during whole-body vibration the body has a similar thixotropic behaviour as individual relaxed muscles. With upright seated subjects, Mansfield (1998) found no significant difference between the resonance frequencies of the apparent masses measured with continuous random vibration and an intermittent random vibration alternated at 0.2 and 2.0 ms^{-2} r.m.s. This might be because that each of the high and low magnitude sections lasted for 60 seconds and the stiffness recovery time constant for the whole body could be smaller than that measured with the finger (Lakie, 1986). For example, the body might only take a couple of seconds to recover. Therefore, the measured responses during the 60 seconds did not reflect the stiffness of the body immediate after prior change in vibration magnitude, or shear history.

Different from the voluntary or involuntary muscle activity which is ‘active’ in controlling the body movement, thixotropy is a ‘passive’ property of tissues. The cause of the thixotropy in muscle tissues is thought to be the breakdown of the bonds between actin and myosin (Hill, 1968). Myosin and actin are contractile proteins in muscles. The thick myosin filament in the isotropic (I) band is overlapped by the thin actin filament in the anisotropic (A) band (Figure 2.72). A large muscle

protein called titin was found to be the primary contributor to the stiffness of relaxed muscles (Wolfgang *et al.*, 1996). The stiffness of the titin protein is dependent on its length. For example, some sections of the titin, such as the 'PEVK' and 'poly-Ig', are suggested to contribute to tissue stiffness. The nonlinear softening effect observed with the relaxed or partially contracted muscles could be due to a combination of the dynamic properties of the passive titin filament and the active contractile myosin and actin filaments. The titin filament could have a high stiffness in response to low magnitudes of excitation but a reduced stiffness during high magnitudes of excitation. Likewise, the breakdown of the myosin-actin bonds develops during high magnitudes of vibration due to high levels of inertial forces, and these bonds recover with increased tissue stiffness during low magnitudes of vibration or stillness. A totally relaxed 'switched-off' muscle fibre would be more likely to breakdown than an activated 'switched-on' fibre. The thixotropy of the body could be influenced by such contractile status of muscle tissues. A small change in the nonlinearity with different muscle tension at the buttocks or abdomen of seated subjects (see Matsumoto and Griffin, 2002b) could be caused by altered contractile status of muscle tissues and therefore altered thixotropy in the body tissues.

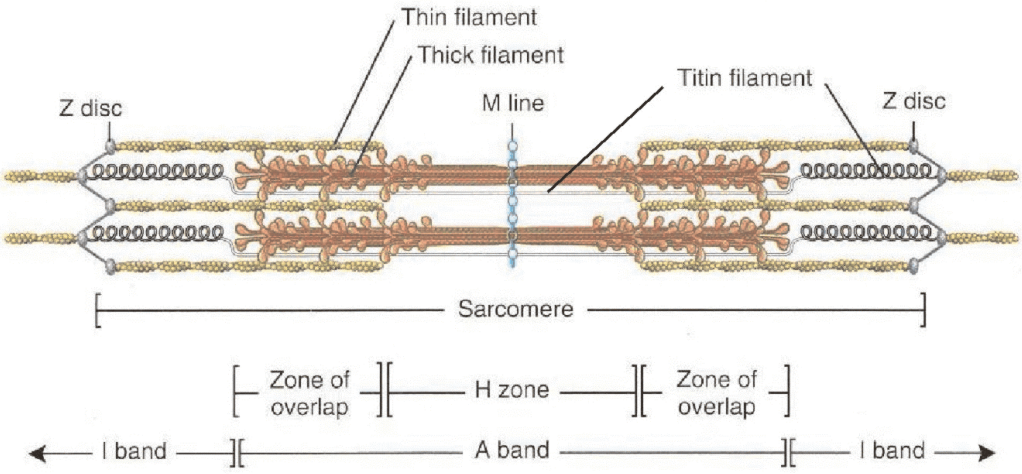

Figure 2.72 The arrangement of filaments within a sarcomere. Narrow, plate-shaped regions of dense material called Z discs separate one sarcomere from the next; a narrow H zone in the centre of each A band contains thick but no thin filament; supporting proteins that hold the thick filaments together at the centre of the H zone form the M line (Tortora and Grabowski, 2003).

Thixotropy has been found in different parts of relaxed human muscle tissues: the wrist (Lakie *et al*., 1979), finger extensor (Lakie, 1986) and flexor (Hagbarth *et al*., 1985; Lakie, 1986), and the relaxed rib cage respiratory muscles (Homma and Hagbarth, 2000). Dynamic responses of skeletal structure depend not only on behaviour of muscles but also soft connective tissues between the skeletal parts, such as the collagen fibres in the cartilage and the annulus fibres in the intervertebral discs. Not many studies have investigated whether the responses of skeletal structures, such as the spinal column and the rib cage, have thixotropic behaviour. But studies reported in the literature have looked at the micro structure and mechanical property of body tissues and implied similar thixotropic behaviour presented in these connective tissues (e.g. Fung, 1981).

2.7 Conclusions

The biodynamic responses of the human body have been studied for about half a century, but there is no study that has revealed the cause of the biodynamic nonlinearity due to vibration magnitude. Previous studies investigating the nonlinearity during whole-body vibration provide speculations and hypothesis about the causes, but there has been no experimental proof.

This thesis aims to discover the principal mechanism(s) causing the biodynamic nonlinearity (in apparent mass and transmissibility) of the human body during whole-body vibration. Section 2.6 above summarizes the possible causes of the nonlinearity and suggests that some active muscle activity or some passive property of soft tissues (i.e. thixotropy) could be the primary cause(s). The present studies are primarily designed to test these two hypotheses.

Previous studies were designed to identify conditions that could significantly change the nonlinearity, but such conditions have not been identified. A number of steady-state sitting conditions have been investigated: different upper-body postures and seat-subject interface contact conditions (Mansfield and Griffin, 2002), increased buttocks or abdomen muscle tension (Matsumoto and Griffin, 2002b), increased pressure at buttocks by raising the footrest height (Nawayseh and Griffin, 2003). But the changes in nonlinearity in these studies were found to be insignificant or inconsistent. Studies measuring the back muscle (EMG) activity show that the magnitude and timing of the muscle activity in response to vibration is dependent on the magnitude of vibration (Robertson and Griffin, 1989; Blüthner *et al*., 2002). If muscular activity primarily causes the nonlinearity, decreasing the muscle activity in response to vibration would decrease the nonlinearity. The effect of voluntary periodic contraction of postural muscles, for instance at the back and at the

abdomen, on the dynamic stiffness of the body during whole-body vibration has not been studied. Assuming voluntary periodic contraction decreases the muscular response to vibration, the nonlinearity would be reduced during such voluntary contraction. In this thesis, the first study was designed to identify a series of voluntary periodic movement conditions that significantly change the nonlinearity (Chapter 4).

Previous studies investigating the nonlinearity used sitting or standing conditions which required considerable muscular postural control of posture. Some relaxed conditions, such as a supine postures, allow the dynamic responses of the body to be measured when there is minimal, or at least reduced, active muscle control. This allows further investigations of the passive thixotropy during whole-body vibration.

According to studies showing thixotropic behaviour of relaxed human muscles, the stiffness of a thixotropic system depends on a recovering time constant immediately after excitation (Figure 2.71, Lakie, 1986). The stiffness is reported to increase rapidly in the first 30 seconds. However, Mansfield (1998) found there was no significant effect of an intermittent vibration alternated at 2.0 and 0.2 ms^{-2} r.m.s. (with each lasted for 60 seconds) on the stiffness of the seated body during whole-body vibration. One possible reason for the absence of the typical thixotropy in Mansfield's study is that the stiffness recovery time constant for the whole body could be very short, for example around a second. A second study in this thesis compares the dynamic stiffness of the relaxed supine human body during vertical continuous and intermittent vibration alternately at a high and a low magnitude with each lasting for only a couple of seconds (Chapter 5). This would confirm whether the behaviour of the body is consistent with thixotropy during whole-body vibration.

The nonlinearity has been extensively reported not only during vertical excitation but also during horizontal excitation (e.g. Mansfield and Lundström, 1999a; Nawayseh and Griffin, 2005a; Abdul Jalil, 2005). A study reported in Chapter 6 investigated the effect of intermittent vibration on the relaxed supine body during longitudinal horizontal vibration.

Harmonic distortions of the dynamic force measured at the excitation-subject interface during vertical sinusoidal vibration were found to increase with increasing vibration magnitude (Mansfield, 1998). The distortions can relate to the nonlinear biodynamic response of the body. A study investigated the frequency and magnitude dependence of harmonic distortions of the dynamic force by using the relaxed supine posture during vertical and longitudinal horizontal sinusoidal vibration (Chapter 7). It was assumed that any contribution of the muscular activity to the harmonic distortions would be eliminated with the supine posture.

Studies measuring the transmission of vibration to various locations along the spine and the pelvis show that the resonance in apparent mass is primarily caused by some rocking mode of the entire body associated with the deformation of the buttocks tissues, bending of the spine and pitching the pelvis (e.g. Kitazaki and Griffin, 1998; Matsumoto and Griffin, 1998b). The biodynamic nonlinearity is closely related to several resonance modes of the body. The transmissibilities measured along the spine and around the abdomen of seated subjects with different vibration magnitudes suggest that the nonlinearity arises from some 'common transmission path', such as the tissues beneath the pelvis (Mansfield and Griffin, 2000; Matsumoto and Griffin, 2002a). The transmissibility measured with relaxed supine subjects would allow the identification of the resonance modes and the common transmission path with minimal interference from voluntary or involuntary muscle activity (Chapter 8).

According to both the active muscle activity hypothesis and the passive thixotropy hypothesis, the nonlinearity is caused by body tissues, including muscles. A vibration transmission path that consists of more soft tissues would yield a more nonlinear response; while a transmission path consisting of more hard skeletal structures would behave less nonlinearly. It is difficult to separate the two types of transmission paths by measuring the transmissibilities with a seated or standing subject. The common transmission path (i.e. the buttocks) contains large amounts of soft tissue which are suggested to cause the nonlinearity (Mansfield and Griffin, 2000; Matsumoto and Griffin, 2002a). The subject contact interface of the relaxed supine posture, however, bypasses the buttocks tissues. The transmissibility measured to the abdomen of supine subjects would be dominated by responses of soft tissues, while the transmissibility measured to the sternum would mainly represent the responses of the joints of the skeletal structures (Chapter 8).

Although inconsistent, some studies show that the nonlinearity tends to be more significant at lower magnitudes of vibration (e.g. Mansfield and Griffin, 2000; Matsumoto and Griffin, 2002a; see Figure 2.16). The degree of the nonlinearity is explored at extremely low magnitudes of vibration (e.g., less than 0.125 ms^{-2} r.m.s.) in Chapter 8.

Various lumped-parameter mathematical models have been proposed to represent the mechanisms causing the resonance modes of the body (e.g. Wei and Griffin, 1998a; Matsumoto and Griffin, 2001; Nawayseh, 2003). These models have the advantages of simple forms and being able to characterize the dynamic response of the body over the full measuring frequency range. By this means, the nonlinearity can be quantified not only by the resonance frequency but also the model

parameters describing the dynamic response of the body over wide frequency ranges (see Chapter 3). Some other models were designed to describe the nonlinearity (e.g. Smith, 1994; Mansfield, 1998). Lacking knowledge about the properties of living human tissues and the relationship between the muscular activity and the dynamic property of the whole body, these models need the measured responses of human subjects at various vibration magnitudes to obtain the model parameters. Having identified the causal mechanisms of the nonlinearity, it would be possible to propose mechanistic models that can 'predict' the responses at different vibration magnitudes.

In conclusion, the literature review reveals that the nonlinearity, in which the resonance frequencies in frequency response functions decrease with increasing vibration magnitude, is most likely to be caused by either some muscle activity or some passive thixotropic behaviour of soft tissues, or both. Previous studies have speculated upon these hypotheses but no conclusive experimental evidence during whole-body vibration has been provided. Various experimental conditions have been employed to change the nonlinear response, but the effects of these variations in conditions were found to be small or inconsistent. Models designed to represent the nonlinear response have been developed but without considering the mechanistic nature of the nonlinearity. This limits the capacity of any biodynamic model trying to 'predict' the response at various magnitudes.

Chapter 3

Apparatus and analysis

3.1 Introduction

This chapter describes the apparatus and data analysis methods used in this thesis. All the experiments were conducted in the laboratory of the Human Factors Research Unit (in the Tizard Building, i.e. Building 13), the Institute of Sound and Vibration Research, University of Southampton. All experiments were approved by the Human Experimentation, Safety and Ethics Committee of the Institute of Sound and Vibration Research at the University of Southampton advised by British Standards Institution (1987) BS 6841 and Guide to Experimentation involving Human Subjects (1996).

3.2 Vibrators

3.2.1 1-metre vertical electro-hydraulic vibrator

The vibrator was used to produce vibration in the vertical direction (i.e., *z*-axis of an upright seated subject or *x*-axis of a supine subject). The 1-metre vertical electro-hydraulic vibrator was capable of accelerations up to ±10 ms^{-2}, a peak-to-peak displacement of 1 m, a dynamic load of 10 kN with a preload of 8.8 kN in the vertical direction. A 150.0 x 89.0 x 1.5 cm aluminium alloy vibrator platform was bolted rigidly on to the top of the vibrator. Experimental equipments, such as force platform, accelerometers, seat, footrest, supine back support, headrest and leg rest, were mounted rigidly onto the aluminium alloy platform (Figure 3.1).

3.2.2 1-metre horizontal electro-hydraulic vibrator

The vibrator was used to produce vibration in the longitudinal horizontal (i.e., *z*-axis) direction of supine subjects. The vibrator was capable of a peak-to-peak displacement of 1 m in the horizontal direction. A 150.0 x 100.0 x 1.9 cm aluminium alloy vibrator platform was mounted on the upper carriage frame, which was driven by a servo-hydraulic actuator. Experimental equipment was mounted rigidly on the aluminium alloy platform (Figure 3.2).

The harmonic distortions in sinusoidal input acceleration of the 1-metre vertical and the 1-metre horizontal vibrator were presented in Figure 7.10 a, b in Chapter 7. Without any input motion, the background noise motion presented on the 1-metre vertical vibrator had a magnitude of 0.017 ms^{-2} r.m.s., on the 1-metre horizontal vibrator 0.021 ms^{-2} r.m.s.

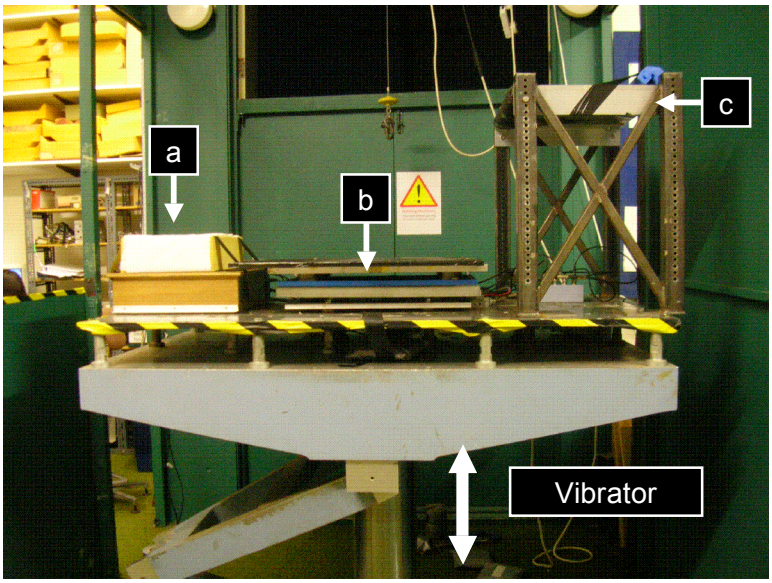

Figure 3.1 A photographic representation of the 1-metre vertical vibrator showing the head rest (a), the force platform with the supine back support attached on its top (b), the leg rest (c) mounted on the 150 x 89 x 1.5 cm aluminium alloy platform, and the travel direction.

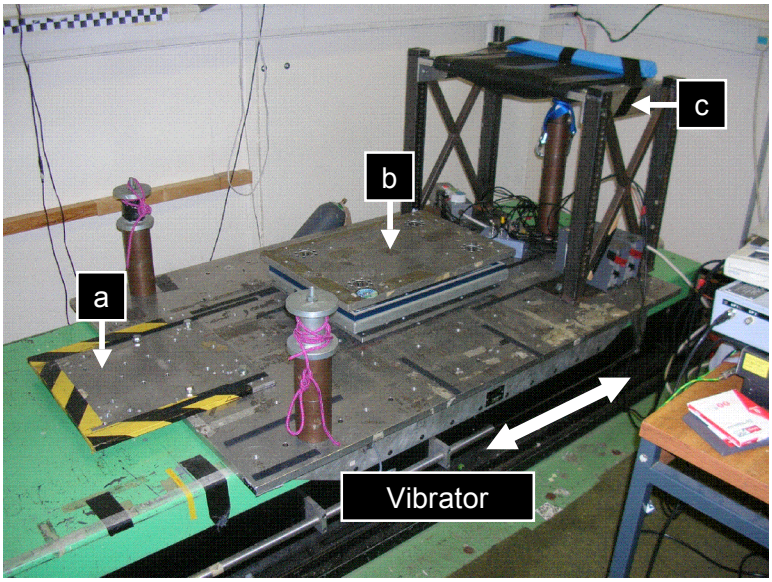

Figure 3.2 A photographic representation of the 1-metre horizontal vibrator showing the extension to accommodate the head rest (a), the force platform (b), the leg rest (c) mounted on the 150.0 x 100.0 x 1.9 cm aluminium alloy platform, and the travel direction.

3.3 Transducers

The excitation acceleration at the vibrator platform and the dynamic forces at the seat-subject interface in the direction of excitation and in the direction perpendicular

to the excitation in the mid-sagittal plane were measured to calculate the apparent mass and the cross-axis apparent mass respectively. Accelerations were also measured at the locations on the body where transmissibilities were calculated.

3.3.1 Accelerometers

In all experiments, the input motion on the vibrator platform was measured and monitored using a capacitive Setra 141A ±2 g accelerometer (Figure 3.3 e). In the case of vertical vibration, the longitudinal horizontal cross-axis acceleration was measured, by using an identical Setra 141A ±2 g accelerometer (Figure 3.3 d), to monitor the cross-axis non-rigidity of the 1-metre vertical vibrator in this direction. The two accelerometers had a sensitivity of approximately 250 mV/g with an operating range of ±2 g.

In a study investigating transmissibilities of the supine body (see Chapter 8), accelerations at the sternum and upper and lower abdomen in the mid-sagittal plane of the supine body were measured using three piezo-resistive accelerometers. These were two identical Endevco 2265-10M2 ±10 g accelerometers (with sensitivities of approximately 34 and 38 mV/g, Figure 3.3 b, c) and one Endevco 2265-20 ±20 g accelerometer (with a sensitivity of approximately 32 mV/g, Figure 3.3 a). The three accelerometers had the same size and weight. The three accelerometers were attached separately to the buckles of three elastic belts via three pieces of 27 x 17 x 2 mm rigid plywood (Figure 3.3). The three identical accelerometer-plywood-buckle blocks were then attached to the skin of the upper and lower abdomen and the sternum. The mounting of these accelerometers and the analysis of the local tissue-accelerometer system is presented in Chapter 8.

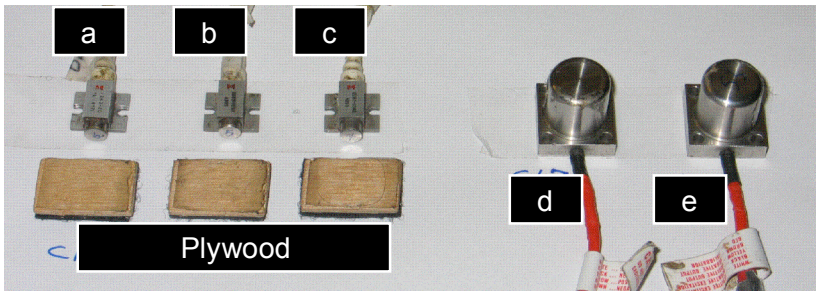

Figure 3.3 Accelerometers used to measure accelerations at: (a) lower abdomen (Endevco 2265-20 ±20 g); (b) upper abdomen (Endevco 2265-10M2 ±10 g); (c) sternum (Endevco 2265-10M2 ±10 g); (d) vibrator platform in the longitudinal horizontal direction during vertical vibration (Setra 141A ±2 g); (e) vibrator platform in the direction of excitation (Setra 141A ±2 g). Three identical pieces of rigid plywood (27 x 17 x 2 mm) are shown below the three accelerometers (a, b and c) used to measure the transmissibilities.

All the accelerometers were calibrated before each experiment and checked during and after the experiment. Each accelerometer was calibrated to give zero reading when it was attached to a vertical surface, +1 g when it was placed on a horizontal flat surface, and –1g when it was inverted. Ideally, the transfer function between two calibrated accelerometers place at two points of the vibrator platform during vibration would give a value of 1.0. Figure 3.4 shows the transfer function (transmissibility) between two calibrated accelerometers attached to the horizontal flat back support and the 1-metre vertical vibrator platform during vertical vibration of 90 seconds.

After the accelerometers were calibrated, the non-rigidities of the vibrators in the cross-axis were checked by measuring the transmissibility between the input acceleration and the cross-axis acceleration perpendicular to direction of input acceleration (see Figure 3.5). Ideally, the cross-axis transmissibility would be zero during vibration.

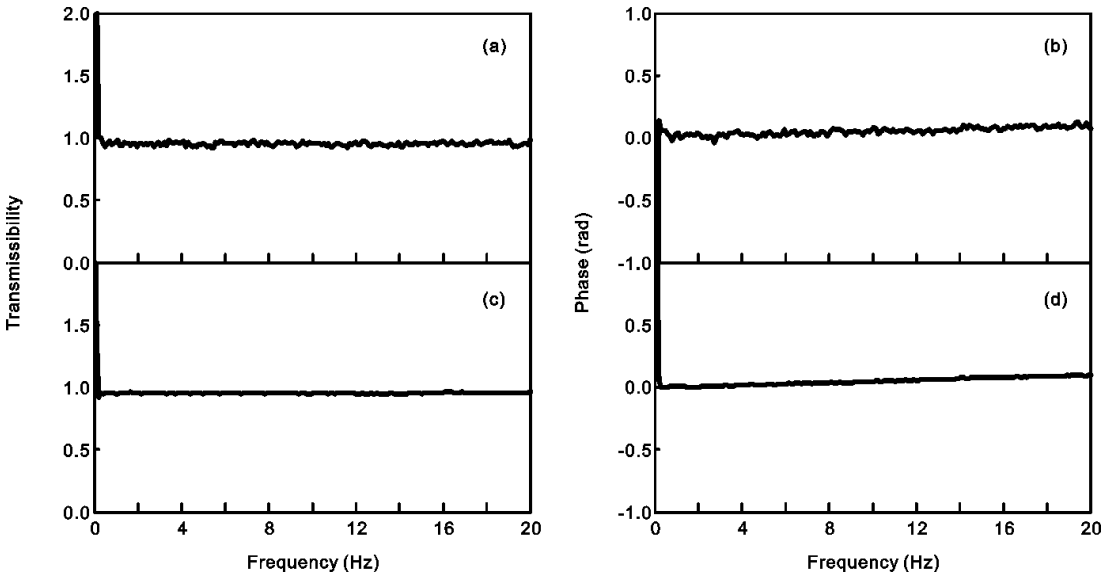

Figure 3.4 Transmissibility modulus and phase between two calibrated accelerometers mounted on the 1-metre vertical vibrator platform and on the horizontal flat supine back support using broadband (0.5 to 20 Hz) random vibration at 0.125 (a and b) and 0.5 (c and d) ms^{-2} r.m.s.

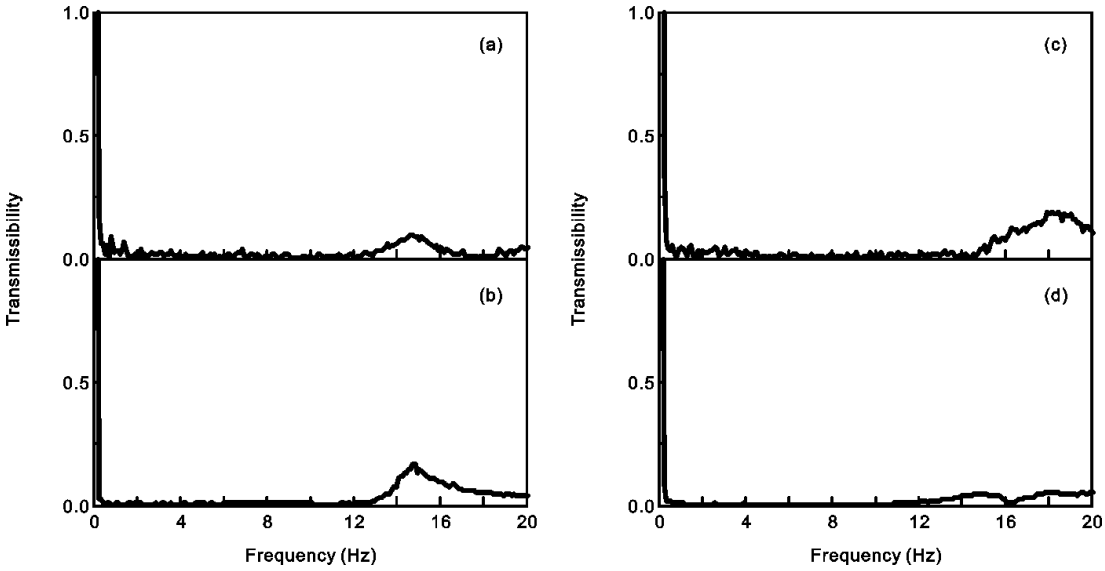

Figure 3.5 Transmissibility modulus between the input vertical acceleration and the cross-axis longitudinal horizontal acceleration during vertical excitation at 0.125 (a) and 1.0 (b) ms^{-2} r.m.s. produced by the 1-metre vertical vibrator. Transmissibility modulus between the input longitudinal horizontal acceleration and the cross-axis vertical acceleration during longitudinal horizontal excitation at 0.125 (c) and 1.0 (d) ms^{-2} r.m.s. produced by the 1-metre horizontal vibrator.

3.3.2 Force transducers

A Kistler 9281 B21 12-channel force platform was used to measure the dynamic forces between the subject and the seat surface (when seated) or between the subject and the back support (when supine). Four quartz piezo-electric force transducers were distributed in the four corners of the force platform in a rectangular arrangement. In experiments with seated subjects, an aluminium alloy plate with a dimension of 60.0 x 40.0 x 4.7 cm and a weight of 29.5 kg was bolted rigidly onto the top of the force transducers. In experiments with supine subjects, the aluminium alloy plate was replaced by another one with a dimension of 60.0 x 40.0 x 2.0 cm and a weight of 12.0 kg. The force platform was capable of measuring the force in three directions (i.e., *x*-, *y*-, and *z*-axes of the body) simultaneously. In the experiments with seated subjects during vertical excitation, only the signals in the vertical direction (i.e. *z*-axis of the subject) were used. In the experiments with supine subjects the four vertical (i.e. *z*-axis) force signals and the four longitudinal horizontal (i.e. *y*-axis) force signals from the four corners of the platform were used. Force signals from the transducers in the four corners were summed and conditioned using two Kistler 5001, or two Kistler 5007, charge amplifiers.

The force platform was calibrated statically and dynamically in the *z*- and *y*-axis to measure the vertical and longitudinal horizontal forces, respectively.

In the vertical direction, the static calibration was carried out individually by adding 10.0 and 5.0 kg weights on the four force sensing elements without any top plate (Figure 3.6). In the horizontal direction, the static calibration was carried out after the aluminium top plate was bolted onto the four force sensing elements by unloading and loading two 2.0 kg weights via a pulley system pulling the edge of the force platform (Figure 3.7 and Figure 3.8).

After the aluminium top plate (12.0 kg) was bolted onto the four force sensing elements, the dynamic calibrations in the vertical and horizontal direction were carried out by broadband (0.25 to 20 Hz) vibration at 0.25 ms^{-2} r.m.s. The apparent mass with vertical vibration was calculated with and without 34.1 kg rigid mass on the top of the force platform (Figure 3.9). Ideally, the apparent mass modulus would be 15.5 kg (i.e. the static mass of the aluminium top plate and all other mass above the force sensing elements), and 49.6 kg after adding 34.1 kg rigid mass. The apparent mass with longitudinal horizontal vibration was calculated with 25.4 kg rigid mass mounted on the four force sensing elements (Figure 3.10). Ideally, the apparent mass modulus would be 25.4 kg. The phase shifts seen in Figures 3.9 and 3.10 were caused by the non-rigidity of the vibrators.

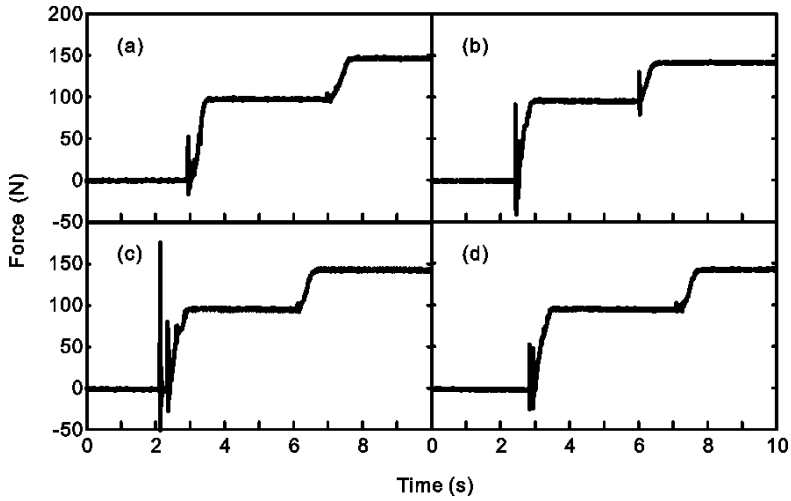

Figure 3.6 Statistically calibrated four force transducers in the four corners of the force platform in the vertical (*z*-axis) direction using 10.0 and 5.0 kg weights.

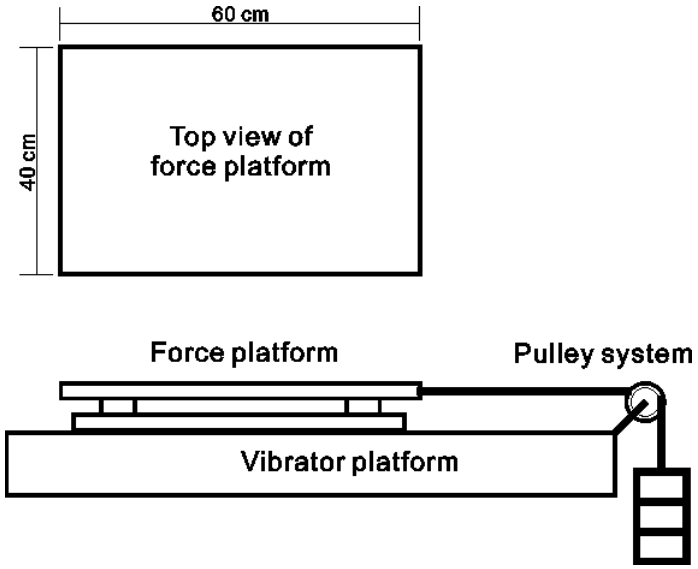

Figure 3.7 Schematic of the pulley system used to calibrate the force platform statically in the longitudinal horizontal (*y*-axis) direction using two 2.0 kg weights.

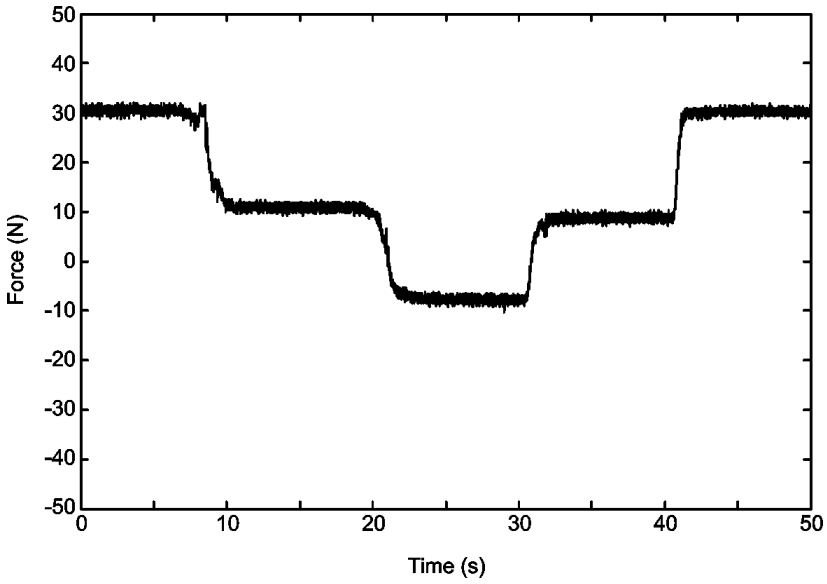

Figure 3.8 Statistically calibrated force transducers in the longitudinal horizontal (*y*-axis) direction using two 2.0 kg weights via the pulley system.

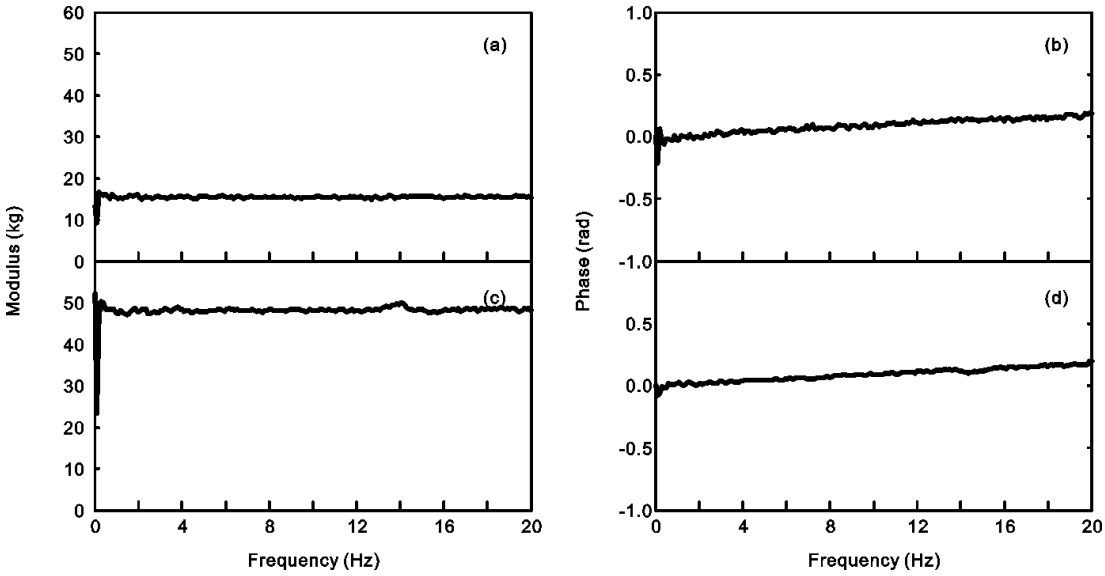

Figure 3.9 Dynamic calibration using vertical broadband vibration at 0.25 ms^{-2} r.m.s.: apparent mass of the force platform with the 12.0 kg aluminium top plate plus 3.5 kg rigid mass on the force sensing elements – (a) and (b); with an addition of 34.1 kg rigid mass – (c) and (d).

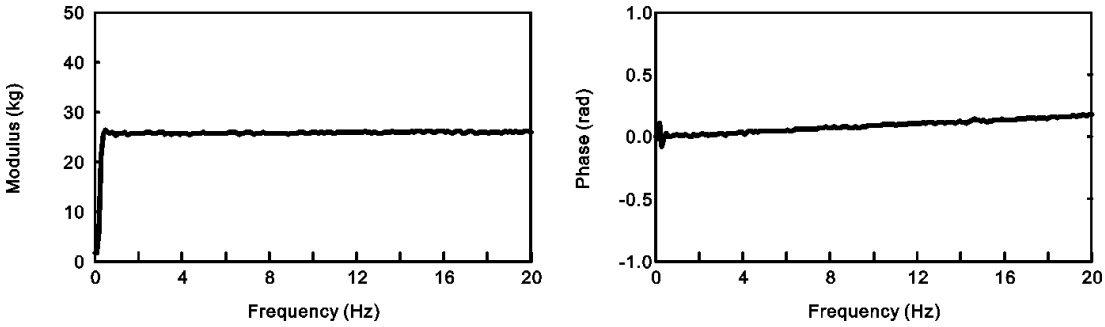

Figure 3.10 Dynamic calibration using longitudinal horizontal broadband vibration at 0.25 ms^{-2} r.m.s.: horizontal apparent mass of the force platform with 25.4 kg rigid mass mounted on the force sensing elements.

3.4 Data acquisition

Input signals were generated using *HVLab* software (version 3.81) which controlled the number of channels, sampling rate, and sampling duration. The generated input signals were sent to the controller of the vibrator via a 16-channel *HVLab* data acquisition and analysis system (Figure 3.11). This system used an *Advantech PCLabs PCL-818* acquisition card at 12-bit and a *Techfilter TF-16* anti-aliasing card. Before the input signals were fed to the vibrator controller, they were low-pass filtered and monitored using an oscilloscope. The output signals from the

accelerometers and the force transducers were acquired using the same *HVLab* system. Before the acquisition, the signals from the accelerometers were amplified using pre-amplifiers and the signals from the force transducers were amplified using charge amplifiers.

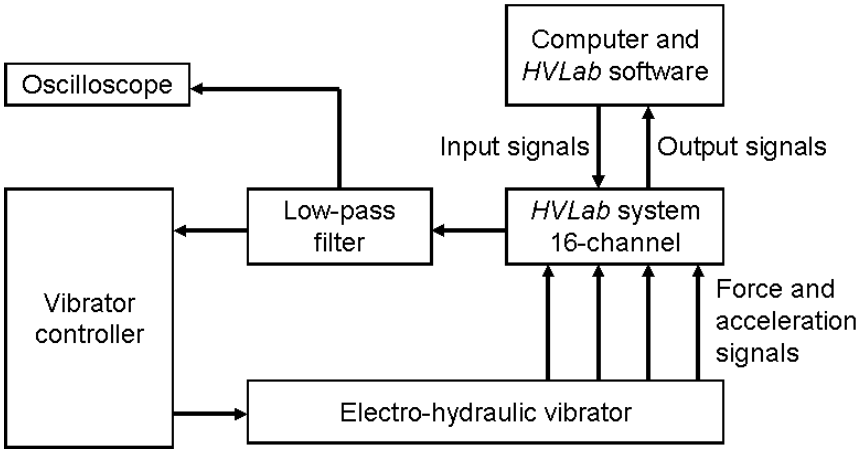

Figure 3.11 Experimental set-up used to control the vibrators and to acquire the output signals.

3.5 Analysis

After the data in the time domain had been acquired by the *HVLab* system, the data were transferred to another computer where the frequency response functions and other analysis, such as the curve-fitting, was performed using *MATLAB* (version 7.0.1, R14, SP1).

3.5.1 Frequency response functions

The vertical dynamic force, the longitudinal horizontal dynamic force, or the vertical accelerations measured at the sternum, the upper or lower abdomen were analyzed relative to the excitation acceleration (vertical or longitudinal horizontal) at the vibrator platform. Five frequency response functions – the apparent mass (where the force was in-line with the excitation acceleration), the cross-axis apparent mass (where the force was perpendicular to the excitation acceleration in the mid-sagittal plane), and the three vertical transmissibilities (to the sternum, and the upper- and lower abdomen) – were calculated using the cross-spectral density (CSD) method:

$$H(f) = S_{io}(f) / S_{ii}(f) \tag{3.1}$$

where, f is the frequency, in Hz; $H(f)$ is the apparent mass, in kg (or cross-axis apparent mass, or transmissibilities); $S_{io}(f)$ is the cross-spectral density between the output, i.e. the force in the direction of excitation (or the cross-axis force perpendicular to the direction of excitation, or the acceleration at the sternum, and

the upper and lower abdomen) and the input excitation acceleration; $S_{ii}(f)$ is the power-spectral density of the input excitation acceleration at the vibrator platform.

Alternatively, the frequency response functions can be calculated using the power-spectral density (PSD) method:

$$| H(f) |^2 = S_{oo}(f) / S_{ii}(f) \quad (3.2)$$

where, $S_{oo}(f)$ is the power-spectral density of the output, i.e. the force in the direction of excitation (or the cross-axis force perpendicular to the direction of excitation, or the acceleration at the sternum, and the upper and lower abdomen).

The CSD method determines the transfer function between the input and that part of the output that is linearly correlated with the input. The PSD method determines the ratio of the output to the input, including all 'noise' at the output including that caused by distortion between the input and the output. In an ideal linear system, the transfer functions obtained by the CSD and PSD method would be identical. If there is noise or distortion in the system, the modulus of the transfer function obtained by the CSD method is lower than the PSD method by an amount that depends on the amount of noise.

Being a complex function, the CSD method gives both the modulus and phase of the transfer function, whereas the PSD method gives only the modulus. The modulus and phase of the apparent mass, or the cross-axis apparent mass, or the transmissibilities using the CSD method can be calculated from:

$$H_{mod}(f) = \sqrt{(ReH(f))^2 + (ImH(f))^2} \quad (3.3)$$

$$H_{ph}(f) = \tan^{-1}(ImH(f) / ReH(f)) \quad (3.4)$$

where $ReH(f)$ and $ImH(f)$ are the real and imaginary parts of the frequency response function $H(f)$; $H_{mod}(f)$ and $H_{ph}(f)$ are the modulus and phase of $H(f)$.

Coherency ($\gamma_{io}^2(f)$) provides another way to examine the linearity of the calculated frequency response functions:

$$\gamma_{io}^2(f) = | S_{io}(f) |^2 / (S_{ii}(f) S_{oo}(f)) \quad (3.5)$$

where $\gamma_{io}^2(f)$ is the coherency of the system with a value always between 0 and 1.

Ideally, the coherency should have a maximum value of 1.0 with a linear system – where the output is always caused by or, correlated with, the input.

In order to obtain the apparent mass of the subject, the masses of the equipment 'above' the force sensing elements must be subtracted from the apparent mass measured during vibration. This 'mass cancellation' can be performed either in the time domain or in the frequency domain. In the time domain, the dynamic force

caused by the masses above the force sensing elements is subtracted from the total force measured with the subjects. The dynamic force caused by the masses above the force sensing elements is obtained dynamically in the frequency range 0.25 to 20 Hz. Alternatively, in the frequency domain, the real and imaginary parts of the frequency response function without a subject are subtracted from those with a subject.

The apparent mass modulus was found to be not greatly affected by the mass cancellation method. However, the coherency is more accurate when calculated after mass cancellation in the time domain as the effect from the masses above the force sensing elements is removed before the coherency is calculated. Therefore, all mass cancellations were performed in the time domain.

No mass cancellation is needed to calculate either the vertical or the longitudinal horizontal cross-axis apparent mass as there was no input motion in the cross-axis direction.

3.5.2 Lumped parameter model and curve-fitting

One of the methods used to quantify the nonlinearity of the frequency response functions is to compare the resonance frequencies obtained at different vibration magnitudes. Higher (i.e. finer) frequency resolution allows smaller differences in resonance frequency to be detected. However, for a fixed sampling duration (i.e. vibration exposure) and a fixed sampling rate, higher frequency resolutions will result in a lower confidence level (i.e., fewer degrees of freedom) in the spectral density functions. Alternatively, a higher frequency resolution requires longer exposure durations to keep the confidence level uncompromised. Reduced confidence level will lower the accuracy of the estimation of the resonance frequency. The exposure duration is limited by the total number of samples and channels that can be acquired simultaneously and, more importantly, restricted by the total duration the subjects are allowed to be exposed to vibration in one day. As a compromise, all experiments described in Chapter 4, Chapter 5, Chapter 6, Chapter 7 and Chapter 8 have a sampling duration of 90 seconds and a sampling rate of 200 samples per second. Apart from a different signal processing procedure described in Chapter 8, the sampled time histories were analyzed using a fast Fourier transform (FFT) length of 2048 samples, 64 degrees of freedom, and an ensuing frequency resolution of 0.098 Hz.

Lumped parameter models developed in the frequency domain have been extensively used to represent the dynamic characteristics of the human body. But these models are restricted to single magnitudes of vibration (e.g. Wei and Griffin, 1998; Matsumoto and Griffin, 2001; Nawayseh, 2003). Without knowing the

response of the body at different magnitudes, a model giving a close fit to the measured response at one magnitude is not be able to 'predict' the responses at the other magnitudes. However, by fitting a model to the measured transfer functions, such as the apparent mass, at individual magnitudes, the dynamic characteristics of the body could be quantified in terms of the parameters of the model. These parameters may include the frequency and magnitude of the frequency response functions at resonance, and the mass, spring and damping components of the model. This allows the nonlinearity to be quantified not only by one single frequency (i.e. the resonance frequency) but also by means of parameters that reflect the dynamic characteristics over the full frequency range interested.

3.5.2.1 Parallel two degree-of-freedom lumped parameter model

To identify the resonance frequency of the apparent mass, a parallel two-degree-of-freedom lumped parameter model was used to fit the apparent mass modulus and phase at each vibration magnitude. The apparent mass of the model has the same frequency resolution as the apparent mass measured with subjects (i.e., 0.098 Hz).

The lumped parameter model was employed as a numerical tool to represent the apparent mass of the human body during broadband random excitation. It is not a mechanistic model representing any physical mechanisms or anatomical parts of the body in response to whole-body vibration.

The resonance frequency is defined as the frequency at which the modulus of the apparent mass is a maximum in the fitted curve as a model response. This procedure was used to obtain the resonance frequencies of individuals and of the median apparent masses.

With vertical excitation, the acceleration and dynamic force of the model acts only in the vertical direction (Figure 3.12 a; Chapter 4 and Chapter 5). With longitudinal horizontal excitation, the acceleration and dynamic force of the model acts only in the horizontal direction (Figure 3.12 b; Chapter 6). Both forms of model are derived from the same equations of motion, and the parameters have the same physical meaning.

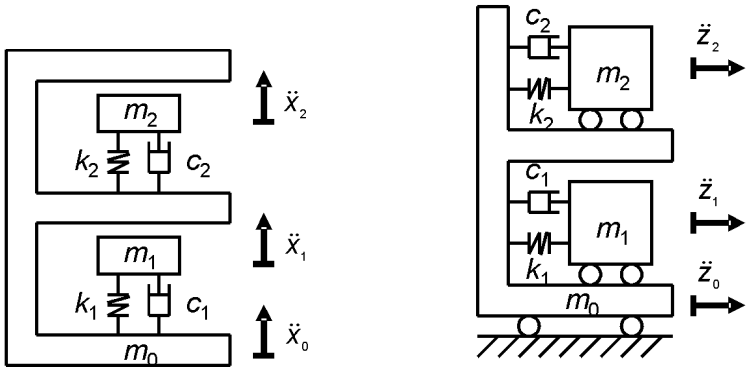

(a) (b)

Figure 3.12 The parallel two-degree-of-freedom lumped parameter models of apparent mass with (a) vertical excitation in the *x*-axis of a semi-supine subject and (b) longitudinal horizontal excitation in the *z*-axis of a semi-supine subject.

From Figure 3.12:

m_0: kg, the frame mass improving fitting results empirically (Wei and Griffin, 1998).

m_1: kg, the primary segmental mass corresponding to the primary resonance.

m_2: kg, the secondary segmental mass corresponding to the secondary resonance.

k_1: N/m, the primary stiffness corresponding to the primary resonance.

k_2: N/m, the secondary stiffness corresponding to the secondary resonance.

c_1: Ns/m, the primary damping corresponding to the primary resonance.

c_2: Ns/m, the secondary damping corresponding to the secondary resonance.

With upright seated subjects exposed to vertical vibration, the primary resonance refers to the dominant resonance peak at around 5 Hz; the secondary resonance refers to the minor resonance peak at around 10 Hz.

When the model is used with semi-supine subjects exposed to vertical (Chapter 5) and longitudinal horizontal (Chapter 6) excitation, '*x*' denotes the vertical direction (i.e. *x*-axis of the supine body), and '*z*' denotes the longitudinal horizontal direction (i.e. *z*-axis of the supine body).

When the model is used with upright seated subjects exposed to vertical vibration (Chapter 4), the model in the vertical direction (Figure 3.12 a) is used but the notation should be '*z*' to denote the vertical *z*-axis of the upright seated subjects.

The equations of motion and the frequency response functions are demonstrated below using the vertical form of the lumped parameter model (i.e. Figure 3.12 a).

The equations of motion are:

$$m_1\ddot{x}_1 = k_1(x_0 - x_1) + c_1(\dot{x}_0 - \dot{x}_1) \tag{3.6}$$

$$m_2\ddot{x}_2 = k_2(x_0 - x_2) + c_2(\dot{x}_0 - \dot{x}_2) \tag{3.7}$$

By using the Laplace Transform ($x \rightarrow X$, $\dot{x} \rightarrow sX$, and $\ddot{x} \rightarrow s^2X$) with the assumption, at equilibrium, that $x(0) = 0$, $\dot{x}(0) = 0$, and $\ddot{x}(0) = 0$, and by mathematical manipulation, the equations of motion can be expressed as:

$$\frac{X_1(s)}{X_0(s)} = \frac{k_1 + c_1 s}{m_1 s^2 + k_1 + c_1 s} \tag{3.8}$$

$$\frac{X_2(s)}{X_0(s)} = \frac{k_2 + c_2 s}{m_2 s^2 + k_2 + c_2 s} \tag{3.9}$$

By Newton's Second Law, the total dynamic forces acting at the base are:

$$F(t) = m_0\ddot{x}_0 + m_1\ddot{x}_1 + m_2\ddot{x}_2 \tag{3.10}$$

$$F(s) = m_0 s^2 X_0(s) + m_1 s^2 X_1(s) + m_2 s^2 X_2(s) \tag{3.11}$$

The apparent mass of the model can be calculated by dividing both sides by $s^2 X_0(s)$:

$$M(s) = m_0 + m_1 \frac{B}{A} + m_2 \frac{D}{C} \tag{3.12}$$

where

$$\begin{aligned} A &= m_1 s^2 + k_1 + c_1 s \\ B &= k_1 + c_1 s \\ C &= m_2 s^2 + k_2 + c_2 s \\ D &= k_2 + c_2 s \end{aligned} \tag{3.13}$$

The modulus AM (i.e. $|M|$) and the phase PH (i.e. $\arctan^{-1}(M)$) of the apparent mass can then be calculated by replacing the Laplace Transform operator s with angular frequency ω ($s = \omega i$, i is the imaginary operator).

3.5.2.2 Curve-fitting and optimization method

The resonance frequency of the apparent mass (f_r) and the parameters (m_0, m_1, m_2, k_1, k_2, c_1, and c_2,) of the two degree-of-freedom model are obtained by minimizing the difference between the apparent mass (modulus and phases) of the model and the measured apparent mass (modulus and phases) of the subjects.

The minimization uses a nonlinear constrained optimization search function *fmincon()*, provided by the optimization toolbox of *MATLAB* version 7.0.1, R14, SP1. The target error is calculated by summing the square of errors in modulus (kg) and phase (rad) at each frequency point between the measurement and the fitted curve of the model. Before the summation, the error in modulus is re-scaled to have an equivalent scale to the error in phase by multiplying the modulus by a normalisation factor *P* (at each frequency point):

$$P = |\mathrm{PH_s}|_{max} / |\mathrm{AM_s}|_{max} \tag{3.14}$$

where s denotes the measured apparent mass, $|AM_s|_{max}$ is the maximum value of the measured apparent mass modulus (in kg), and $|\mathrm{PH_s}|_{max}$ is the maximum absolute value of measured phase (in rad). So the normalisation is based on the values at two frequencies: one giving the maximum modulus and the other giving the maximum absolute phase.

The errors in the apparent mass modulus at different frequency steps was then summed over the frequency range of interest. The procedure to calculate the error in the phase was similar to that for the modulus except that the error in the phase was not normalised by the factor *P* but multiplied by an empirical phase weighting factor *Q* (given a value of 5.0). The value of the weighting factor was determined by maximizing the 'R-Square', a statistic parameter measures how successful the fit is in explaining the variation of the measured data. R-square was defined as the ratio of the sum of squares of the regression (SSR) to the total sum of squares (SST). The value of R-square can take on any value between 0 and 1, with a value closer to 1 indicating a better fit.

The overall target error (penalty function) was expressed in the form:

$$E = \sum_N \{ P [\mathrm{AM_m}(f) - \mathrm{AM_s}(f)]^2 \} + \sum_N \{ Q [\mathrm{PH_m}(f) - \mathrm{PH_s}(f)]^2 \} \tag{3.15}$$

$$\mathrm{R\text{-}square} = \frac{\mathrm{SSR}}{\mathrm{SST}} \tag{3.16}$$

$$\mathrm{SSR} = \sum_N [\mathrm{AM_m}(f) - \overline{\mathrm{AM_s}}]^2 \tag{3.17}$$

$$\mathrm{SST} = \sum_N [\mathrm{AM_s}(f) - \overline{\mathrm{AM_s}}]^2 \tag{3.18}$$

where E is the overall target error between the fitted curve and the measured apparent mass; N is the number of frequency points in the measured apparent mass; f denotes the frequency; $AM_m(f)$ and $PH_m(f)$ are the apparent mass modulus and phase of the model at each frequency; $AM_s(f)$ and $PH_s(f)$ are the measured apparent mass modulus and phase at each frequency; $\overline{AM_s}$ is the mean value of the measured apparent mass modulus (kg) averaged over the full frequency range; P is the normalisation factor for apparent mass modulus defined by Equation (3.14); Q = 5.0 is the phase weighting factors.

The above curve-fitting procedure was performed independently at each individual vibration magnitude.

3.5.3 Statistical tests

Statistical tests were used to identify the statistical significance of different experimental conditions and of correlations between two variables. To avoid making assumptions as to the distribution of the population, non-parametric statistical techniques were used, and all subjects were drawn from an unknown population. All statistical tests were performed using *SPSS* (version 14.0) statistical analysis software. The following sections give brief descriptions of the statistical tests performed in this thesis, with cases in which they were used. More detailed descriptions and examples of how these non-parametric statistical tests work can be found in Siegel and Castellan (1988).

Friedman two-way analysis of variance

The Friedman two-way analysis of variance was used to test the null hypothesis with k dependent (matched) conditions (samples) drawn from the same population. This test compares repeated measures within a group of samples. In this thesis, the samples were dependent (or matched) because the same subjects were tested using k different conditions. The Friedman test was used to examine whether a particular variable (e.g. apparent mass resonance frequency, apparent mass at resonance, parameters of fitted model, and harmonic distortion) was dependent on different excitation conditions (e.g. vibration magnitude, vibration waveform, direction of excitation, and posture). For example, the test was used to examine whether the apparent mass resonance frequency measured from 14 subjects was significantly different with five (k = 5) magnitudes of vibration (0.125, 0.25, 0.5, 0.75, and 1.0 ms^{-2} r.m.s.). The null hypothesis was accepted if there was no significant difference in the resonance frequency between the five vibration magnitudes. If there was a significant difference in the resonance frequencies, there was a

difference between at least two of the vibration magnitudes. In order to find out the vibration magnitudes where the differences in resonance frequency occurred, another statistical test was needed to deal with two sets of data.

Wilcoxon matched-pairs signed ranks test

The Wilcoxon matched-pairs signed ranks test was used to determine whether two dependent (matched) conditions (samples) were different. The Wilcoxon test takes into account the direction and the magnitude of the difference between the two samples. For instance, in the above example, if there was a significant effect of vibration magnitude on the resonance frequency, the Wilcoxon test would be used to identify between which two vibration magnitudes there was a significant difference. The resonance frequencies obtained at each of the five vibration magnitudes was tested against the resonance frequencies obtained at the other four vibration magnitudes (i.e., ten tests were needed).

Spearman rank-order correlation

The spearman rank-order correlation test was used to compare the ranking of data between two variables (samples) and to identify whether the two are related. For example, this method was used to investigate whether there was a correlation between the resonance frequency of the inline vertical apparent mass and the peak frequency of the horizontal cross-axis apparent mass of the supine human body exposed to vertical vibration. The correlation coefficient, r (rho), has a value between -1.0 and 1.0. It measures how linear the two variables (samples) are related. An r value of 1.0 indicates that the two variables are perfectly related with a positive correlation. An r value of -1.0 indicates that the two variables are perfectly related but with a negative correlation. An r value of zero suggests that there is no relation between the two variables.

Chapter 4

Effect of voluntary periodic muscular activity on nonlinearity in the apparent mass of the seated human body during vertical random whole-body vibration

4.1 Introduction

The principal resonance frequency in the driving-point impedance of the human body decreases with increasing vibration magnitude – a nonlinear softening effect during whole-body vibration. This nonlinearity is seen in the vertical and the fore-and-aft responses of the seated human body exposed to vertical whole-body vibration (e.g. Fairley and Griffin, 1989; Mansfield and Griffin, 2000; Mansfield and Griffin, 2002; Matsumoto and Griffin, 2002a; Matsumoto and Griffin, 2002b; Nawayseh and Griffin, 2003), in the fore-and-aft and vertical response to fore-and-aft excitation of the seated body (e.g. Mansfield and Lundström, 1999a; Holmlund and Lundström, 2001; Nawayseh and Griffin, 2005a), and in the response of the standing body (e.g. Matsumoto and Griffin, 1998a). The absolute difference between resonance frequencies at two vibration magnitudes appears to be greater between two low vibration magnitudes than between two high vibration magnitudes (e.g. Mansfield and Griffin, 2000; Matsumoto and Griffin, 2002a). The mechanisms causing the nonlinearity are not understood, and this restricts the modelling of biodynamic responses and the prediction of responses to whole-body vibration, including injury, at different magnitudes of vibration.

In attempts to identify factors influencing the nonlinearity, the effects of different seating conditions have been explored, but the nonlinearity has been found in all postures previously investigated. Mansfield and Griffin (2002) exposed twelve subjects to three vibration magnitudes with nine sitting postures and found that the change in resonance frequency (over three vibration magnitudes) was similar in all postures. With postures involving varying degrees of contact between the thighs and a rigid seat, Nawayseh and Griffin (2003) found reductions in nonlinearity when decreasing the thigh contact area with a rigid seat by raising the foot height (from feet-hanging, to feet supported with maximum thigh contact, feet supported with average thigh contact, and feet supported with minimum thigh contact), but the nonlinearity was clear in all conditions. With both sinusoidal and random vibration, Masumoto and Griffin (2002b) observed reduced nonlinearity when subjects were asked to tense muscles in the buttocks and the abdomen, although the nonlinearity was not eliminated.

Section 2.6.1 summarized the most relevant studies of the nonlinear response of the human body and identified three variables that had been considered responsible for the nonlinearity: the geometry of the body, the dynamic properties of the buttocks tissue, and muscle activity. If the nonlinearity is caused by the geometric characteristics of the human body, it should be possible to model the nonlinear behaviour with a passive dynamic system with fixed parameters, but such a model has not been found. The dynamic properties of the buttocks tissue have been associated with the vertical mode of the body at the primary resonance in some mathematical models (Masumoto and Griffin, 2001; Kitazaki and Griffin, 1997), but variation in pressure at the buttocks has little affect on the nonlinearity (Nawayseh and Griffin, 2003), consistent with pressure at the ischial tuberosities having little effect on the resonance frequency (Mansfield and Griffin, 2002). Reduced stiffness of muscles with increased vibration magnitude might be the cause of the reduced resonance frequency. During static sitting, many muscles can be involved in supporting the body with 'tonic' activity. When exposed to oscillatory motion, the muscle activity varies with a 'phasic' response, so it is assumed that during vibration excitation, muscle activity has both 'tonic' and 'phasic' components. Studies have found that the phasic muscular activity varies with vibration magnitude (Robertson and Griffin, 1989; Blüthner *et al*., 2001 and 2002). Assuming the erector spinae muscles influence the biodynamic responses of the body, or that they are typical of muscles that are involved, these studies imply that a nonlinearity, possibly the nonlinear softening effect, is associated with the phasic muscle response.

The published studies often assume that the nonlinearity is caused by reduced effective stiffness at higher vibration magnitudes. Alternatively, the nonlinearity could arise from increased effective stiffness at low vibration magnitudes. The studies of phasic muscle activity suggest that, relative to a static sitting condition, the muscle forces are increased during parts of a cycle of vibration and decreased during other parts. With increases in the vibration magnitude, the peaks and troughs tend to change nonlinearly and there may be variations in the timing of the forces. Without a dynamic model, it is not possible to predict whether the force variations corresponding to the observed variations in EMG response with vibration magnitude will increase the effective stiffness or reduce the effective stiffness. However, the known variation in muscle activity with vibration magnitude is such that it can be assumed to have a nonlinear effect. The reduction in resonance frequency of the body with increased vibration magnitude suggests that either the phasic muscle activity increases stiffness at low magnitudes or the muscle activity decreases stiffness at high magnitudes, or both.

If the phasic activity of the muscles increases the effective stiffness of the body at low vibration magnitudes, the resonance frequency at low magnitudes will be reduced if the phasic activity is reduced. If the phasic activity of the muscles reduces the effective stiffness of the body at high vibration magnitudes, the resonance frequency at high magnitudes will be increased if the phasic activity is reduced.

The phasic activity of muscles arising from whole-body vibration, and therefore the nonlinearity, will be altered if the relevant muscles contract in response to other stimuli. Studies which involve voluntary steady-state contraction have found little change in the nonlinearity, possibly because such contractions involve other muscles or because the contractions are voluntary (Mansfield and Griffin, 2002; Masumoto and Griffin, 2002b). There have been no reported studies of the effects of periodic muscular contractions on the nonlinearity.

This experiment was designed to investigate whether voluntary periodic muscular activity affects the nonlinearity in the apparent mass resonance frequency. It was hypothesised that periodic muscle activity would reduce body stiffness at low vibration magnitudes, so reducing the resonance frequency at low magnitudes and reducing the difference in the resonance frequency at low and high vibration magnitudes.

4.2 Method

4.2.1 Apparatus

The experiment was conducted using a rigid flat horizontal seat (600 mm by 400 mm) without backrest mounted on the platform of a 1-metre stroke electro-hydraulic vertical vibrator. A footrest 310 mm below the seat surface moved with the seat. A loose lap strap was fastened around the subjects.

A force platform (Kistler 9281 B21) was secured to the supporting surface of the seat and the four vertical force signals from the corners of the platform were summed and conditioned using a Kistler 5011 charge amplifier. The acceleration of the seat surface was measured using a Setra 141A accelerometer attached directly to the rigid seat surface. The force and acceleration signals were acquired at 200 samples per second via 67 Hz anti-aliasing filters.

Subjects were exposed to random vertical vibration with an approximately flat constant-bandwidth acceleration power spectrum over the frequency range 0.5 to 20 Hz. The duration of each exposure was 90 seconds. There were 14 combinations of two vibration magnitudes (0.25 and 2.0 ms^{-2} r.m.s.) and seven sitting conditions.

4.2.2 Experimental design

Fourteen fit and healthy male subjects with mean (minimum to maximum) stature 1.75 m (1.63 m to 1.85 m) and total body mass 70.3 kg (55.0 kg to 84.0 kg) participated in the experiment.

Subjects adopted an upright sitting posture as a reference condition (A: upright, Figure 4.1), broadly similar to the minimum thigh contact condition used by Nawayseh and Griffin (2003). The minimum thigh contact condition was adopted so as to minimise inter-subject variability – less variation in the apparent mass resonance frequency has been found in this posture. Sitting conditions B, C, D, E, F and G (Figure 4.1) were based on condition A. In condition B (upper-body tensed), subjects were asked to tense their upper-body while holding their breath (to assist maintenance of tension) and exhaling-inhaling every 15 seconds or longer. There were five conditions with periodic movements of the body: C (back-abdomen bending), D (back-to-front), E (rest-to-front), F (arm folding), and G (deep breathing). In these five conditions, subjects were instructed to move smoothly and continuously with 3 seconds per complete cycle. Back muscle activity produced by the cyclical movements was expected to decrease from condition C (back-abdomen bending) to condition G (deep breathing). Condition C (back-abdomen bending) required alternate flexing of the trunk with abdominal contraction and extension of the trunk with back muscle contraction. Conditions D (back-to-front), E (rest-to-front) and F (arm folding) required subjects to make normal arm movements without otherwise unnecessary muscular activity in the remainder of the body. Condition G (deep breathing) required subjects to use their maximum lung capacity. Subjects practiced the conditions for 20 minutes prior to commencing the experiment by following the instruction (see Appendix A). Subjects counted the number of cycles completed during each session so as to encourage a constant 3-second-per-cycle rate of movement.

The seven sitting conditions and the two vibration magnitudes were presented in a single session lasting approximately 45 minutes. The seven sitting conditions were presented in a balanced random order. The 14 subjects were divided into two equal groups, so that for each sitting condition, one group was tested in the order low-to-high vibration magnitude and the other group was tested in the order high-to-low vibration magnitude.

The experiment was approved by the Human Experimentation, Safety and Ethics Committee of the Institute of Sound and Vibration Research at the University of Southampton.

Condition	Description	Illustration
A. Upright	Upright with reduced thigh contact	
B. Upper-body tensed	Upright with reduced thigh contact – upper-body tensed	
C. Back-abdomen bending	Upright with reduced thigh contact – back-abdomen bending	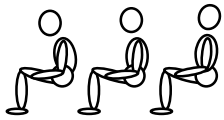
D. Back-to-front	Upright with reduced thigh contact – folding-stretching arms from back to front	
E. Rest-to-front	Upright with reduced thigh contact – stretching arms from rest to front	
F. Arm folding	Upright with reduced thigh contact – folding arms from elbow	
G. Deep breathing	Upright with reduced thigh contact – deep breathing	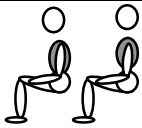

Figure 4.1 Seven sitting conditions – two stationary sitting conditions (A and B) and five with voluntary periodic movement (C, D, E, F and G).

4.2.3 Analysis

Mass cancellation was carried out in the time domain so as to subtract the force caused by the mass of platform above the force transducers:

$$F_s(t) = F_t(t) - (M_{top} \times a_s(t)) \quad (4.1)$$

where $F_s(t)$ is the vertical force generated by the subject, $F_t(t)$ is the total measured vertical force, M_{top} is the mass of the platform above the force transducers (determined dynamically over the range 0.5 to 20 Hz without a subject), and $a_s(t)$, is the measured vertical acceleration on the seat surface. The time histories of the vertical force generated by the subject, $F_s(t)$, and the vertical acceleration of the

surface supporting the subject, $a_s(t)$, were used to calculate the apparent mass of the subject, $M(f)$, in the frequency domain using the cross-spectral density method:

$$M(f) = S_{af}(f) / S_{aa}(f), \quad (4.2)$$

where $M(f)$ is the apparent mass, $S_{af}(f)$ is the cross spectral density between the vertical seat acceleration and the vertical force at the seat surface (after mass cancellation), and $S_{aa}(f)$ is the power-spectral density of the vertical seat acceleration. The cross spectral density method assumes that the output (vertical force) is linearly related to the input (vertical acceleration) excluding nonlinear effects including noise.

The moduli and phases of the apparent masses of the 14 subjects were calculated for each condition. The normalised apparent masses of the subjects were calculated by dividing their individual apparent masses by their apparent mass at 0.5 Hz. It was assumed that the body acts rigidly at 0.5 Hz such that the apparent mass at this frequency can be considered as the sitting weight of the subjects. Median normalised apparent masses and phases were calculated.

The resonance frequencies in the individual apparent masses and the median normalised apparent masses were obtained by curve-fitting the measured apparent masses and phases (over the frequency range 2 to 20 Hz) to a two-degree-of-freedom lumped parameter model (see Figure 3.12 a). The 'resonance frequency' was defined as the frequency where the modulus of the apparent mass had a maximum value in the fitted curve.

The two-degree-of-freedom lumped parameter model was defined in Section 3.5.2.1; the optimization method used to minimize the error in apparent mass modulus and phase between the model and the measurement was described in Section 3.5.2.2.

The optimization produced the resonance frequency (f_r) and seven parameters of the two-degree-of-freedom mathematical model (i.e. m_0, m_1, k_1, c_1, m_2, k_2 and c_2).

The frequency range of fitting was restricted to frequencies greater than 2 Hz because the periodic movements of the body (in conditions C to G) resulted in low coherency between resultant force and input acceleration at frequencies less than 2 Hz.

Statistical analysis was performed using non-parametric tests: Friedman two-way analysis of variance for k-sample cases and Wilcoxon matched-pairs signed ranks tests for two-sample cases.

4.3 Results

An example of the moduli and phases of the apparent mass of an individual subject with two magnitudes of vibration in the seven sitting conditions is shown in Figure 4.2. The median normalised apparent masses of the group of 14 subjects are shown in Figures 4.3 and Figures 4.4, and the resonance frequencies are shown in Table 4.1.

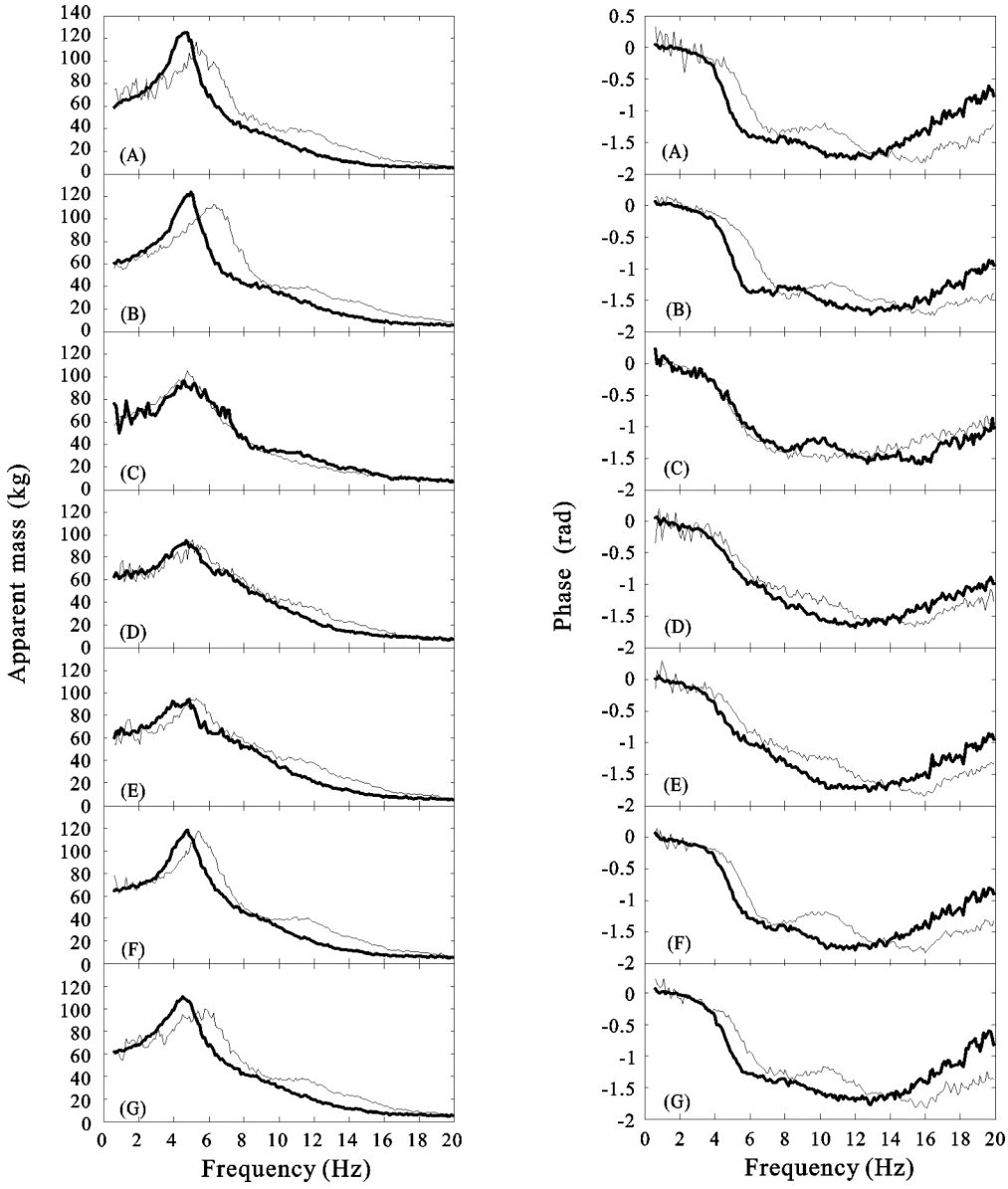

Figure 4.2 Apparent masses and phases for a single subject in seven sitting conditions: A: upright; B: upper-body tensed; C: back-abdomen bending; D: back-to-front; E: rest-to-front; F: arm folding; G: deep breathing at two vibration magnitudes (——— 0.25 ms^{-2} r.m.s.; ▬▬▬ 2.0 ms^{-2} r.m.s.).

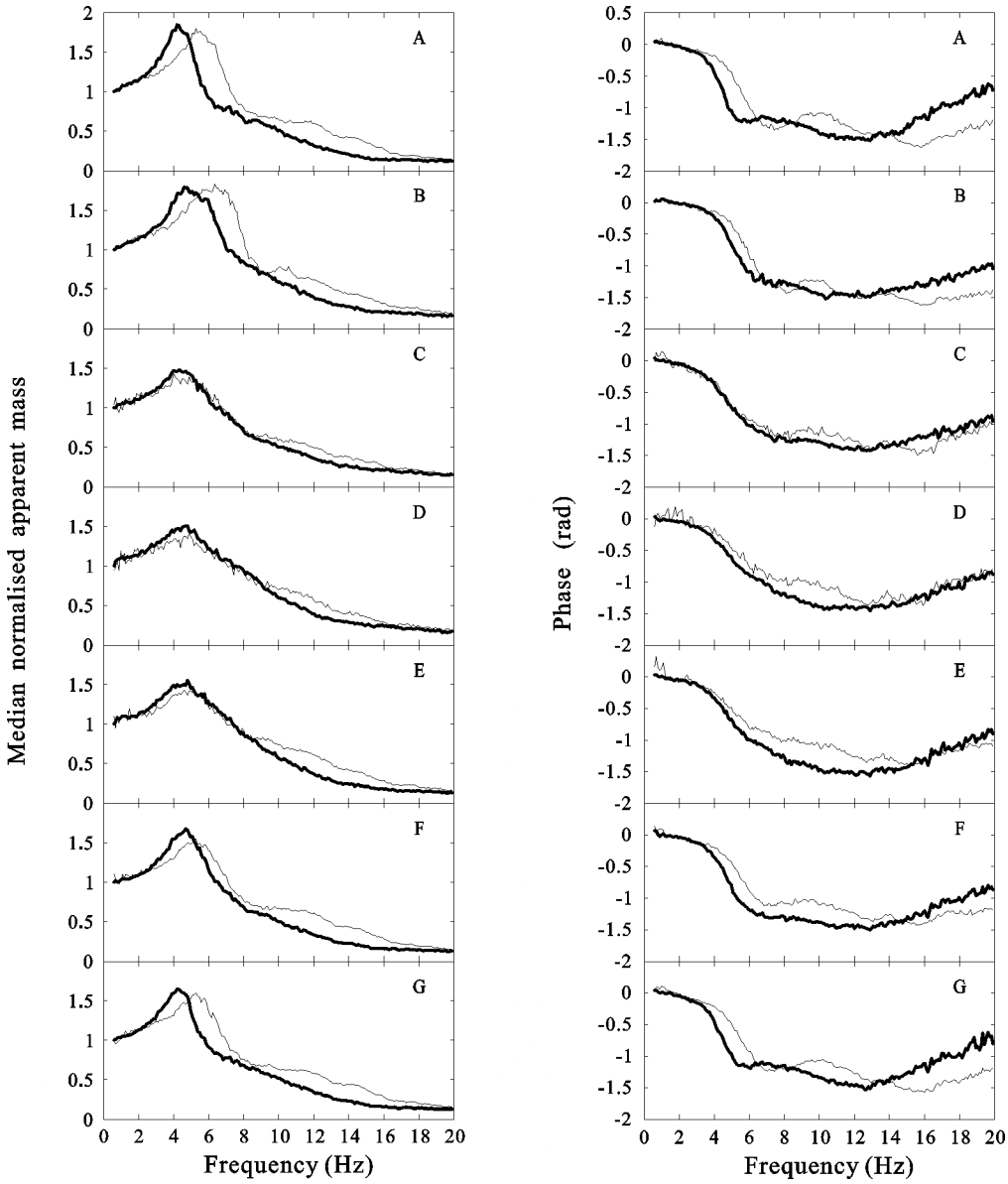

Figure 4.3 Median normalised apparent masses and phases of 14 subjects in seven sitting conditions: A: upright; B: upper-body tensed; C: back-abdomen bending; D: back-to-front; E: rest-to-front; F: arm folding; G: deep breathing at two vibration magnitudes (——— 0.25 ms^{-2} r.m.s.; ▬▬▬ 2.0 ms^{-2} r.m.s.).

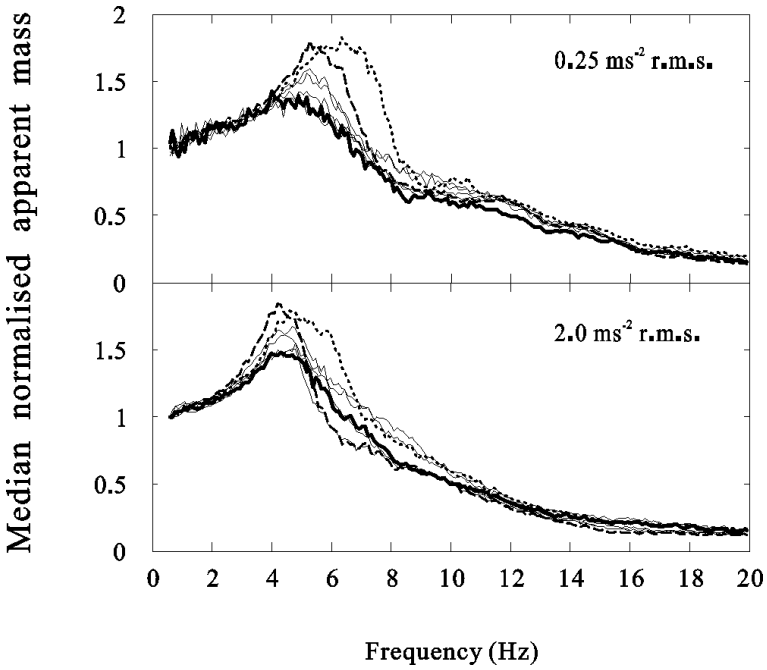

Figure 4.4 Median normalised apparent masses of 14 subjects in seven sitting conditions (A: upright -----; B: upper-body tensed ……; C: back-abdomen bending ▬▬▬; D: back-to-front ———; E: rest-to-front ———; F: arm folding ———; G: deep breathing ———) at two vibration magnitudes (0.25 ms^{-2} r.m.s. - top); 2.0 ms^{-2} r.m.s. - bottom).

Table 4.1 Median resonance frequencies of the apparent mass for seven sitting conditions at two vibration magnitudes.

Condition	Vibration magnitude (ms^{-2} r.m.s.)		Absolute difference (Hz)	Resonance difference ratio
	0.25	2.0		
	$f_{0.25}$ (Hz)	$f_{2.0}$ (Hz)	$\Delta f = f_{0.25} - f_{2.0}$ (Hz)	$\Delta f / f_{2.0}$
A: upright	5.47	4.39	1.08	24.60%
B: upper-body tensed	5.96	5.08	0.88	17.32%
C: back-abdomen bending	4.69	4.59	0.10	2.18%
D: back-to-front	5.08	4.59	0.49	10.68%
E: rest-to-front	4.98	4.69	0.29	6.18%
F: arm folding	5.27	4.69	0.58	12.37%
G: deep breathing	5.27	4.30	0.97	22.56%

$f_{0.25}$ and $f_{2.0}$: resonance frequencies at two magnitudes (0.25 and 2.0 ms^{-2} r.m.s.);

Δf: ($f_{0.25} - f_{2.0}$), absolute difference of two resonance frequencies.

The coherency varied between conditions but was generally in excess of 0.7 in the frequency range 3 to 20 Hz. Condition D (back-to-front) showed the lowest coherency.

As in a previous study (Wei and Griffin, 1998a), the two-degree-of-freedom model provided a good fit to the moduli and phases of all 14 subjects at both vibration magnitudes and in all seven sitting conditions. An example of the fitting for one subject in sitting conditions A (upright) and C (back-abdomen bending) is shown in Figure 4.5. The model also provided a good fit to the scaled normalised apparent mass (Figure 4.6).

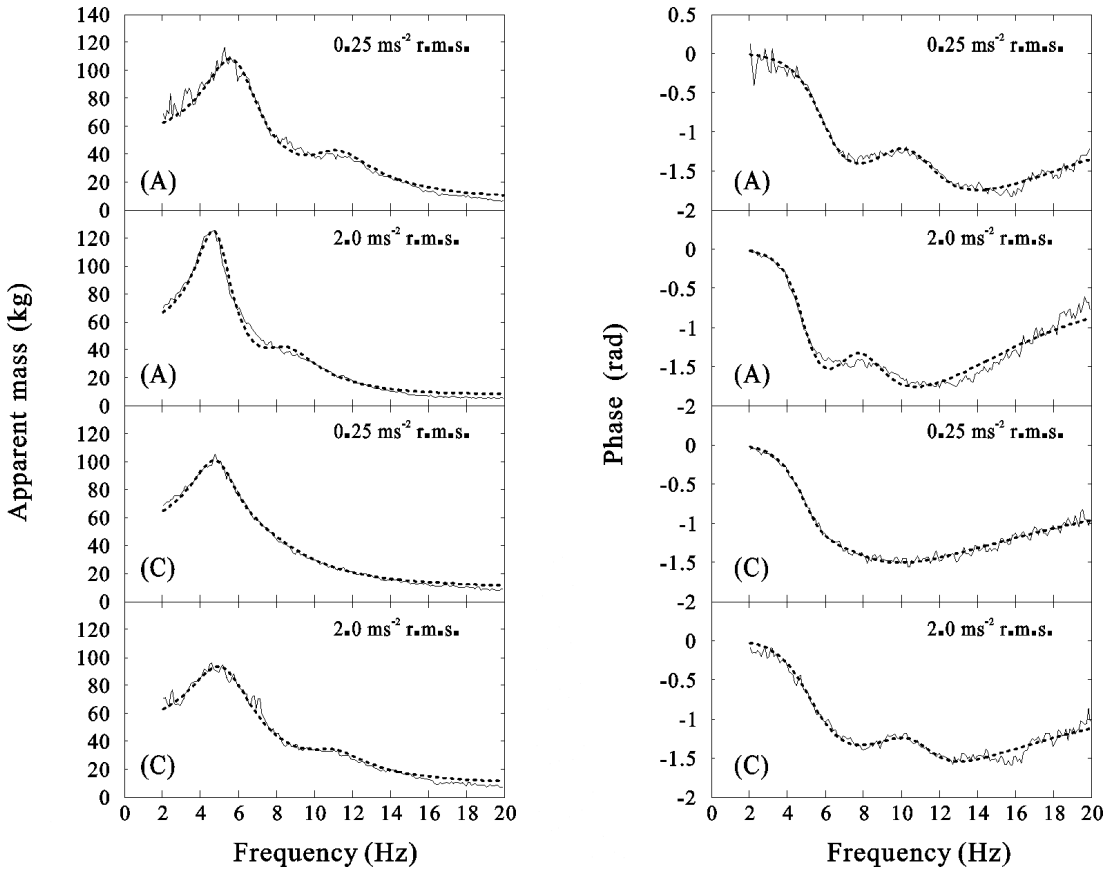

Figure 4.5 Curve-fitting (—— measurement; ..... fitting curve) the apparent mass and phase to obtain the resonance frequency of the apparent mass for a single subject in condition A (upright) and C (back-abdomen bending) at the low vibration magnitude (0.25 ms^{-2} r.m.s.) and the high vibration magnitude (2.0 ms^{-2} r.m.s.).

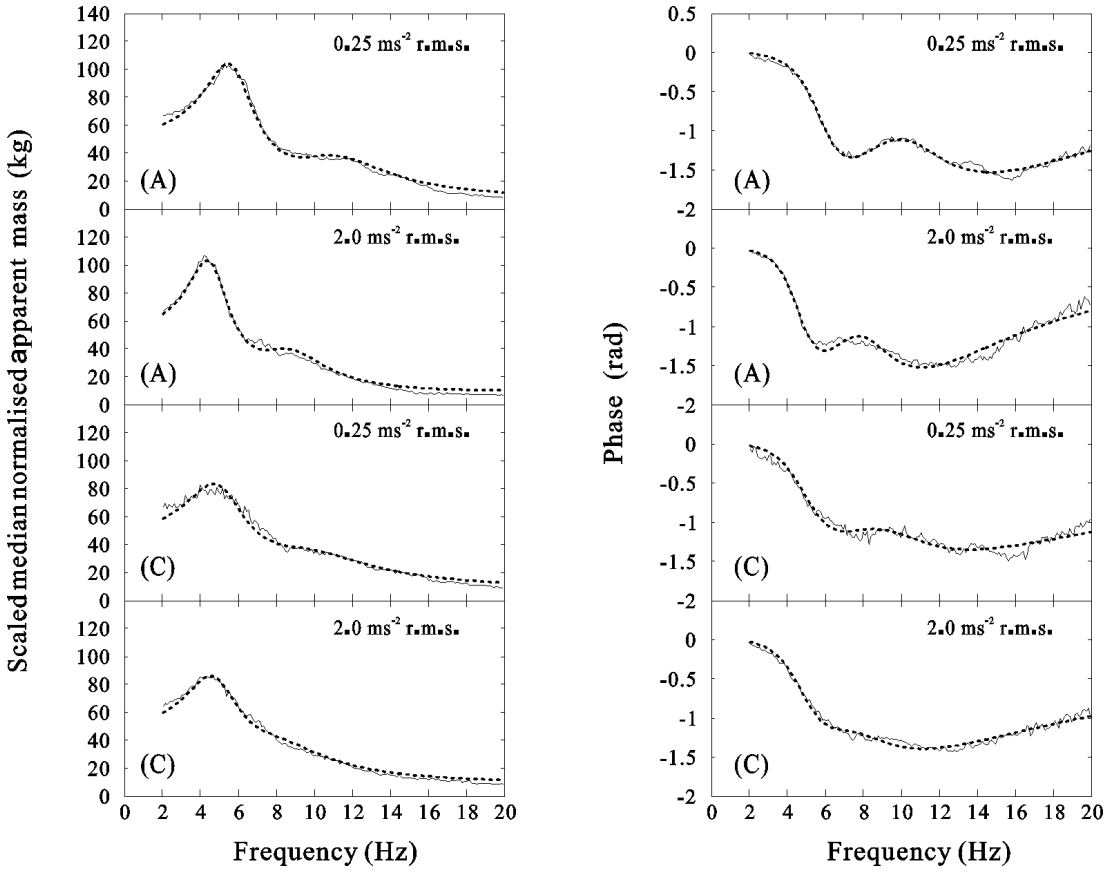

Figure 4.6 Curve-fitting (—— measurement; ..... fitting curve) the scaled median normalised apparent mass and phase to obtain the resonance frequency of the median normalised apparent mass in conditions A (upright) and C (back-abdomen bending) at the low vibration magnitude (0.25 ms^{-2} r.m.s.) and the high vibration magnitude (2.0 ms^{-2} r.m.s.).

4.3.1 Individual apparent mass resonance frequencies

The resonance frequencies at the high vibration magnitude were significantly less than the resonance frequencies at the low vibration magnitude in the two static sitting conditions (A: upright; B: upper-body tensed) and in two of the periodic moving conditions (F: arm folding; G: deep breathing) (p<0.05, Wilcoxon matched-pairs signed ranks test). The resonance frequencies at the two vibration magnitudes were not significantly different for three of the periodic movement conditions (C: back-abdomen bending; D: back-to-front; E: rest-to-front) (p>0.2, Wilcoxon).

Sitting condition B (upper-body tensed) gave a significantly greater resonance frequency than sitting condition A (upright) at both vibration magnitudes (p<0.01, Table 4.2 and Table 4.3, Wilcoxon), indicating an effect of static posture on the biodynamic response of the body.

Table 4.2 Statistical significance of the difference in apparent mass resonance frequencies at the low vibration magnitude (0.25 ms^{-2} r.m.s.) between the seven sitting conditions (*p* values for Wilcoxon matched-pairs signed ranks test; * $p < 0.05$).

	A (upright)	B (upper-body tensed)	C (back-abdomen bending)	D (back-to-front)	E (rest-to-front)	F (arm folding)	G (deep breathing)
A (upright)	_____	0.001*	0.000*	0.000*	0.000*	0.060	0.004*
B (upper-body tensed)	_____	_____	0.000*	0.000*	0.000*	0.000*	0.000*
C (back-abdomen bending)	_____	_____	_____	0.397	0.087	0.000*	0.001*
D (back-to-front)	_____	_____	_____	_____	0.088	0.001*	0.000*
E (rest-to-front)	_____	_____	_____	_____	_____	0.004*	0.002*
F (arm folding)	_____	_____	_____	_____	_____	_____	0.278
G (deep breathing)	_____	_____	_____	_____	_____	_____	_____

Table 4.3 Statistical significance of the difference in apparent mass resonance frequencies at the high vibration magnitude (2.0 ms^{-2} r.m.s.) between the seven sitting conditions (*p* values for Wilcoxon matched-pairs signed ranks test; * $p < 0.05$).

	A (upright)	B (upper-body tensed)	C (back-abdomen bending)	D (back-to-front)	E (rest-to-front)	F (arm folding)	G (deep breathing)
A (upright)	_____	0.000*	0.037*	0.002*	0.002*	0.000*	0.218
B (upper-body tensed)	_____	_____	0.001*	0.016*	0.009*	0.006*	0.000*
C (back-abdomen bending)	_____	_____	_____	0.027*	0.066	0.005*	0.002*
D (back-to-front)	_____	_____	_____	_____	0.201	0.648	0.002*
E (rest-to-front)	_____	_____	_____	_____	_____	0.408	0.002*
F (arm folding)	_____	_____	_____	_____	_____	_____	0.000*
G (deep breathing)	_____	_____	_____	_____	_____	_____	_____

Over the seven sitting conditions, there were significant differences in the resonance frequencies at 0.25 ms^{-2} r.m.s. (p<0.01, Friedman) and at 2.0 ms^{-2} r.m.s. (p<0.01, Friedman). When sitting condition B (upper-body tensed) was removed, an overall significant difference remained at both 0.25 ms^{-2} r.m.s. and at 2.0 ms^{-2} r.m.s. (p<0.01). At 0.25 ms^{-2} r.m.s., the resonance frequencies did not differ between conditions A and F, C and D, C and E, D and E, and F and G (p>0.05, Wilcoxon; Table 4.2). At 2.0 ms^{-2} r.m.s., the resonance frequencies did not differ between conditions A and G, C and E, D and E, D and F, and E and F (p>0.05; Table 4.3).

There was a significant overall effect of sitting condition on the absolute difference in resonance frequency at the two vibration magnitudes (p<0.01, Friedman). In four conditions with voluntary periodic movement (C: back-abdomen bending; D: back-to-front; E back-to-front; F: arm folding) the difference in resonance frequency was significantly less that in condition A (upright) (p<0.05, Wilcoxon; Table 4.4). There was no significant difference in the change in resonance frequency between low and high magnitudes in the two static sitting conditions (A: upright; B: upper-body tensed) (p>0.5, Wilcoxon; Table 4.4), or between condition G (deep breathing) and condition A (p>0.05, Wilcoxon). There was no significant difference in the change in resonance frequency between low and high magnitudes between conditions C (back-abdomen bending) and D (back-to-front) (p>0.2, Wilcoxon), or between conditions C (back-abdomen bending) and E (rest-to-front) (p>0.8, Wilcoxon).

Table 4.4 Statistical significance of the size of the absolute difference in apparent mass resonance frequencies at the low and the high vibration magnitudes ($\Delta f = f_{0.25} - f_{2.0}$) between the seven sitting conditions (p values for Wilcoxon matched-pairs signed ranks test; * $p < 0.05$).

	A (upright)	B (upper-body tensed)	C (back-abdomen bending)	D (back-to-front)	E (rest-to-front)	F (arm folding)	G (deep breathing)
A (upright)	———	0.484	0.001*	0.001*	0.001*	0.001*	0.059
B (upper-body tensed)	———	———	0.010*	0.002*	0.004*	0.064	0.814
C (back-abdomen bending)	———	———	———	0.208	0.814	0.020*	0.001*
D (back-to-front)	———	———	———	———	0.007*	0.004*	0.002*
E (rest-to-front)	———	———	———	———	———	0.010*	0.002*
F (arm folding)	———	———	———	———	———	———	0.002*
G (deep breathing)	———	———	———	———	———	———	———

4.3.2 *Median normalised apparent mass resonance frequencies*

The median normalised apparent masses and phases of the 14 subjects in the seven conditions at the two vibration magnitudes are shown in Figure 4.3 and Figure 4.4. Table 4.1 and Figure 4.7 show that the difference in the resonance frequencies at the two vibration magnitudes decreased markedly in the periodic moving conditions, especially C (back-abdomen bending), E (rest-to-front) and D (back-to-front) compared with condition A (upright), G (deep breathing) and B (upper-body tensed). Condition C (back-abdomen bending) produced the least change in median resonance frequency (0.10 Hz, 2.18%) compared with condition A (upright) that produced the greatest change (1.08 Hz, 24.60%).

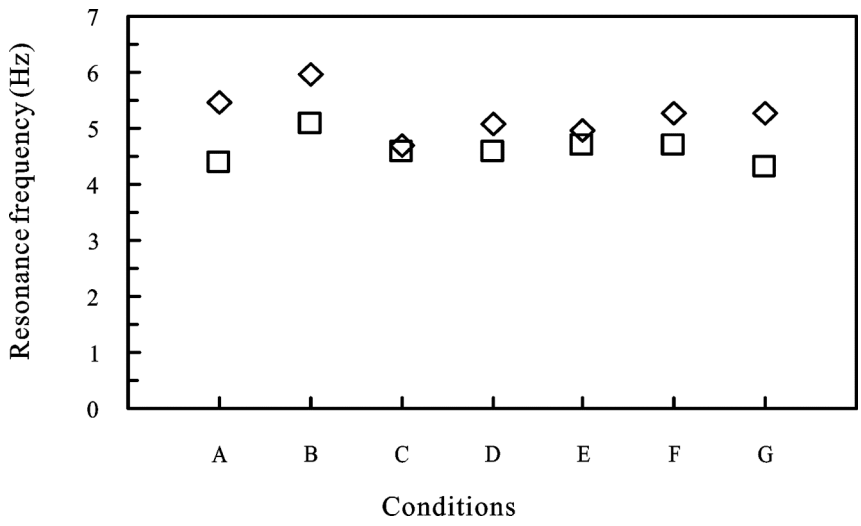

Figure 4.7 Resonance frequencies of median normalised apparent masses – effect of two vibration magnitudes (◊, 0.25 ms^{-2} r.m.s. and □, 2.0 ms^{-2} r.m.s.) and seven sitting conditions (A: upright; B: upper-body tensed; C: back-abdomen bending; D: back-to-front; E: rest-to-front; F: arm folding; G: deep breathing).

4.3.3 *Parameters of the two-degree-of-freedom model*

The parameters of the two-degree-of-freedom model fitted to the rescaled median normalised apparent masses are shown in Table 4.5. The ranges of the parameters of the two-degree-of-freedom model fitted to the individual subject apparent masses are shown in Table 4.6.

Since the two-degree-of-freedom model provided a good fit to the modulus and phase of all 14 individual subjects at both vibration magnitudes and in all seven sitting conditions it seems appropriate to investigate which parameters in this model changed with vibration magnitude and sitting condition (Figure 4.8).

Table 4.5 Parameters generated by fitting the two-degree-of-freedom model (Figure 3.12 a) to the scaled median normalised apparent masses and phases of 14 subjects at two vibration magnitudes with seven sitting conditions.

Condition	Vibration magnitude (ms^{-2} r.m.s.)	m_0 (kg)	m_1 (kg)	k_1 (N/m)	c_1 (Ns/m)	m_2 (kg)	k_2 (N/m)	c_2 (Ns/m)	f_r (Hz)
A: upright	0.25	9.13	36.00	49440	615	10.45	54444	367	5.47
	2.0	10.45	36.64	32513	522	9.46	29816	236	4.39
B: upper-body tensed	0.25	7.14	38.48	61707	718	11.51	56144	501	5.96
	2.0	9.59	37.41	44119	644	11.18	33976	376	5.08
C: back-abdomen bending	0.25	8.26	34.58	38039	719	9.89	41598	411	4.69
	2.0	8.78	34.08	34519	655	10.17	28736	352	4.59
D: back-to-front	0.25	12.83	29.28	38179	653	11.72	48585	405	5.08
	2.0	10.11	31.99	33388	658	14.24	36868	406	4.59
E: rest-to-front	0.25	10.39	31.66	39402	727	12.81	53238	505	4.98
	2.0	9.12	32.83	34757	611	12.88	33569	339	4.69
F: arm folding	0.25	9.71	33.08	44068	669	11.06	53900	449	5.27
	2.0	9.32	35.23	36631	567	8.83	27264	266	4.69
G: deep breathing	0.25	8.60	34.19	44969	641	10.45	54684	387	5.27
	2.0	10.04	34.79	30676	538	9.52	30391	253	4.30

Table 4.6 Inter-subject variability – ranges of parameters generated by fitting the two-degree-of-freedom model (Figure 3.12 a) to individual subject apparent masses and phases of 14 subjects at two vibration magnitudes with seven sitting conditions.

Condition	Vibration magnitude (ms^{-2} r.m.s.)		m_0 (kg)	m_1 (kg)	k_1 (N/m)	c_1 (Ns/m)	m_2 (kg)	k_2 (N/m)	c_2 (Ns/m)	f_r (Hz)
A: upright	0.25	max	5.65	26.46	31453	476	6.35	31951	154	4.30
		min	12.53	43.68	62262	773	12.90	69587	536	6.35
	2.0	max	6.70	23.48	20742	276	4.92	19611	92	3.61
		min	12.25	41.29	42910	706	11.06	34189	423	5.18
B: upper-body tensed	0.25	max	3.90	21.03	30145	282	3.70	28237	225	4.49
		min	12.62	44.14	73527	764	16.71	86562	663	7.42
	2.0	max	2.96	26.58	28378	453	2.19	11632	42	4.00
		min	10.92	41.47	74593	1052	31.50	57066	678	7.03
C: back-abdomen bending	0.25	max	3.82	23.94	20455	565	6.48	19791	239	3.32
		min	12.01	37.70	44716	927	14.14	58575	737	5.37
	2.0	max	4.51	23.90	23662	494	2.83	12648	53	3.81
		min	11.69	44.22	59810	1441	13.32	33137	936	5.08
D: back-to-front	0.25	max	2.65	21.36	22957	567	2.50	11943	38	3.81
		min	13.23	35.50	44782	791	16.30	74923	689	5.47
	2.0	max	4.60	21.79	27368	448	5.79	19871	128	4.30
		min	11.87	33.22	35005	857	19.16	42043	586	5.57
E: rest-to-front	0.25	max	3.60	22.48	25209	588	4.34	22416	89	3.91
		min	11.72	34.34	45654	799	15.78	70354	711	5.57
	2.0	max	3.57	23.16	26334	431	5.28	18158	100	4.20
		min	11.02	36.99	56578	1067	15.86	42247	604	5.47
F: arm folding	0.25	max	4.19	24.46	32383	524	7.00	28035	222	4.39
		min	13.57	38.25	58108	839	14.82	72467	592	6.25
	2.0	max	6.84	25.78	26672	422	4.99	14373	111	4.00
		min	11.64	40.12	62726	995	12.49	40426	544	5.96
G: deep breathing	0.25	max	5.49	26.32	29639	538	7.41	34879	195	4.20
		min	11.58	41.53	51480	739	15.31	76284	593	5.86
	2.0	max	7.00	25.95	22213	369	4.99	16558	101	3.71
		min	12.79	40.99	37674	617	11.56	35470	356	4.69

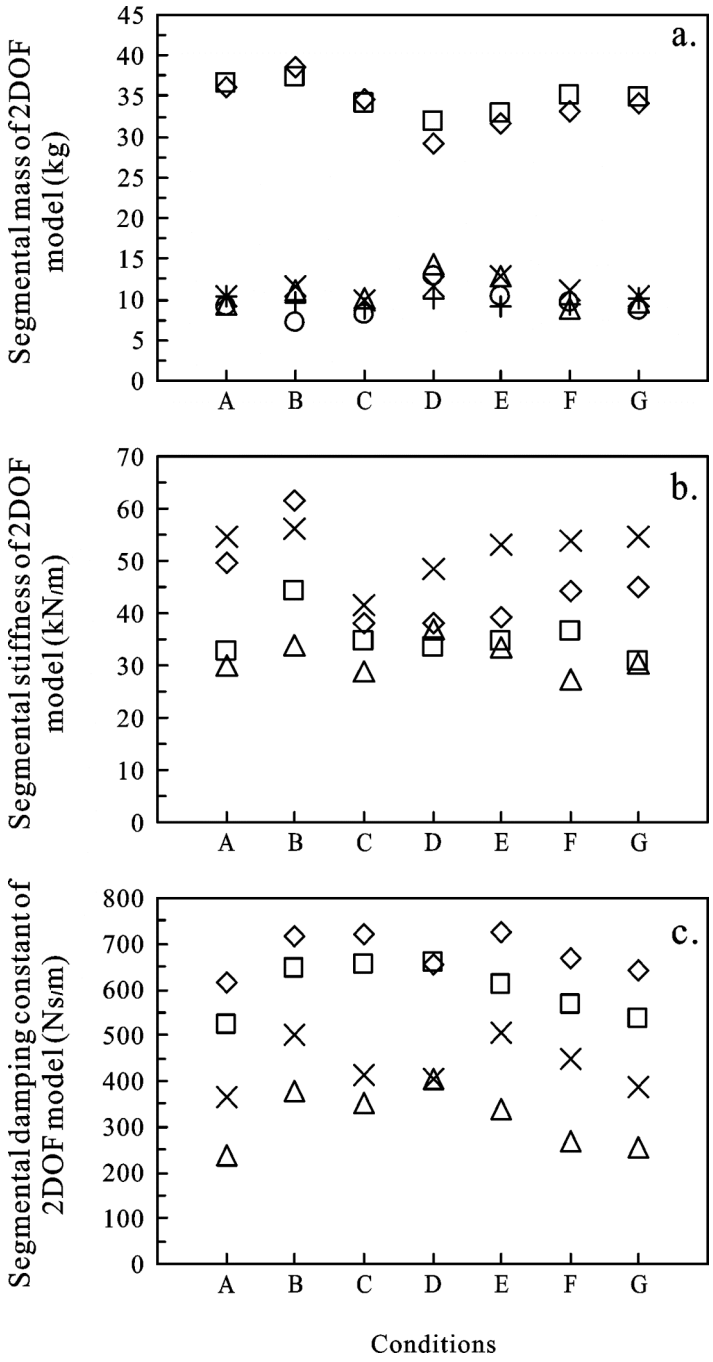

Figure 4.8 Parameters of the two-degree-of-freedom (segmental mass: m_0, m_1 and m_2; segmental stiffness: k_1 and k_2; segmental damping constant: c_1 and c_2) – effect of two vibration magnitudes (0.25 ms^{-2} r.m.s. and 2.0 ms^{-2} r.m.s.) and seven sitting conditions (A: upright; B: upper-body tensed; C: back-abdomen bending; D: back-to-front; E: rest-to-front; F: arm folding; G: deep breathing). a. segmental mass: o, m_0 at 0.25 ms^{-2} r.m.s.; +, m_0 at 2.0 ms^{-2} r.m.s.; ◊, m_1 at 0.25 ms^{-2} r.m.s.; □, m_1 at 2.0 ms^{-2} r.m.s.; x, m_2 at 0.25 ms^{-2} r.m.s.; Δ, m_2 at 2.0 ms^{-2} r.m.s. b. segmental stiffness: ◊, k_1 at 0.25 ms^{-2} r.m.s.; □, k_1 at 2.0 ms^{-2} r.m.s.; x, k_2 at 0.25 ms^{-2} r.m.s.; Δ, k_2 at 2.0 ms^{-2} r.m.s. c. segmental damping constant: ◊, c_1 at 0.25 ms^{-2} r.m.s.; □, c_1 at 2.0 ms^{-2} r.m.s.; x, c_2 at 0.25 ms^{-2} r.m.s.; Δ, c_2 at 2.0 ms^{-2} r.m.s.

Frame mass, m_0

Effect of vibration magnitude

The vibration magnitude had little effect on the frame mass (m_0). However, m_0 was significantly greater at the high vibration magnitude than at the low magnitude in conditions A (upright) and G (deep breathing) (p<0.05, Wilcoxon). There was no significant change in the frame mass with vibration magnitude in any other condition.

Effect of sitting condition

Over the seven sitting conditions, there were significant differences in m_0 at both 0.25 ms^{-2} r.m.s. and 2.0 ms^{-2} r.m.s. (p<0.05, Friedman). At 0.25 ms^{-2} r.m.s., m_0 differed between conditions C and A, E and A, E and B, F and E, and G and E (p<0.05, Wilcoxon). At 2.0 ms^{-2} r.m.s., m_0 differed between conditions B and A, C and A, D and A, E and A, F and A, D and C, G and C, E and D, and G and D (p<0.05, Wilcoxon).

The first segmental mass, m_1

Effect of vibration magnitude

There was only one significant change in the first segmental mass, m_1: in condition F (arm folding), m_1 was significantly greater at the high vibration magnitude than at the low vibration magnitude (p<0.05, Wilcoxon).

Effect of sitting condition

Over the seven sitting conditions, significant differences were found in m_1 at 0.25 ms^{-2} r.m.s. and at 2.0 ms^{-2} r.m.s. (p<0.05, Friedman). At 0.25 ms^{-2} r.m.s., m_1 differed between conditions C and A, D and A, E and A, F and A, G and A, D and B, E and B, D and C, E and C, G and C, F and D, G and D, F and E, and G and E (p<0.05, Wilcoxon). At 2.0 ms^{-2} r.m.s., m_1 differed between conditions D and A, E and A, G and A, D and B, E and B, G and B, D and C, E and C, E and D, F and D, G and D, F and E, and G and E (p<0.05, Wilcoxon).

The first segmental stiffness, k_1

Effect of vibration magnitude

At the high vibration magnitude, the first segmental stiffness, k_1 was significantly less than at the low vibration magnitude in conditions A (upright), B (upper-body tensed), F (arm folding), and G (deep breathing) (p<0.05, Wilcoxon).

Effect of sitting condition

Over the seven sitting conditions, there were significant differences in k_1 at 0.25 ms^{-2} r.m.s. (p<0.05, Friedman) and at 2.0 ms^{-2} r.m.s. (p<0.05, Friedman). At 0.25 ms^{-2} r.m.s., k_1 differed between all conditions (p<0.05, Wilcoxon), except between conditions D and C, E and C, E and D, G and F (p>0.1, Wilcoxon). At 2.0 ms^{-2} r.m.s., k_1 did not differ between condition C and A, D and A, E and A, G and A, D and C, E and C, E and D, or G and D (p>0.05, Wilcoxon). This shows that voluntary movement had less effect on the first segmental stiffness, k_1, at the high vibration magnitude than at the low vibration magnitude.

The first segmental damping constant, c_1

Effect of vibration magnitude

At the high vibration magnitude, the first segmental damping constant, c_1, was significantly less than at the low vibration magnitude in condition A (upright), D (back-to-front), E (rest-to-front), F (arm folding), and G (deep breathing) (p<0.05, Wilcoxon).

Effect of sitting condition

Over the seven sitting conditions, there were significant changes in c_1 at both 0.25 ms^{-2} r.m.s. and 2.0 ms^{-2} r.m.s. (p<0.05, Friedman). At 0.25 ms^{-2} r.m.s., c_1 differed between conditions C and A, D and A, E and A, D and B, E and B, G and C, F and D, G and D, and G and E (p<0.05, Wilcoxon). At 2.0 ms^{-2} r.m.s., c_1 differed between conditions B and A, C and A, D and A, E and A, F and A, F and B, G and B, F and C, G and C, E and D, F and D, G and D, and G and E (p<0.05, Wilcoxon).

The second segmental mass, m_2

Effect of vibration magnitude

At the high vibration magnitude, the second segmental mass, m_2, was significantly less than that at the low vibration magnitude in condition F (arm folding) and G (deep breathing) (p<0.05, Wilcoxon).

Effect of sitting condition

Over the seven sitting conditions, there were significant changes in m_2 at 0.25 ms^{-2} r.m.s. (p<0.05, Friedman) and at 2.0 ms^{-2} r.m.s. (p<0.05, Friedman). At 0.25 ms^{-2} r.m.s., m_2 differed between conditions B and A, C and A, D and A, E and A, F and A, G and A, G and D, and G and E (p<0.05, Wilcoxon). At 2.0 ms^{-2} r.m.s., m_2 differed between conditions D and A, E and A, D and C, E and D, F and D, G and D, and F and E (p<0.05, Wilcoxon).

The second segmental stiffness, k_2

Effect of vibration magnitude

At the high vibration magnitude, the second segmental stiffness, k_2, was significantly less than at the low vibration magnitude in all conditions A to G (p<0.01, Wilcoxon).

Effect of sitting condition

Over the seven sitting conditions, there were significant differences in k_2 at both 0.25 ms^{-2} r.m.s. and 2.0 ms^{-2} r.m.s. (p<0.05, Friedman). At 0.25 ms^{-2} r.m.s., k_2 differed between conditions C and A, C and B, D and B, E and B, E and C, F and C, G and C, E and D, and G and D (p<0.05, Wilcoxon). At 2.0 ms^{-2} r.m.s., k_2 differed between conditions D and A, C and B, F and B, D and C, E and C, F and D, and F and E (p<0.05, Wilcoxon).

The second segmental damping constant, c_2

Effect of vibration magnitude

At the high vibration magnitude, the second segmental damping constant, c_2, was significantly less than at the low vibration magnitude in all conditions A to G (p<0.05, Wilcoxon).

Effect of sitting condition

Over the seven sitting conditions, there were significant differences in c_2 at both 0.25 ms^{-2} r.m.s. and 2.0 ms^{-2} r.m.s. (p<0.05, Friedman). At 0.25 ms^{-2} r.m.s., c_2 differed between conditions B and A, C and A, D and A, E and A, F and A, G and B, G and D, and G and E (p<0.05, Wilcoxon). At 2.0 ms^{-2} r.m.s., c_2 differed between conditions B and A, C and A, D and A, E and A, F and A, F and B, G and B, E and D, F and D, and G and D (p<0.05, Wilcoxon).

4.4 Discussion

The results show that voluntary periodic movement can affect the nonlinearity in the apparent mass resonance frequency. The changes in nonlinearity found here are far greater than those found as a result of postural changes in previous studies. Conditions involving periodic movement significantly reduced the difference in resonance frequencies between low and high vibration magnitudes compared with the difference during static sitting in the same posture. The voluntary periodic movements primarily reduced the resonance frequency at low vibration magnitudes,

with little change in the resonance frequency at high vibration magnitudes (Figure 4.4).

Voluntary periodic body movement reduced the effective stiffness of the body at the low vibration magnitude, but had less effect on the effective stiffness of the body at the high vibration magnitude. This is apparent in the stiffness of both k_1 and k_2 in the equivalent two degree-of-freedom model (Table 4.5 and Figure 4.8). At the low vibration magnitude, there were also increases in the damping, as reflected in c_1 and c_2 of the equivalent model, although the pattern of changes in damping over the conditions with voluntary movement differs from the changes in stiffness. Although there were also some statistically significant changes in the masses in the equivalent two degree-of-freedom model as a result of voluntary movement, the nonlinearity is most obviously reflected in the changes in stiffness.

Compared to a normal sitting posture (A: upright), a voluntary sustained increase in muscle tension (B: upper-body tensed) increased the resonance frequency at both low and high vibration magnitudes, and this was reflected in significant increases in the stiffness k_1 in the equivalent model at both vibration magnitudes. However, the stiffness k_2 in the equivalent model did not increase significantly with the increased voluntary sustained muscle tension in condition B. The damping, as reflected in c_1 and c_2 of the equivalent model also increased with increased voluntary muscle tension.

The results suggest that body movement influences of the effective stiffness of the body but that voluntary steady-state tensing of the body and voluntary movements have different effects. Whereas tensing increased stiffness at both high and low magnitudes of vibration, periodic voluntary muscular contractions primarily affected the dynamic response of the body at low magnitudes.

Condition C (back-abdomen bending) had the least nonlinearity in the apparent mass resonance frequency and had similar resonance frequencies at the two vibration magnitudes. The variation in the characteristic nonlinearity with the different involvement of back muscles in the different sitting conditions may suggest that back muscles, or other muscles involved in making the voluntary periodic movements, influence the biodynamic responses of the body and are in some way responsible for the nonlinearity.

The nonlinearity might be caused by muscular activity that acts differently at high and low vibration magnitudes. Limitations to muscles might restrict their force at high magnitudes, but the addition of voluntary movement as in this experiment would then be expected to change response at high magnitudes more than low

magnitudes. The timing of the phasic muscle activity may vary with vibration magnitude so that the peak muscle force occurs at different times during high magnitude and low magnitude vibration, but if voluntary muscle activity alters the timing of phasic muscular activity this might be expected to alter response with both high and low magnitudes of vibration.

The greater effect of periodic body movement at low vibration magnitudes suggests the nonlinearity arises from a change at low magnitudes rather than a change at high magnitudes. At high magnitudes the inertial forces are greater, so it will require greater muscular force to influence the apparent mass, whereas at low magnitudes the inertial forces are less and it will require less muscle activity to influence the apparent mass. If the phasic muscle activity results in low forces that do not increase in proportion to vibration magnitude, they will influence the equivalent stiffness of the body more at low magnitudes than at high magnitudes. Voluntary periodic muscular activity may activate these same muscles, modify their phasic activity and reduce their contribution to the nonlinearity.

Periodic voluntary body movement might change the dynamic response of relevant body parts without muscle activity. For example, the thixotropy of tissues might allow both whole-body vibration and voluntary body movements to reduce the equivalent stiffness of the body. This would reduce the resonance frequency of the body if the movements occur in the soft tissues contributing to the stiffness of the body that controls the resonance frequency. High vibration magnitudes or increased voluntary movement would then reduce the resonance frequency of the body. The nonlinearity would be less evident when the stiffness of relevant body tissues has been reduced by body movements, as found in the present experiment.

4.5 Conclusion

The nonlinearity in apparent mass resonance frequency during static sitting can be significantly reduced by suitable voluntary periodic muscular activity.

Voluntary periodic muscle activity alters the equivalent stiffness of the body more at low vibration magnitudes (e.g. 0.25 ms^{-2} r.m.s.) than at high vibration magnitudes (e.g. 2.0 ms^{-2} r.m.s.).

Active control, or alternatively some passive property (e.g. thixotropy), of muscles, or other tissues involved during movement of the back and the upper body, significantly influence the biodynamic responses of the body to vibration.

Chapter 5

Nonlinear dual-axis biodynamic response of the semi-supine human body during vertical whole-body vibration

5.1 Introduction

Biodynamic responses of the human body to whole-body vibration are nonlinear: the resonance frequencies in frequency response functions (e.g., the apparent mass) decrease with increasing vibration magnitude. This nonlinearity has been observed in the vertical and the fore-and-aft responses of the seated human body exposed to vertical whole-body vibration (e.g. Fairley and Griffin, 1989; Mansfield and Griffin, 2000; Mansfield and Griffin, 2002; Matsumoto and Griffin, 2002a; Nawayseh and Griffin, 2003), in the fore-and-aft and the vertical responses of the seated human body exposed to fore-and-aft whole-body vibration (Fairley and Griffin, 1989; Mansfield and Lundström, 1999a; Holmlund and Lundström, 2001; Nawayseh and Griffin, 2005a; Abdul Jalil, 2005), and in the vertical and the fore-and-aft responses of the standing human body exposed to vertical whole-body vibration (Matsumoto and Griffin, 1998a; Subashi *et al*., 2006).

To identify factors influencing the nonlinearity, the effects of various steady-state sitting conditions have been studied, but the nonlinearity has been found in all sitting postures investigated. Increased constant muscle tension at some locations of the body had no significant effect on the nonlinearity (Mansfield and Griffin, 2002; Matsumoto and Griffin, 2002b) and there are insignificant changes in the nonlinearity with different contact pressures on the buttocks (Nawayseh and Griffin, 2003; Nawayseh and Griffin, 2005a).

Electromyographic (EMG) measurements show that muscle activity in the back varies with vibration magnitude (Robertson and Griffin, 1989; Blüthner *et al*., 2002). It has been found that voluntary periodic upper-body movement can greatly reduce the nonlinearity in the vertical apparent mass resonance frequency of the seated body (see Chapter 4). With voluntary movements, the resonance frequency was 4.7 Hz at 0.25 ms^{-2} r.m.s. and 4.6 Hz at 2.0 ms^{-2} r.m.s., whereas the resonance frequency was 5.5 Hz at 0.25 ms^{-2} r.m.s. and 4.4 Hz at 2.0 ms^{-2} r.m.s. without voluntary movement. The authors suggested that the reduction in the nonlinearity might be due to a change in the involuntary phasic activity of the muscles stimulated by the whole-body vibration when the muscles are contracted voluntarily by the periodic upper-body movement. Alternatively, both the voluntary body movement

and the associated muscular contraction may have altered the dynamic stiffness of the body by changes in the passive thixotropic behaviour.

Fairley and Griffin (1989) speculated that the nonlinear loosening effect of the musculo-skeletal structure had a similar mechanism to the thixotropic property of relaxed human muscles. 'Thixotropy' has been used to describe a passive property of human tissues: the stiffness of tissues decreases with prior perturbation, while the stiffness increases with prior stillness or low magnitude stimuli: the dynamic stiffness of tissues depends on the immediate 'shear history'. Following a perturbation applied to the relaxed finger extensor, the stiffness increased back to normal after a recovery time of between 5 to 10 seconds (Lakie, 1986). This thixotropic behaviour has been found in different parts of the human body: passive movement of the human wrist (Lakie *et al*., 1979), finger extensor (Lakie, 1986) and finger flexor (Hagbarth *et al*., 1985; Lakie, 1986). Homma and Hagbarth (2000) found that the rib cage respiratory muscles exhibit thixotropic properties similar to those observed in other skeletal muscles.

Considering the ubiquity of the nonlinearity with different sitting conditions and the prevalent thixotropic property of different parts of the body, it may be hypothesised that the intrinsic passive thixotropy of local body parts accumulatively produces the previously observed whole-body nonlinearity.

An intermittent stimulus with alternately high magnitudes and low magnitudes can be used to investigate the effect of shear history on the dynamic response of the body. Mansfield (1998) found no significant difference between the resonance frequencies of apparent masses measured with continuous random vibration and alternately high-low vibration at 0.2 and 2.0 ms^{-2} r.m.s. This may have been because the durations of the high and low magnitudes were 60 seconds and far longer than the recovery time of relaxed muscles and other tissues. Immediately after a tap perturbation, the stiffness of relaxed finger muscles recovered by 80% in only a couple of seconds (Lakie, 1986).

A relaxed semi-supine posture will involve less, or at least different, trunk muscle activity than sitting and standing postures. Measuring responses in a relaxed semi-supine position may therefore allow analysis of the nonlinearity with minimal muscle activity. The primary resonance frequency in the mechanical impedance of the semi-supine human body during vertical excitation has been found near 6 Hz with both 2 to 20 Hz sinusoidal vibration at 3.5 ms^{-2} r.m.s. (Vogt *et al*., 1973) and 1 to 20 Hz sinusoidal vibration at 2.1 ms^{-2} r.m.s. (Vogt *et al*., 1978). With 0.69 ms^{-2} peak-to-peak sinusoidal vibration between 2 and 20 Hz, the resonance was reported to be around 5 Hz for transmissibility to the chest, and 5 to 11 Hz for transmissibility to the

abdomen of supine subjects (Liu *et al.*, 1996). With semi-supine space crew, the primary resonance frequency of the mechanical impedance was observed between 7 and 11 Hz during 1 to 70 Hz sinusoidal vibration at 2.8 ms^{-2} r.m.s. (Vykukal, 1968). The variation in resonance frequency between these studies might be due to differences in the magnitudes of vibration, variations in the supine postures, the measuring locations, the frequency resolutions, and inter-subject variability. Most of these studies were conducted with a single magnitude of vibration and some with a sustained acceleration.

It is not known whether with vertical excitation of subjects in a relaxed semi-supine posture the 'in-line' dynamic response is as nonlinear as in sitting and standing postures, or whether the nonlinearity will be present in the horizontal cross-axis direction in the mid-sagittal plane of the body.

It was hypothesized that, in a relaxed semi-supine posture, both the vertical apparent mass resonance frequencies and the longitudinal horizontal cross-axis apparent mass peak frequencies would decrease with increasing vibration magnitude. It was also hypothesized that with random vibration consisting of intermittent periods at a low magnitude (0.25 ms^{-2} r.m.s.) and a high magnitude (1.0 ms^{-2} r.m.s.) the stiffness of the body would be decreased by prior high magnitude vibration and increased by prior low magnitude vibration, so reducing and raising, respectively, the resonance frequency.

5.2 Method

5.2.1 Apparatus

A supine support was constructed with three parts: back support, leg rest and headrest (Figure 5.1).

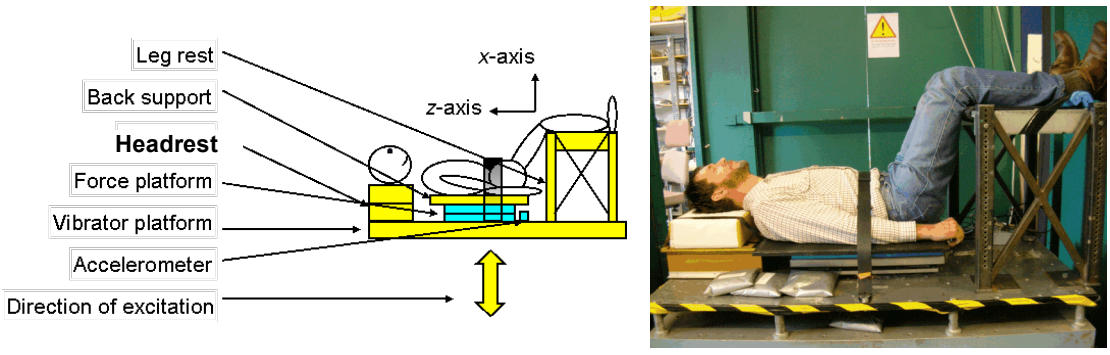

Figure 5.1 Schematic diagram of the supine support showing the semi-supine position and the axes of the force (*z*-axis and *x*-axis) and the acceleration (*x*-axis) transducers. A photographic representation of a test subject in the relaxed semi-supine position for vertical whole-body vibration.

The back support was a horizontal flat rigid 660 mm by 660 mm by 10 mm aluminium plate with a high stiffness 3 mm thick laterally treaded rubber layer attached to the upper surface. The complete back support was bolted rigidly to the upper surface of the force platform which monitored the vertical (*x*-axis of the semi-supine subject) and horizontal (*z*-axis of the semi-supine subject) forces exerted by the subject on the back support. The force platform was bolted rigidly to the vibrator platform. The horizontal distance between the edge of the back support and the edge of the leg rest was 50 mm (Figure 5.1).

The legs of subjects rested on a horizontal flat rigid aluminium support with an 8-mm thick high stiffness rubber layer attached to the top. The height of the leg rest was adjusted to allow the lower legs to rest horizontally.

The headrest was a horizontal flat rigid wooden block with 75-mm thick car-seat foam attached to the upper surface. The top surface of the complete headrest was approximately 50 mm higher than the back support. The horizontal distance between the back support and the headrest was adjusted by moving the headrest so that a subject's head could rest comfortably.

Vertical vibration was produced by a 1-metre stroke electro-hydraulic vertical vibrator capable of accelerations up to ±10 ms^{-2} in the laboratory of the Human Factors Research Unit.

The vertical (*x*-axis) and the horizontal (*z*-axis) accelerations of the vibrator platform were measured using two identical Setra 141A ±2 g accelerometers fixed on the plane of vibrator platform below the back support and between the leg rest and the force platform (Figure 5.1). The vertical (*x*-axis) and the horizontal (*z*-axis) forces at the back support were measured using a Kistler 9281 B21 12-channel force platform. The four vertical (*x*-axis) force signals and the four horizontal (*z*-axis) force signals from the four corners of the platform were summed and conditioned using two Kistler 5001 charge amplifiers.

An *HVLab* v3.81 data acquisition and analysis system was used to generate test stimuli and acquire the vertical and horizontal accelerations and the vertical and horizontal forces from the transducers. The two acceleration signals and the two force signals were acquired at 200 samples per second via 67 Hz analogue anti-aliasing filters.

5.2.2 Stimuli

The random stimuli used in this study had approximately flat constant-bandwidth acceleration power spectra over the frequency range 0.25 to 20 Hz.

Two types of vertical vibration were employed:

(i) Continuous random vibration with a duration of 90 seconds tapered at the start and end with 0.5-second cosine tapers. Five accelerations at 0.125, 0.25, 0.5, 0.75, and 1.0 ms^{-2} r.m.s. (unweighted) were generated using different random seeds (giving different time histories). Twelve subjects were randomly divided into six groups with two persons per group. With different groups, different random seeds were used to generate the random stimuli.

(ii) Intermittent random vibration, alternately at 0.25 and 1.0 ms^{-2} r.m.s. (unweighted) with a total duration of 828 seconds. The 828-second intermittent stimulus was divided evenly into four identical 207-second sections (Figure 5.2 a). During each 207-second section, 18 high magnitude slices and 18 low magnitude slices (generated using different random seeds) were presented alternately. The duration of 828 seconds was determined so that there were sufficient high magnitude and low magnitude slices for the concatenated signals (at high or low magnitude) to have the same duration as each of the continuous signals (i.e., 90 seconds). One single cycle of the intermittent signal was defined as one high magnitude slice followed by one low magnitude slice. During a single cycle of the intermittent motion, the high magnitude slice (at 1.0 ms^{-2} r.m.s.) lasted for 6 seconds (tapered at the start and end with a 0.25-second cosine taper) followed by a low magnitude slice (at 0.25 ms^{-2} r.m.s.) for 5.5 seconds (Figure 5.2 b). The durations of the high or low magnitude slices were determined so that the effective high or low magnitude signals (after removing the tapering) could be analysed with a frequency resolution of about 0.391 Hz (see Section 5.2.5.2)

All test motions were presented in one session lasting approximately 100 minutes. The order of presentation of the six random stimuli (the continuous stimuli at five magnitudes and the intermittent stimulus) was balanced across the twelve subjects.

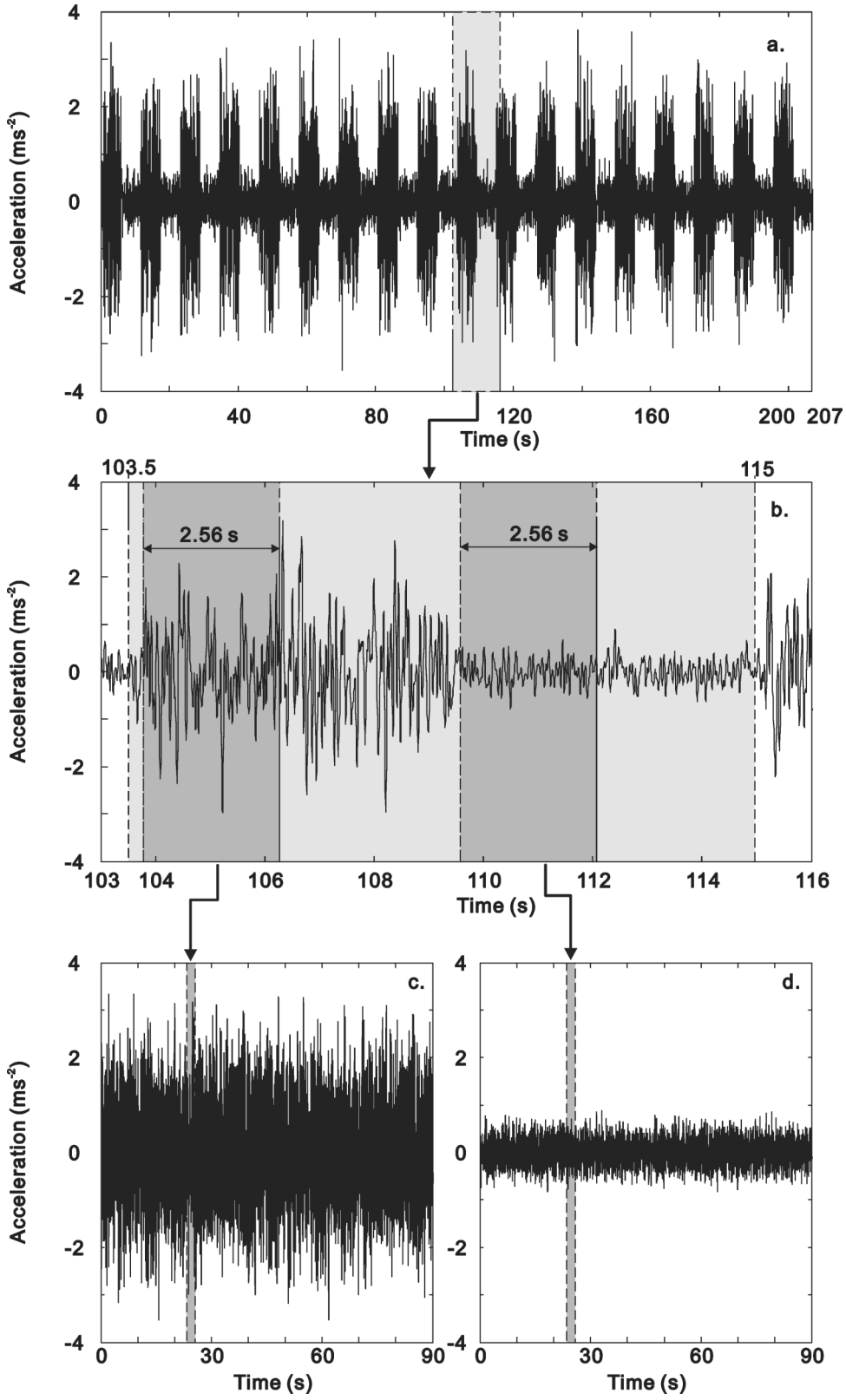

Figure 5.2 A vertical input acceleration time history measured with the high-low (1.0-0.25 ms^{-2} r.m.s.) magnitude intermittent random stimuli showing: (a) one complete 207-second intermittent time history; (b) one period of the intermittent time history starting with 6-second high magnitude slice followed by a 5.5-second low magnitude slice; (c) extracted and concatenated high magnitude (1.0 ms^{-2} r.m.s.) time slices (2.56 seconds each); (d) extracted and concatenated low magnitude (0.25 ms^{-2} r.m.s.) time slices (2.56 seconds each). The same procedure was applied to vertical force and horizontal cross-axis force time histories.

5.2.3 Posture

While experiencing each motion, subjects maintained a relaxed semi-supine position with their lower legs lifted and resting on the horizontal leg rest so as to give maximum back contact with the back support (Figure 5.1). The horizontal distance between the bottom of buttocks (aligned with the edge of the back support) and the near edge of the leg rest was 50 mm for all subjects. Subjects were instructed to relax totally with their eyes closed. A loose safety belt passed around the subject abdomen and arms but did not constrain the body. The instruction for subjects is shown in Appendix B.

5.2.4 Subjects

Twelve male subjects, aged between 20 to 42 years, with mean (minimum and maximum) stature 1.73 m (1.66 m and 1.80 m) and mean total body mass 70.3 kg (58.3 kg and 86.2 kg) participated in the study.

The experiment was approved by the Human Experimentation, Safety and Ethics Committee of the Institute of Sound and Vibration Research at the University of Southampton.

5.2.5 Analysis

5.2.5.1 Continuous random vibration

The vertical (*x*-axis) and horizontal (*z*-axis) forces measured at the supine back support were analysed relative to the vertical (*x*-axis) acceleration (Figure 5.1). Two frequency response functions – apparent mass (where the force was in-line with the acceleration in the vertical direction) and horizontal cross-axis apparent mass (where the horizontal force was perpendicular to the vertical acceleration in the sagittal plane, i.e. the *z*-axis) – were calculated using the cross-spectral density method:

$$M(f) = S_{af}(f) / S_{aa}(f) \tag{5.1}$$

where, $M(f)$ is the vertical apparent mass or the horizontal z-axis cross-axis apparent mass, in kg; $S_{af}(f)$ is the cross spectral density between the measured forces and the vertical excitation acceleration; $S_{aa}(f)$ is the power spectral density of the vertical excitation acceleration.

Before calculating the vertical apparent mass, mass cancellation (of the equipment above the force sensing elements) was carried out in the time domain to subtract the force caused by the masses above the force sensing elements (a total of 30.5 kg obtained dynamically in the frequency range 0.25 to 20 Hz). No mass cancellation

was needed to calculate the horizontal cross-axis apparent mass as there was no input motion in this direction.

The apparent masses at the five magnitudes were normalised by dividing by the apparent mass modulus measured at frequencies between 0.25 and 1.5 Hz, where the body was considered rigid. For motion at 0.125 ms^{-2} r.m.s., the normalisation was carried out at 1.37 Hz; for 0.25 ms^{-2} r.m.s. at 1.37 Hz; for 0.5 ms^{-2} r.m.s. at 0.59 Hz; for 0.75 ms^{-2} r.m.s. at 0.59 Hz; for 1.0 ms^{-2} r.m.s. at 0.39 Hz. The median normalised apparent masses at the five magnitudes were then calculated. The horizontal *z*-axis cross-axis apparent masses at the five magnitudes were normalised by dividing by the vertical apparent mass modulus measured at the same frequencies as the vertical apparent mass at each magnitude. The median normalised *z*-axis cross-axis apparent masses were then calculated.

The cross spectral densities and the power spectral densities were both estimated via Welch's method at frequencies between 0.25 and 20 Hz. The frequency response functions for each of the 90-second continuous random signals used a fast Fourier transform (FFT) windowing length of 2048 samples, a Hamming window with 100% overlap, a sampling rate of 200 samples per second and an ensuing frequency resolution of 0.098 Hz. This signal processing procedure applied to signals measured with continuous vibration is referred as the 0.098-Hz procedure.

5.2.5.2 Intermittent random vibration

Before the intermittent signals (vertical acceleration excitation, vertical force and horizontal force) were analysed according to the procedure applied to the continuous signals (Section 5.2.5.1), the intermittent signals described in Section 5.2.2 (ii) were processed as follow.

Each of the high magnitude (1.0 ms^{-2} r.m.s.) and low magnitude (0.25 ms^{-2} r.m.s.) time slices of the accelerations and forces measured with each of the 828-second intermittent signals was extracted and concatenated into a processed high magnitude signal (90 s duration) and a processed low magnitude signal (90 s duration) (Figure 5.2 c and d). The duration of each extracted time slice was 2.56 seconds to allow the apparent masses to be measured and calculated before the dynamic stiffness of the body recovered from the prior immediate high magnitude or low magnitude vibration. Each of the force and acceleration time histories measured with the continuous random stimuli and each of the processed force and acceleration time histories measured with the intermittent random stimuli lasted for 90 seconds, allowing the apparent masses to be calculated with the same frequency resolution of 0.391 Hz for both stimuli.

The same procedure used to analyse the signals measured with continuous random vibration (Section 5.2.2 (i)) was used to calculate the apparent masses and cross-axis apparent masses with each of the 90-second high magnitude (1.0 ms^{-2} r.m.s.) or low magnitude (0.25 ms^{-2} r.m.s.) processed intermittent signals, except for a different signal processing procedure (0.391-Hz procedure, Table 5.1). The 0.391-Hz criterion was used to generate apparent masses and cross-axis apparent masses with each of the 90-second processed intermittent acceleration and force signals. The 0.391-Hz procedure was also used to analyse accelerations and forces measured with the continuous vibration at 0.25 and 1.0 ms^{-2} r.m.s. so that the apparent masses measured with the intermittent and the continuous vibration could be compared using the same frequency resolution (0.391 Hz) with the same signal duration (90 seconds). Finally, the frequency resolution obtained using the 0.391-Hz procedure with both intermittent and continuous signals at 0.25 and 1.0 ms^{-2} r.m.s. was increased to 0.10 Hz by linearly interpolating the apparent mass moduli and phases in the frequency domain. The 0.391-Hz procedure used 0% overlap (with a Hamming window) to eliminate discontinuity caused by the concatenation of the 2.56-s slices.

Table 5.1 Two signal processing procedures used to analyse measurement with the continuous random stimuli and with the intermittent random stimuli.

A. 0.098-Hz procedure – for measured accelerations and forces with continuous random vibration at 0.125, 0.25, 0.5, 0.75 and 1.0 ms^{-2} r.m.s.

Duration (s)	Sampling rate (Hz)	FFT length	Degrees of freedom	Windowing overlap	Frequency resolution (Hz)
90	200	2048	36	100%	0.098

B. 0.391-Hz procedure – for processed accelerations and forces measured at 0.25 and 1.0 ms^{-2} r.m.s. for both the intermittent and continuous random vibration

Duration (s)	Sampling rate (Hz)	FFT length	Degrees of freedom	Windowing overlap	Frequency resolution (Hz)
90	200	512	70	0%	0.391 (then linearly interpolated to 0.098 in the frequency domain)

5.2.5.3 Curve-fitting, apparent mass resonance frequencies and cross-axis apparent mass peak frequencies

The parallel two-degree-of-freedom parametric model defined in Section 3.5.2.1 (see Figure 3.12 a) was used to fit the vertical in-line individual apparent masses and phases in order to obtain primary resonance frequencies. The optimization method used to minimize the error in apparent mass modulus and phase between the model and the measurement was described in Section 3.5.2.2. The resonance frequencies in the individual apparent masses and the median normalised apparent masses were obtained by curve-fitting the measured apparent masses and phases (over the frequency range 0.5 to 20 Hz) to the two-degree-of-freedom lumped parameter model. The 'resonance frequency' was defined as the frequency where the modulus of the apparent mass had a maximum value in the fitted curve.

The horizontal *z*-axis cross-axis apparent mass 'peak frequency' was defined as the frequency at which the modulus of the measured cross-axis apparent mass had a maximum value within a limited frequency range where coherency was reasonably high (more than 0.7). The peak frequencies were considered to be a representation of the stiffness of some parts of the body system similar to the resonance frequencies. This simplification was necessary as the *z*-axis cross-axis response of the body exhibited the behaviour of a multi-degree-of-freedom system with several peaks and troughs.

The same curve-fitting procedure was carried out with the vertical apparent masses at the five magnitudes (0.125, 0.25, 0.5, 0.75 and 1.0 ms^{-2} r.m.s) of continuous random vibration and the two magnitudes (0.25 and 1.0 ms^{-2} r.m.s.) of processed intermittent random vibration.

By fitting the parallel two-degree-of-freedom model to vertical in-line apparent masses with the curve-fitting procedure, the apparent mass resonance frequency (f_r), the apparent mass at resonance (AM_r), segmental masses (m_0, m_1 and m_2), stiffnesses (k_1 and k_2) and damping constants (c_1 and c_2) were obtained.

5.3 Results

5.3.1 Response in the vertical (x-axis) direction

5.3.1.1 Overview

The individual apparent masses and phases of twelve subjects with five vibration magnitudes of continuous random vibration are shown in Figure 5.3. The median normalised apparent masses and phases of the group of 12 subjects are shown in

Figure 5.4. The medians and full ranges of individual apparent mass resonance frequencies are shown in Table 5.2. The individual apparent masses and phases of the 12 subjects at two vibration magnitudes (0.25 and 1.0 ms^{-2} r.m.s.) with both continuous and intermittent random vibration are shown in Figure 5.5.

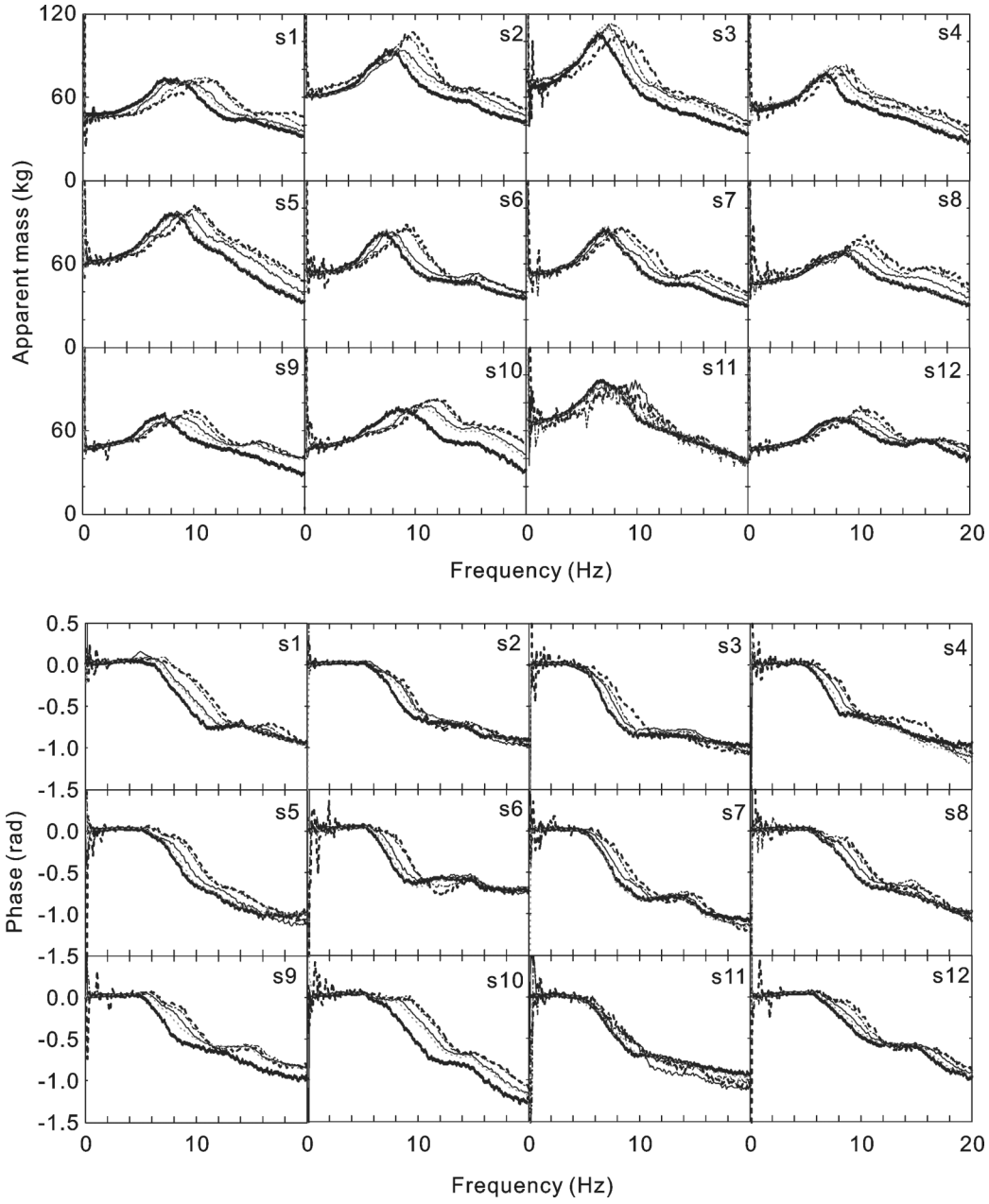

Figure 5.3 Individual apparent masses (upper) and phases (lower) of 12 subjects (s1 to s12) at five vibration magnitudes (- - - - - 0.125 ms^{-2} r.m.s.; _.-_.-_.-_ 0.25 ms^{-2} r.m.s.; ——— 0.5 ms^{-2} r.m.s.; ..... 0.75 ms^{-2} r.m.s.; ▬▬▬ 1.0 ms^{-2} r.m.s.) of continuous random stimuli.

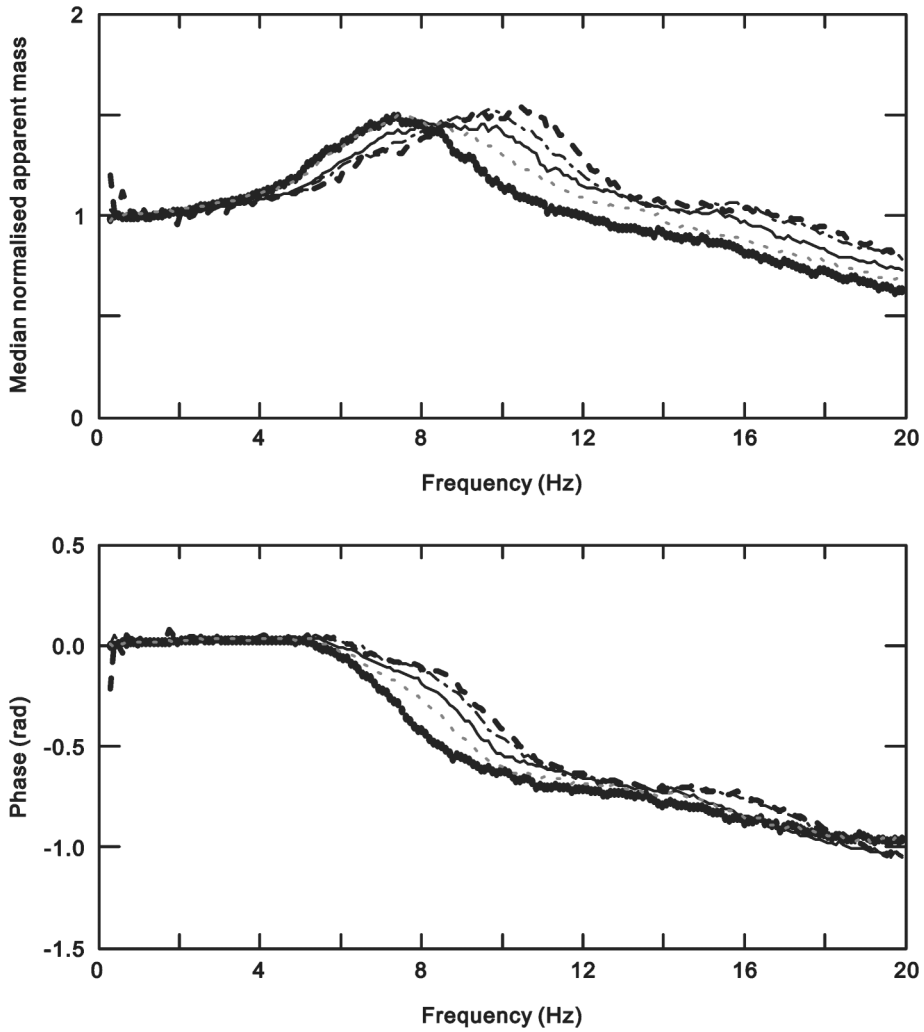

Figure 5.4 Median normalised apparent masses (upper) and phases (lower) of the group of 12 subjects at five vibration magnitudes (- - - - - 0.125 ms^{-2} r.m.s.; _ . _ . _ . _ . _ 0.25 ms^{-2} r.m.s.; ——— 0.5 ms^{-2} r.m.s.; ..... 0.75 ms^{-2} r.m.s.; ▬▬▬ 1.0 ms^{-2} r.m.s.) of continuous random stimuli.

Consistently low target errors were obtained by curve-fitting to the two-degree-of-freedom model. The results of the curve-fitting for the subject with the greatest error (S11) is shown for five magnitudes of continuous random vibration in Figure 5.6.

The lowest coherency occurred with the lowest vibration magnitude (0.125 ms^{-2} r.m.s.), probably due to involuntary and voluntary subject movement (e.g. breathing and stretching), mainly at frequencies less than 1.0 to 2.0 Hz. The coherencies were generally in excess of 0.9 in the frequency range 0.5 to 20 Hz.

There was one dominant primary resonance frequency of the vertical apparent mass between 6.0 Hz and 12.0 Hz. A minor secondary resonance occurred in the frequency range 14.0 to 20.0 Hz, which was most distinct with subjects 1, 2, 6, 7, 8, 9, 10, and 12.

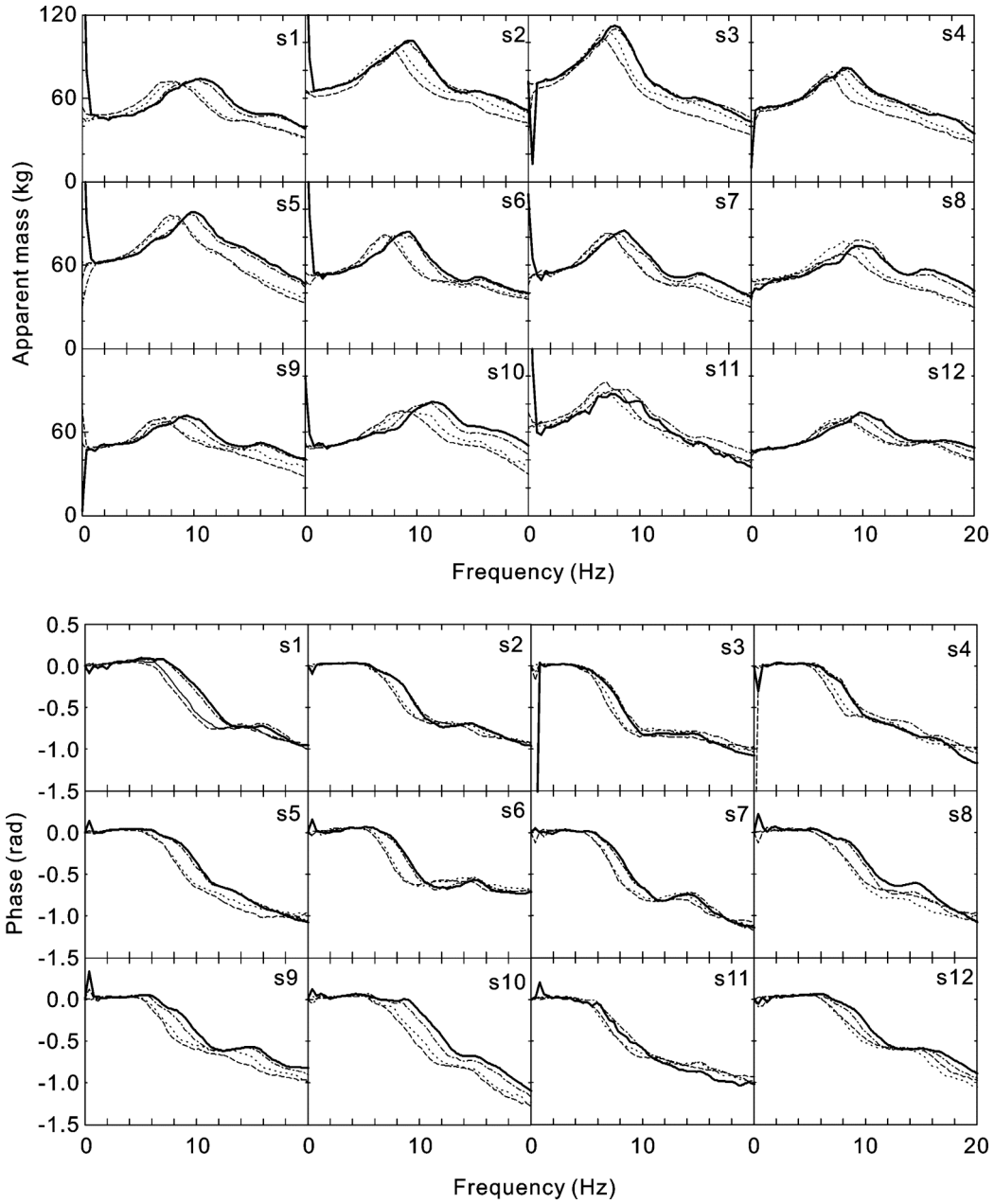

Figure 5.5 Individual apparent masses (upper) and phases (lower) of 12 subjects (s1 to s12) at two vibration magnitudes (_ ._ ._. 0.25 ms^{-2} r.m.s. intermittent; ..... 1.0 ms^{-2} r.m.s. intermittent; ——— 0.25 ms^{-2} r.m.s. continuous; _ _ _ _ _ 1.0 ms^{-2} r.m.s. continuous) of both intermittent and continuous random stimuli.

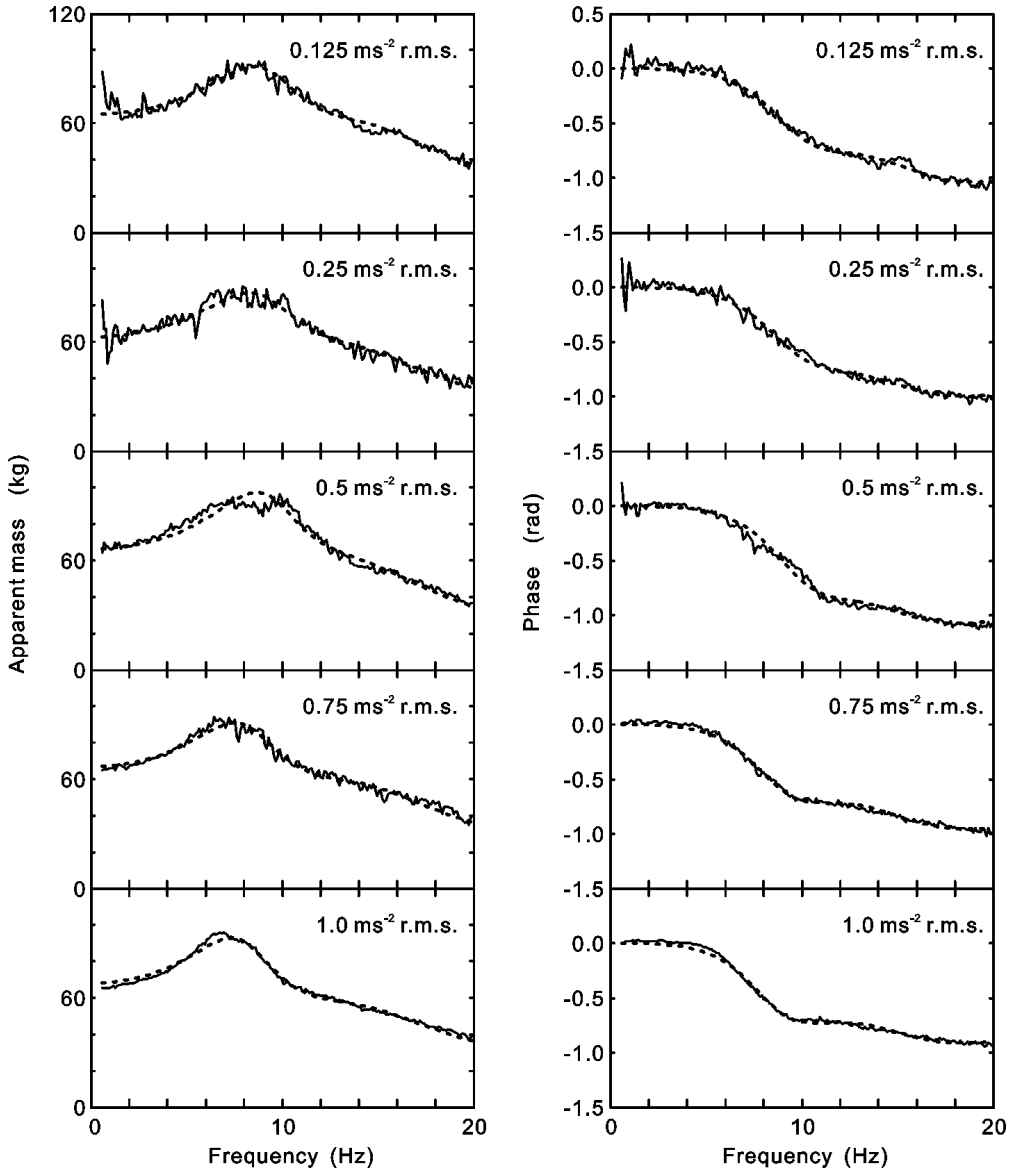

Figure 5.6 An example of curve-fitting (——— measurement; - - - - - fitted curve) the apparent masses and phases of one subject (s11) at five magnitudes (0.125, 0.25, 0.5, 0.75 and 1.0 ms^{-2} r.m.s.) of continuous random stimuli to obtain the resonance frequencies (Hz). Frequency range of curve-fitting: 0.5 to 20 Hz.

5.3.1.2 Apparent mass resonance frequencies with continuous random vibration

The apparent mass resonance frequency decreased significantly with increasing vibration magnitude ($p < 0.01$, Friedman two-way analysis of variance). There was a significant difference between each of the resonance frequencies at the five magnitudes ($p < 0.01$, Wilcoxon matched-pairs signed ranks test).

The median resonance frequencies of the apparent masses of the 12 subjects decreased from 10.01 Hz to 7.81 Hz as the vibration magnitude increased from 0.125 ms^{-2} r.m.s. to 1.0 ms^{-2} r.m.s. (Table 5.2).

The resonance frequencies of the median normalised apparent masses (Figure 5.4) of the group of 12 subjects were 10.35, 9.67, 8.01, 7.42, and 7.32 Hz with vibration magnitudes of 0.125, 0.25, 0.5, 0.75 and 1.0 ms^{-2} r.m.s., respectively.

Table 5.2 Median and ranges of resonance frequencies of apparent masses generated by fitting the two-degree-of-freedom parametric model to the apparent masses and phases of 12 subjects at five vibration magnitudes (0.125, 0.25, 0.5, 0.75 and 1.0 ms^{-2} r.m.s.) of continuous random stimuli.

Resonance frequency	Minimum	Median	Maximum
$f_{0.125}$ (Hz)	8.50	10.01	12.11
$f_{0.25}$ (Hz)	8.01	9.62	11.82
$f_{0.5}$ (Hz)	7.62	9.08	10.94
$f_{0.75}$ (Hz)	7.13	8.50	10.65
$f_{1.0}$ (Hz)	6.84	7.81	9.18

$f_{0.125}$, $f_{0.25}$, $f_{0.5}$, $f_{0.75}$ and $f_{1.0}$: resonance frequencies at five vibration magnitudes (0.125, 0.25, 0.5, 0.75 and 1.0 ms^{-2} r.m.s.).

5.3.1.3 Parameters of the two-degree-of-freedom model fitted to the apparent masses with continuous random vibration

The medians and ranges of the parameters of the two-degree-of-freedom model fitted to individual apparent masses and phases are shown in Table 5.3. The effect of vibration magnitude on the model parameters has been investigated. The segmental mass m_1, stiffness k_1, and damping constant c_1, correspond to the primary resonance between 6.0 and 12.0 Hz. The segmental mass m_2, stiffness k_2, and damping constant c_2, correspond to the secondary resonance between 14.0 and 20.0 Hz.

Table 5.3 Median and ranges of parameters generated by fitting the two-degree-of-freedom parametric model to the apparent masses and phases of 12 subjects at five vibration magnitudes (0.125, 0.25, 0.5, 0.75 and 1.0 ms^{-2} r.m.s.) of continuous random stimuli.

Vibration magnitude (ms^{-2} r.m.s.)		m_0 (kg)	m_1 (kg)	k_1 (N/m)	c_1 (Ns/m)	m_2 (kg)	k_2 (N/m)	c_2 (Ns/m)	f_r (Hz)
0.125	Minimum	16.5	9.5	51876	226	9.9	107118	531	8.50
	Median	21.2	15.0	75373	421	17.7	226389	1280	10.01
	Maximum	25.9	32.7	125815	1436	31.6	332926	2193	12.11
0.25	Minimum	13.5	9.6	47403	210	7.9	86288	472	8.01
	Median	19.3	13.3	59658	343	21.9	237016	1634	9.62
	Maximum	24.0	34.7	128742	1656	32.7	351234	2321	11.82
0.5	Minimum	15.2	10.0	30358	190	2.8	33311	92	7.62
	Median	18.2	12.4	54952	332	20.6	219720	1585	9.08
	Maximum	22.8	45.0	178344	2343	32.9	294682	2662	10.94
0.75	Minimum	13.6	11.7	40154	245	18.1	166046	1178	7.13
	Median	17.7	13.4	50844	379	20.1	193479	1578	8.50
	Maximum	22.4	28.5	71239	835	33.8	280341	2929	10.65
1.0	Minimum	14.3	10.5	25239	193	14.2	149178	744	6.84
	Median	16.9	14.8	52365	429	21.2	163275	1730	7.81
	Maximum	22.1	27.6	81153	708	30.6	234006	2675	9.18

m_0, m_1 and m_2 – segmental masses. k_1 and k_2 – segmental stiffnesses. c_1 and c_2 – segmental damping constants. f_r – apparent mass resonance frequency of the model.

The five vibration magnitudes had a significant overall effect on the frame mass, m_0 (p < 0.01, Friedman). The frame mass tended to decrease with increasing magnitude (p < 0.05, Wilcoxon), except between 0.25 and 0.5 ms^{-2} r.m.s. (p = 0.126, Wilcoxon), between 0.25 and 0.75 ms^{-2} r.m.s. (p = 0.239, Wilcoxon), between 0.5 and 0.75 ms^{-2} r.m.s. (p = 0.844, Wilcoxon), between 0.5 and 1.0 ms^{-2} r.m.s. (p = 0.071, Wilcoxon), and between 0.75 and 1.0 ms^{-2} r.m.s. (p = 0.136, Wilcoxon). There was no significant effect of vibration magnitude on the primary segmental mass, m_1 (p = 0.615, Friedman) or the secondary segmental mass, m_2 (p = 0.194, Friedman).

The vibration magnitude had an overall effect on the primary segmental stiffness, k_1 (p < 0.01, Friedman), which tended to decrease with increasing vibration magnitude (p < 0.05, Wilcoxon) except between 0.5 and 0.75 ms^{-2} r.m.s. (p = 0.117, Wilcoxon), and between 0.75 and 1.0 ms^{-2} r.m.s. (p = 0.433, Wilcoxon). The vibration magnitude also had an overall effect on the secondary segmental stiffness, k_2 (p < 0.01, Friedman), which tended to decrease with increasing magnitude (p < 0.05, Wilcoxon) except between 0.125 and 0.25 ms^{-2} r.m.s. (p = 0.347, Wilcoxon), between 0.125 and 0.5 ms^{-2} r.m.s. (p = 0.136, Wilcoxon), and between 0.125 and 0.75 ms^{-2} r.m.s. (p = 0.071, Wilcoxon).

There was no significant effect of vibration magnitude on the primary segmental damping constant, c_1 (p = 0.748, Friedman) or the secondary segmental damping constant, c_2 (p = 0.220, Friedman).

The variations in the parameters with varying vibration magnitude allowed consistently good fits between the model and the measured apparent mass. However, the parameters are not suggested as representative of the dynamic characteristics of specific parts of the human body or differences in specific body parts between different subjects.

5.3.1.4 Apparent mass resonance frequencies with intermittent random vibration

As vibration magnitude increased from 0.25 to 1.0 ms^{-2} r.m.s., the median resonance frequency of the apparent mass decreased from 9.28 Hz to 8.06 Hz with intermittent random vibration, and from 9.62 Hz to 7.81 Hz with continuous random vibration (Table 5.4 A).

The resonance frequencies with intermittent random vibration at 0.25 ms^{-2} r.m.s. were significantly lower than those with continuous random vibration at the same magnitude (p =0.025, Wilcoxon). This effect was apparent for all except subjects 3 and 11 (Table 5.4 A and Figure 5.5). The resonance frequencies with intermittent random vibration at 1.0 ms^{-2} r.m.s. were significantly higher than those with

continuous random vibration at the same magnitude (p = 0.034, Wilcoxon). This effect was apparent for all except subjects 11 and 12 (Table 5.4 A and Figure 5.5).

Table 5.4 Median and ranges of resonance frequencies and model parameters generated by fitting the two-degree-of-freedom parametric model to the apparent masses and phases of 12 subjects at two vibration magnitudes (0.25 and 1.0 ms^{-2} r.m.s.) of both continuous and intermittent random stimuli.

A. Resonance frequency (Hz)				
Subject	0.25 ms^{-2} r.m.s. intermittent	0.25 ms^{-2} r.m.s. continuous	1.0 ms^{-2} r.m.s. intermittent	1.0 ms^{-2} r.m.s. continuous
s1	10.65	11.04	9.18	8.59
s2	9.38	9.47	8.20	8.01
s3	8.01	7.91	7.23	6.84
s4	8.69	8.79	7.71	7.13
s5	9.96	10.25	8.50	8.40
s6	9.18	9.38	7.91	7.62
s7	8.40	8.79	7.52	7.42
s8	10.16	10.25	8.69	8.59
s9	8.98	9.77	7.62	7.32
s10	11.13	11.82	9.77	9.18
s11	8.50	8.20	7.03	7.32
s12	9.86	10.55	8.50	8.79
Minimum	8.01	7.91	7.03	6.84
Median	9.28	9.62	8.06	7.81
Maximum	11.13	11.82	9.77	9.18

B. Model parameters									
Vibration magnitude (ms^{-2} r.m.s.)		m_0 (kg)	m_1 (kg)	k_1 (N/m)	c_1 (Ns/m)	m_2 (kg)	k_2 (N/m)	c_2 (Ns/m)	f_r (Hz)
0.25 intermittent	Minimum	15.1	10.6	39883	237	13.8	162269	737	8.01
	Median	18.8	14.4	70758	407	19.5	232477	1454	9.28
	Maximum	24.2	28.3	106650	1135	32.0	296319	2864	11.13
0.25 continuous	Minimum	13.3	9.7	47817	223	6.7	73096	355	7.91
	Median	18.9	13.2	60506	341	22.2	243550	1533	9.62
	Maximum	25.2	35.3	131477	1702	32.1	352212	2296	11.82
1.0 intermittent	Minimum	14.8	12.4	35956	277	13.8	141198	847	7.03
	Median	17.7	16.1	59117	456	20.8	182644	1669	8.06
	Maximum	21.4	32.0	90193	1326	29.9	264476	2625	9.77
1.0 continuous	Minimum	14.3	10.4	24859	193	14.0	147512	742	6.84
	Median	16.9	14.9	52442	433	21.3	161898	1743	7.81
	Maximum	22.0	27.7	82605	720	30.3	234212	2664	9.18

m_0, m_1 and m_2 – segmental masses. k_1 and k_2 – segmental stiffnesses. c_1 and c_2 – segmental damping constants. f_r – apparent mass resonance frequency of the model.

The absolute difference between the resonance frequencies at 0.25 and 1.0 ms^{-2} r.m.s. was significantly less with intermittent random vibration than with the continuous random vibration (p = 0.015, Wilcoxon). This effect was present for all except subject 11 (Table 5.4 A and Figure 5.5). The median reduction in resonance frequency between 1.0 ms^{-2} r.m.s. and 0.25 ms^{-2} r.m.s. was less with intermittent random vibration (1.37 Hz) than with continuous random vibration (1.71 Hz).

5.3.1.5 Parameters of the two-degree-of-freedom model fitted to the apparent masses with intermittent random vibration

The median and range of the parameters of the two-degree-of-freedom model fitted to individual apparent masses and phases are shown in Table 5.4 B. The effect of intermittent random vibration compared to continuous random vibration on the model parameters has been investigated by comparing the parameters.

The primary segmental stiffness (k_1) was significantly greater (p = 0.023, Wilcoxon) with the intermittent signal than with the continuous signal at 1.0 ms^{-2} r.m.s. (only subjects 1 and 12 showed the reverse trend), consistent with the characteristics of thixotropy. However, intermittency had no significant effect at 0.25 ms^{-2} r.m.s. (p = 0.695, Wilcoxon, with six subjects having a higher k_1 with the intermittent signal and six having a higher k_1 with the continuous signal).

There was no significant difference in the secondary segmental stiffness (k_2) between the continuous and the intermittent stimulus at either 1.0 ms^{-2} r.m.s. (p = 0.084, Wilcoxon) or 0.25 ms^{-2} r.m.s. (p = 0.754, Wilcoxon). However, 10 of the 12 subjects showed a higher k_2 at 1.0 ms^{-2} r.m.s. with the intermittent signal than with the continuous signal, consistent with thixotropy.

For the other parameters in the two-degree-of-freedom model, there were no significant differences between the continuous and the intermittent stimulus at either 0.25 or 1.0 ms^{-2} r.m.s.

5.3.2 Response in the horizontal (z-axis) cross-axis direction

5.3.2.1 Overview

The individual horizontal (z-axis) cross-axis apparent masses of the 12 subjects with the five magnitudes of continuous random vibration are shown in Figure 5.7. The median normalised cross-axis apparent masses of the group of 12 subjects are shown in Figure 5.8. The median and ranges of the individual peak frequencies are shown in Table 5.5. The individual horizontal cross-axis apparent masses of the 12 subjects with two vibration magnitudes (0.25 and 1.0 ms^{-2} r.m.s.) with both continuous and intermittent random vibration are shown in Figure 5.9.

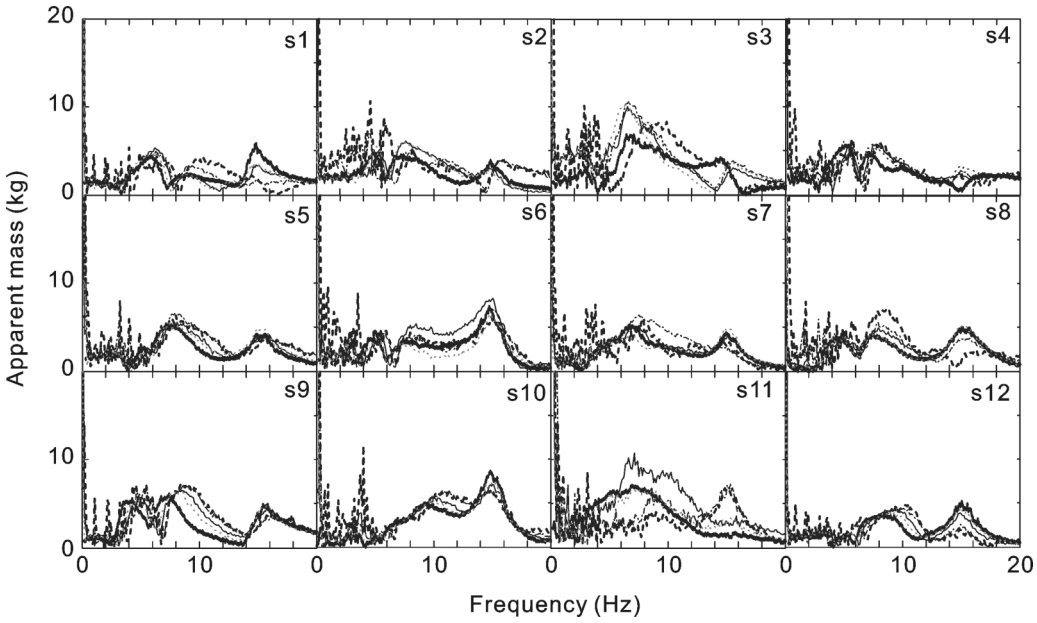

Figure 5.7 Individual horizontal *z*-axis cross-axis apparent masses of 12 subjects (s1 to s12) at five vibration magnitudes (- - - - - 0.125 ms^{-2} r.m.s.; _·_·_·_ 0.25 ms^{-2} r.m.s.; ——— 0.5 ms^{-2} r.m.s.; ..... 0.75 ms^{-2} r.m.s.; ▬▬▬ 1.0 ms^{-2} r.m.s.) of continuous random stimuli.

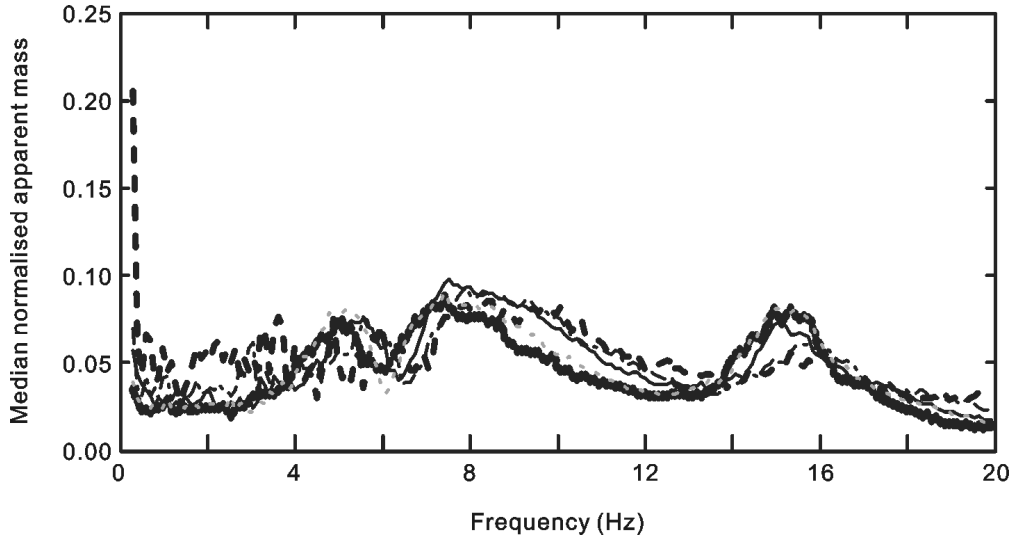

Figure 5.8 Median normalised horizontal *z*-axis cross-axis apparent masses of the group of 12 subjects at five vibration magnitudes (- - - - - 0.125 ms^{-2} r.m.s.; _·_·_·_ 0.25 ms^{-2} r.m.s.; ——— 0.5 ms^{-2} r.m.s.; ..... 0.75 ms^{-2} r.m.s.; ▬▬▬ 1.0 ms^{-2} r.m.s.) of continuous random stimuli.

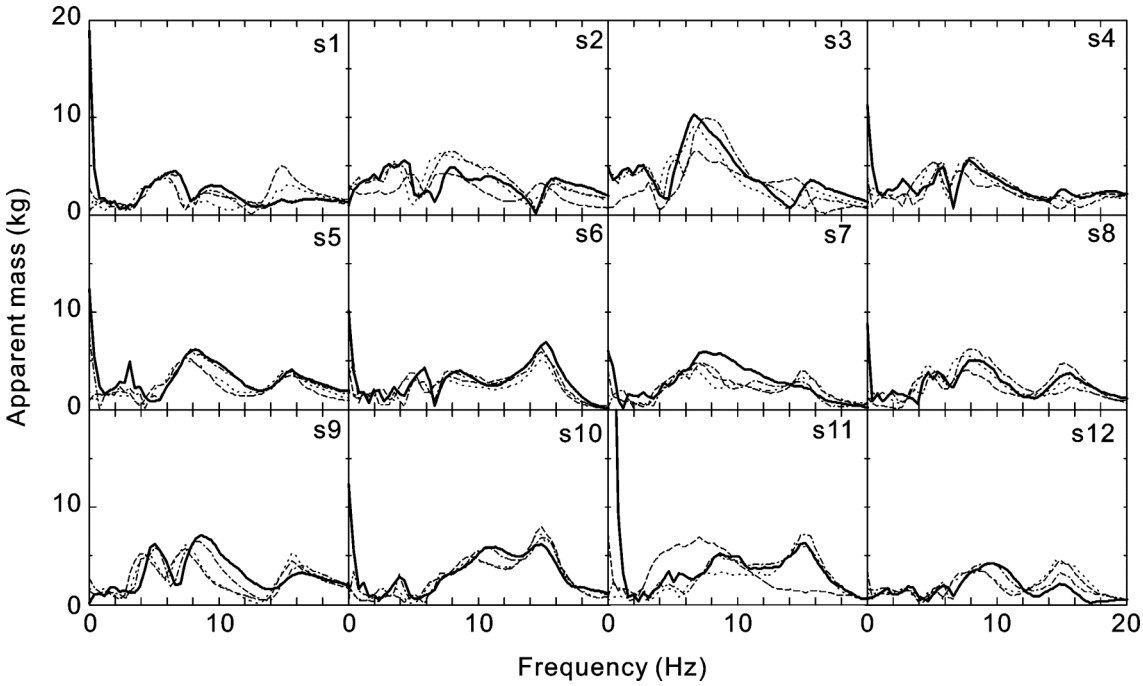

Figure 5.9 Individual horizontal *z*-axis cross-axis apparent masses of 12 subjects (s1 to s12) at two vibration magnitudes (_ ._ ._._ 0.25 ms^{-2} r.m.s. intermittent; …… 1.0 ms^{-2} r.m.s. intermittent; ——— 0.25 ms^{-2} r.m.s. continuous; _ _ _ _ _ 1.0 ms^{-2} r.m.s. continuous) of both intermittent random stimuli and continuous random stimuli.

Table 5.5 Median and ranges of peak frequencies of horizontal *z*-axis cross-axis apparent masses of 12 subjects at five vibration magnitudes (0.125, 0.25, 0.5, 0.75 and 1.0 ms^{-2} r.m.s.) of continuous random stimuli.

A. Cross-axis peak frequencies of continuous random stimuli (Hz)

Vibration magnitude (ms^{-2} r.m.s.)	Minimum	Median	Maximum
0.125	7.81	8.89	11.04
0.25	6.64	8.26	10.74
0.5	6.54	8.01	9.86
0.75	6.35	7.47	9.86
1.0	6.45	7.42	9.28

B. Cross-axis peak frequencies of intermittent random stimuli (Hz)				
Subject	0.25 ms^{-2} r.m.s. intermittent	0.25 ms^{-2} r.m.s. continuous	1.0 ms^{-2} r.m.s. intermittent	1.0 ms^{-2} r.m.s. continuous
s1	9.38	9.38	8.98	8.98
s2	8.20	8.20	7.03	7.03
s3	7.42	6.64	6.64	6.64
s4	7.81	7.81	7.42	7.03
s5	7.81	8.20	7.42	7.42
s6	7.81	8.59	7.42	7.81
s7	7.03	7.42	6.64	7.03
s8	8.20	8.20	7.42	7.81
s9	8.20	8.59	7.42	7.42
s10	10.55	11.33	9.77	9.38
s11	8.59	8.59	8.98	7.03
s12	9.78	9.38	8.98	8.20
Minimum	7.03	6.64	6.64	6.64
Median	8.20	8.40	7.42	7.42
Maximum	10.55	11.33	9.77	9.38

The coherencies were generally lower than 0.5 with the lowest vibration magnitude (0.125 ms^{-2} r.m.s.) at frequencies less than 4.0 to 6.0 Hz. At 0.125 ms^{-2} r.m.s. the coherencies were generally in excess of 0.7 in the frequency range from about 6.0 Hz to between 14.0 and 16.0 Hz. At 1.0 ms^{-2} r.m.s. the coherencies were in excess of 0.8 in the frequency range from about 4.0 Hz to about 18.0 Hz.

There were three distinguishable peaks in each cross-axis apparent mass curve: the first below about 4.0 to 8.0 Hz, the second from around 4.0 or 8.0 Hz to around 12.0

Hz, the third between 14 and 16 Hz (Figures 5.7 and 5.8). The third peak was caused by non-rigidity of the vibrator in the horizontal longitudinal direction during the vertical excitation. With no subject on the platform, the power spectral density of the measured horizontal acceleration showed a peak between 14 and 16 Hz with a magnitude less than 5% of the vertical acceleration excitation. The third peak was therefore excluded from further consideration. The first two peaks were caused by the biodynamic response of the human body and are of interest. The first peak had a low coherency (less than 0.3) below about 6.0 Hz, so the second peak was used to obtain the horizontal *z*-axis cross-axis apparent mass peak frequency as described in Section 5.2.5.3. The magnitudes of the horizontal *z*-axis cross-axis apparent masses at the peaks were less than 10% of the apparent masses at this frequency in the vertical direction.

5.3.2.2 Horizontal (z-axis) cross-axis apparent mass peak frequencies with continuous random vibration

There was a significant effect of vibration magnitude on the horizontal (*z*-axis) cross-axis apparent mass peak frequencies ($p < 0.01$, Friedman). The peak frequency decreased significantly with increasing vibration magnitude from 0.125 to 0.75 ms^{-2} r.m.s. ($p < 0.05$, Wilcoxon). There was no significant difference in the peak frequencies between 0.75 and 1.0 ms^{-2} r.m.s. ($p = 0.14$, Wilcoxon).

The median peak frequencies of the cross-axis apparent masses of the 12 subjects decreased from 8.89 Hz to 7.42 Hz as the vibration magnitude increased from 0.125 to 1.0 ms^{-2} r.m.s. (Table 5.5 A).

The peak frequencies of the median normalised cross-axis apparent masses of the group of 12 subjects were 8.40, 7.91, 7.52, 7.42, and 7.42 Hz with vibration magnitudes of 0.125, 0.25, 0.5, 0.75, and 1.0 ms^{-2} r.m.s., respectively (Figure 5.8).

There were significant correlations between the cross-axis peak frequencies and the inline resonance frequencies at 1.0 ms^{-2} r.m.s. ($r = 0.858$, $p < 0.01$, Spearman rank order correlation test), 0.75 ms^{-2} r.m.s. ($r = 0.785$, $p < 0.01$, Spearman), 0.5 ms^{-2} r.m.s. ($r = 0.835$, $p < 0.01$, Spearman) and 0.25 ms^{-2} r.m.s. ($r = 0.703$, $p = 0.011$, Spearman) ms^{-2} r.m.s. However, the correlation was not statistically significant at 0.125 ms^{-2} r.m.s. ($r = 0.469$, $p = 0.124$, Spearman).

5.3.2.3 Cross-axis apparent mass peak frequencies with intermittent random vibration

The median peak frequency of the cross-axis apparent masses with intermittent random vibration decreased from 8.20 Hz to 7.42 Hz as the vibration magnitude increased from 0.25 to 1.0 ms^{-2} r.m.s. With continuous random vibration, the median

peak frequency decreased from 8.40 Hz to 7.42 Hz as the vibration magnitude increased from 0.25 to 1.0 ms^{-2} r.m.s. (Table 5.5 B).

There was no significant difference between the peak frequency with 0.25 ms^{-2} r.m.s. intermittent random vibration and the peak frequency with continuous random vibration at the same magnitude (p = 0.257, Wilcoxon). However, five subjects showed a lower peak frequency and only 2 subjects showed a higher peak frequency (five subjects showed no change) with intermittent stimuli than with continuous vibration at this magnitude (Figure 5.9 and Table 5.5 B). This implies that with some subjects the dynamic stiffness of the body in the horizontal cross-axis at the low magnitude was lowered due to prior high magnitude vibration in the vertical direction. At 1.0 ms^{-2} r.m.s., there was no significant difference between the peak frequency with intermittent random vibration and the peak frequency with continuous random vibration (p = 0.705, Wilcoxon).

The absolute differences between the peak frequencies at 0.25 and 1.0 ms^{-2} r.m.s. were marginally not significantly different between the intermittent random vibration and the continuous random vibration (p = 0.095, Friedman).

5.4 Discussion

5.4.1 Response in the vertical (x-axis) direction

5.4.1.1 Effect of the magnitude of continuous random vibration on apparent mass resonance frequency

The vertical in-line apparent masses at five magnitudes show that the semi-supine body is nonlinear: the resonance frequencies decreased significantly with increasing vibration magnitude. The relaxed semi-supine posture was assumed to involve less voluntary muscular postural control of the body than sitting and standing postures used in most previous studies of the nonlinearity of the body. The consistent nonlinear response found here suggests that the nonlinearity is not primarily caused by voluntary control of postural muscles but as a result of some passive property of the body (e.g. thixotropy) or, alternatively, an involuntary reflex response of the body.

A passive thixotropic characteristic implies that the dynamic stiffness of muscles, or other body components, undergoes a reduction as a result of mechanical perturbation, with a recovery after a period of stillness (Lakie, 1986). Fairley and Griffin (1989) speculated that the nonlinear loosening effect of the musculo-skeletal structure had a similar mechanism to the thixotropic property of relaxed human muscles. However, there was no experimental data to support their hypothesis. The

current study shows that the nonlinearity is present not only in postures where there is muscular control of posture but also in postures where muscular activity is not required to maintain posture. Previous studies with upright sitting and standing postures have found that variations in posture, so as to vary the muscular tension, have little effect on the nonlinearity. This is consistent with thixotropy rather than muscle activity being the primary cause of the nonlinearity.

The fore-and-aft apparent mass resonance frequency at the backrest for subjects sitting upright with average thigh contact while exposed to fore-and-aft random whole-body vibration reduced from 5 Hz to 2 Hz (with normalised apparent mass at resonance between 1.5 and 1.2) as the vibration magnitude increased from 0.125 to 1.25 ms^{-2} r.m.s. (Nawayseh and Griffin, 2005b). Compared to that upright sitting posture with fore-and-aft excitation from the backrest, the semi-supine body exhibited higher equivalent stiffness (and a higher resonance frequency) but lower damping (indicated by the magnitude of the apparent mass at resonance). The lower resonance frequency of the fore-and-aft apparent mass on the backrest might be due to a pitching mode of the upper body pivoting upon the pelvic structure, whereas in the present study the response of the semi-supine body may be dominated by axial movement normal to the back inline with the vertical *x*-axis excitation.

5.4.1.2 Effect of intermittency on apparent mass resonance frequency

The present results appear to be characteristic of thixotropic changes in the dynamic stiffness of the body during whole-body vibration: the resonance frequency at a low magnitude (0.25 ms^{-2} r.m.s.) was lower with intermittent vibration than with the continuous vibration, whereas the resonance frequency at a high magnitude (1.0 ms^{-2} r.m.s.) was higher with intermittent vibration than with continuous vibration. The resonance frequency at the low magnitude reflected the dynamic stiffness of the body 2.56 s after high magnitude 'perturbation'; the resonance frequency at the high magnitude reflected the dynamic stiffness of the body 2.56 s after low magnitude perturbation. With minimal postural muscle activity, the characteristics of the semi-supine body seem consistent with thixotropy being a cause of the characteristic nonlinearity, but the change found here was small and so if thixotropy is the primary cause of the nonlinearity it must have a time-constant much less than 2.56 s.

A statistically significant variation in the stiffness of the body during the intermittent stimuli was only found for the stiffness of k_1 in the parametric model at 1.0 ms^{-2} r.m.s. (Section 5.3.1.5 and Table 5.4 B). This suggests that the effect of the different shear histories on the dynamic stiffness of the body was small, or that the body stiffness recovered very quickly after perturbation, for example in less than 2.56 s.

The nonlinearity in steady-state sitting conditions has been found to be significantly reduced by some periodic muscle activity associated with voluntary body movement, with the reduction mainly due to a change in the resonance frequency with low magnitudes of vibration (see Chapter 4). With normal steady-state sitting, the biodynamic response of the body may be influenced by voluntary muscular control of posture in response to the vibration, by involuntary muscular reflex responses, and by the passive dynamic property of muscles and tissues (including thixotropy). In addition to these three components, voluntary periodic movement involves muscular control. If the passive thixotropy of tissues is a cause of the nonlinearity and if voluntary periodic muscular activity has the same effect on the thixotropy at low and at high magnitudes of vibration, the resonance frequencies might be expected to decrease at both low and high magnitudes. However, voluntary periodic muscular activity was more effective in reducing the resonance frequency at low magnitudes, suggesting that the voluntary movement had a different effect on thixotropy at different magnitudes of vibration. At high magnitudes of vibration, the passive deformation and shearing stress on muscles and other tissues from the vibration may have already reduced the dynamic stiffness, so that the effect of voluntary muscle activity on dynamic stiffness was less at higher vibration magnitudes.

Thixotropy is a passive response of the body and muscle reflex responses are involuntary. During whole-body vibration, both responses could be present in the relaxed semi-supine body. Neuromuscular reflex responses are a necessary component in the control of spinal stability (Moorhouse and Granata, 2007), and by measuring trunk muscle EMG (Granata *et al*., 2004) found reflex responses of paraspinal muscles associated with movement disturbances. Possibly, with low magnitudes of vibration, involuntary muscular reflex response may increase the dynamic stiffness of the body, whereas at high magnitudes the relative contribution from reflex response may be less than the contribution with low magnitudes of vibration, resulting in a softer body at higher magnitudes. The relaxed semi-supine conditions of the present study allowed the subjects to lie with minimal voluntary and involuntary muscular activity, or at least, less voluntary and involuntary muscular activity than when sitting and standing. The consistent nonlinear response with relaxed passive body tissues suggests muscle activity may not be the primary cause of the nonlinearity.

5.4.2 Response in the horizontal z-axis cross-axis direction

5.4.2.1 Effect of the magnitude of continuous random vibration on horizontal z-axis cross-axis apparent mass peak frequency

The peak frequencies of the horizontal *z*-axis cross-axis apparent masses were significantly correlated with the resonance frequencies of the vertical *x*-axis inline apparent masses at four (0.25, 0.5, 0.75 and 1.0 ms^{-2} r.m.s.) of the five vibration magnitudes (Section 5.3.2.2). This may suggest that the responses in the two axes are cross-coupled by a common mechanism. The horizontal *z*-axis cross-axis apparent masses at five magnitudes also show that the semi-supine body is nonlinear: the peak frequency decreased significantly with increasing vibration magnitude. The consistent nonlinear response in both the vertical *x*-axis and horizontal *z*-axis suggests the nonlinearities in these two directions may have a common cause.

Using upright sitting posture with a backrest and minimal thigh contact, Nawayseh and Griffin (2005b) found that the dominant vertical *z*-axis cross-axis apparent mass peak frequency at the back during fore-and-aft *x*-axis whole-body vibration was in the range 5 to 7 Hz at vibration magnitudes between 0.625 and 0.125 ms^{-2} r.m.s. This frequency range differed from the resonance frequencies in the fore-and-aft inline direction at the back while seated (i.e., 3 to 5 Hz). The magnitude of the vertical cross-axis forces present on the backrest was small (less than 4 kg at the peak). The authors explained that the expected magnitudes of rotational modes in the mid-sagittal plane of the head, the spine and the pelvis were reduced by some vertical motion of the spine counteracting the pitching motions. In the present study, the horizontal cross-axis peak frequencies were in the range 7 to 9 Hz which coincides with the vertical inline resonance frequency between 7 and 10 Hz, suggesting common modes in the vertical inline and horizontal cross-axis responses. The magnitude of the cross-axis apparent mass of the semi-supine body is also small in the present study (up to 5 kg at peak and less than 10% of the vertical inline apparent mass at resonance).

5.4.2.2 Effect of intermittency on z-axis cross-axis apparent mass peak frequency

The apparent dependence of the response on the shear-history in the vertical in-line response was not significant in the cross-axis direction. This could be due to a lower magnitude of cross-axis response and less nonlinearity presented in the cross-axis than in the vertical direction. The magnitudes of the cross-axis apparent masses are less than 10% of the vertical in-line apparent masses – the maximum values of the median normalised apparent mass and the median normalised cross-axis apparent

mass were 1.60 and 0.10, respectively (Figure 5.9). The absolute difference between the peak frequencies of the median normalised cross-axis apparent masses at 0.125 ms^{-2} r.m.s. (8.40 Hz) and at 1.0 ms^{-2} r.m.s. (7.42 Hz) was 0.98 Hz. The absolute difference for the vertical in-line apparent mass was 3.03 Hz (10.35 Hz at 0.125 ms^{-2} r.m.s. and 7.32 Hz at 1.0 ms^{-2} r.m.s.). On this basis, the nonlinearity in the cross-axis direction was only 32% (0.98 Hz / 3.03 Hz) of the nonlinearity in the vertical direction.

5.5 Conclusions

With minimal voluntary and involuntary muscular activity, the relaxed semi-supine body showed a consistent nonlinear biodynamic response, both in the vertical (*x*-axis) direction and in the horizontal (*z*-axis) cross-axis direction, during vertical whole-body vibration.

The responses of the semi-supine body during intermittent random vibration had a typical thixotropic characteristic at both a low magnitude of vibration (0.25 ms^{-2} r.m.s.) and a high magnitude of vibration (1.0 ms^{-2} r.m.s.). This resulted in less nonlinearity than with continuous random vibration. It is concluded that the passive thixotropic properties of the body could be the principal cause of the nonlinearity seen in measures of the apparent mass and transmissibility of the human body.

Chapter 6

Nonlinear dual-axis biodynamic response of the semi-supine human body during longitudinal horizontal whole-body vibration

6.1 Introduction

The resonance frequencies in frequency response functions of the human body (e.g. apparent mass and transmissibility) decrease with increasing vibration magnitude – the median apparent mass resonance frequencies of a group of 12 seated human subjects were, respectively, 5.4, 5.0, 4.7, 4.6, 4.4 and 4.2 Hz with vibration magnitudes of 0.25, 0.5, 1.0, 2.0 and 2.5 ms^{-2} r.m.s. (Mansfield and Griffin, 2000). This nonlinear biodynamic response has been found in studies of apparent mass and transmissibility with various sitting postures (e.g. Mansfield and Griffin, 2002; Nawayseh and Griffin, 2003; Nawayseh and Griffin, 2005a) and standing postures (Matsumoto and Griffin, 1998a; Subashi *et al*., 2006) that require muscular postural control. The nonlinearity is evident in both the vertical and the fore-and-aft responses of the seated human body during vertical whole-body vibration (Nawayseh and Griffin, 2003), and in both the fore-and-aft and vertical responses of the seated human body during fore-and-aft whole-body vibration (Holmlund and Lundström, 2001; Nawayseh and Griffin, 2005a).

Electromyographic (EMG) studies indicate that the activity of the back muscles varies with vibration magnitude (Robertson and Griffin, 1989; Blüthner *et al*., 2002). So muscular activity could be a cause of the nonlinearity: muscles may stabilize or stiffen the body at low magnitudes of vibration but be incapable of a sufficient response at high magnitudes where there are greater inertial forces. With 12 subjects sitting upright without a backrest, the study described in Chapter 4 found that the nonlinearity could be significantly reduced by some voluntary periodic upper-body movements. The apparent mass resonance frequencies were 5.47 Hz at 0.25 ms^{-2} r.m.s. and 4.39 Hz at 2.0 ms^{-2} r.m.s. without voluntary movements, but 4.69 Hz at 0.25 ms^{-2} r.m.s. and 4.59 Hz at 2.0 ms^{-2} r.m.s. with voluntary movements. The change in nonlinearity due to voluntary movement was considered to be due to either a change in muscular activity stimulated by the voluntary periodic contraction or a change in the stiffness of the body due to the thixotropic behaviour of body tissues.

'Thixotropy' refers to a recovery behaviour of colloidal materials after the breakdown of structural linkages (Tanner, 1985). Perturbations break down the structures but after a period of stillness the structures reform. Some human body tissues

(protoplasm, mucus, etc.) have a similar thixotropic behaviour (Fung, 1981). Lakie (1986) found a thixotropic response in human index fingers in response to tap stimuli – the dynamic stiffness of the finger increased back to normal about 10 seconds after an impulse. The nonlinearity in the human body during whole-body vibration could be a consequence of thixotropy: the equivalent stiffness of the body decreasing during high magnitude vibration and the stiffness increasing after vibration or with low magnitudes of vibration.

The preceding study described in Chapter 5 compared the apparent mass of the semi-supine body measured with intermittent vertical vibration and continuous vertical vibration. The intermittent vibration (alternately 1.0 and 0.25 ms^{-2} r.m.s.) allowed the apparent mass to be measured 2.56 s after the commencement of high magnitude or the low magnitude vibration. With continuous random vibration, the apparent mass resonance frequencies were 9.62 and 7.81 Hz with magnitudes of 0.25 and 1.0 ms^{-2} r.m.s., respectively. Whereas with intermittent vibration, the resonance frequencies were 9.28 and 8.06 Hz at 0.25 and 1.0 ms^{-2} r.m.s., respectively. The responses with intermittent vibration were consistent with the resonance frequency, or the dynamic stiffness, of the body depending on the shear history of the body, typical of thixotropy. However, the changes could be caused by either muscle activity (involuntary or voluntary) or a passive change in the body tissues. In a relaxed semi-supine posture there is little muscle activity compared to sitting and standing postures, so the nonlinear response may be more likely due to thixotropic changes than muscular contractions. If thixotropy is the primary cause of the nonlinearity in the in-line and cross-axis responses with various directions of excitation, the dependence on the shear history found with vertical excitation of the semi-supine body should also be present with longitudinal horizontal excitation.

As part of a series of studies to explore the biodynamic nonlinearity, the present study investigated the longitudinal horizontal in-line and the cross-axis vertical biodynamic responses of the relaxed semi-supine body exposed to longitudinal horizontal whole-body vibration. It was designed to find out whether the response of the body is nonlinear with both continuous and intermittent random vibration, and if the intermittency (changed shear history) has an effect on the nonlinearity.

It was hypothesized that, with continuous random whole-body vibration, the longitudinal in-line apparent mass resonance frequencies and vertical cross-axis apparent mass peak frequencies would decrease with increasing vibration magnitude. It was also hypothesized that with intermittency the in-line resonance frequencies and the cross-axis peak frequencies would be decreased by prior high magnitude vibration and increased by prior low magnitude vibration compared to the

resonance frequencies and peak frequencies measured at the same high and low magnitudes of continuous vibration.

6.2 Method

6.2.1 Apparatus

A supine support was constructed with three parts: back support, leg rest and headrest (Figure 6.1). The experimental set-up was the same as used in the preceding study with vertical vibration (Chapter 5) to allow the same semi-supine postures to be tested.

The back support was a horizontal flat rigid 660 mm by 660 mm by 10 mm aluminium plate with a high stiffness 3 mm thick laterally treaded rubber layer attached to the upper surface. The complete back support was bolted rigidly to the upper surface of the force platform which monitored the longitudinal forces (in the *z*-axis of the semi-supine subject) and the vertical forces (in the x-axis of the semi-supine subject) exerted by the subject on the back support. The force platform was bolted rigidly to the vibrator platform. The horizontal distance between the edge of the back support and the edge of the leg rest was 50 mm (Figure 6.1).

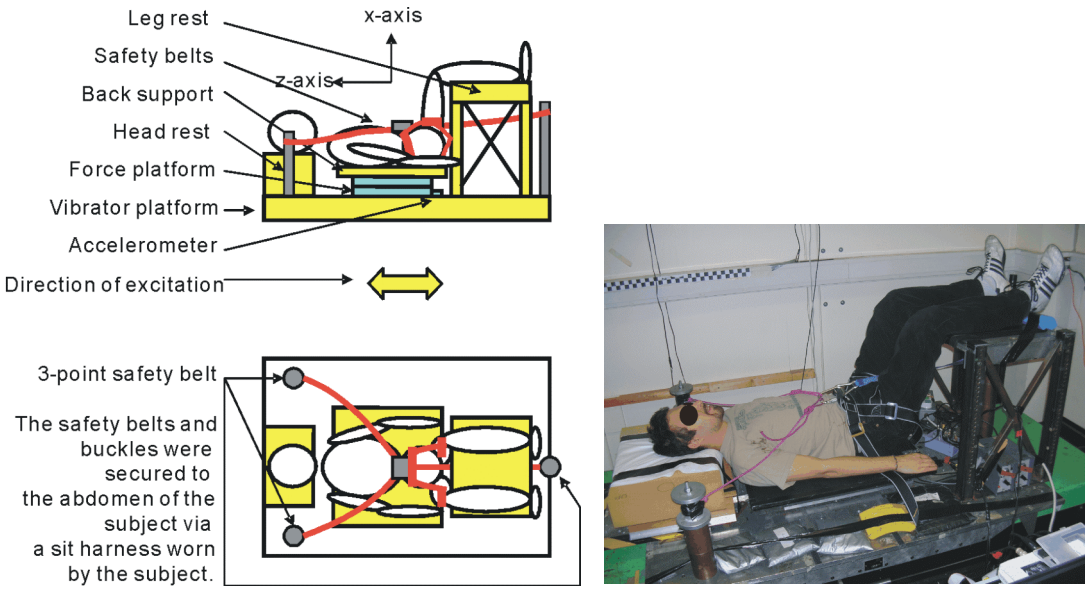

Figure 6.1 Schematic diagram of the supine support showing the semi-supine posture and the axes of the forces (*z*-axis and *x*-axis) and the acceleration (*z*-axis) transducers. A photographic representation of a test subject in the relaxed semi-supine position for longitudinal horizontal (*z*-axis) whole-body vibration.

The legs of subjects rested on a horizontal flat rigid aluminium support with an 8-mm thick high stiffness rubber layer attached to the top. The height of the leg rest was adjusted to allow the lower legs to rest horizontally.

The headrest was a horizontal flat rigid wooden block with 75-mm thick car-seat foam attached to the upper surface. The top surface of the complete headrest was approximately 50 mm higher than the back support. The horizontal distance between the back support and the headrest was adjusted by moving the headrest so that a subject's head could rest comfortably.

Longitudinal horizontal vibration (in the *z*-axis of the subjects) was produced by a 1-metre stroke electro-hydraulic horizontal vibrator capable of accelerations up to ±10 ms^{-2} in the laboratory of the Human Factors Research Unit.

The longitudinal horizontal (*z*-axis) acceleration of the vibrator platform was measured using a Setra 141A ±2 g accelerometer fixed on the plane of vibrator platform below the back support and between the leg rest and the force platform (Figure 1). The longitudinal horizontal (*z*-axis) and the vertical (*x*-axis) forces at the back support were measured using a Kistler 9281 B21 12-channel force platform. The four longitudinal horizontal (*z*-axis) force signals and the four vertical (*x*-axis) force signals from the four corners of the platform were summed and conditioned using two Kistler 5001 charge amplifiers.

An *HVLab* v3.81 data acquisition and analysis system was used to generate test stimuli and acquire the longitudinal acceleration and the longitudinal and vertical forces from the transducers. The one acceleration and the two force signals were acquired at 200 samples per second via 67 Hz analogue anti-aliasing filters.

6.2.2 Stimuli

The random stimuli used in this study had approximately flat constant-bandwidth acceleration power spectra over the frequency range 0.25 to 20 Hz.

The two types of longitudinal horizontal vibration were exactly the same as the ones used in the previous study of vertical vibration:

(i) Continuous random vibration with a duration of 90 seconds tapered at the start and end with 0.5-second cosine tapers. Five magnitudes of acceleration (0.125, 0.25, 0.5, 0.75, and 1.0 ms^{-2} r.m.s., unweighted) were generated using five different random seeds. Twelve subjects were randomly divided into six groups with two persons per group. With different groups, different random seeds were used to generate the random stimuli.

(ii) Intermittent random vibration, alternately at 0.25 and 1.0 ms^{-2} r.m.s. (unweighted) with a total duration of 828 seconds. The 828-second intermittent stimulus was divided evenly into four identical 207-second sections (Figure 6.2 a). During each 207-second section, 18 high magnitude slices and 18 low magnitude slices (generated using different random seeds) were presented alternately. The duration of 828 seconds was determined so that there were sufficient high magnitude and low magnitude slices for the concatenated signals (at high or low magnitude) to have the same duration as each of the continuous signals (i.e., 90 seconds). One single cycle of the intermittent signal was defined as one high magnitude slice followed by one low magnitude slice. During a single cycle of the intermittent motion, the high magnitude slice (at 1.0 ms^{-2} r.m.s.) lasted for 6 seconds (tapered at the start and end with a 0.25-second cosine taper) followed by a low magnitude slice (at 0.25 ms^{-2} r.m.s.) for 5.5 seconds (Figure 6.2 b). The durations of the high or low magnitude slices were determined so that the effective high or low magnitude signals (after removing the tapering) could be analysed with a frequency resolution of about 0.4 Hz (see Section 6.2.5.2).

All test motions were presented in one session lasting approximately 100 minutes. The order of presentation of the six random stimuli (the continuous stimuli at five magnitudes and the intermittent stimulus) was balanced across the twelve subjects.

6.2.3 Posture

While experiencing each motion, subjects maintained a relaxed semi-supine position with their lower legs lifted and resting on the horizontal leg rest so as to give maximum back contact with the back support (Figure 6.1). The longitudinal horizontal distance between the bottom of the buttocks (aligned with the edge of the back support) and the near edge of the leg rest was 50 mm for all subjects. Subjects were instructed to relax totally with their eyes closed. The semi-supine posture was the same as described in the previous study in Chapter 5 with the same instruction to subjects (Appendix B).

For safety, subjects wore a light harness connected by three loose safety belts to the vibrator platform without constraining the movement of the body. The total weight of the harness and buckles was less than 0.5 kg.

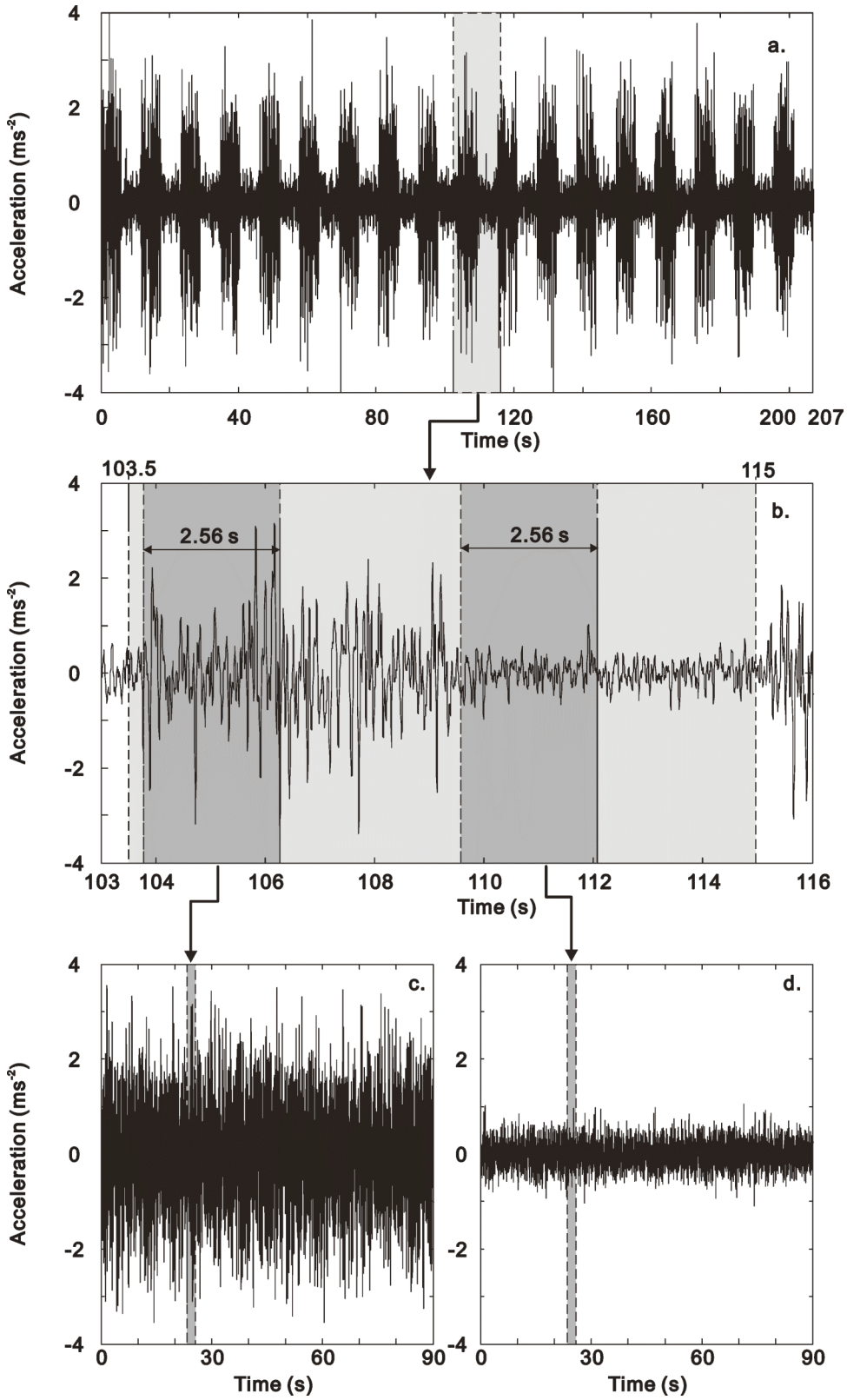

Figure 6.2 A longitudinal input acceleration time history measured with the high-low (1.0-0.25 ms^{-2} r.m.s.) magnitude intermittent random stimuli showing: (a) one complete 207-second intermittent time history; (b) one period of the intermittent time history starting with 6-second high magnitude slice followed by a 5.5-second low magnitude slice; (c) extracted and concatenated high magnitude (1.0 ms^{-2} r.m.s.) time slices (2.56 seconds each); (d) extracted and concatenated low magnitude (0.25 ms^{-2} r.m.s.) time slices (2.56 seconds each). The same procedure was applied to longitudinal horizontal and vertical cross-axis force time histories.

6.2.4 Subjects

Twelve male subjects, aged between 20 to 42 years, with mean (minimum and maximum) stature 1.73 m (1.66 m and 1.80 m) and mean total body mass 70.3 kg (58.3 kg and 86.2 kg) participated in the study. The study used the same subjects and the same testing order as the preceding study with vertical excitation described in Chapter 5.

The experiment was approved by the Human Experimentation, Safety and Ethics Committee of the Institute of Sound and Vibration Research at the University of Southampton.

6.2.5 Analysis

The analysis was similar to that used with vertical excitation (in Chapter 5). The data were analysed over the frequency 0.25 to 20 Hz, but the presentation of results is limited to 0.5 to 10 Hz. The magnitude of the horizontal apparent mass at frequencies greater than 10 Hz was small (about 5% to 15% of the static body mass and 2% to 6% of the apparent mass at resonance).

6.2.5.1 Continuous random vibration

The longitudinal horizontal (*z*-axis) and vertical (*x*-axis) forces measured at the supine back support were analysed relative to the longitudinal horizontal (*z*-axis) acceleration (Figure 6.1). Two frequency response functions – longitudinal apparent mass (where the force was in-line with the acceleration in the longitudinal horizontal direction, i.e. the *z*-axis) and vertical cross-axis apparent mass (where the vertical force was perpendicular to the longitudinal acceleration in the sagittal plane, i.e. the *x*-axis) – were calculated using the cross-spectral density method:

$$M(f) = S_{af}(f) / S_{aa}(f) \qquad (6.1)$$

where, $M(f)$ is the longitudinal apparent mass or the vertical x-axis cross-axis apparent mass, in kg; $S_{af}(f)$ is the cross spectral density between the measured forces and the longitudinal excitation acceleration; $S_{aa}(f)$ is the power spectral density of the longitudinal excitation acceleration.

Before calculating the longitudinal apparent mass, mass cancellation was carried out in the time domain to subtract the force caused by the masses above the force sensing elements (a total of 30.5 kg obtained dynamically in the frequency range 0.25 to 20 Hz). No mass cancellation was needed to calculate the vertical cross-axis apparent mass as there was no input motion in this direction.

The relation of the output motion to the input motion in the calculated frequency response functions was investigated using the coherency:

$$\gamma_{io}^2(f) = | S_{af}(f) |^2 / (S_{aa}(f) S_{ff}(f)) \quad (6.2)$$

where $S_{ff}(f)$ is the power spectral density of the longitudinal force and $\gamma_{io}^2(f)$ is the coherency of the system with a value between 0 and 1. The coherency has a maximum value of 1.0 in a linear single-input system with no noise – the output motion being entirely due to, and linearly correlated with, the input motion.

The apparent masses at the five magnitudes were normalised by dividing by the apparent mass modulus measured at frequencies between 0.25 and 1.5 Hz, where the body was considered rigid. For motion at 0.125 ms^{-2} r.m.s., the normalisation was carried out at 0.98 Hz; for 0.25 ms^{-2} r.m.s. at 0.98 Hz; for 0.5 ms^{-2} r.m.s. at 0.59 Hz; for 0.75 ms^{-2} r.m.s. at 0.59 Hz; for 1.0 ms^{-2} r.m.s. at 0.39 Hz. The median normalised apparent masses at the five magnitudes were then calculated. The same normalisation procedure was applied to calculate the normalised vertical cross-axis apparent mass at the five magnitudes. The median normalised *x*-axis cross-axis apparent masses were then calculated.

The cross spectral densities and the power spectral densities were estimated via Welch's method at frequencies between 0.25 and 20 Hz (data shown 0.25 to 10 Hz). The frequency response functions for each of the 90-second continuous random signals used a fast Fourier transform (FFT) windowing length of 2048 samples, a Hamming window with 100% overlap, a sampling rate of 200 samples per second and an ensuing frequency resolution of 0.098 Hz (see Table 6.1). This signal processing procedure applied to signals measured with continuous vibration is referred as the 0.098-Hz procedure.

Table 6.1 Two signal processing procedures used to analyse measurement with the continuous random stimuli and with the intermittent random stimuli.

A. 0.098-Hz procedure – for measured accelerations and forces with continuous random vibration at 0.125, 0.25, 0.5, 0.75 and 1.0 ms^{-2} r.m.s.

Duration (s)	Sampling rate (Hz)	FFT length	Degrees of freedom	Windowing overlap	Frequency resolution (Hz)
90	200	2048	36	100%	0.098

B. 0.391-Hz procedure – for processed accelerations and forces measured at 0.25 and 1.0 ms^{-2} r.m.s. for both the intermittent and continuous random vibration					
Duration (s)	Sampling rate (Hz)	FFT length	Degrees of freedom	Windowing overlap	Frequency resolution (Hz)
90	200	512	70	0%	0.391 (then linearly interpolated to 0.098 in the frequency domain)

6.2.5.2 Intermittent random vibration

Before the intermittent signals (longitudinal acceleration, longitudinal force and vertical force) were analysed according to the procedure applied to the continuous signals (Section 6.2.5.1), the acquired intermittent signals described in Section 6.2.2 (ii) were processed as described below.

Each of the high magnitude (1.0 ms^{-2} r.m.s.) and low magnitude (0.25 ms^{-2} r.m.s.) time slices of the acceleration and forces measured with each of the 828-second intermittent signals was extracted and concatenated into a processed high magnitude signal (90 s duration) and a processed low magnitude signal (90 s duration) (Figure 6.2 c, d). The duration of each extracted time slice was 2.56 seconds to allow the apparent masses to be measured and calculated before the dynamic stiffness of the body recovered from the prior high magnitude or low magnitude vibration. Each of the force and acceleration time histories measured with the continuous random stimuli and each of the processed force and acceleration time histories measured with the intermittent random stimuli lasted for 90 seconds, allowing the apparent masses to be calculated with the same frequency resolution of 0.391 Hz for both stimuli. The 0.391-Hz procedure used 0% overlap; any discontinuity caused by the concatenation of the 2.56-s slices had an effect at frequencies lower than of interest in the present study (Table 6.1).

The same procedure used to analyse the signals measured with continuous random vibration (Section 6.2.2 (i)) was used to calculate the apparent masses and cross-axis apparent masses with each of the 90-second high magnitude (1.0 ms^{-2} r.m.s.) and low magnitude (0.25 ms^{-2} r.m.s.) processed intermittent signals, except for a different signal processing procedure (0.391-Hz procedure, Table 6.1). The 0.391-Hz procedure was used to generate apparent masses and cross-axis apparent

masses with each of the 90-second processed intermittent acceleration and force signals. The 0.391-Hz procedure was also used to analyse accelerations and forces measured with the continuous vibration at 0.25 and 1.0 ms^{-2} r.m.s. so that the apparent masses measured with the intermittent and the continuous vibration could be compared using the same frequency resolution (0.391 Hz) with the same signal duration (90 seconds). Finally, the frequency resolution obtained using the 0.391-Hz procedure with both intermittent and continuous signals at 0.25 and 1.0 ms^{-2} r.m.s. was increased to 0.098 Hz by linearly interpolating the apparent mass moduli and phases in the frequency domain.

6.2.5.3 Curve-fitting, apparent mass resonance frequencies and cross-axis apparent mass peak frequencies

The parallel two-degree-of-freedom parametric model used to fit the vertical in-line individual apparent masses and phases was adapted to fit the longitudinal in-line individual apparent masses and phases in order to obtain primary resonance frequencies. The horizontal model was described in Section 3.5.2.1 (see Figure 3.12 b). The lumped parameter model was employed as a numerical tool to characterize the apparent mass of the human body. It was not a mechanistic model representing any physical mechanisms or anatomical parts of the body in response to whole-body vibration.

The optimization method used to minimize the error in apparent mass modulus and phase between the model and the measurement was described in Section 3.5.2.2. The resonance frequencies in the individual apparent masses and the median normalised apparent masses were obtained by curve-fitting the measured apparent masses and phases (over the frequency range 0.5 to 10 Hz) to the two-degree-of-freedom lumped parameter model. The 'resonance frequency' was defined as the frequency where the modulus of the apparent mass had a maximum value in the fitted curve.

The vertical *x*-axis cross-axis apparent mass 'peak frequency' was defined as the frequency at which the modulus of the measured cross-axis apparent mass had a maximum value in the frequency range 0.5 to 10 Hz. In this frequency range, there were one, two or three peaks depending on the vibration magnitude and inter-subject variability. The first dominant peak below about 5 Hz was used to represent the dynamic characteristic of the vertical cross-axis response of the body (Section 6.3.2.1).

The same curve-fitting procedure was carried out with the longitudinal apparent masses at the five magnitudes (0.125, 0.25, 0.5, 0.75 and 1.0 ms^{-2} r.m.s) of

continuous random vibration and the two magnitudes (0.25 and 1.0 ms^{-2} r.m.s.) of processed intermittent random vibration.

By fitting the parallel two-degree-of-freedom model to the longitudinal apparent mass, the apparent mass resonance frequency (f_r), the apparent mass at resonance (AM_r), segmental masses (m_0, m_1 and m_2), stiffnesses (k_1 and k_2) and damping constants (c_1 and c_2) were obtained.

6.3 Results

6.3.1 Response in the longitudinal horizontal (z-axis) direction

6.3.1.1 Overview

The individual apparent masses and phases of twelve subjects with five vibration magnitudes of continuous random vibration are shown in Figure 6.3. The median normalised apparent masses and phases of the group of 12 subjects are shown in Figure 6.4. The medians and full ranges of individual apparent mass resonance frequencies are shown in Table 6.2. The individual apparent masses and phases of the 12 subjects at two vibration magnitudes (0.25 and 1.0 ms^{-2} r.m.s.) with both continuous and intermittent random vibration are shown in Figure 6.5.

Consistently low target errors were obtained by curve-fitting to the two-degree-of-freedom model. The results of the curve-fitting for one subject (Subject 11) are shown for five magnitudes of continuous random vibration in Figure 6.6. The fitting results of the vertical in-line apparent mass of the same semi-supine subject were shown in Chapter 5.

The coherencies were generally in excess of 0.9 in the frequency range 0.5 to 6.0 Hz. The coherency reduced over a band of higher frequencies, with the frequency of the coherency drop decreasing with increasing vibration magnitude (e.g., 8 to 20 Hz at 0.125 ms^{-2} r.m.s. and 6 to 18 at 1.0 ms^{-2} r.m.s.). The lowest coherency (0.1 to 0.5) occurred with the highest vibration magnitude (1.0 ms^{-2} r.m.s.) in the range 10 to 16 Hz. The lowest coherency tended to decrease from about 0.5 to about 0.1 as the vibration magnitude increased from 0.125 to 1.0 ms^{-2} r.m.s. The coherencies obtained with intermittent random vibration had a similar pattern to those with continuous random vibration.

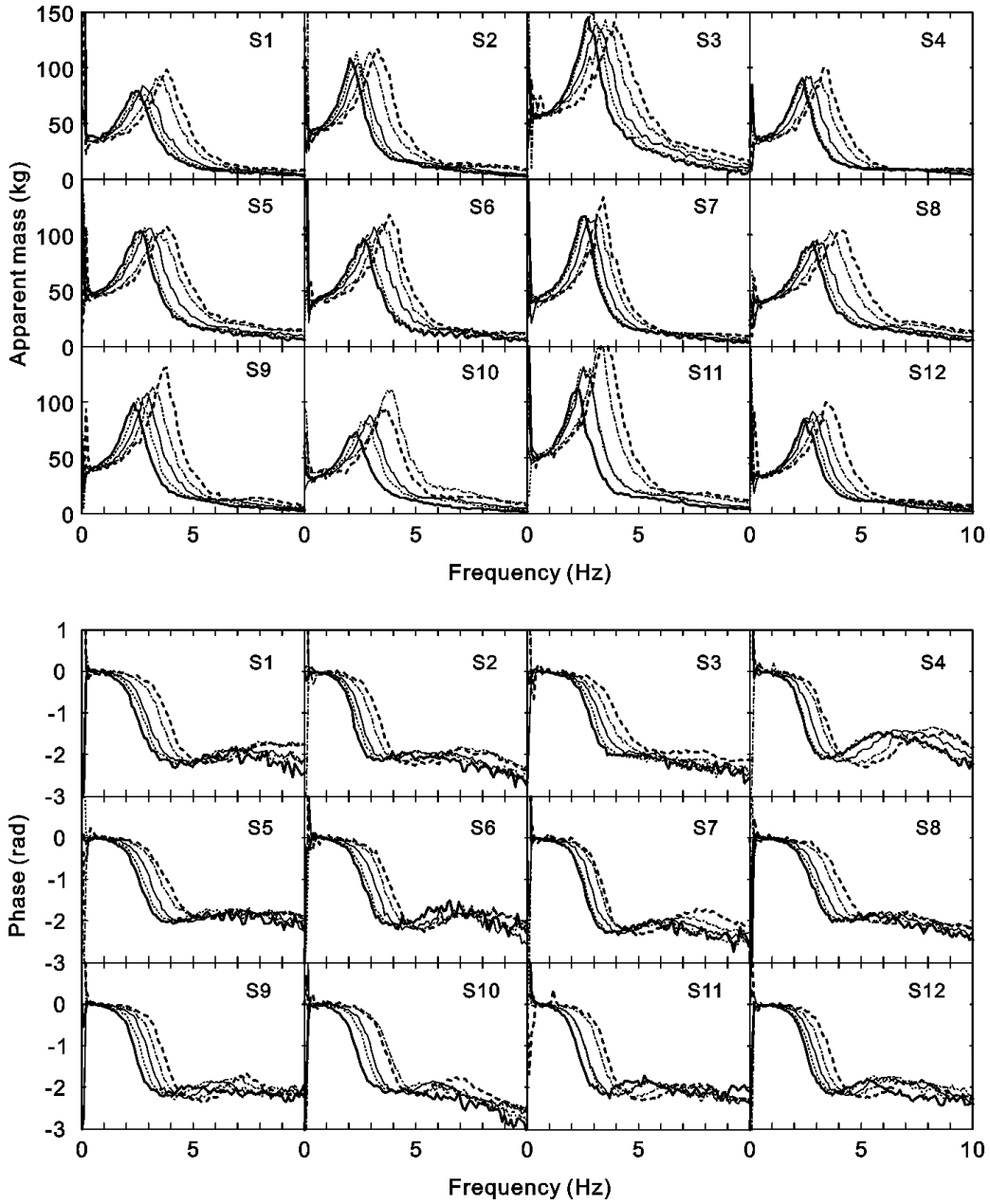

Figure 6.3 Individual apparent masses (upper) and phases (lower) of 12 subjects (S1 to S12) at five vibration magnitudes (- - - - - 0.125 ms^{-2} r.m.s.; _·_·_·_ 0.25 ms^{-2} r.m.s.; ——— 0.5 ms^{-2} r.m.s.; ..... 0.75 ms^{-2} r.m.s.; ▬▬▬ 1.0 ms^{-2} r.m.s.) of continuous random vibration.

There was one dominant resonance frequency in the longitudinal apparent mass between 2.0 and 4.0 Hz. Since the magnitude of the apparent mass at frequencies greater than 5 Hz was small (less than 8% of the apparent mass at resonance), the minor secondary resonance expected at a higher frequency than the primary resonance was not clear. The secondary resonance was expected as it occurs in the apparent mass at the back when subjects seated upright with a backrest are exposed to vertical whole-body vibration, especially at low magnitudes (Nawayseh and Griffin, 2004). In the present results, the secondary resonances between about 6 and 10 Hz could be seen with only some subjects (Subjects 2, 8, 9 and 12) and only at very low vibration magnitudes by referring to the phase (Figure 6.3).

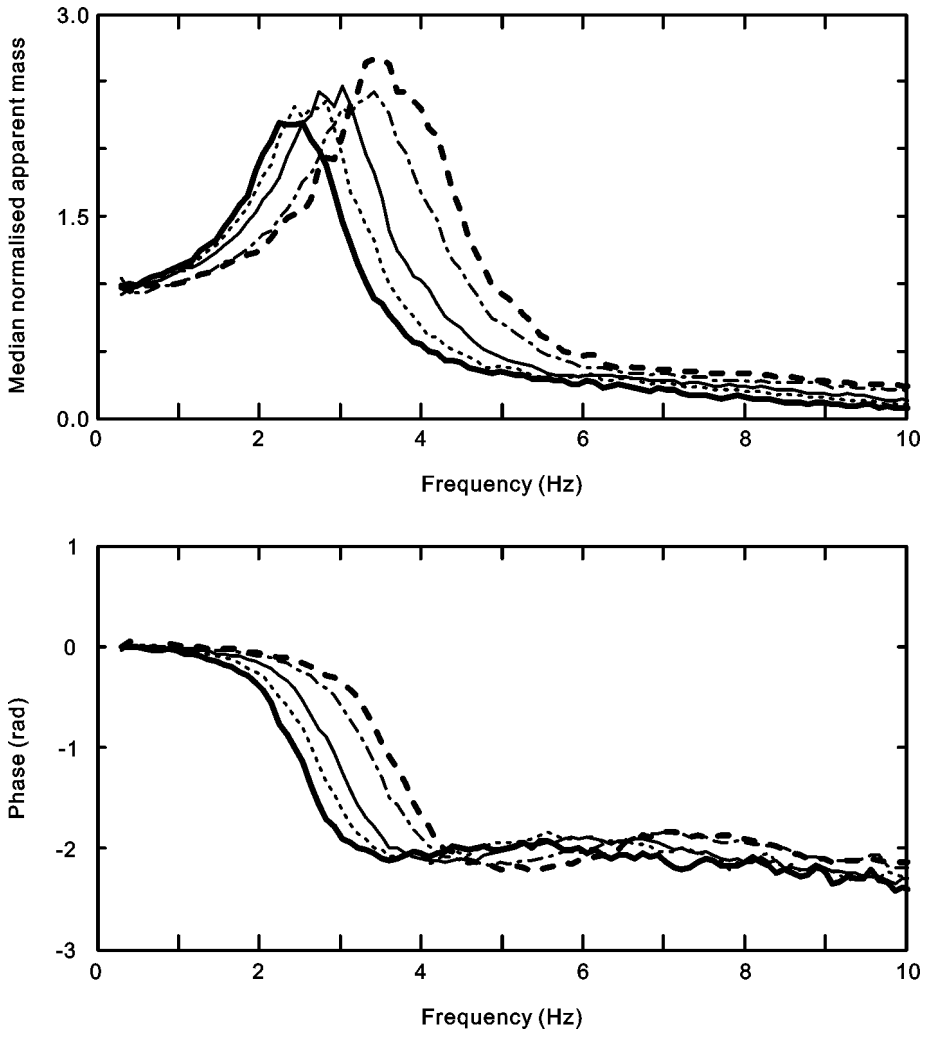

Figure 6.4 Median normalised apparent masses (upper) and phases (lower) of the group of 12 subjects at five vibration magnitudes (- - - - - 0.125 ms^{-2} r.m.s.; _.._.._.._ 0.25 ms^{-2} r.m.s.; ——— 0.5 ms^{-2} r.m.s.; ..... 0.75 ms^{-2} r.m.s.; ▬▬▬ 1.0 ms^{-2} r.m.s.) of continuous random vibration.

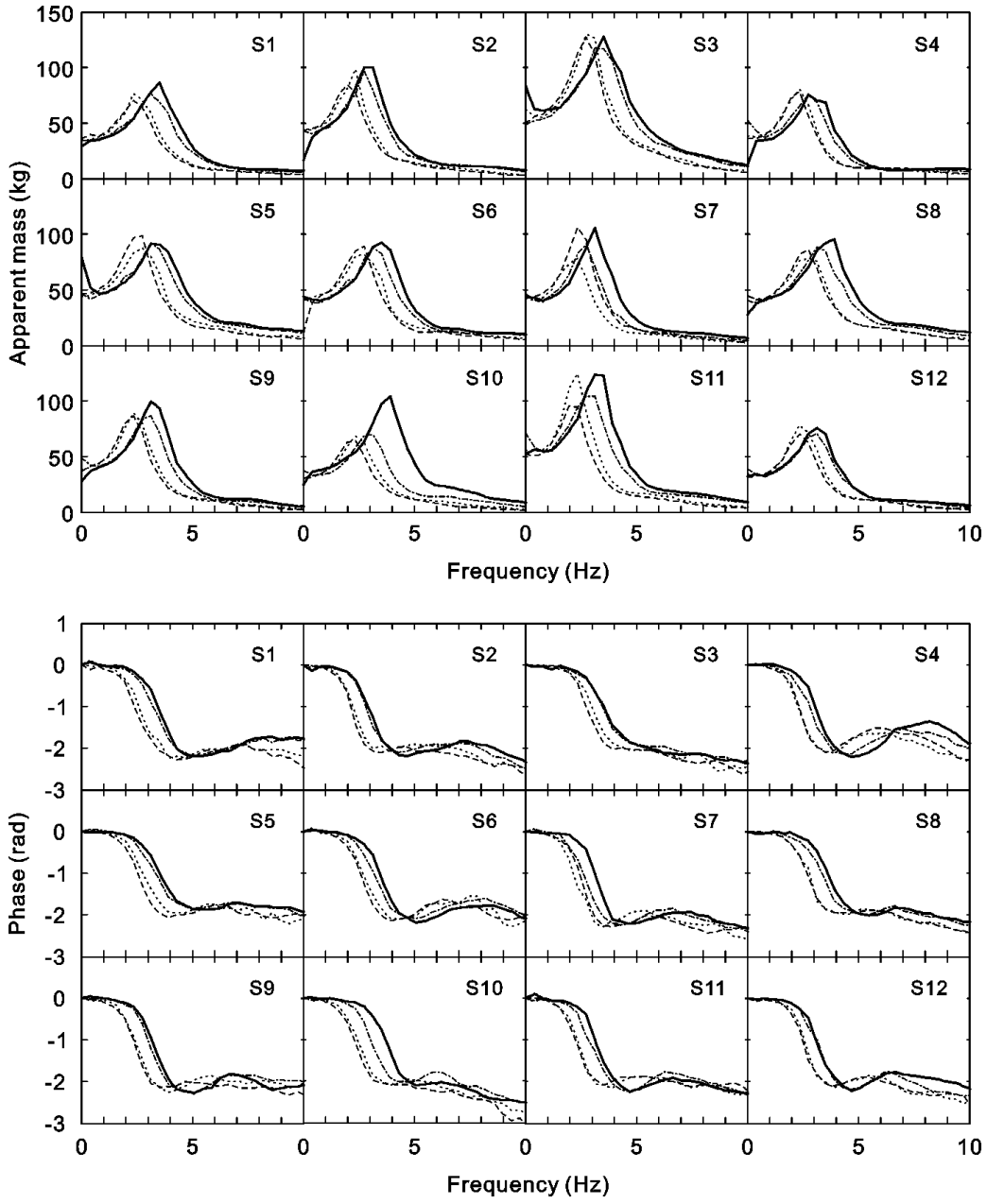

Figure 6.5 Individual apparent masses (upper) and phases (lower) of 12 subjects (S1 to S12) at two vibration magnitudes (_ ._ ._ ._. 0.25 ms^{-2} r.m.s. intermittent; ..... 1.0 ms^{-2} r.m.s. intermittent; ——— 0.25 ms^{-2} r.m.s. continuous; _ _ _ _ _ 1.0 ms^{-2} r.m.s. continuous) of both intermittent random vibration and continuous random vibration.

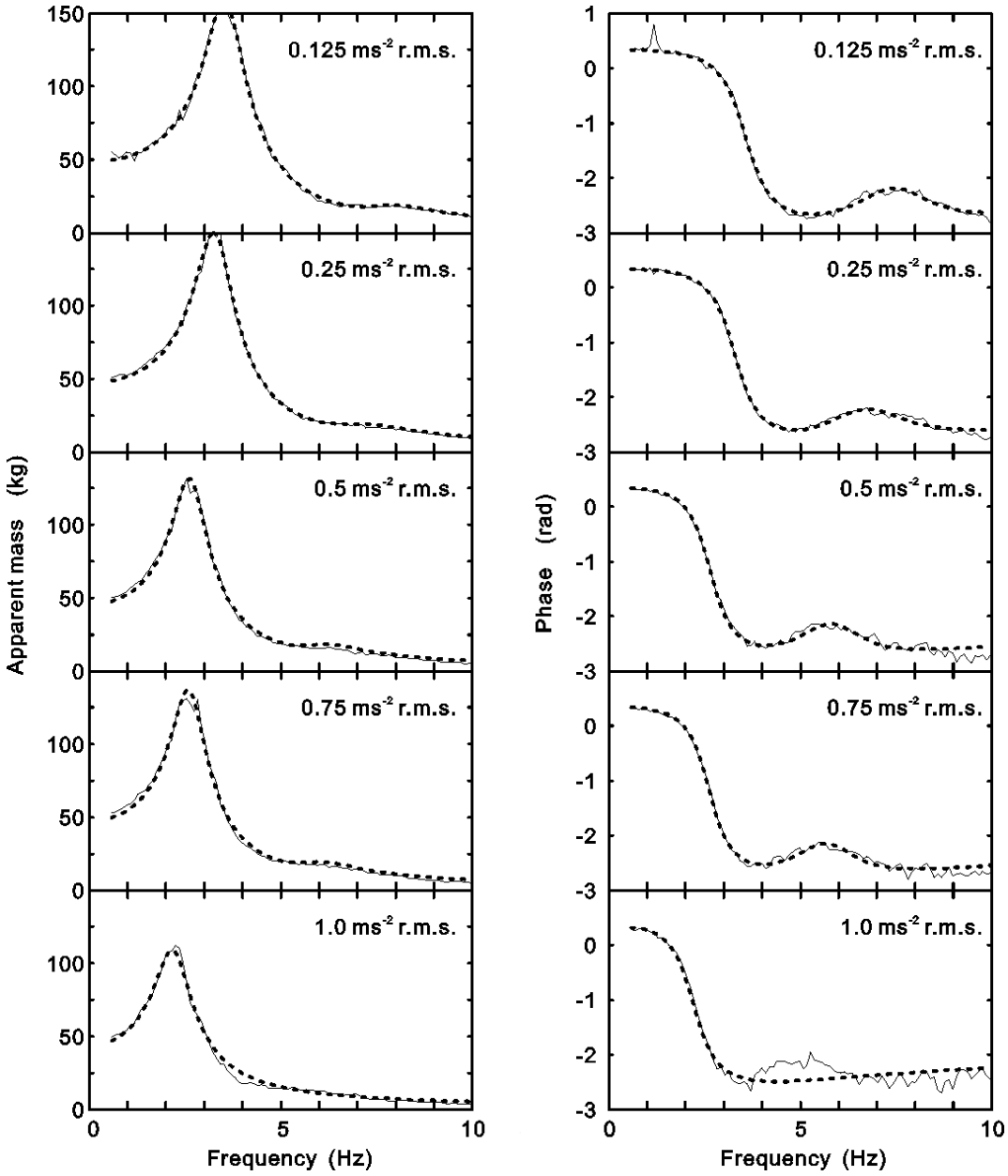

Figure 6.6 An example of curve-fitting (——— measurement; - - - - - fitted curve) the apparent masses and phases of one subject (S11) at five magnitudes (0.125, 0.25, 0.5, 0.75 and 1.0 ms^{-2} r.m.s.) of continuous random vibration to obtain the resonance frequencies (Hz). Frequency range of curve-fitting: 0.5 to 10 Hz.

6.3.1.2 Apparent mass resonance frequencies with continuous random vibration

The median resonance frequencies of the apparent masses of the 12 subjects decreased from 3.66 Hz to 2.44 Hz as the vibration magnitude increased from 0.125 ms^{-2} r.m.s. to 1.0 ms^{-2} r.m.s. (Table 6.2).

Table 6.2 Median and ranges of resonance frequencies of apparent masses generated by fitting the two-degree-of-freedom parametric model to the apparent masses and phases of 12 subjects at five vibration magnitudes (0.125, 0.25, 0.5, 0.75 and 1.0 ms^{-2} r.m.s.) of continuous random vibration.

Resonance frequency	Minimum	Median	Maximum
$f_{0.125}$ (Hz)	3.32	3.66	4.00
$f_{0.25}$ (Hz)	2.93	3.37	3.71
$f_{0.5}$ (Hz)	2.44	2.83	3.22
$f_{0.75}$ (Hz)	2.25	2.59	2.93
$f_{1.0}$ (Hz)	2.15	2.44	2.73

$f_{0.125}$, $f_{0.25}$, $f_{0.5}$, $f_{0.75}$ and $f_{1.0}$: resonance frequencies at five vibration magnitudes (0.125, 0.25, 0.5, 0.75 and 1.0 ms^{-2} r.m.s.).

Over the five vibration magnitudes, the apparent mass resonance frequency (f_r) decreased significantly with increasing magnitude ($p < 0.01$, Friedman two-way analysis of variance). There was a significant difference between the resonance frequencies at each of the five magnitudes ($p < 0.01$, Wilcoxon matched-pairs signed ranks test).

The resonance frequencies of the median normalised apparent masses (Figure 6.4) of the group of 12 subjects were 3.61, 3.32, 2.83, 2.64, and 2.44 Hz with vibration magnitudes of 0.125, 0.25, 0.5, 0.75 and 1.0 ms^{-2} r.m.s., respectively.

6.3.1.3 Parameters of the two-degree-of-freedom model fitted to the apparent masses with continuous random vibration

The medians and ranges of the parameters of the two-degree-of-freedom model fitted to individual apparent masses and phases are shown in Table 6.3. The segmental mass m_1, stiffness k_1, and damping constant c_1, determine the primary resonance between 2.0 and 4.0 Hz. The apparent mass at resonance, AM_r (i.e. the maximum value of the apparent mass modulus of the fitted curve), reflects the damping characteristic of the primary resonance. The segmental mass m_2, stiffness

k_2, and damping constant c_2, determine to the secondary resonance between 6.0 and 10.0 Hz.

According to the curve-fitting, 20 of 60 cases (12 subjects and 5 vibration magnitudes) showed a zero secondary segmental mass (m_2), and most cases exhibited the response of a single-degree-of-freedom system (Figure 6.3). Nevertheless, the two-degree-of-freedom model gave a better fit than a single-degree-of-freedom model. The fitting error caused by the phase of the secondary resonance peak was reduced by adding the second degree of freedom in the model (see phases of MAG1 to MAG4, Figure 6.6). The changes in the parameters of the minor secondary resonance (m_2, k_2 and c_2,) at varying magnitudes were not apparent and they are not discussed.

The frame mass, m_0

The median value of the frame mass, m_0, decreased from 1.8 to 1.1 kg when the magnitude increased from 0.125 to 0.25 ms^{-2} r.m.s. (Table 6.3). The median m_0 was zero at the three highest magnitudes (0.5, 0.75 and 1.0 ms^{-2} r.m.s.). The five vibration magnitudes had a significant overall effect on the frame mass ($p < 0.001$, Friedman). The frame mass decreased with increasing magnitude ($p < 0.01$, Wilcoxon), except between 0.5 and 0.75 ms^{-2} r.m.s. ($p = 0.116$, Wilcoxon), between 0.5 and 1.0 ms^{-2} r.m.s. ($p = 0.075$, Wilcoxon), and between 0.75 and 1.0 ms^{-2} r.m.s. ($p = 0.066$, Wilcoxon).

The primary segmental mass, m_1

The median value of m_1 increased from 33.0 to 36.5 kg with increasing vibration magnitude from 0.125 to 1.0 ms^{-2} r.m.s. except for 0.75 ms^{-2} r.m.s. (Table 6.3). There were small but significant increases in the primary segmental mass with increasing vibration magnitude ($p = 0.017$, Friedman): the primary segmental mass increased with increasing magnitude only between 0.125 and 0.5 ms^{-2} r.m.s. ($p = 0.028$, Wilcoxon), and between 0.125 and 0.75 ms^{-2} r.m.s. ($p = 0.008$, Wilcoxon).

The primary segmental stiffness, k_1

The median value of k_1 decreased from 17743 to 8565 N/m as vibration magnitude increased from 0.125 to 1.0 ms^{-2} r.m.s. (Table 6.3). The vibration magnitude had a significant effect on the primary segmental stiffness ($p < 0.01$, Friedman): the primary segmental stiffness decreased with increasing magnitude ($p < 0.05$, Wilcoxon) with no exception for all five vibration magnitudes.

Table 6.3 Median and ranges of parameters generated by fitting the two-degree-of-freedom parametric model to the apparent masses and phases of 12 subjects at five vibration magnitudes (0.125, 0.25, 0.5, 0.75 and 1.0 ms^{-2} r.m.s.) of continuous random vibration.

Vibration magnitude (ms^{-2} r.m.s.)		m_0 (kg)	m_1 (kg)	k_1 (N/m)	c_1 (Ns/m)	m_2 (kg)	k_2 (N/m)	c_2 (Ns/m)	f_r (Hz)	AM_r (kg)
0.125	Min	0.3	27.4	13429	192	0.9	2777	16	3.32	96.0
	Median	1.8	33.0	17743	230	1.9	5037	29	3.66	112.2
	Max	3.5	49.1	33581	528	3.7	8651	114	4.00	158.8
0.25	Min	0.0	27.7	11219	184	0.0	0	8	2.93	90.6
	Median	1.1	34.3	16119	259	1.9	3813	34	3.37	109.3
	Max	3.3	50.3	27163	475	3.1	7106	105	3.71	150.1
0.5	Min	0.0	28.5	8699	171	0.0	0	20	2.44	83.0
	Median	0.0	35.8	12307	248	1.8	3497	46	2.83	103.4
	Max	1.2	49.0	21314	393	2.8	6284	112	3.22	140.7
0.75	Min	0.0	29.3	6862	165	0.0	0	27	2.25	79.0
	Median	0.0	35.5	10296	235	1.1	1408	66	2.59	99.9
	Max	0.5	49.6	18211	343	3.0	5701	115	2.93	150.1
1.0	Min	0.0	25.8	5832	132	0.0	0	26	2.15	80.9
	Median	0.0	36.5	8565	217	0.0	0	98	2.44	98.1
	Max	0.4	47.4	15288	305	3.1	5732	130	2.73	144.5

m_0, m_1 and m_2 – segmental masses. k_1 and k_2 – segmental stiffnesses. c_1 and c_2 – segmental damping constants. f_r – apparent mass resonance frequency obtained by model. AM_r – apparent mass at resonance by model.

The primary segmental damping constant, c_1

The median value of c_1 decreased from 259 to 217 Ns/m as vibration magnitude increased from 0.25 to 1.0 ms^{-2} r.m.s. (Table 6.3). The vibration magnitude had a small but significant effect on the primary segmental damping constant (p = 0.005,

Friedman): the primary segmental damping constant decreases with increasing magnitude only between 0.125 and 1.0 ms^{-2} r.m.s. (p = 0.012, Wilcoxon), between 0.25 and 1.0 ms^{-2} r.m.s. (p = 0.003, Wilcoxon), and between 0.5 and 1.0 ms^{-2} r.m.s. (p = 0.012, Wilcoxon).

The apparent mass at resonance, AM_r

The median apparent mass at resonance decreased from 112.2 to 98.1 kg as vibration magnitude increased from 0.125 to 1.0 ms^{-2} r.m.s. (Table 6.3).The vibration magnitudes had a significant overall effect on the apparent mass at resonance (p = 0.002, Friedman). The apparent mass at resonance decreased with increasing magnitude (p < 0.05, Wilcoxon), except between 0.125 and 0.25 ms^{-2} r.m.s. (p = 0.05, Wilcoxon), between 0.5 and 0.75 ms^{-2} r.m.s. (p = 0.784, Wilcoxon), between 0.5 and 1.0 ms^{-2} r.m.s. (p = 0.239, Wilcoxon), and between 0.75 and 1.0 ms^{-2} r.m.s. (p = 0.388, Wilcoxon).

6.3.1.4 Apparent mass resonance frequencies with intermittent random vibration

With intermittent random vibration, the median resonance frequency of the apparent mass was 3.03 Hz at 0.25 ms^{-2} r.m.s. and 2.44 Hz at 1.0 ms^{-2} r.m.s. Whereas, with continuous random vibration, the resonance frequency was 3.32 Hz at 0.25 ms^{-2} r.m.s. and 2.44 Hz at 1.0 ms^{-2} r.m.s. (Table 6.4 A).

The resonance frequencies with intermittent random vibration at 0.25 ms^{-2} r.m.s. were significantly lower than those with continuous random vibration at the same magnitude (p =0.003, Wilcoxon). The effect was apparent for all except Subject 3 (Table 6.4 A and Figure 6.5). There was no significant difference in the resonance frequencies with intermittent and continuous vibration at 1.0 ms^{-2} r.m.s. (p =0.103, Wilcoxon). However, eight of the twelve subjects (subjects 1, 2, 3, 6, 9, 10, 11 and 12) had higher resonance frequencies with intermittent vibration than with continuous vibration (Table 6.4 A and Figure 6.5).

The absolute difference between the resonance frequencies at 0.25 and 1.0 ms^{-2} r.m.s. was less with intermittent random vibration than with the continuous random vibration for all 12 subjects (p = 0.002, Wilcoxon; Table 6.4 A and Figure 6.5).

Table 6.4 Median and ranges of resonance frequencies (A) and model parameters (B) generated by fitting the two-degree-of-freedom parametric model to the apparent masses and phases of 12 subjects at two vibration magnitudes (0.25 and 1.0 ms^{-2} r.m.s.) of both continuous and intermittent random vibration.

A. Resonance frequency (Hz)				
Subject	0.25 ms^{-2} r.m.s. intermittent	0.25 ms^{-2} r.m.s. continuous	1.0 ms^{-2} r.m.s. intermittent	1.0 ms^{-2} r.m.s. continuous
s1	3.22	3.42	2.54	2.44
s2	2.73	2.93	2.15	2.05
s3	3.42	3.42	2.93	2.73
s4	2.73	3.03	2.25	2.25
s5	3.22	3.42	2.64	2.64
s6	3.13	3.42	2.64	2.54
s7	2.64	3.13	2.15	2.44
s8	3.22	3.61	2.64	2.64
s9	3.03	3.22	2.34	2.25
s10	2.93	3.81	2.34	2.25
s11	2.83	3.22	2.25	2.15
s12	3.03	3.13	2.54	2.44
Minimum	2.64	2.93	2.15	2.05
Median	3.03	3.32	2.44	2.44
Maximum	3.42	3.81	2.93	2.73

B. Model parameters

Vibration magnitude (ms^{-2} r.m.s.)		m_0 (kg)	m_1 (kg)	k_1 (N/m)	c_1 (Ns/m)	m_2 (kg)	k_2 (N/m)	c_2 (Ns/m)	f_r (Hz)	AM_r (kg)
0.25 Int	Min	0.0	27.9	9860	229	0.0	0	4	2.64	71.7
	Median	0.0	34.2	12725	268	0.0	0	130	3.03	91.4
	Max	2.0	50.2	25315	530	5.7	4125	310	3.42	120.4
0.25 Con	Min	0.0	28.0	11045	207	0.4	0	14	2.93	81.8
	Median	0.0	34.2	15995	285	2.4	2339	54	3.32	101.7
	Max	1.4	45.8	23015	475	6.9	7106	1487	3.81	131.4
1.0 Int	Min	0.0	29.7	6915	197	0.0	0	11	2.15	70.6
	Median	0.0	36.4	8897	263	0.0	0	128	2.44	88.0
	Max	0.7	50.1	18416	417	2.2	3717	183	2.93	129.1
1.0 Con	Min	0.0	14.8	4430	80	0.0	0	1	2.05	69.5
	Median	0.0	36.8	7899	242	0.0	0	158	2.44	91.2
	Max	1.0	51.6	16294	427	29.8	6893	282	2.73	126.1

int – intermittent. con – continuous. m_0, m_1 and m_2 – segmental masses. k_1 and k_2 – segmental stiffnesses. c_1 and c_2 – segmental damping constants. f_r – apparent mass resonance frequency of the model. AM_r – apparent mass at resonance by model.

6.3.1.5 Parameters of the two-degree-of-freedom model fitted to the apparent masses with intermittent random vibration

The median and range of the parameters of the two-degree-of-freedom model fitted to individual apparent masses and phases are shown in Table 6.4 B.

At 1.0 ms^{-2} r.m.s., the primary segmental stiffness (k_1) was significantly greater (p = 0.028, Wilcoxon) with intermittent vibration than with continuous vibration (only subject 7 showed the reverse trend), consistent with the characteristics of thixotropy. At 0.25 ms^{-2} r.m.s., the primary segmental stiffness (k_1) was significantly less (p = 0.008, Wilcoxon) with intermittent vibration than with the continuous vibration (only subject 3 showed the reverse trend), also consistent with the thixotropy.

At 1.0 ms^{-2} r.m.s., the primary segmental damping constant (c_1) was significantly greater (p = 0.038, Wilcoxon) with intermittent vibration than with continuous vibration (4 subjects showed the reverse trend). However, at 0.25 ms^{-2} r.m.s. there was no significant difference in the secondary segmental damping constant (c_2) between the continuous and the intermittent stimulus (p = 0.456, Wilcoxon).

At 0.25 ms^{-2} r.m.s., the apparent mass at resonance (AM_r) was significantly less (p = 0.002, Wilcoxon) with intermittent vibration than with continuous vibration for all twelve subjects. However, at 1.0 ms^{-2} r.m.s. there was no significant difference in the apparent mass at resonance (AM_r) between the continuous and the intermittent stimulus (p = 0.61, Wilcoxon).

For the other parameters in the two-degree-of-freedom model, there were no significant differences between the continuous and the intermittent vibration at either 0.25 or 1.0 ms^{-2} r.m.s.

6.3.2 Response in the vertical (x-axis) cross-axis direction

6.3.2.1 Overview

The individual vertical (x-axis) cross-axis apparent masses of the 12 subjects with the five magnitudes of continuous random vibration are shown in Figure 6.7. The median normalised cross-axis apparent masses of the group of 12 subjects are shown in Figure 6.8. The median and ranges of the individual peak frequencies are shown in Table 6.5. The individual cross-axis apparent masses of the 12 subjects with two vibration magnitudes (0.25 and 1.0 ms^{-2} r.m.s.) with both continuous and intermittent random vibration are shown in Figure 6.9. The magnitude of the vertical x-axis cross-axis apparent mass at peak were about 60% of the static weight of each subject and were about between 20% and 40% of the magnitude of the horizontal apparent mass at resonance (Figure 6.8).

The coherencies were generally in excess of 0.8 at frequencies between 2 and 6 Hz. Some subjects exhibited the lowest coherency (0.1 to 0.4) at frequencies between 8 and 14 Hz, while some occurred above 18 Hz. Similar to the coherency of the horizontal in-line apparent mass, there was a drop in the coherency, with the frequency range of the coherency drop decreasing with increasing vibration magnitude. The coherencies with intermittent vibration were of the same pattern as observed with the continuous vibration (Section 6.3.1.1).

There were two or three distinguishable peaks in each cross-axis apparent mass curve: the number and the magnitude of the peaks depended varied between subjects and depended on the magnitude of vibration (Figure 6.7). At 0.125 ms^{-2} r.m.s., all twelve subjects showed a dominant primary peak between 3.3 and 4.5 Hz,

with some (subjects 1, 2, 4, 5, 7, 8, 11 and 12) showing a secondary peak between 6.0 and 10.0 Hz. At 1.0 ms^{-2} r.m.s., the primary peak frequency was between 2.2 and 3.0 Hz, with no apparent second peak (Figures 6.7). The primary peak was used to investigate the effects of magnitude and intermittency on the dynamic characteristic of the cross-axis response (Section 6.2.5.3).

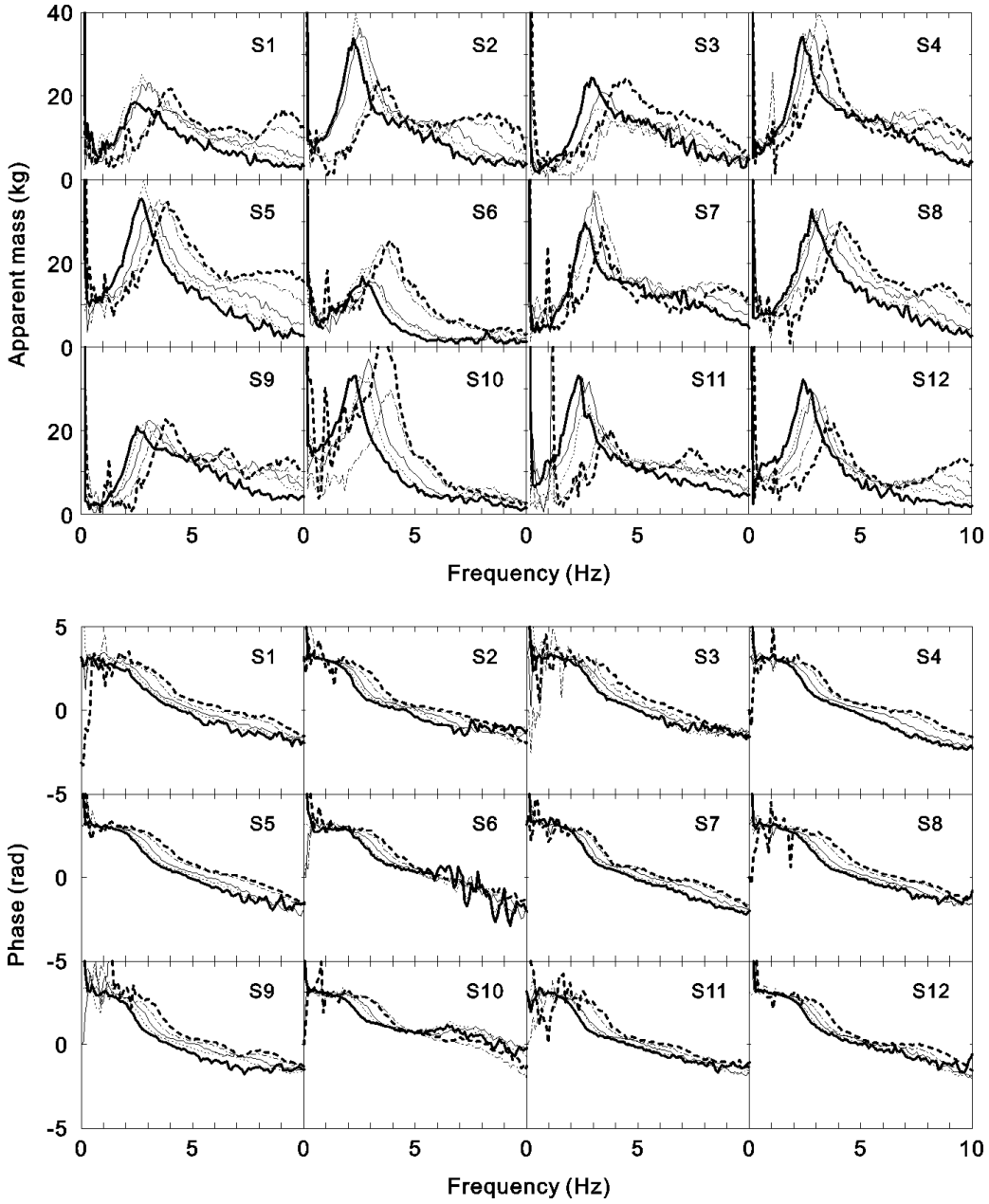

Figure 6.7 Individual vertical *x*-axis cross-axis apparent masses (upper) and phases (lower) of 12 subjects (S1 to S12) at five vibration magnitudes (- - - - - 0.125 ms^{-2} r.m.s.; _ ._ ._ ._ ._ 0.25 ms^{-2} r.m.s.; ——— 0.5 ms^{-2} r.m.s.; ..... 0.75 ms^{-2} r.m.s.; ▬▬▬ 1.0 ms^{-2} r.m.s.) of continuous random vibration.

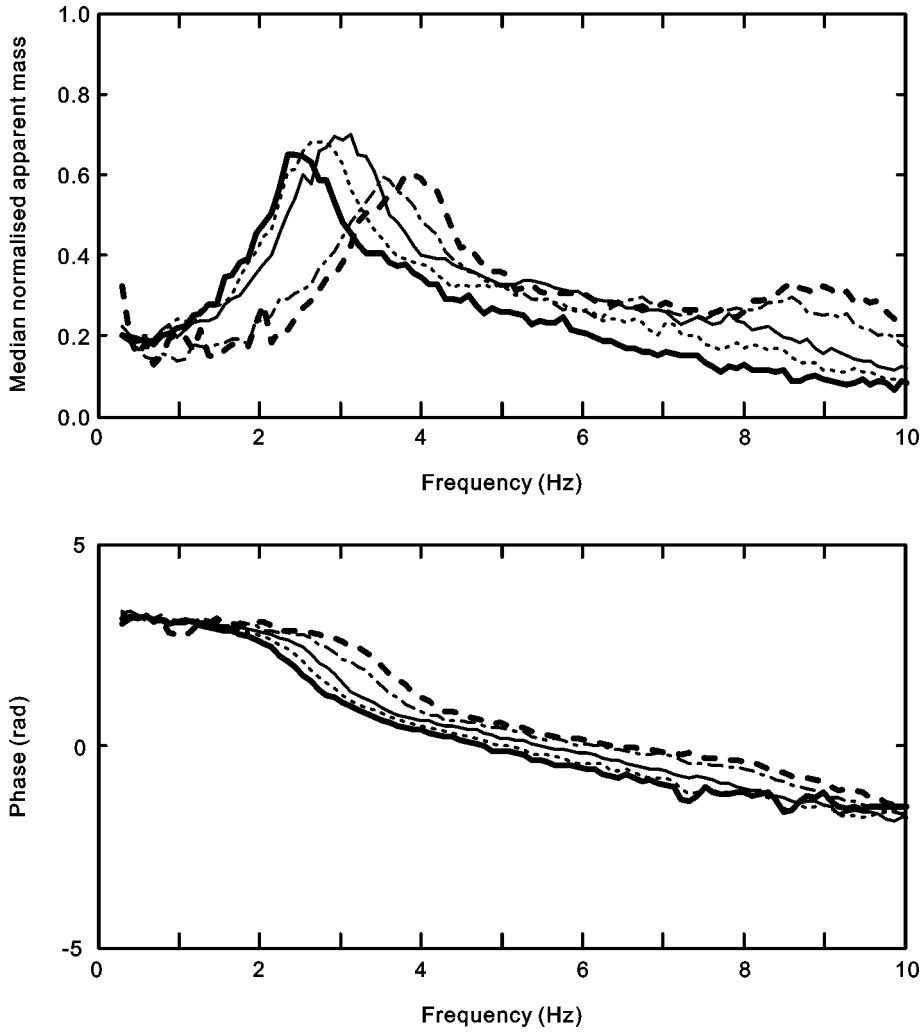

Figure 6.8 Median normalised vertical *x*-axis cross-axis apparent masses (upper) and phases (lower) of the group of 12 subjects at five vibration magnitudes (- - - - - 0.125 ms^{-2} r.m.s.; _.._.._.._ 0.25 ms^{-2} r.m.s.; ——— 0.5 ms^{-2} r.m.s.; ..... 0.75 ms^{-2} r.m.s.; ▬▬▬ 1.0 ms^{-2} r.m.s.) of continuous random vibration.

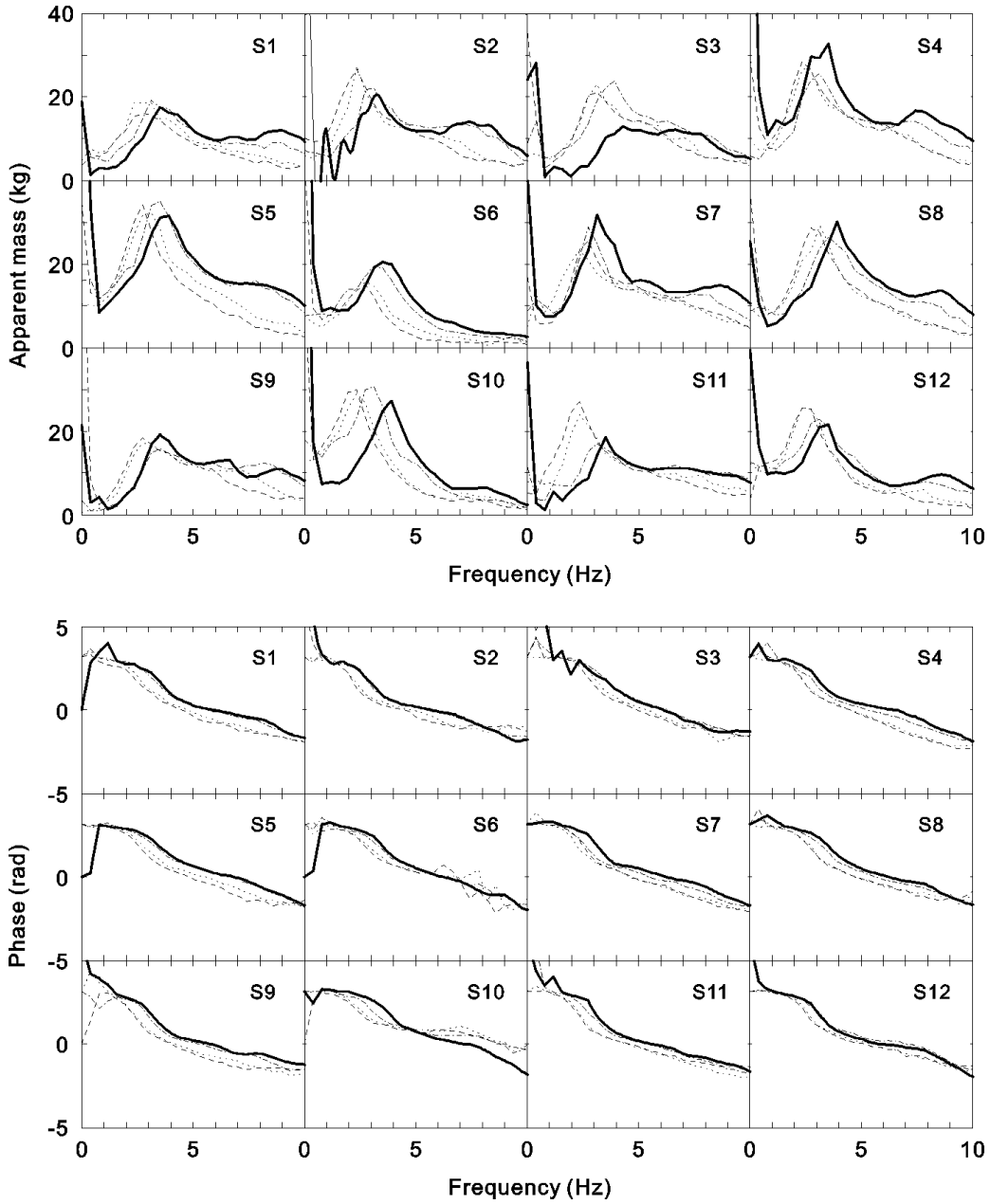

Figure 6.9 Individual vertical *x*-axis cross-axis apparent masses (upper) and phases (lower) of 12 subjects (S1 to S12) at two vibration magnitudes (_ . _ . _ . _ 0.25 ms^{-2} r.m.s. intermittent; ..... 1.0 ms^{-2} r.m.s. intermittent; ▬▬▬ 0.25 ms^{-2} r.m.s. continuous; _ _ _ _ _ 1.0 ms^{-2} r.m.s. continuous) of both intermittent random vibration and continuous random vibration.

Table 6.5 Median and ranges of peak frequencies of vertical *x*-axis cross-axis apparent masses of 12 subjects at five vibration magnitudes (0.125, 0.25, 0.5, 0.75 and 1.0 ms^{-2} r.m.s.) of continuous random vibration (A), and individual peak frequencies with intermittent and continuous random vibration of 12 subjects at 1.0 and 0.25 ms^{-2} r.m.s. (B).

A. Cross-axis peak frequencies of continuous random vibration (Hz)

Vibration magnitude (ms^{-2} r.m.s.)	Minimum	Median	Maximum
0.125	3.32	3.81	4.49
0.25	3.13	3.52	4.30
0.5	2.54	3.03	3.32
0.75	2.34	2.83	3.22
1.0	2.25	2.49	2.93

B. Cross-axis peak frequencies of intermittent random vibration (Hz)

Subject	0.25 ms^{-2} r.m.s. intermittent	0.25 ms^{-2} r.m.s. continuous	1.0 ms^{-2} r.m.s. intermittent	1.0 ms^{-2} r.m.s. continuous
s1	3.13	3.52	2.34	2.73
s2	3.13	3.23	2.34	2.34
s3	3.91	4.30	3.13	3.13
s4	3.13	3.52	2.73	2.34
s5	3.52	3.91	3.13	2.73
s6	3.13	3.52	2.73	2.73
s7	2.73	3.13	2.34	2.73
s8	3.52	3.91	3.13	2.73
s9	3.52	3.52	2.73	2.73
s10	3.13	3.91	2.34	2.34
s11	3.13	3.52	2.34	2.34
s12	3.13	3.52	2.34	2.34
Minimum	2.73	3.13	2.34	2.34
Median	3.13	3.52	2.54	2.73
Maximum	3.91	4.30	3.13	3.13

6.3.2.2 Vertical (x-axis) cross-axis apparent mass peak frequencies with continuous random vibration

The median peak frequencies of the cross-axis apparent masses of the twelve subjects decreased from 3.81 Hz to 2.49 Hz as the vibration magnitude increased from 0.125 to 1.0 ms^{-2} r.m.s. (Table 6.5 A).

There was a significant effect of vibration magnitude on the vertical (*x*-axis) cross-axis apparent mass peak frequencies ($p < 0.001$, Friedman). The peak frequency decreased significantly with increasing vibration magnitude from 0.125 to 1.0 ms^{-2} r.m.s. ($p < 0.02$, Wilcoxon). There was no significant difference in the peak frequencies between 0.75 and 1.0 ms^{-2} r.m.s. ($p = 0.14$, Wilcoxon). No significant difference was found among the cross-axis apparent masses at peak at the five vibration magnitudes ($p = 0.287$, Friedman).

The peak frequencies of the median normalised cross-axis apparent masses of the group of the twelve subjects were 3.81, 3.52, 3.13, 2.73, and 2.34 Hz with vibration magnitudes of 0.125, 0.25, 0.5, 0.75, and 1.0 ms^{-2} r.m.s., respectively (Figure 6.8).

There were significant correlations between the cross-axis peak frequencies and the in-line resonance frequencies at 1.0 ms^{-2} r.m.s. ($r = 0.903$, $p < 0.001$, Spearman's rank order correlation test), 0.75 ms^{-2} r.m.s. ($r = 0.661$, $p = 0.019$, Spearman), 0.5 ms^{-2} r.m.s. ($r = 0.83$, $p = 0.001$, Spearman), 0.25 ms^{-2} r.m.s. ($r = 0.898$, $p < 0.001$, Spearman) ms^{-2} r.m.s., and 0.125 ms^{-2} r.m.s. ($r = 0.952$, $p < 0.001$, Spearman) ms^{-2} r.m.s. This may imply that the primary resonance occurred in the longitudinal direction and primary peak occurred in the vertical cross-axis direction are correlated to the same mode(s) of the body.

6.3.2.3 Vertical (x-axis) cross-axis apparent mass peak frequencies with intermittent random vibration

The median peak frequency of the apparent masses with intermittent random vibration was 3.13 Hz at 0.25 ms^{-2} r.m.s. and 2.54 Hz at 1.0 ms^{-2} r.m.s. With continuous random vibration, the median peak frequency was 3.52 Hz at 0.25 ms^{-2} r.m.s. and 2.73 Hz at 1.0 ms^{-2} r.m.s. (Table 6.5 B).

At 0.25 ms^{-2} r.m.s., the peak frequency with intermittent random vibration was significantly lower than the peak frequency with continuous random vibration ($p = 0.002$, Wilcoxon). Only one of the twelve subjects showed the same peak frequencies with the intermittent and the continuous vibration at this magnitude (Table 6.5 B). This implies that the dynamic stiffness of the body in the vertical cross axis at the low magnitude was lowered by the prior high magnitude longitudinal

vibration. However, at 1.0 ms^{-2} r.m.s., there was no significant difference in the peak frequency with intermittent and continuous vibration (p = 0.334, Wilcoxon).

The absolute differences between the peak frequencies with 0.25 and 1.0 ms^{-2} r.m.s. were significantly less with the intermittent random vibration than with the continuous random vibration (p = 0.005, Wilcoxon). Only subjects 1 and 9 showed marginally reverse trends (Table 6.5 B). The median absolute difference in peak frequency between at 1.0 and 0.25 ms^{-2} r.m.s. was considerably less with intermittent random vibration (about 0.8 Hz) than with continuous random vibration (about 1.2 Hz).

At either the low magnitude or the high magnitude of vibration, the intermittency had no effect on the cross-axis apparent mass at peak (at 1.0 ms^{-2} r.m.s., p = 0.373, Wilcoxon; at 0.25 ms^{-2} r.m.s., p = 1.0, Wilcoxon).

6.4 Discussion

6.4.1 Effect of vibration magnitude on apparent mass resonance frequency and cross-axis apparent mass peak frequency

6.4.1.1 Response in the horizontal (z-axis) direction

The longitudinal horizontal in-line apparent masses at five magnitudes show that the semi-supine body is nonlinear: the resonance frequencies decreased significantly with increasing vibration magnitude. This is apparent in the primary stiffness, k_1, of the parametric two-degree-of-freedom-model (Section 6.3.1.3 and Table 6.3). The characteristic nonlinearity found here is consistent with the nonlinearity in the vertical in-line apparent masses of the same semi-supine subjects during vertical excitation (see Chapter 5). With both longitudinal horizontal and vertical excitation, the relaxed semi-supine posture is assumed to require no voluntary muscular postural control and minimal involuntary reflex responses for postural control compared to sitting and standing postures. The consistent nonlinear response suggests that the nonlinearity is not primarily caused by voluntary control of postural muscles, but the result of some passive property of the body (e.g. thixotropy) or, alternatively, an involuntary reflex response of the body.

For subjects sitting upright with minimum thigh contact during vertical whole-body vibration, the vertical apparent mass resonance frequency at the backrest reduced from 7 Hz to 5 Hz as the vibration magnitude increased from 0.125 to 1.25 ms^{-2} r.m.s. (Nawayseh and Griffin, 2004). The semi-supine posture in the present study showed a considerably lower resonance frequency – the resonance frequency of the

median normalised horizontal in-line apparent mass changed from 3.61 Hz to 2.44 Hz as the magnitude increased from 0.125 to 1.0 ms^{-2} r.m.s. The absence of the seat surface perpendicular to the horizontal direction (*z*-axis) of the body in the present semi-supine condition allows more body movement in the longitudinal horizontal direction. The movement of semi-supine body might involve shear in the tissues between the supine support surface and the skeletal structure, or within other tissues inside the body.

6.4.1.2 Response in the vertical (x-axis) cross-axis direction

The vertical *x*-axis cross-axis apparent masses at the five magnitudes show that the semi-supine body is nonlinear: the peak frequency decreased with increasing vibration magnitude (Table 6.5 A).

The peak frequencies of the vertical *x*-axis cross-axis apparent masses were correlated with the resonance frequencies of the horizontal *z*-axis in-line apparent masses at all five vibration magnitudes (Section 6.3.2.2). This implies that the responses in the two axes are cross-coupled by some common mechanism. The consistent nonlinear responses in both the horizontal and the vertical cross axes suggest the nonlinearities in these two directions may have a common cause.

Correlations between the in-line and cross-axis resonance frequencies are also found in the apparent mass and cross-axis apparent mass at the backs of upright sitting subjects during vertical excitation. Nawayseh and Griffin (2004) measured the apparent mass and fore-and-aft cross-axis apparent mass on a vertical backrest with upright sitting subjects. The dominant fore-and-aft (*x*-axis) cross-axis apparent mass peak frequency at the back during vertical (*z*-axis) whole-body vibration varied over the range 5 to 10 Hz when the vibration magnitude varied from 1.25 to 0.125 ms^{-2} r.m.s. This is similar to the resonance frequency in the vertical in-line direction at the back while seated (i.e., 5 to 7 Hz), and similar to the peak in the fore-and-aft and pitch transmissibilities to the spine (T1, T5, T10 and L1) and the pelvis during vertical vibration (Matsumoto and Griffin, 2002a).

In the present study with longitudinal horizontal excitation of the semi-supine body, there were large responses in the vertical cross-axis direction: the maximum of the median normalised cross-axis apparent mass (0.6 to 0.7) was about 26% of the median normalised longitudinal horizontal in-line apparent mass at resonance (2.2 to 2.7). This was not the case with vertical excitation of the semi-supine body seen in Chapter 5: the maximum median normalised longitudinal cross-axis apparent mass (about 0.1) was only about 7% of the maximum median normalised vertical in-line apparent mass (about 1.5).

With subject sitting upright while exposed to vertical excitation, the median fore-and-aft cross-axis apparent mass at the backrest was a maximum of about 25 kg, while the median vertical in-line apparent mass at the backrest was a maximum of about 5 kg (Nawayseh and Griffin, 2004). With the same sitting conditions and the same subjects but with fore-and-aft excitation, Nawayseh and Griffin (2005b) found that the vertical cross-axis apparent mass of one subject at the back was less than 3 kg at all frequencies, while the fore-and-aft in-line apparent mass at the back was between about 60 and 100 kg at resonance, depending on the subject and the vibration magnitude. With subjects either sitting upright or semi-supine, comparing *z*-axis and *x*-axis excitation, the cross-axis response in the *x*-axis is always larger than the cross-axis response in the *z*-axis. It seems that the cross-coupling mechanism in the human body is stronger for excitations in the *z*-axis of the body.

6.4.2 Effect of intermittency on apparent mass resonance frequency and cross-axis apparent mass peak frequency

6.4.2.1 Response in the horizontal (z-axis) direction

The results with intermittent vibration appear characteristic of thixotropic changes in the dynamic stiffness of the body: the resonance frequency at a low magnitude (0.25 ms^{-2} r.m.s.) was lower with intermittent vibration than with the continuous vibration. The resonance frequency at the low magnitude reflected the dynamic stiffness of the body 2.56 s after high magnitude 'perturbation'.

With vertical excitation of the semi-supine body, the median resonance frequency at 0.25 ms^{-2} r.m.s. was 9.28 Hz with intermittent vibration and 9.62 Hz with continuous vibration (see Chapter 5). So the relative percentage change due to intermittency was 3.5% (i.e. (9.62–9.28) / 9.62). In the present study, the relative percentage change was 8.7% (i.e. (3.03–3.32) / 3.32, Table 6.4 A), 2½ times greater than with vertical excitation. So the effect of intermittency tended to be greater in the present study with horizontal longitudinal excitation.

It was hypothesized that the resonance frequency at the high magnitude (1.0 ms^{-2} r.m.s.) would be higher with intermittent vibration than with continuous vibration, because the resonance frequency at the high magnitude would reflect the dynamic stiffness of the body 2.56 s after the low magnitude 'stillness'. The difference was not statistically significant, but eight subjects (1, 2, 3, 6, 9, 10, 11, and 12) of the twelve subjects showed this effect at 1.0 ms^{-2} r.m.s. (Figure 6.5 and Table 6.4 A). The study reported in Chapter 4 found that voluntary periodic muscular activity was less effective in changing the resonance frequency at high magnitudes, consistent with voluntary movement having less effect on thixotropy at high magnitudes. At

greater magnitudes of vibration there are greater inertial forces that may be sufficient to change thixotropy quickly, so voluntary muscle activity was not needed to reduce the dynamic stiffness of the body. This may explain why intermittency did not significantly alter the stiffness of the body at high magnitudes of vibration. It may be assumed that the dynamic stiffness of the body cannot continue to decrease with ever-increasing vibration magnitude – there must be a limitation for the body to be able to withstand high magnitude inertial forces without collapsing. This will limit the maximum reduction in stiffness with high magnitudes and may be expected to differ for different people.

Intermittency had a significant effect on the primary segmental mass (k_1) of the parametric model at both 0.25 and 1.0 ms^{-2} r.m.s. and the primary damping constant (c_1) at 1.0 ms^{-2} r.m.s. (Section 6.3.1.5 and Table 6.4 B). Using a similar parametric model, the study described in Chapter 5 found that the effect of intermittency was only significant in k_1 and only at 1.0 ms^{-2} r.m.s. for the semi-supine body exposed to vertical excitation. So the effect of intermittency was apparent in more parameters during longitudinal excitation than during vertical excitation.

6.4.2.2 Response in the vertical (x-axis) cross-axis direction

Similar to the responses in the longitudinal horizontal in-line direction, the effect of intermittency was found in the vertical cross-axis direction with 0.25 ms^{-2} r.m.s. but not with 1.0 ms^{-2} r.m.s. excitation. Since the frequency resolution of the apparent mass during intermittent vibration was originally 0.391 Hz and then linearly interpolated to 0.098 Hz, the small changes in the cross-axis peak frequencies may be masked by the 0.391 Hz resolution. However, this was not the case in the in-line responses as the in-line apparent mass was fitted by the parametric model with 0.098 Hz resolution.

6.4.3 Effect of vibration magnitude on apparent mass coherency

The frequency band of the reduction in coherency (over the range 6 to 20 Hz) showed a similar pattern to the nonlinearity in the apparent mass resonance frequency (over the range 2 to 4 Hz): the frequency band of the coherency drop decreased with increasing vibration magnitude (Figure 6.10 c). And the lowest coherency decreased with increasing vibration magnitude.

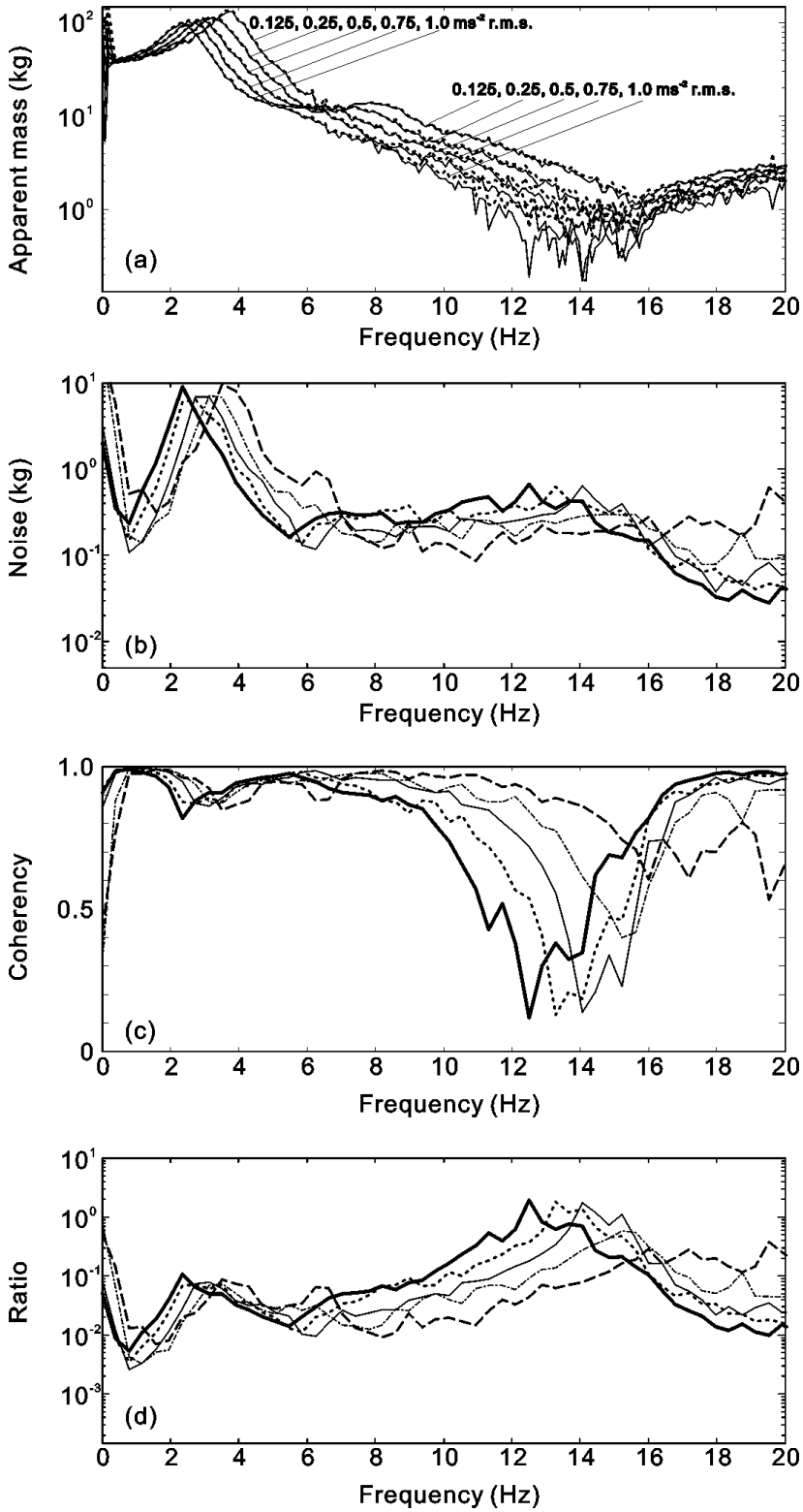

Figure 6.10 Comparison of the PSD and the CSD method for one individual subject (S9) with a frequency resolution 0.4 Hz. (a). Apparent mass modulus using the CSD (_____) and the PSD (- - - - -) method at five magnitudes of vibration (0.125, 0.25, 0.5, 0.75, 1.0 ms^{-2} r.m.s.); (b). Noise – absolute difference between the apparent mass modulus using the PSD method and the CSD method at five vibration magnitudes (▬ ▬ ▬ 0.125 ms^{-2} r.m.s.; _ . _ . _ . _ . _ 0.25 ms^{-2} r.m.s.; —— — 0.5 ms^{-2} r.m.s.; - - - - - 0.75 ms^{-2} r.m.s.; ▬▬▬ 1.0 ms^{-2} r.m.s.); (c). Coherencies at five magnitudes of vibration; (d). Ratio of the absolute noise (see (b)) over the apparent mass modulus using the CSD method at five vibration magnitudes with continuous random vibration.

The cross spectral density (CSD) method of calculating the apparent mass used here assumes that the output force is linearly correlated with the input acceleration. The apparent mass might alternatively be calculated using the power spectral density (PSD) method that includes noise and distortion that are not correlated between the input and the output. For measurements from a typical subject, Figure 6.10 a shows that at all five magnitudes the CSD and the PSD method give similar absolute apparent masses at all frequencies between 0.25 and 20 Hz. Figure 6.10 b shows the absolute difference between the apparent mass estimated using the CSD and PSD methods at each of the five magnitudes. This difference is the total 'noise' or distortion between the input acceleration and the output dynamic force. The peak 'noise' occurs over the frequency range of the apparent mass resonance (2 to 4 Hz), so the absolute 'noise' is proportionally greater with greater body movement. At frequencies greater than 6 Hz, the output force is much less and, as a consequence, the 'noise' has a relatively greater effect on the coherency, as shown in Figure 6.10 c. The noise-output ratio (the absolute difference between the apparent mass modulus obtained by the PSD method and the apparent mass modulus obtained by the CSD method divided by the apparent mass modulus obtained using the CSD method) is shown in Figure 6.10 d. The frequency with the greatest noise-output ratio decreases with increasing vibration magnitude and the ratio at the peak frequency tends to be greater with greater magnitudes of vibration. These changes around 10 to 16 Hz (as seen in Figure 6.11 c, d) probably occur because the nonlinearity results in reductions in the output force at high frequencies rather than because there is greater 'noise' at these frequencies. The same trends were observed for all twelve subjects.

Previous studies with standing, sitting, and semi-supine postures during vertical excitation have not reported systematic drops in coherency. Normally, coherency drops with low magnitude excitation (e.g. 0.125 to 0.25 ms^{-2} r.m.s.) and at low frequencies (e.g. less than 1 to 2 Hz) due to small input signals and noise at the output (e.g. subject voluntary or involuntary movement). In the present study with longitudinal horizontal excitation, subjects reported more overall movement and more local movement (e.g. from body components within the trunk and hip) along the direction of excitation than during vertical (*x*-axis) excitation (seen in Chapter 5).

6.5 Conclusions

With continuous random longitudinal horizontal excitation, the longitudinal horizontal in-line apparent mass resonance frequencies and vertical cross-axis apparent mass

peak frequencies of the relaxed semi-supine human body decrease with increasing vibration magnitude from 0.125 to 1.0 ms^{-2} r.m.s.

With intermittent excitation, the in-line resonance frequency and the cross-axis peak frequency measured at a low magnitude (0.25 ms^{-2} r.m.s.) decreased immediately after prior exposure to a higher magnitude of vibration (1.0 ms^{-2} r.m.s.), compared to the resonance frequency and peak frequency measured at 0.25 ms^{-2} r.m.s. with continuous vibration. With intermittent vibration, the in-line resonance frequency and the cross-axis peak frequency were similar at a high magnitude (1.0 ms^{-2} r.m.s.) to that measured with continuous vibration.

It is concluded that the passive thixotropic behaviour of the human body is likely to be at least partially responsible for reduced resonance frequencies with higher vibration magnitudes – as the vibration magnitude increases, the movement of tissues reduces their overall stiffness. However, reflex muscle activity may also have an influence.

Chapter 7

Nonlinear response of the semi-supine human body during vertical and longitudinal horizontal sinusoidal whole-body vibration

7.1 Introduction

The nonlinearity in the dynamic response of the human body exposed to broad-band random excitation is evident in two ways. The frequency response functions (e.g. apparent mass and transmissibility) show a reduction in resonance frequency with increasing vibration magnitude (e.g. Fairley and Griffin, 1989; Matsumoto and Griffin, 2002a; Nawayseh and Griffin, 2003). The nonlinearity has also been found with a relaxed semi-supine posture reported in Chapters 5 and 6. With increasing magnitude of excitation, there is a reduction in the coherency between the excitation force and acceleration used to calculate the apparent mass at some frequencies, with the frequency at which coherency is least reducing as the magnitude of the excitation increases (see Chapter 6). The reductions in coherency with relaxed semi-supine subjects exposed to longitudinal horizontal random vibration suggest both reduced apparent mass and increased force distortion with increasing magnitude of excitation (see Figure 6.10 in Chapter 6).

In a linear system, the resonance frequency is the same at all vibration magnitudes and sinusoidal acceleration excitation results in sinusoidal forces at the point of excitation: distortion in the force in response to sinusoidal acceleration is a measure of the degree of nonlinearity. With subjects sitting erect and exposed to vertical sinusoidal excitation, Wittman and Phillips (1969) reported that the magnitude of the force time history on the seat during the positive loading phase (around the peak downward displacement) was greater than during the negative unloading phase (around the peak upward displacement). The duration of the negative unloading phase was longer than the duration of the positive loading phase. Hinz and Seidel (1987) also reported that for seated subjects force time histories deviated from vertical sinusoidal input acceleration waveforms and they expressed the deviations by magnitude quotients (the ratio of the maximum or minimum force to the maximum or minimum acceleration) and phase quotients (the ratio of the phase of the maximum or minimum force to the phase of the maximum or minimum acceleration). With one seated subject exposed to 1.5 ms^{-2} r.m.s. vertical sinusoidal excitation at 4.5 and 8.0 Hz, vertical and fore-and-aft accelerations measured at the third and fourth lumbar vertebrae (i.e. L3, L4) were found to be non-sinusoidal (Hinz *et al.*, 1988). Vertical sinusoidal excitation of seated subjects has been reported to

produce greater distortion of vertical acceleration on the pelvis around the 5-Hz resonance than at other frequencies, with distortion in the vertical acceleration of the pelvis and the vertical force at the seat increasing with increasing vibration magnitude (from 0.5 to 1.5 ms^{-2} r.m.s.) over the frequency range 4.0 to 12.5 Hz (Mansfield, 1995).

The distortion in output force at the subject-excitation interface during sinusoidal acceleration excitation can be used to examine the nature of the nonlinear change in the dynamic stiffness (or resonance frequency of apparent mass) of the body with varying vibration magnitude. Voluntary or involuntary muscular activity could cause nonlinearity, especially in postures that require muscle activity for postural stability (e.g. Matsumoto and Griffin, 2002b). Almost all studies investigating distortion in acceleration or force generated by the body have investigated the response of seated subjects where a degree of muscular postural control is necessary for stability. However, appreciable nonlinearity has also been found in relaxed semi-supine postures when using both random vertical excitation (Chapter 5) and random horizontal excitation (Chapter 6). The findings of these studies, which included intermittent random excitation, were consistent with the nonlinearity being caused by passive thixotropy of soft tissues, such that the stiffness of the body decreased during, and for a very short period immediately after, excitation. The distortions seen in the output force in relaxed semi-supine postures reduces the probability that voluntary or involuntary muscular activity is the primary cause of the distortion and nonlinearity.

There is evidence of harmonic force distortion during sinusoidal excitation at frequencies around the resonance frequency where nonlinearity is most apparent (e.g. Hinz and Seidel, 1987; Mansfield, 1995) – suggesting the distortion may be associated with the nonlinearity. With a change in the magnitude of intermittent random vibration, the dynamic stiffness of the body changes within about 2 seconds (Chapters 5 and 6). If quick changes in thixotropy are sufficient to be the primary cause of the nonlinearity, the output force will be distorted within a cycle of sinusoidal excitation. Harmonic force distortion would be greatest when the relative motion within the body is greatest – around the resonance frequency and at higher magnitudes of excitation. If thixotropy changes slowly relative to the duration of one cycle of oscillation, the force will not be distorted during a cycle, but the overall change in stiffness will result in a change in the response over a longer time. Greater understanding of how the harmonic force distortion depends on the magnitude and frequency of sinusoidal oscillation will indicate whether a quick change in thixotropy is likely to be responsible for the nonlinearity.

The distortion in the force arising during acceleration excitation can also be used to investigate the reason for the reductions in coherency evident with increasing magnitude of excitation (Chapter 6). The coherency between broad-band random input acceleration and the output force used to calculate the apparent mass of the body reflects the linearity of the transfer function between the acceleration and force, with unity coherence if the force arises solely from the input acceleration. With low magnitude excitation (e.g. less than 0.125 or 0.25 ms^{-2} r.m.s.) at low frequencies (e.g. less than 1 or 2 Hz), low coherency can be caused by incoherent forces arising from voluntary and involuntary movements of the body (e.g., Fairley, 1986; Abdul Jalil, 2005). With semi-supine subjects exposed to horizontal longitudinal acceleration, the coherency between acceleration and force is also reduced over the range 10 to 16 Hz, with the coherency, and the frequency at which coherency is least, reducing with increasing magnitude of vibration (Chapter 6). These authors showed that the reduced coherency was due to a combination of increased incoherent force (i.e. noise) and reduced apparent mass (and therefore reduced total output force) at these frequencies. Measurements of force during horizontal sinusoidal excitation at frequencies between 10 and 16 Hz would assist understanding of whether the high incoherent forces in this range are due to distortion. Since the reduction in coherency found with horizontal excitation of the semi-supine body (Chapter 6) was not observed with vertical excitation (Chapter 5), it is expected that there would be increased force distortion between 10 to 16 Hz with horizontal excitation but not with vertical excitation.

This study was designed to determine how the distortion in the dynamic force at the surface supporting relaxed semi-supine subjects depends on the frequency and magnitude of vertical and horizontal sinusoidal acceleration excitation. It was hypothesized that with both vertical and horizontal sinusoidal excitation the harmonic distortion in the force would exhibit a peak around the resonance frequency, and that the distortion would increase with increasing excitation magnitude. The observation of force distortion also provided an opportunity to examine the cause of variations in coherency during random excitation – it was hypothesized that there would be high force distortion between 10 and 16 Hz with horizontal excitation but not with vertical excitation.

7.2 Method

7.2.1 Apparatus

The experimental arrangement during vertical sinusoidal excitation is shown in Figure 5.1 (Chapter 5); the arrangement during longitudinal horizontal excitation is shown in Figure 6.1 (Chapter 6). With both vertical and longitudinal horizontal excitation, subjects maintained the same relaxed semi-supine posture. The support was constructed with three parts: back support, leg rest, and headrest.

The back support was a horizontal flat rigid aluminium plate (660 mm by 660 mm by 10 mm) covered with high stiffness 3-mm thick laterally treaded rubber attached to the upper surface. The back support was bolted rigidly to the upper surface of the force platform that monitored the vertical (*x*-axis of the supine subject) and longitudinal horizontal (*z*-axis of the supine subject) forces exerted by the subject on the back support. The force platform was bolted rigidly to the vibrator platform. The horizontal distance between the edge of the back support and the edge of the leg rest was 50 mm.

The legs of subjects rested on a horizontal flat rigid aluminium support covered with an 8-mm thick high-stiffness rubber. The height of the leg rest was adjusted to allow the lower legs to rest horizontally on the leg rest.

The headrest was a horizontal flat rigid wooden block with 75-mm thick uncompressed foam on the upper surface. The top surface of the complete uncompressed headrest was approximately 50 mm higher than the back support. The longitudinal horizontal distance between the back support and headrest was adjusted by moving the headrest so that the head of each subject could rest comfortably.

Vertical vibration (in the *x*-axis of the supine subject) was produced by a 1-metre stroke electro-hydraulic vertical vibrator, while the longitudinal horizontal vibration (in the *z*-axis of the supine subject) was produced by a 1-metre stroke electro-hydraulic horizontal vibrator in the laboratory of the Human Factors Research Unit. Both vibrators were capable of accelerations up to ±10 ms^{-2}.

The vertical (*x*-axis) acceleration and the longitudinal horizontal (*z*-axis) acceleration of the vibrator platform was measured using two identical Setra 141A ±2 g accelerometers fixed to the vibrator platform between the leg rest and the force platform (Figure 5.1 and Figure 6.1). The vertical (*x*-axis) and the longitudinal horizontal (*z*-axis) forces at the back support were measured using a Kistler 9281 B21 12-channel force platform. The four vertical (*x*-axis) force signals and the four

longitudinal horizontal (*z*-axis) force signals from the four corners of the platform were summed and conditioned using two Kistler 5001 charge amplifiers.

An *HVLab* data acquisition and analysis system (version 3.81) was used to generate motion stimuli and to acquire the vertical and horizontal accelerations and the vertical and horizontal forces from the transducers. The two acceleration signals and the two force signals were acquired at 200 samples per second via 67 Hz analogue anti-aliasing filters.

7.2.2 Stimuli

Sinusoidal vibration with a duration of 90 seconds was tapered at the start and end with 0.5-second cosine tapers. Two magnitudes of sinusoidal acceleration (0.25 and 1.0 ms^{-2} r.m.s.) were generated at each of nine preferred 1/3rd-octave centre frequencies (2.5, 3.15, 4.0, 5.0, 6.3, 8.0, 10.0, 12.5, and 16.0 Hz).

All subjects were tested first with vertical (*x*-axis) vibration and later with longitudinal horizontal (*z*-axis) vibration. The twelve subjects were divided into two equal groups, so that one group was tested with 0.25 ms^{-2} r.m.s. before 1.0 ms^{-2} r.m.s., and the other group was tested with 1.0 ms^{-2} r.m.s. before 0.25 ms^{-2} r.m.s. The order of presentation of the nine sinusoidal frequencies was randomised.

7.2.3 Posture

While experiencing each vertical or longitudinal horizontal motion, subjects had their eyes closed and maintained a relaxed supine position with their lower legs lifted and resting on the horizontal flat leg rest so as to achieve maximum contact with the back support (Figure 5.1 and Figure 6.1). Instruction for subjects is shown in Appendix B.

During vertical excitation, subjects wore a loose safety belt (passing around their abdomen and their arms resting at the two sides of the body) that did not constrain the body. During horizontal excitation, subjects wore a light harness connected by three loose safety belts to the vibrator platform without constraining the movement of the body. The total weight of the harness and buckles was less than 0.5 kg.

7.2.4 Subjects

Twelve male subjects, aged between 20 to 42 years, with mean (minimum and maximum) stature 1.73 m (1.66 m and 1.80 m) and mean total body mass 70.3 kg (58.3 kg and 86.2 kg) participated in the study. The study used the same subjects investigated with vertical random vibration (i.e. Chapter 5) and longitudinal horizontal random vibration (i.e. Chapter 6).

The experiment was approved by the Human Experimentation, Safety and Ethics Committee of the Institute of Sound and Vibration Research at the University of Southampton.

7.2.5 Analysis

All time histories were low-pass filtered at 46.0 Hz before the distortion of the input excitation acceleration and the output force in the direction of excitation were calculated at each of the nine frequencies from 2.5 to 16.0 Hz. The distortion, referred to here as the 'harmonic distortion', was calculated from:

$$D(\%) = \sqrt{\frac{G_3 - G_2}{G_2 - G_1}} x100 \tag{7.1}$$

where, with f_e as the excitation frequency, G_1 was obtained from the integration of the power spectral densities from 0 Hz to $1/\sqrt{2}\, f_e$ Hz, G_2 by integration from 0 Hz to $\sqrt{2}\, f_e$ Hz, and G_3 by integration from 0 Hz to $2\sqrt{2}\, f_e$ Hz. The power at the fundamental excitation frequency was assumed to be contained in the band $1/\sqrt{2}\, f_e$ to $\sqrt{2}\, f_e$ Hz (i.e. G_2 - G_1). The power of the harmonic distortion was assumed to be contained in the first harmonic in the band $\sqrt{2}\, f_e$ to $2\sqrt{2}\, f_e$ Hz (i.e. G_3 - G_2).

The force distortion was calculated using two types of output force. One was the dynamic force at the supine support after mass cancellation in the time domain (see Chapters 5 and 6), called the 'total output force', with power spectral density function $G_{oo}(f)$. The other, called 'coherent output force', with power spectral density function $G_{oo}'(f)$, was estimated by:

$$G_{oo}'(f) = G_{ii}(f) \mid H(f) \mid^2 \tag{7.2}$$

where

$$H(f) = G_{io}(f) / G_{ii}(f) \tag{7.3}$$

and $G_{ii}(f)$ is the power spectral density function of the input acceleration, $H(f)$ is the transfer function of the body (i.e. apparent mass) with modulus $\mid H(f) \mid$ in kg, and $G_{io}(f)$ is the cross spectral density function between the output force at the supine support and the input acceleration (Figure 7.1).

With Equation (7.1), the 'acceleration distortion', D_a, was calculated using the power spectrum of the input acceleration (i.e., $G_{ii}(f)$). The 'total-force distortion', D_{psd}, was calculated using the power spectrum of the total force (i.e., $G_{oo}(f)$), taking into account all harmonic distortion caused by coherent and incoherent output force. The 'coherent-force distortion', D_{csd}, was calculated using the power spectrum of the

coherent force (i.e., $G_{oo}'(f)$) and solely contains distortion arising from the slightly non-sinusoidal nature of the excitation (i.e. arising from the acceleration distortion). The difference between the 'total-force distortion' and the 'coherent-force distortion' indicates the distortion in 'incoherent force' caused by noise or nonlinearity (i.e. D_{psd} – D_{csd}). If the coherent-force distortion is similar to the total-force distortion, the harmonic distortions in the force are primarily caused by distortions in the input acceleration rather than distortions arising from the nonlinearity of the body.

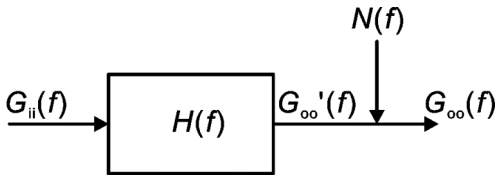

Figure 7.1 Frequency domain input-output diagram describing the relationship between the input acceleration (with subscript i), output force (with subscript o). $G_{ii}(f)$ denotes the power spectral density of the input acceleration; $G_{oo}(f)$ denotes the power spectral density of the output force which includes all coherent force (caused by input acceleration) and incoherent force (caused by noise and distortions of the body); $G_{oo}'(f)$ denotes the coherent output force estimated by multiplying the input acceleration power spectral density function $G_{ii}(f)$ with the transfer function, i.e. the apparent mass $H(f)$. $N(f)$ denotes the noise caused by the body, i.e. $G_{oo}(f) – G_{oo}'(f)$.

7.3 Results

Example acceleration and force time history waveforms, re-scaled to a peak value of unity by dividing the time histories by their absolute maximum peak values, are shown in Figure 7.2. The peak positive acceleration (loading phase) corresponded to the 'bottom' of the motion (i.e., the lowest position of the displacement cycle relative to the body) and so the peak negative acceleration (unloading phase) corresponded to the 'top' of the motion (i.e., the highest position of the displacement cycle). With 1.0 ms^{-2} r.m.s. horizontal excitation at 2.5 Hz (i.e., F1) Subject 10 in Figure 4 showed an approximately 180-degree lag in dynamic force. This lag was evident in 11 of the 12 subjects (not Subject 6) with 1.0 ms^{-2} r.m.s. horizontal excitation at 2.5 Hz, and 4 of the 12 subjects (i.e. Subjects 2, 7, 11 and 12) with 0.25 ms^{-2} r.m.s. horizontal excitation at 2.5 Hz. Possible causes of the lag could be voluntary or involuntary muscle activity pushing the legs against the raised leg rest or a cross-axis response in the mid-sagittal plane associated with the geometry of the body and the semi-supine posture.

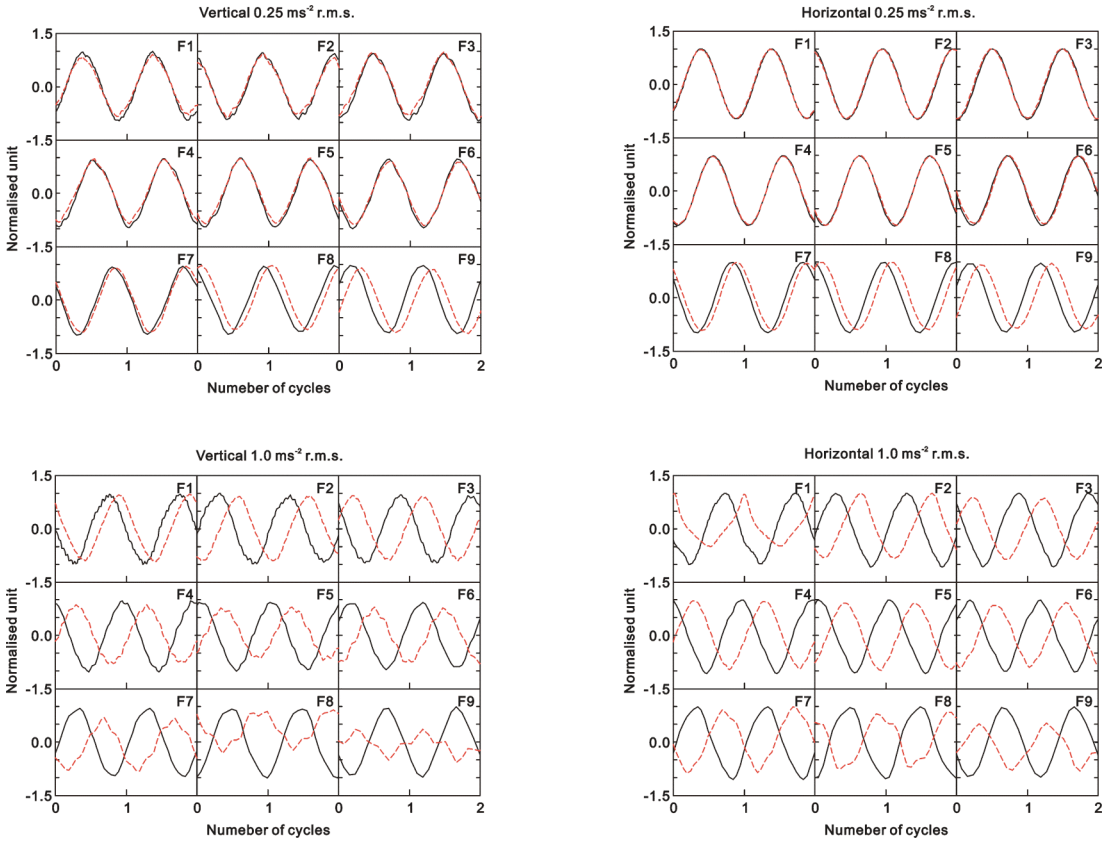

Figure 7.2 Example waveforms (Subject 10) of the excitation acceleration (——) and the output force (— — —) during vertical (*x*-axis) and horizontal (*z*-axis) sinusoidal vibration at 0.25 ms^{-2} r.m.s. and 1.0 ms^{-2} r.m.s. F1 – 2.5 Hz; F2 – 3.15 Hz; F3 – 4.0 Hz; F4 – 5.0 Hz; F5 – 6.3 Hz; F6 – 8.0 Hz; F7 – 10.0 Hz; F8 – 12.5 Hz; F9 – 16.0 Hz. The duration of each sampled time history varies to give two cycles. The *x* axis of each illustrated time history plot was normalised by the period of the excitation signal so as to show two cycles of signals. The illustrated time histories were sampled after the 10th second of the 90-second total duration.

The acceleration power spectral densities (i.e., G_{ii}) and the total-force power spectral densities (i.e., G_{oo}) for Subject 10 at both vibration magnitudes and the nine frequencies are shown for vertical excitation in Figure 7.3 and for horizontal excitation in Figure 7.4.

Acceleration distortion (i.e., D_a), total-force distortion (i.e., D_{psd}) and incoherent-force distortion (i.e., $D_{psd} - D_{csd}$) with the 12 subjects at both vibration magnitudes are shown for vertical excitation in Figure 7.5 and Table 7.1 and for horizontal excitation in Figure 7.6 and Table 7.2. The effect of excitation frequency on the distortions with vertical and horizontal excitation is shown with medians in Figure 7.7. The effect of excitation magnitude on the distortions with vertical and horizontal excitation is shown with medians in Figure 7.8. The effect of excitation magnitude on the square-rooted power spectra of the total force in the first harmonic is shown with medians and ranges in Figure 7.9.

7.3.1 Effect of excitation frequency

7.3.1.1 Vertical x-axis excitation

Ideally, harmonic distortion in the excitation acceleration would have been zero, or very low and the same for all subjects at each excitation frequency and magnitude. However, due to limitations of the vibrator, the harmonic distortion in the vertical excitation acceleration varied between 0.9% and 3.1% at 0.25 ms^{-2} r.m.s., and between 0.4% and 1.3% at 1.0 ms^{-2} r.m.s. over the nine selected frequencies (see Table 7.1).

At each of the two vibration magnitudes (0.25 and 1.0 ms^{-2} r.m.s.) and at each of the nine selected frequencies, Wilcoxon matched-pairs signed ranks tests were performed to determine whether the total-force distortion or the coherent-force distortion differed from the acceleration distortion.

With 0.25 ms^{-2} r.m.s. excitation, the harmonic distortion in total output force showed a similar frequency-dependent characteristic to the harmonic distortion in the excitation acceleration at all frequencies (see Figure 7.7, Table 7.1, and Figure 7.5 a, c). From 2.5 to 5.0 Hz, the total-force distortion was greater than the acceleration distortion ($p < 0.01$). At 6.3, 8.0 and 16.0 Hz, the acceleration and the total-force distortions were not significantly different ($p = 0.158$, 0.071, and 0.71, respectively). From 10.0 to 12.5 Hz, the total-force distortion was less than the acceleration distortion ($p < 0.01$). The coherent-force distortion was less than the acceleration distortion at all nine frequencies ($p < 0.01$; Figure 7.7 c).

With 1.0 ms^{-2} r.m.s. excitation, the total-force distortion and the coherent-force distortion showed a peak around 5 Hz with a different frequency-dependent characteristic from the harmonic distortion in the excitation acceleration (see Figure 7.7 d, Table 7.1, and Figure 7.5 b, d). At 2.5 Hz, the total-force distortion was less than the acceleration distortion ($p < 0.01$). From 3.15 to 16.0 Hz, the total-force distortion was greater than the acceleration distortion ($p < 0.01$). At 2.5 Hz, the coherent-force distortion was less than the acceleration distortion ($p < 0.01$). At 3.15 Hz, the coherent-force distortion was not significantly different from the acceleration distortion ($p = 0.099$). From 4.0 to 16.0 Hz, the coherent-force distortion was greater than the acceleration distortion ($p < 0.01$).

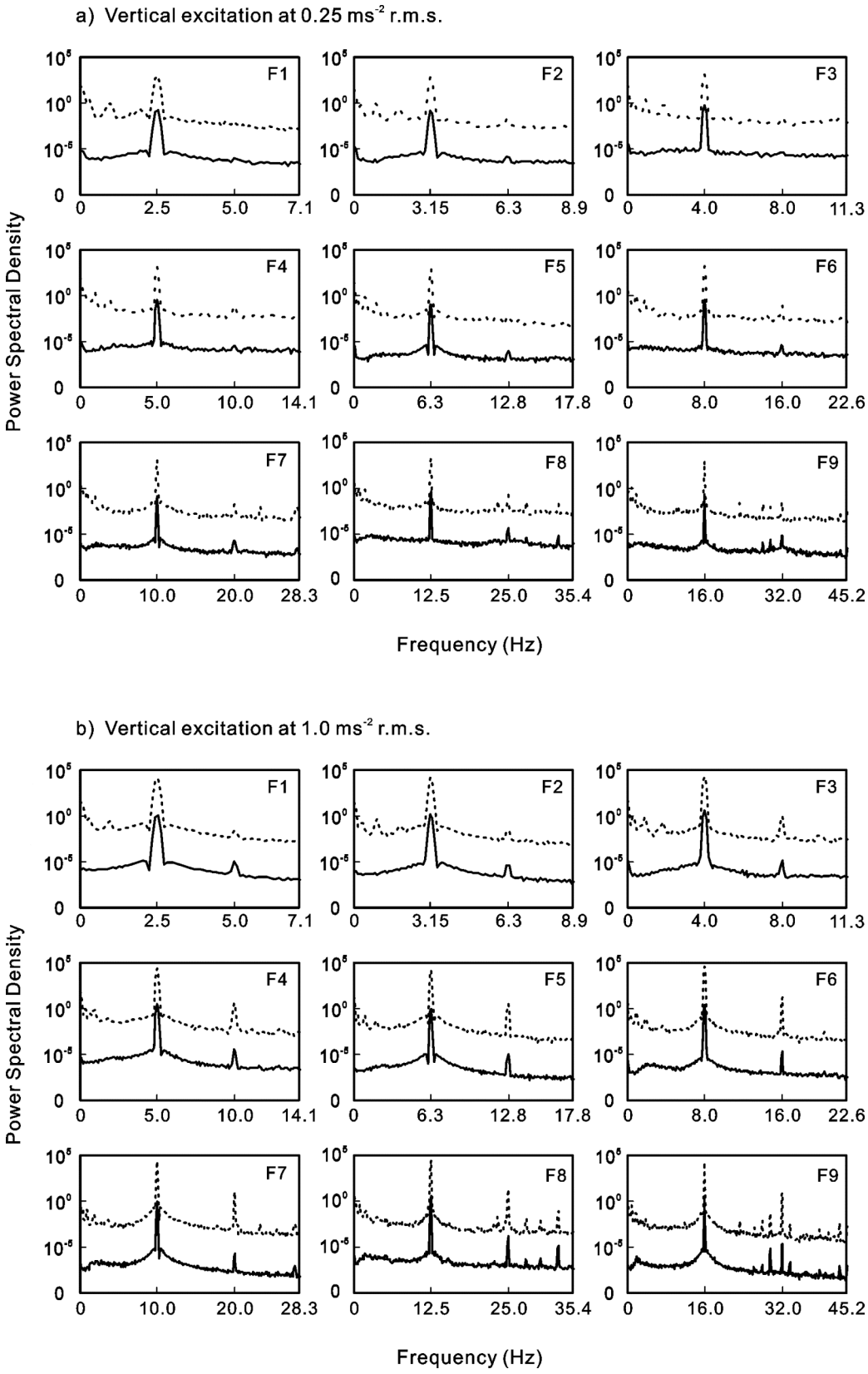

Figure 7.3 Example power spectral density (Subject 10) of the excitation acceleration (▬▬), in $(ms^{-2})^2$/Hz, and the total output force (……), in N^2/Hz, during vertical (*x*-axis) sinusoidal excitation at 0.25 ms^{-2} r.m.s. (a) and 1.0 ms^{-2} r.m.s. (b) showing the fundamental component and the first harmonic. Excitation frequency: F1 – 2.5 Hz; F2 – 3.15 Hz; F3 – 4.0 Hz; F4 – 5.0 Hz; F5 – 6.3 Hz; F6 – 8.0 Hz; F7 – 10.0 Hz; F8 – 12.5 Hz; F9 – 16.0 Hz. The upper limit of the frequency scale is $2\sqrt{2}$ times the excitation frequency.

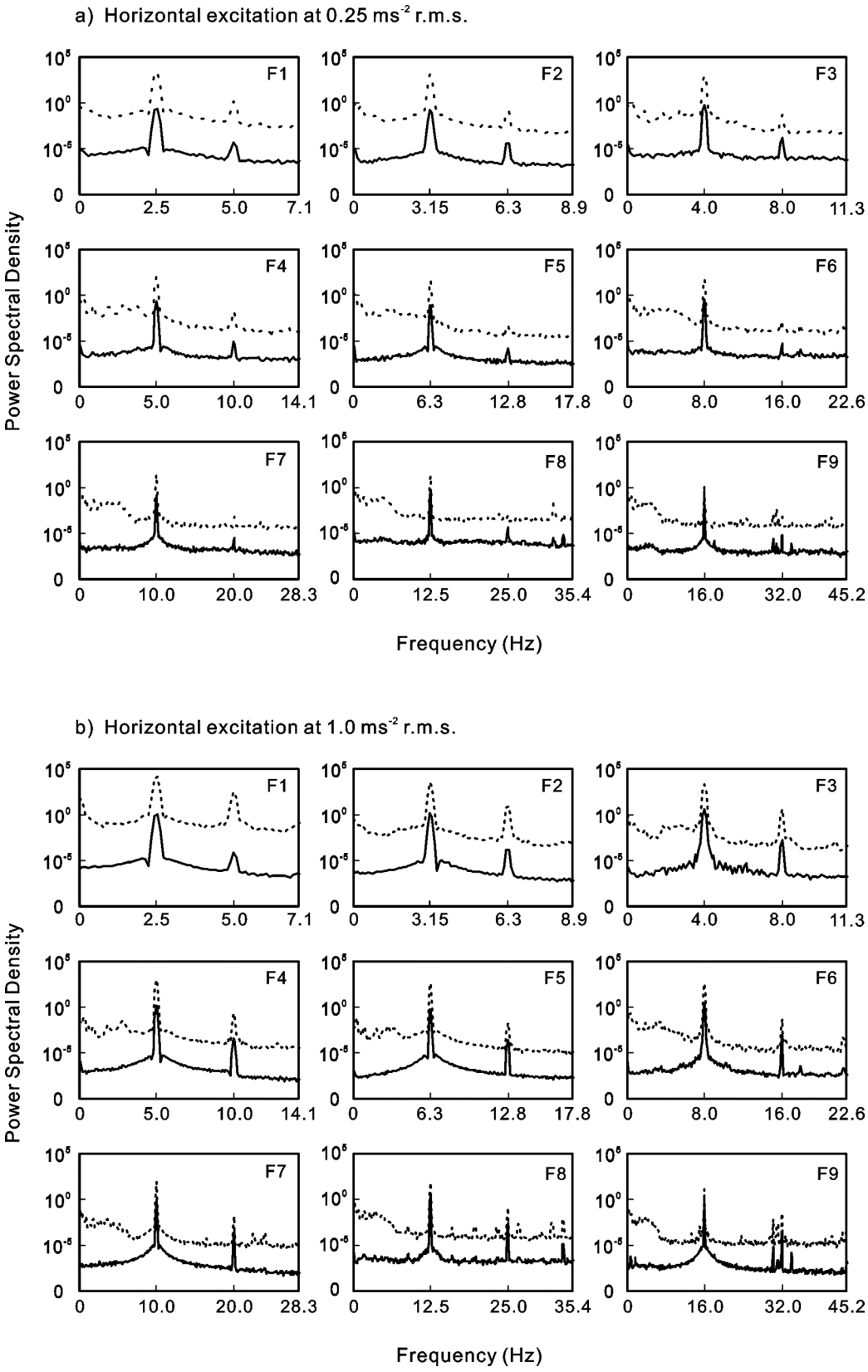

Figure 7.4 Example power spectral density (Subject 10) of the excitation acceleration (——), in $(ms^{-2})^2$/Hz, and the total output force (……), in N^2/Hz, during horizontal (*z*-axis) sinusoidal excitation at 0.25 ms^{-2} r.m.s. (a) and 1.0 ms^{-2} r.m.s. (b) showing the fundamental component and the first harmonic. Excitation frequency: F1 – 2.5 Hz; F2 – 3.15 Hz; F3 – 4.0 Hz; F4 – 5.0 Hz; F5 – 6.3 Hz; F6 – 8.0 Hz; F7 – 10.0 Hz; F8 – 12.5 Hz; F9 – 16.0 Hz. The upper limit of the frequency scale is $2\sqrt{2}$ times the excitation frequency.

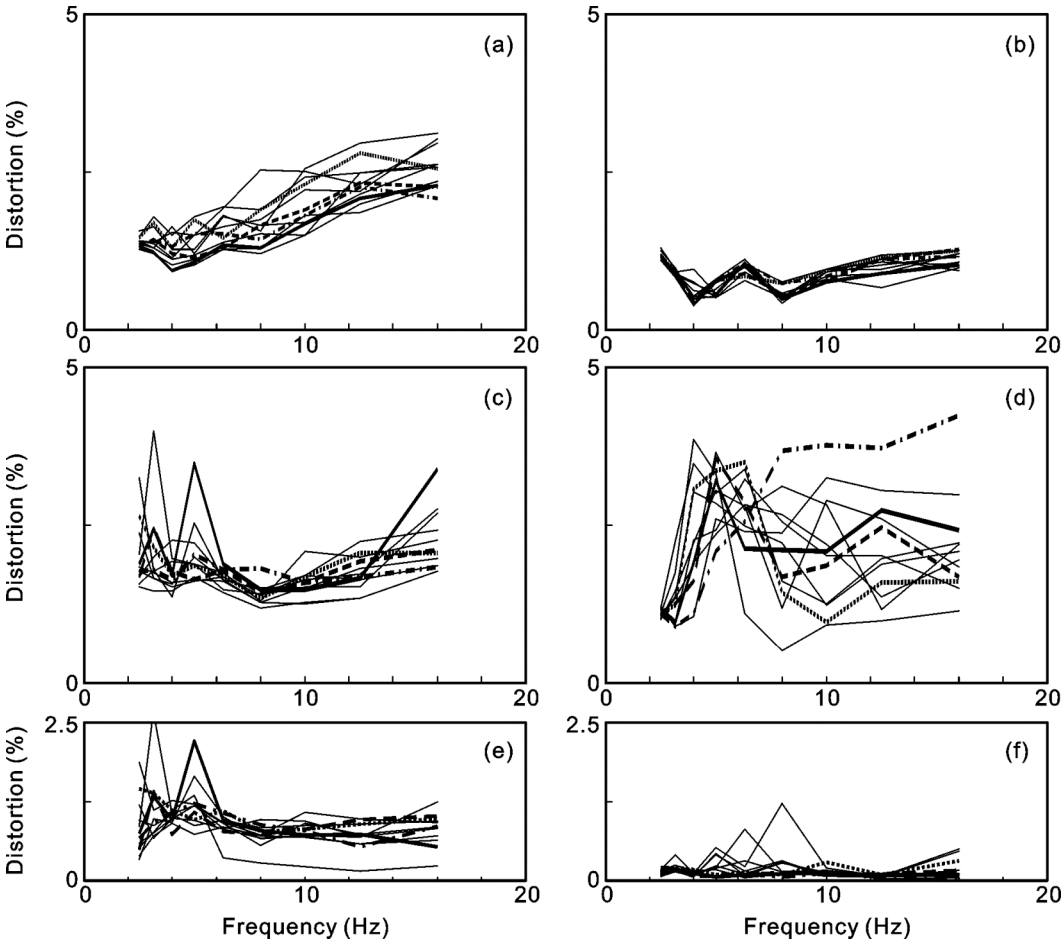

Figure 7.5 Vertical *x*-axis sinusoidal excitation – individual distortion at 0.25 ms^{-2} r.m.s. in: (a) excitation acceleration, (c) total force, (e) incoherent force; individual distortion at 1.0 ms^{-2} r.m.s. in: (b) excitation acceleration; (d) total force; (f) incoherent force. ——— Subject 1; ..... Subject 6; — — — Subject 9; —.—.— Subject 10; ——— others. Nine excitation frequencies: 2.5, 3.15, 4.0, 5.0, 6.3, 8.0, 10.0, 12.5, and 16.0 Hz.

Table 7.1 Median and ranges of the harmonic distortions (%) over the 12 subjects exposed to vertical (*x*-axis) sinusoidal excitation at the nine selected frequencies and the two vibration magnitudes (0.25 and 1.0 ms^{-2} r.m.s.).

Freq. (Hz)	2.5	3.15	4.0	5.0	6.3	8.0	10.0	12.5	16.0
Distortion in input acceleration at 0.25 ms^{-2} r.m.s. (%)									
Minimum	1.3	1.2	0.9	1.0	1.3	1.2	1.5	1.8	2.1
Median	1.4	1.4	1.2	1.2	1.5	1.6	1.9	2.3	2.6
Maximum	1.6	1.8	1.6	1.8	1.9	2.5	2.5	3.0	3.1
Distortion in total force at 0.25 ms^{-2} r.m.s. (%)									
Minimum	1.5	1.4	1.4	1.6	1.4	1.2	1.3	1.3	1.8
Median	1.8	1.8	1.7	1.9	1.7	1.4	1.6	1.7	2.1
Maximum	3.2	4.0	2.3	3.5	1.9	1.8	2.1	2.2	3.4
Distortion in input acceleration at 1.0 ms^{-2} r.m.s. (%)									
Minimum	1.1	0.8	0.4	0.5	0.8	0.4	0.7	0.7	0.9
Median	1.2	0.9	0.5	0.6	1.0	0.5	0.9	1.0	1.2
Maximum	1.3	1.0	1.0	0.8	1.1	0.8	1.0	1.2	1.3
Distortion in total force at 1.0 ms^{-2} r.m.s. (%)									
Minimum	1.0	0.9	1.0	2.1	1.1	0.5	0.9	1.0	1.1
Median	1.1	1.2	2.1	3.0	2.8	2.1	2.0	2.0	2.0
Maximum	1.2	2.2	3.8	3.6	3.5	3.7	3.7	3.7	4.2

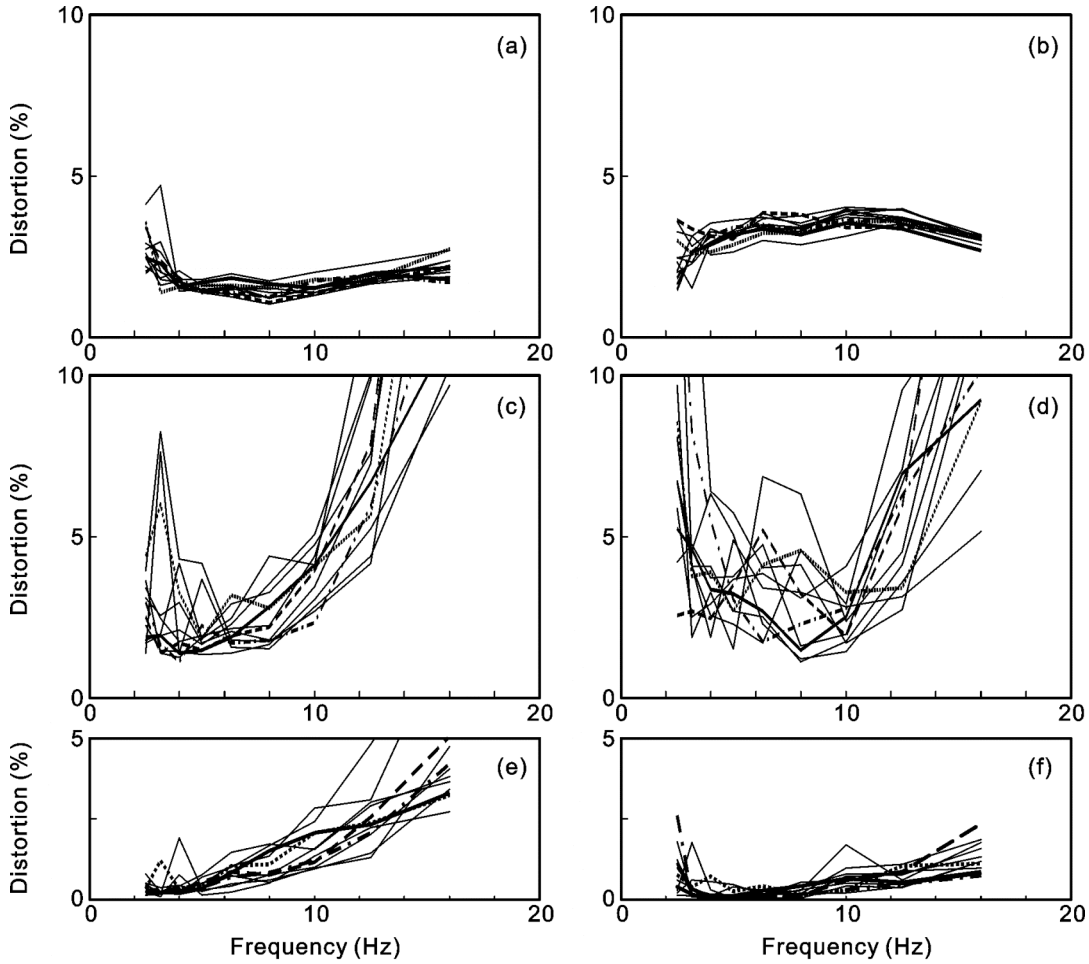

Figure 7.6 Horizontal *z*-axis sinusoidal excitation – individual distortion at 0.25 ms^{-2} r.m.s. in: (a) excitation acceleration, (c) total force, (e) incoherent force; individual distortion at 1.0 ms^{-2} r.m.s. in: (b) excitation acceleration; (d) total force; (f) incoherent force. ▬▬▬ Subject 1; ..... Subject 6; ▬ ▬ ▬ Subject 9; ▬.▬.▬ Subject 10; ——— others. Nine excitation frequencies: 2.5, 3.15, 4.0, 5.0, 6.3, 8.0, 10.0, 12.5, and 16.0 Hz.

Table 7.2 Median and ranges of the harmonic distortions (%) of the 12 subjects exposed to horizontal (*z*-axis) sinusoidal excitation at the nine selected frequencies and the two vibration magnitudes (0.25 and 1.0 ms^{-2} r.m.s.).

Freq. (Hz)	2.5	3.15	4.0	5.0	6.3	8.0	10.0	12.5	16.0
Distortion in input acceleration at 0.25 ms^{-2} r.m.s. (%)									
Minimum	2.0	1.4	1.4	1.4	1.2	1.0	1.3	1.7	1.7
Median	2.7	2.2	1.6	1.5	1.5	1.3	1.5	1.8	2.1
Maximum	4.1	4.7	2.0	1.8	2.0	1.7	2.0	2.3	2.7
Distortion in total force at 0.25 ms^{-2} r.m.s. (%)									
Minimum	1.3	1.4	1.1	1.3	1.3	1.5	2.3	4.2	9.7
Median	2.7	1.9	1.7	1.8	2.0	2.2	4.0	6.9	22.3
Maximum	4.4	8.2	4.3	4.1	3.2	4.4	5.0	12.5	34.5
Distortion in input acceleration at 1.0 ms^{-2} r.m.s. (%)									
Minimum	1.5	1.5	2.5	2.6	3.0	2.8	3.1	3.3	2.7
Median	2.4	2.6	3.0	3.2	3.4	3.4	3.7	3.6	3.0
Maximum	3.6	3.3	3.5	3.6	3.9	3.8	4.0	4.0	3.2
Distortion in total force at 1.0 ms^{-2} r.m.s. (%)									
Minimum	2.5	1.9	1.9	1.5	1.7	1.1	1.4	2.7	5.1
Median	7.4	4.1	3.5	3.3	3.6	3.1	2.4	5.2	12.1
Maximum	17.2	14.7	6.4	5.7	6.9	6.3	4.1	9.5	22.2

7.3.1.2 Horizontal z-axis excitation

Due to limitations of the 1-m horizontal vibrator, the harmonic distortion in the horizontal excitation acceleration varied between 1.0% and 4.7% at 0.25 ms^{-2} r.m.s., and between 1.5% and 4.0% at 1.0 ms^{-2} r.m.s. over the nine selected frequencies (see Table 7.2).

With 0.25 ms^{-2} r.m.s. excitation, the harmonic distortion in the total output force only showed a similar frequency-dependent characteristic to the harmonic distortion in the excitation acceleration at frequencies less than about 6.3 Hz (see Figure 7.7 a, Table 7.2, and Figure 7.6 a, c). From 2.5 to 4.0 Hz, the total-force distortion was not significantly different from the acceleration distortion (p = 0.754, 0.875, and 0.388, respectively). From 5.0 to 16.0 Hz, the total-force distortion was greater than the acceleration distortion ($p < 0.05$). From 2.5 to 8.0 Hz, the coherent-force distortion was not significantly different from the acceleration distortion (p = 0.05 to 0.937).

From 10.0 to 16.0 Hz, the coherent-force distortion was greater than the acceleration distortion ($p < 0.02$).

With 1.0 ms^{-2} r.m.s. excitation, the total-force distortion and the coherent-force distortion showed very different frequency-dependencies from the harmonic distortion in the excitation acceleration across the nine frequencies (see Figure 7.7 b, Table 7.2, and Figure 7.6 b, d). At 2.5 and 3.15 Hz, the total-force distortion was greater than the acceleration distortion ($p < 0.02$). From 4.0 to 8.0 Hz, the total-force distortion was not significantly different from the acceleration distortion ($p = 0.136$ to 0.937). At 10.0 Hz, the total-force distortion was lower than the acceleration distortion ($p < 0.02$). At 12.5 and 16.0 Hz, the total-force distortion was greater than the acceleration distortion ($p < 0.05$). The statistical difference between the coherent-force distortion and the acceleration distortion was similar to that between the total-force distortion and the acceleration distortion, except at 12.5 Hz. At 12.5 Hz, the coherent-force distortion was not significantly different from the acceleration distortion ($p = 0.58$).

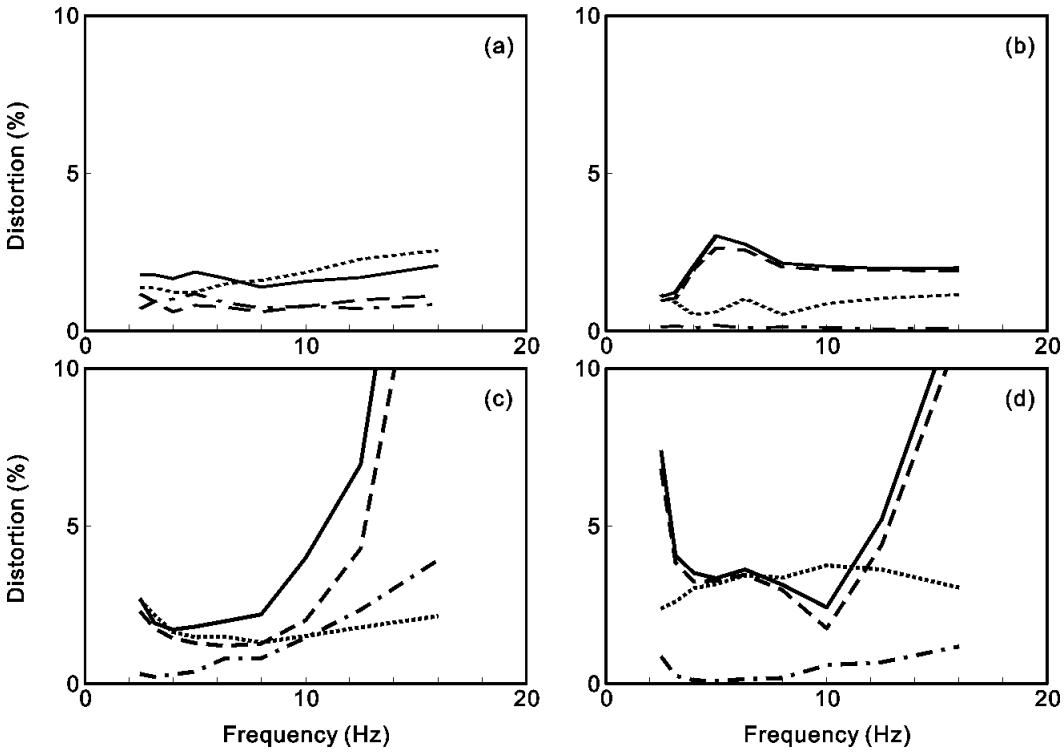

Figure 7.7 Effect of excitation frequency: median distortion during *x*-axis vertical excitation at 0.25 (a) and 1.0 ms^{-2} r.m.s. (b); median distortion during *z*-axis horizontal excitation at 0.25 (c) and 1.0 ms^{-2} r.m.s. (d). Distortion in excitation acceleration: ..... ; distortion in total force: ——— ; distortion in coherent force: — — — ; distortion in incoherent force: — . — . — . Nine excitation frequencies: 2.5, 3.15, 4.0, 5.0, 6.3, 8.0, 10.0, 12.5, and 16.0 Hz.

7.3.2 Effect of excitation magnitude

7.3.2.1 Vertical x-axis excitation

The acceleration distortion at 0.25 ms^{-2} r.m.s. was greater than the acceleration distortion at 1.0 ms^{-2} r.m.s. at all nine frequencies ($p < 0.01$, Wilcoxon; Figure 7.8 a).

The total-force distortion at 0.25 ms^{-2} r.m.s. was greater than the total-force distortion at 1.0 ms^{-2} r.m.s. with 2.5 and 3.15 Hz ($p < 0.02$; Figure 7.8 c). The total-force distortion at 0.25 ms^{-2} r.m.s. was less than the total-force distortion at 1.0 ms^{-2} r.m.s. with 5.0, 6.3 and 8.0 Hz ($p < 0.02$). With 4.0, 10.0, 12.5 and 16.0 Hz, the influence of vibration magnitude on total-force distortion was not statistically significant ($p = 0.05$ to 0.388).

The coherent-force distortion at 0.25 ms^{-2} r.m.s. was greater than the coherent-force distortion at 1.0 ms^{-2} r.m.s. with 2.5 Hz ($p < 0.03$, Wilcoxon). The coherent-force distortion at 0.25 ms^{-2} r.m.s. was less than the coherent-force distortion at 1.0 ms^{-2} r.m.s. from 4.0 to 12.5 Hz ($p < 0.01$). With 3.15 and 16.0 Hz, the effect of vibration magnitude on the coherent-force distortion was not statistically significant ($p = 0.347$ and 0.084, respectively).

7.3.2.2 Horizontal z-axis excitation

The acceleration distortion with 0.25 ms^{-2} r.m.s. was less than the acceleration distortion with 1.0 ms^{-2} r.m.s. from 4.0 to 16.0 Hz ($p < 0.01$, Wilcoxon; Figure 7.8 b). The effect of excitation magnitude on the distortion in acceleration was not statistically significant at 2.5 and 3.15 Hz ($p = 0.05$ and 0.84, respectively).

The total-force distortion was less at 0.25 ms^{-2} r.m.s. than at 1.0 ms^{-2} r.m.s. from 2.5 to 6.3 Hz ($p < 0.01$, Wilcoxon; Figure 7.8 d) except with 3.15 Hz ($p = 0.071$, Wilcoxon). The total-force distortion at 0.25 ms^{-2} r.m.s. was greater than the total-force distortion at 1.0 ms^{-2} r.m.s. from 10.0 to 16.0 Hz ($p < 0.01$). With 8.0 Hz, the effect of vibration magnitude on total-force distortion was not significant ($p = 0.209$).

The coherent-force distortion at 0.25 ms^{-2} r.m.s. was less than the coherent-force distortion at 1.0 ms^{-2} r.m.s. from 2.5 to 8.0 Hz ($p < 0.05$, Wilcoxon). The coherent-force distortion at 0.25 ms^{-2} r.m.s. was greater than the coherent-force distortion at 1.0 ms^{-2} r.m.s. with 16.0 Hz ($p < 0.05$). With 10.0 and 12.5 Hz, the effect of vibration magnitude on total-force distortion was not significant ($p = 0.239$ and 0.695, respectively).

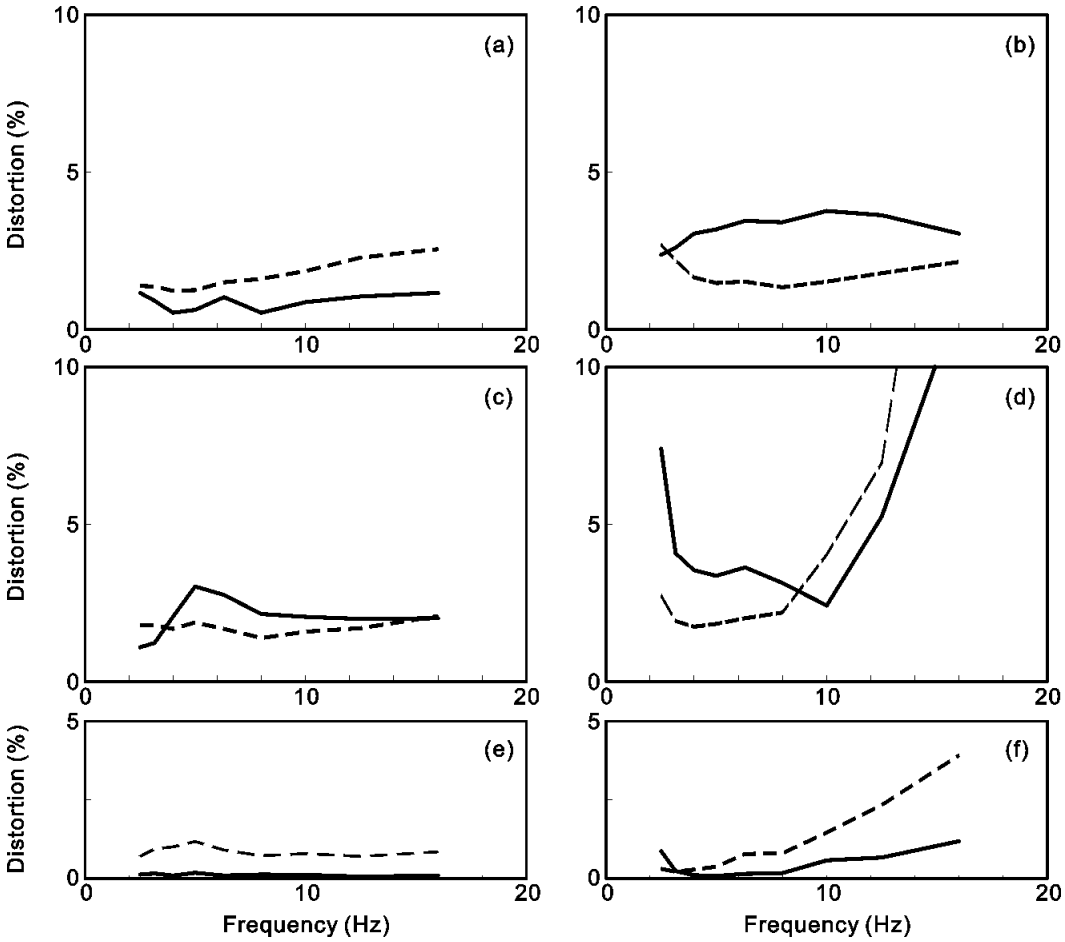

Figure 7.8 Effect of excitation magnitude: median distortion during *x*-axis vertical excitation in (a) excitation acceleration, (c) total force, (e) incoherent force; median distortion during *z*-axis horizontal excitation in (b) excitation acceleration, (d) total force, (f) incoherent force. — — — 0.25 ms^{-2} r.m.s.; ——— 1.0 ms^{-2} r.m.s. Nine excitation frequencies: 2.5, 3.15, 4.0, 5.0, 6.3, 8.0, 10.0, 12.5, and 16.0 Hz.

7.4 Discussion

7.4.1 Total output force distortion – dependence on excitation frequency

With 0.25 ms^{-2} r.m.s. vertical excitation, the total force distortion was marginally greater than the acceleration distortion at frequencies from 2.5 to 5.0 Hz (Figure 7.7). There was no evident peak in distortion around 9.6 Hz – the median normalised apparent mass resonance frequency of the same group of subjects during vertical random excitation at 0.25 ms^{-2} r.m.s. (Chapter 5). The force distortion at this magnitude was low and at frequencies greater than 5.0 Hz it was mainly caused by the distortion in the input acceleration. However, with 1.0 ms^{-2} r.m.s. vertical excitation, the total force distortion was greater than the acceleration distortion at frequencies from 3.15 to 16.0 Hz. This range encompasses the median

normalised apparent mass resonance frequency at 7.8 Hz obtained for the subjects during 1.0 ms^{-2} r.m.s. vertical random excitation.

With 0.25 ms^{-2} r.m.s. horizontal excitation, the total force distortion was greater than the acceleration distortion at frequencies greater than 4.0 Hz (Figure 7.7). Similar to the force distortion with vertical excitation at the same magnitude, there was no evident peak around 3.4 Hz, the median normalised apparent mass resonance frequency of the same group of subjects during horizontal random excitation at 0.25 ms^{-2} r.m.s. (Chapter 6). At this magnitude, the force distortion was less than the acceleration distortion at frequencies less than about 4.0 Hz. With 1.0 ms^{-2} r.m.s. horizontal excitation, the total force distortion was considerably greater than the acceleration distortion at frequencies less than 4.0 Hz, including the median normalised apparent mass resonance frequency at 2.4 Hz obtained for the subjects during 1.0 ms^{-2} r.m.s. horizontal random excitation.

7.4.2 Total output force distortion – dependence on excitation magnitude

Over the frequency range of the apparent mass resonance during random excitation, the force distortion was significantly greater at 1.0 ms^{-2} r.m.s. than at 0.25 ms^{-2} r.m.s. with both vertical and horizontal sinusoidal excitation (Figure 7.8 c, d). With this four-fold change in vibration magnitude in both axes of excitation, the ratio between the r.m.s. total force in the first harmonic (i.e. the square-root of the power spectrum of the force integrated between $\sqrt{2}\,f_e$ and $2\sqrt{2}\,f_e$ Hz) at 1.0 and 0.25 ms^{-2} r.m.s. generally exceeded a ratio of 4.0 (Figure 7.9). With this change in magnitude, the corresponding ratio for r.m.s. acceleration distortion was less than 4.0 (see Figure 7.8 a, b). This shows that at frequencies around the resonance a four-fold increase in the magnitude of the excitation acceleration results in a disproportionally greater increase in the force distortion at the first harmonic. The filtering effect seen with the apparent mass of the body during random vibration would decrease the distortion of the dynamic force in the first harmonic with excitation frequencies near the resonance. However, even with this effect there is a greater increase in the force distortion at the first harmonic.

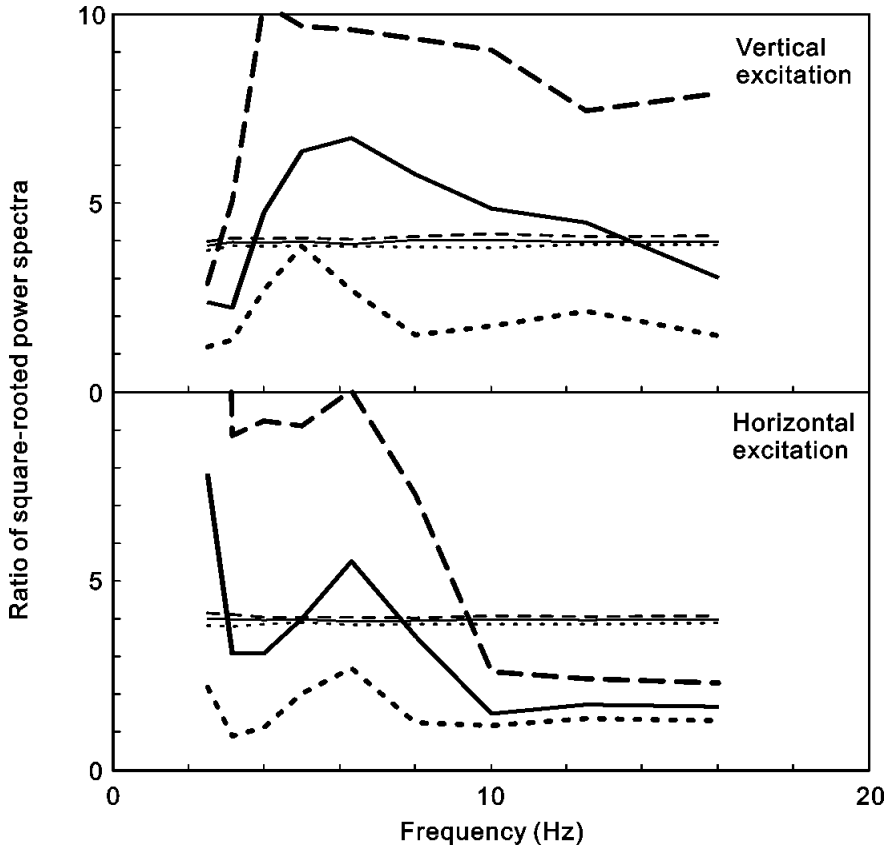

Figure 7.9 Effect of excitation magnitude on harmonic force distortion: the ratios between the r.m.s. total force at the first harmonic at 1.0 ms^{-2} r.m.s. and the r.m.s. total force at the first harmonic at 0.25 ms^{-2} r.m.s. during both vertical and horizontal excitation at each of the nine frequencies (f_e). For each excitation frequency, the r.m.s. acceleration at excitation was obtained from integration of the acceleration power spectral densities from $1/\sqrt{2}\,f_e$ Hz to $\sqrt{2}\,f_e$ Hz (— — — maximum; ——— median; . . . . . minimum); the r.m.s. total force at the first harmonic distortion was obtained from the integration of the total force power spectral densities from $\sqrt{2}\,f_e$ Hz to $2\sqrt{2}\,f_e$ Hz (— — — maximum; ——— median; - - - - - minimum). Nine excitation frequencies: 2.5, 3.15, 4.0, 5.0, 6.3, 8.0, 10.0, 12.5, and 16.0 Hz.

7.4.3 Nonlinearity and force distortion

The results indicate that force distortion of the supine human body depends on the frequency and magnitude of vibration similarly to how they vary in the upright body (Mansfield, 1995). This similarity suggests that the involvement of muscular control of posture does not greatly affect the force distortion. In both postures, the distortion may be associated with the nonlinearity evident with varying magnitudes of excitation.

The low distortion in total force around the resonance frequency at low magnitudes suggests that the nonlinearity evident in the reduction in the resonance frequency

with an increase in the vibration magnitudes was associated with the increased force distortion present at the higher magnitudes. At 1.0 ms^{-2} r.m.s. the increase in total force distortion around the resonance frequencies was primarily caused by increased coherent force generated by the response of the body (Figure 7.7 b, d). In other words, especially around the resonance, the force distortion increased when the acceleration increased and was due to an increase in force at the first harmonic causing distortion. This was evident in a similar departure from a sinusoidal force waveform in each successive cycle of oscillation.

If passive thixotropy of body tissues is the primary cause of the nonlinearity, a biodynamic model incorporating such a mechanism should take into account two variables: (i) the instantaneous reduction in the proportional change of resultant force when increasing or decreasing the magnitude of excitation, and (ii) the time constant associated with the change in body stiffness when altering the excitation magnitude. According to Hooke's law, the force imposed by a linear spring is the product of the stiffness and displacement of the spring. But thixotropy will reduce the resonance frequency associated with reduced equivalent stiffness of the body as the velocity increases. The dependence on velocity as well as displacement will cause the dynamic force to change nonlinearly with variations in the acceleration. The results of the present study may allow the estimation of the velocity-dependence of the force (by comparing the force at harmonic frequencies with the force at the excitation frequency), but this and the development of a dynamic model of the nonlinearity due to thixotropy are outside the scope of this study.

Although the semi-supine posture was intended to minimise muscular activity of the body, it is possible that some muscular activity, such as involuntary reflexes, contributed to the force distortion and the nonlinearity. Transfer functions between vertical forces at a seat and the EMG activity of back muscles in seated subjects, and the transfer function between acceleration at the seat and EMG muscular activity, suggest that 'muscular reaction' does not primarily cause the nonlinearity evident with varying magnitudes of vibration at frequencies greater than 1 Hz (see Section 4.2 in Blüthner *et al.*, 2002). In the present study, appreciable force distortion evident at frequencies much lower than the excitation frequency (see Figure 7.3 and Figure 7.4) may have been caused by muscle activity. Such activity may have caused the 'phase reversal' visible in Figure 7.2 (with 1.0 Hz horizontal excitation at 1.0 ms^{-2} r.m.s.) of the present study. The phase reversal represents a time lag between the input acceleration and the dynamic force by about 180 degree. A change in time lag of the muscular activity when the vibration magnitude increases has been suggested to cause the nonlinearity (Chapter 4). The

nonlinearity can be changed by some voluntary periodic back and abdomen muscular contraction (Chapter 4), possibly because the timing of the dynamic force generated by muscular activity is changed by the voluntary contraction.

7.4.4 The coherency drop and force distortion

During horizontal excitation at both 0.25 and 1.0 ms^{-2} r.m.s., the coherent force distortion caused the total force distortion to be greater than the acceleration distortion at frequencies greater than about 8.0 Hz (Figure 7.7 c, d). This frequency range coincides with the drop in coherency during random excitation of the same subjects (Chapter 6). The increased distortion and reduced coherency were not observed with either sinusoidal or random vertical vibration, suggesting the force distortion with horizontal excitation at these frequencies could be contributing to the reduced coherency.

7.5 Conclusions

During both vertical and longitudinal horizontal sinusoidal acceleration excitation of the semi-supine human body, there is an increase in force distortion around the apparent mass resonance frequency as the vibration magnitude increases from 0.25 ms^{-2} r.m.s. to 1.0 ms^{-2} r.m.s. The findings are consistent with thixotropy being a primary cause of the nonlinearity.

Chapter 8

Nonlinearity in apparent mass and transmissibility of the supine human body during vertical whole-body vibration

8.1 Introduction

During vertical whole-body vibration, the resonance frequencies of the apparent mass and transmissibilities of the upright seated or standing human body decrease with increasing vibration magnitude (e.g. Matsumoto and Griffin, 1998b; Mansfield and Griffin, 2000; Matsumoto and Griffin, 2002a). This nonlinearity has also been found in the apparent mass of the relaxed semi-supine human body exposed to vertical vibration (Chapter 5) and longitudinal horizontal vibration (Chapter 6). With the response of the human body represented by a passive single degree-of-freedom mass-spring-damper model, the change in the resonance frequency can be represented by either a decrease in the stiffness or an increase in the sprung mass.

The transmissibilities to various locations on the body may be used to identify the modes contributing to resonances seen in the apparent mass. Improved understanding of the modes contributing to the resonances might improve understanding of the cause of the nonlinearity. Transmissibilities to the pelvis and the spinal column show that the resonance of the seated body is primarily caused by a whole-body rocking mode associated with bending and rotational modes of the spine, possibly caused by axial and shear deformation of the tissues beneath the pelvis (i.e. parts of the buttocks, e.g. Kitazaki and Griffin, 1998; Matsumoto and Griffin, 1998b). Transmissibilities to the pelvis, thoracic and lumbar spine, and abdominal wall have been found to be nonlinear in upright seated subjects during vertical excitation (e.g. Mansfield and Griffin, 2000; Matsumoto and Griffin, 2002a). These studies with seated subjects suggest that the nonlinearity is caused by either a passive softening effect of the soft tissues beneath the ischial tuberosities (e.g. thixotropy) or some combination of voluntary and involuntary activity of the postural muscles.

With vertical intermittent vibration, the stiffness of the relaxed supine body has been reported to decrease during, and for about 3 seconds after, exposure to high magnitude vibration, and increase during and for about 3 seconds after exposure to low magnitude vibration – a response typical of thixotropy (Chapter 5). Thixotropy, in which stiffness reduces during excitation, might be the primary cause of the nonlinearity found with the seated, standing, and supine human body. Thixotropy has been found in various parts of the human body: wrist (Lakie *et al*., 1979), finger

extensor (Lakie, 1986), finger flexor (Hagbarth *et al*., 1985; Lakie, 1986), and rib cage respiratory muscles (Homma and Hagbarth, 2000). It might be suspected that vibration transmission paths comprising more soft tissues (e.g. the abdomen of a supine subject) would be more thixotropic and therefore more nonlinear than paths dominated by boney structures (e.g. the spinal column and sternum of a supine subject). Transmissibilities measured to different locations (e.g., the abdomen and the sternum) with varying magnitudes of vibration will indicate whether some parts of the supine body are more nonlinear than other parts.

Whereas increased steady-state muscle contraction has not been found to influence the nonlinearity (e.g. Matsumoto and Griffin, 2002b), The study described in Chapter 4 found that some voluntary periodic upper-body movements reduced the nonlinearity seen in the apparent mass of seated persons. The movements were assumed to involve various postural muscles that are normally involved in supporting the body with 'tonic' activity (i.e. a state of continuous contraction). During vibration, in order to stabilise the body in the presence of the externally applied motion, muscle activity varies with a 'phasic' response (i.e. muscles try to compensate for the inertial forces of the oscillatory motion). Phasic responses may be voluntary or involuntary, although voluntary phasic contractions may only be effective at low frequencies (e.g., at frequencies less than about 1 to 2 Hz, Griffin, 1990). The present study was undertaken with supine postures so as to eliminate the need for voluntary or involuntary phasic activity of the postural muscles to support the body.

It is not known whether the posture of the supine body affects the nonlinearity. Changing posture, contact conditions, and constraints of seated and standing subjects changes the resonance frequencies of the body, but the responses of the seated and standing body appears to remain nonlinear in all postures (e.g. Mansfield and Griffin, 2002; Subashi *et al*., 2006). Nawayseh and Griffin (2003) reported a small reduction in the nonlinearity when seated subjects changed their posture from 'maximum thigh contact' to 'minimum thigh contact' by raising the feet. The 'maximum thigh contact' allowed more soft tissues of the thighs to couple with the seat, while the 'minimum thigh contact' reduced the soft tissues in contact with the seat. Mansfield and Griffin (2002) found no significant change in the nonlinearity when an abdominal constraining belt was worn by upright seated subjects during vertical vibration. The present study employed three postures to vary the contact between the body and the excitation. In a 'flat supine' posture, the excitation involved the soft tissues of the lower back and part of the thighs, whereas in a 'semi-supine' posture with the lower legs raised there was less contact with these soft

tissues (but greater contact with the skeletal structure of the entire back), and in a 'constrained semi-supine' posture the upper-body was constrained by a four-point harness so as to maximise the contact between the subjects and source of excitation. The 'semi-supine' posture was the same as that described in Chapters 5 and 6.

From previous studies it is not clear whether the human body is 'more nonlinear' at low magnitudes or high magnitudes of vibration. Voluntary periodic movement of the upper bodies of seated subjects changed the resonance frequency more at low vibration magnitudes (0.25 ms^{-2} r.m.s.) than at high magnitudes (2.0 ms^{-2} r.m.s.; Chapter 4). The lowest vibration magnitudes investigated in previous studies with seated or standing subjects have been between 0.1 and 0.25 ms^{-2} r.m.s. To investigate the nonlinearity at lower magnitudes, the present study measured apparent mass and transmissibility at vibration magnitudes as low as 0.03 ms^{-2} r.m.s.

With vertical excitation at seven vibration magnitudes (from about 0.03 to 1.0 ms^{-2} r.m.s.), this study investigated the apparent mass and transmissibility of subjects in three supine postures. It was hypothesized that there would be nonlinearity in the apparent mass and also in transmissibilities to the sternum and the upper and lower abdomen: the resonance frequencies would decrease with increasing vibration magnitude. Evidence of greater nonlinearity in transmissibility to the abdomen would suggest that soft tissues primarily cause the nonlinearity. The vibration transmission path in the semi-supine posture involved less soft tissues on the back than the flat supine posture. For this reason, it was hypothesized that the semi-supine posture would be less nonlinear than the flat supine posture. Constraining the body of a seated subject does not appear to affect the nonlinearity, so the constrained semi-supine posture was expected to have similar nonlinearity to the relaxed semi-supine posture.

8.2 Method

8.2.1 Apparatus

Subjects lay face up supported by a back support, leg rest, and headrest on the same apparatus described in Chapter 5 (see Figure 8.1). The back support was a horizontal flat rigid aluminium plate (660 mm by 660 mm by 10 mm) covered with a high stiffness 3-mm thick laterally treaded rubber layer. The back support was bolted to the upper surface of a force platform (Kistler 9281 B21 12-channel force platform) that monitored the vertical (*x*-axis of the supine subject) and longitudinal horizontal

(*z*-axis of the supine subject) forces. The four vertical (*x*-axis) force signals, and the four longitudinal (*z*-axis) force signals, from the four corners of the platform were summed and conditioned using two Kistler 5001 charge amplifiers. The force platform was bolted to the vibrator platform. The horizontal gap between the back support and the leg rest was 50 mm (Figure 8.1).

The headrest was a horizontal flat rigid wooden block with 75-mm thick uncompressed car-seat foam attached to the upper surface. The top surface of the uncompressed foam was approximately 50-mm higher than the back support. The horizontal distance between the back support and headrest was adjusted by moving the headrest so that a subject's head could rest comfortably.

Vertical vibration was produced by a 1-metre stroke electro-hydraulic vertical vibrator capable of accelerations up to ±10 ms^{-2} in the laboratory of the Human Factors Research Unit at the Institute of Sound and Vibration Research. Vertical (*x*-axis of the supine subjects) acceleration and longitudinal (*z*-axis) acceleration of the vibrator platform were measured using two identical Setra 141A ±2 g accelerometers (Figure 8.2) on the vibrator platform.

Vertical (*x*-axis) acceleration at the middle of the sternum (4 cm above, i.e., superior to, the lower end of the sternum), at the upper abdomen (4 cm above the navel), and at the lower abdomen (4 cm below the navel) were measured using two Endevco 2265-10M2 ±10 g accelerometers and one Endevco 2265-20 ±20 g accelerometer, respectively (Figure 8.2). The three accelerometers had the same size and weight. The base of each accelerometer was attached to rigid plywood (27x17x2 mm) by double-sided adhesive tape, and the other side of the plywood was attached to a plastic buckle connected to two ends of an elastic belt (Figure 8.3 a). The weight of the block, including the accelerometer, the plywood, and the buckle, was approximately 8 g. The contact area of the block to the skin was 12.8 mm (longitudinal) by 7.2 mm (lateral). The block was then fastened by tightening the elastic belt with a stiffness of approximately 75 N/m for all subjects. The locations of the accelerometers on the body surface are shown in Figure 8.3 b.

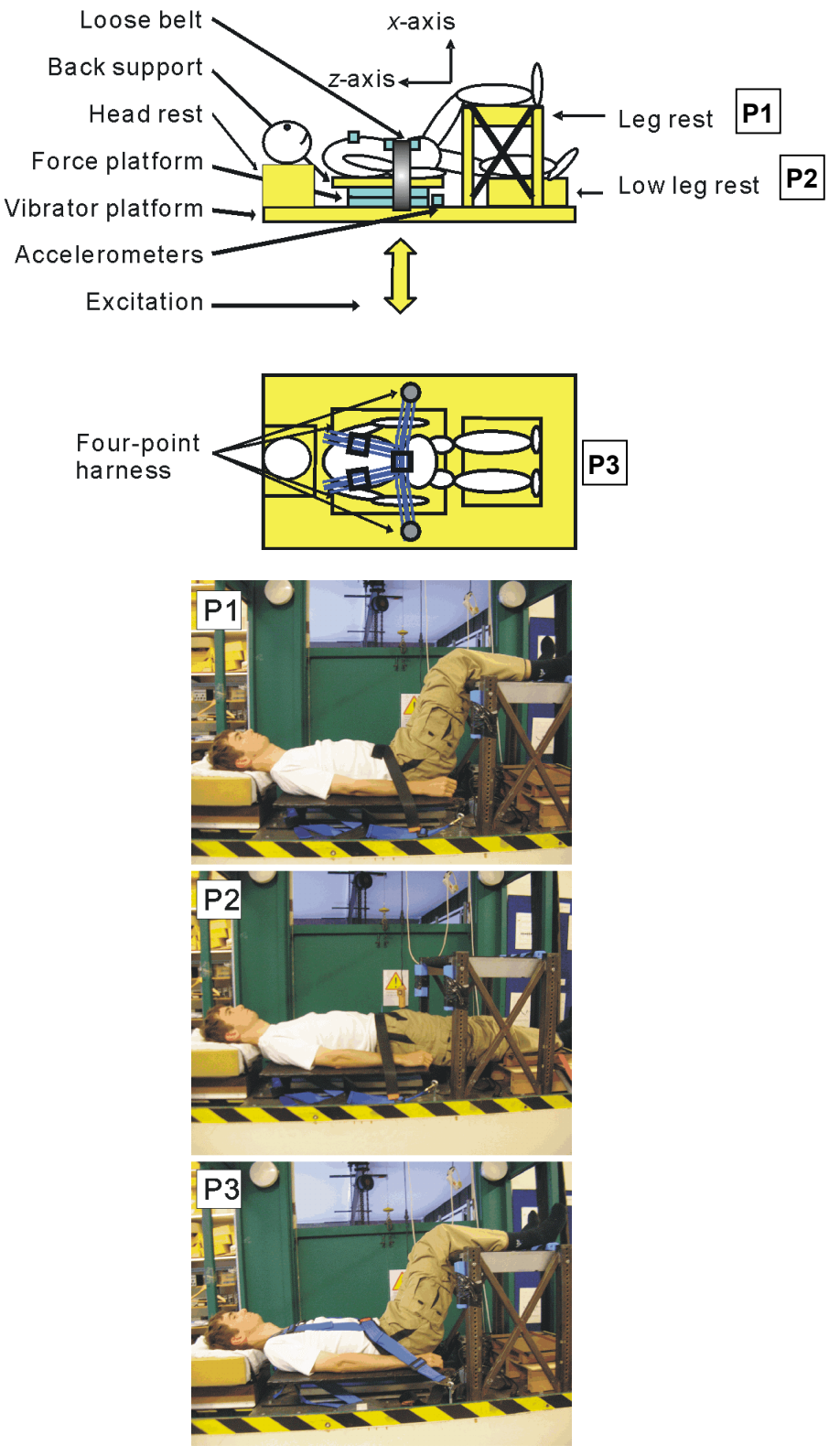

Figure 8.1 Schematic (upper) and photographic (lower) representations of the supine support showing the supine postures (P1: semi-supine posture; P2: flat supine posture; P3: constrained semi-supine posture) and the axes of force (*x*-axis and *z*-axis) and acceleration (*x*-axis) transducers.

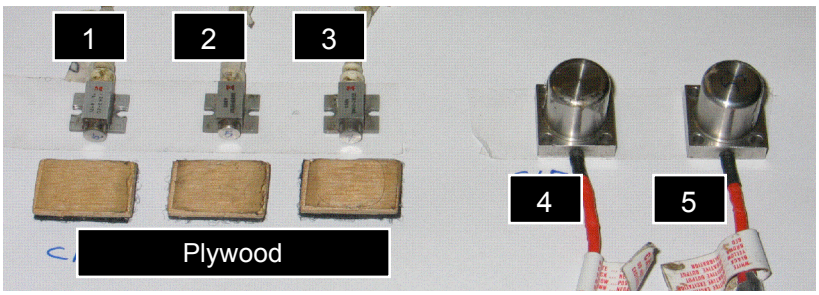

Figure 8.2 Accelerometers used to measure accelerations at: 1: lower abdomen (Endevco 2265-20 ±20 g); 2: upper abdomen (Endevco 2265-10M2 ±10 g); 3: sternum (Endevco 2265-10M2 ±10 g); 4: vibrator platform in the longitudinal (*z*-axis) direction (Setra 141A ±2 g); 5: vibrator platform in the vertical (*x*-axis) direction (Setra 141A ±2 g). Three pieces of identical 27 x 17 x 2 mm rigid plywood are shown below the three accelerometers (1, 2 and 3) used to measure the transmissibilities.

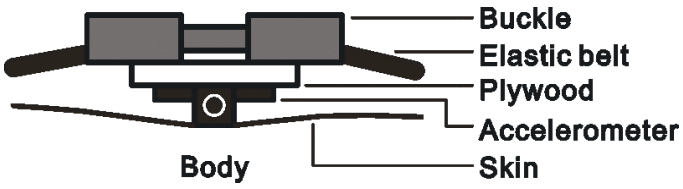

(a)

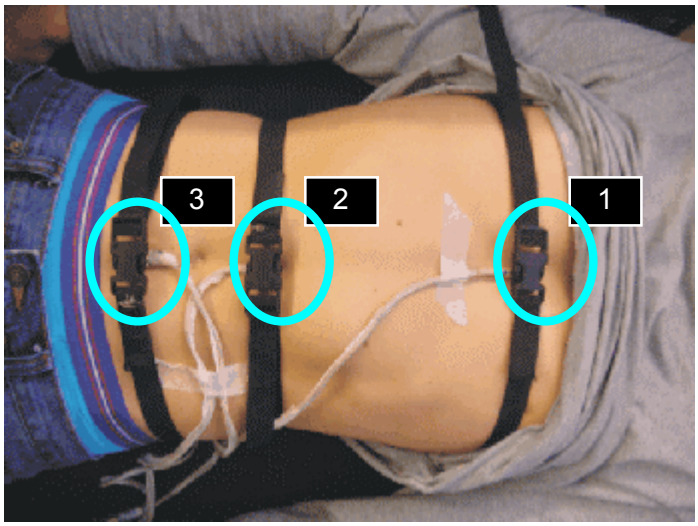

(b)

Figure 8.3 Each accelerometer was in an upside-down position and in contact with the skin (a). The three accelerometers (b) were attached to each buckle via a 27 x 17 x 2 mm rigid plywood along the longitudinal axis of the body at the sternum (1), upper abdomen (2) and lower abdomen (3).

The local tissue-accelerometer motion caused by the mounting of an accelerometer can be corrected with an impulse response function obtained from its free vibration (Kitazaki and Griffin, 1995). Previous studies have measured transmissibilities to spinal vertebrae (e.g. Kitazaki and Griffin, 1995; Matsumoto and Griffin, 1998b and 2002a), and to the abdomen above and below the navel (Mansfield and Griffin, 2000) in upright seated subjects during vertical excitation. Using the same correction method described by Kitazaki and Griffin (1995), Mansfield and Griffin (2000) reported that 'corrections for the measurements slightly changed the transmissibilities at frequencies greater than 10 Hz, although resonance frequencies were unaffected for any measurement location'. The present study was designed to compare the nonlinearity around resonances in the supine body where different transmission paths are likely. In the present study, pilot experimentation using the same method described by Kitazaki and Griffin (1995) determined that the natural frequency of the local system was around 25 to 32 Hz at the lower and upper abdomen. Since only much lower frequencies are of current interest (transmissibilities are presented at frequencies less than 20 Hz in this paper), no correction for the local tissue-accelerometer system was applied.

The accelerometers attached to the three locations on the body were adjusted to be perpendicular to the body surface before each vibration exposure. The static inclinations of the accelerometers were approximately 4 to 6 degrees at the sternum, and 0 to 8 degrees at the upper and lower abdomen. In addition to the static inclination, during vibration excitation the accelerometer at the sternum tilted by about 1 to 2 degrees; during vibration the accelerometers at the upper and lower abdomen tilted by about 2 to 4 degrees. Matsumoto and Griffin (1998b) measured the inclination of the surface of the upright seated body at T1 (between 20 and 35 degrees) and linearly compensated for the inclination by adding the sine of vertical transmissibility to the fore-and-aft transmissibility and subtracting the cosine of fore-and-aft transmissibility from the vertical transmissibility. The inclination of the accelerometers to the axis of excitation in the present experiment was less than 10 degrees and the cross-axis longitudinal motion of the supine subjects was less than for seated subjects. The inclination of the accelerometer was therefore not compensated.

The vibration stimuli were generated, and the four vertical accelerations and the vertical and horizontal forces were acquired, using an *HVLab* data acquisition and analysis system (version 3.81). The acceleration and force were acquired at 200 samples per second via 67 Hz analogue anti-aliasing filters.

8.2.2 Stimuli

The random vertical vibration had approximately flat constant-bandwidth acceleration power spectra over the frequency range 0.25 to 20 Hz. Seven unweighted accelerations, nominally at 0.0313, 0.0625, 0.125, 0.25, 0.5, 0.75, and 1.0 ms^{-2} r.m.s., were generated using seven different random seeds. Each test motion had duration of 90 seconds tapered at the start and end with 0.5-second cosine tapers. Twelve subjects were randomly divided into six groups with two persons per group. With different groups, different random seeds were used to generate the random stimuli. The presentation order of the twenty-one test motions (seven magnitudes with three supine postures) was randomised independently for each subject.

8.2.3 Posture

Subjects lay in three different supine postures (Figure 8.1). In the reference posture ('semi-supine'), the lower legs rested on a raised horizontal leg rest so as to give maximum contact between the back and the back support (the same posture as the 'relaxed semi-supine' posture described in Chapters 5, 6 and 7). A loose safety belt passed around the abdomen and arms but did not constrain the body.

In the 'flat supine posture', the legs rested on a horizontally flat rigid wooden support at the same height as the back support allowing the subject to lie horizontally flat.

In the 'constrained semi-supine' posture, subjects maintained the 'semi-supine' posture with the upper body tightly constrained to the back support by a four-point harness. The harness was loosened before each test. Subjects tightened the harness to a 'comfortably tight' setting with the help of the experimenter. The harness was adjusted first at the waist and then the shoulder.

In all three postures, the support for the body, head and legs was exposed to the same vertical vibration. The subjects were instructed to relax with their eyes closed. The instruction for subjects is provided in Appendix C.

8.2.4 Subjects

Twelve male subjects, aged 19 to 33 years, with mean (minimum and maximum) stature 1.79 m (1.72 to 1.89 m), total body mass 74.5 kg (58.9 to 96.7 kg), and waist circumference 0.82 m (0.73 m to 0.96 m) participated in the study. The subjects wore loose and light shirts and trousers with no waist belts.

The experiment was approved by the Human Experimentation, Safety and Ethics Committee of the Institute of Sound and Vibration Research at the University of Southampton.

8.2.5 Analysis

The vertical (*x*-axis) dynamic force and the vertical (*x*-axis) accelerations measured at the middle of the sternum, the upper abdomen, and the lower abdomen were expressed relative to the vertical (*x*-axis) acceleration of the vibrator platform. Four frequency response functions – apparent mass (where the force was in-line with the acceleration in the vertical direction), and three vertical transmissibilities (to the sternum, the upper abdomen, and the lower abdomen) – were calculated using the cross-spectral density method:

$$H(f) = S_{af}(f) / S_{aa}(f) \quad (1)$$

where, $H(f)$ is the apparent mass, in kg (or the transmissibilities to the sternum, the upper abdomen, or the lower abdomen); $S_{af}(f)$ is the cross spectral density between the dynamic forces at the back support (or the accelerations at the sternum, and upper and lower abdomen) and the vertical excitation acceleration; $S_{aa}(f)$ is the power spectral density of the vertical excitation acceleration at the vibrator platform.

Before calculating the apparent mass, mass cancellation was carried out in the time domain to subtract the force caused by the masses above the force sensing elements (a total of 30.5 kg obtained dynamically in the frequency range 0.25 to 20 Hz).

The relation of the output motion to the input motion in the calculated frequency response functions was investigated using the coherency:

$$\gamma_{io}^2(f) = | S_{af}(f) |^2 / (S_{aa}(f) S_{ff}(f)) \quad (2)$$

where $S_{ff}(f)$ is the power spectral density of the vertical force and $\gamma_{io}^2(f)$ is the coherency of the system with a value between 0 and 1. The coherency has a maximum value of 1.0 in a linear single-input system with no noise – the output motion being entirely caused by, and linearly correlated with, the input motion.

The cross spectral densities and the power spectral densities were estimated via Welch's method at frequencies between 0.25 and 20 Hz. The frequency response functions for each 90-second signal were calculated with a frequency resolution of 0.781 Hz (Table 8.1). The coarse 0.781-Hz resolution was used to give a high confidence level (increased degrees of freedom) at each frequency, needed especially for the low magnitudes of vibration (0.0313, 0.0625, and 0.125 ms^{-2} r.m.s.).

The apparent masses at the seven magnitudes were normalised by dividing by the apparent mass modulus measured at frequencies between 0.25 and 2.5 Hz, where the body was considered virtually rigid. For excitation at 0.0313, 0.0625, 0.125, 0.25,

and 0.5 ms^{-2} r.m.s., the normalisation was carried out at 2.34 Hz; for excitation at 0.75 and 1.0 ms^{-2} r.m.s. the normalisation was carried out at 1.56 Hz. The median normalised apparent masses at the seven magnitudes were then calculated.

Differences in apparent mass and transmissibility (both modulus and phase) at different vibration magnitudes and postures were tested using the Friedman two-way analysis of variance and then, if there was a significant overall effect, the Wilcoxon matched-pairs signed ranks tests. These tests were carried out at eight discrete frequencies (3.91, 5.47, 7.03, 8.59, 10.16, 11.72, 13.28 and 14.84 Hz).

Table 8.1 Signal processing procedure used to calculate the apparent mass and the transmissibilities to the sternum, the upper abdomen and the lower abdomen.

	Duration (s)	Samples per second	FFT length	Degrees of freedom	Windowing overlap	Frequency resolution (Hz)
0.781-Hz procedure	90	200	256	284	Hamming 100%	0.781

8.3 Results

8.3.1 Apparent mass

Figure 8.4 shows inter-subject variability in apparent mass in the three postures at the seven magnitudes of vibration.

With the semi-supine posture, the coherency of the apparent mass of all subjects was greater than 0.90 at frequencies between 1 and 20 Hz at vibration magnitudes greater than 0.25 ms^{-2} r.m.s. With the flat supine posture, the coherency was greater than 0.95 at magnitudes greater than 0.0625 ms^{-2} r.m.s. With the constrained semi-supine posture, the coherency was greater than 0.90 at magnitudes greater than 0.5 ms^{-2} r.m.s. An example of the coherency in the three postures for Subject 1 is shown in Figure 8.5.

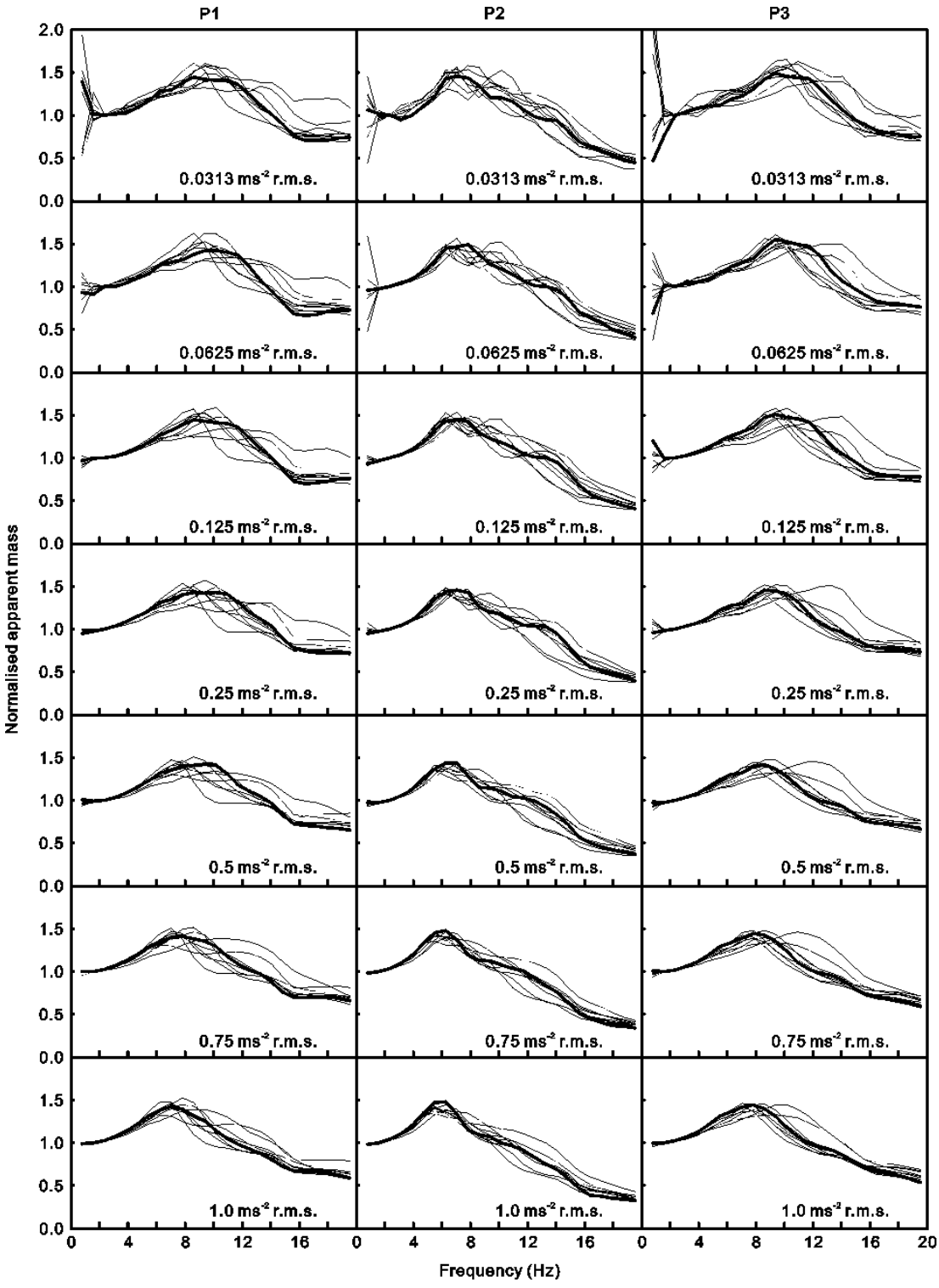

Figure 8.4 Individual normalised apparent mass modulus with three supine postures (P1 – semi-supine, P2 – flat supine, P3 – constrained semi-supine) at seven vibration magnitudes (0.0313, 0.0625, 0.125, 0.25, 0.5, 0.75, 1.0 ms^{-2} r.m.s.) of all twelve subjects. ▬▬ Subject 1; ——— Subjects 2 – 12

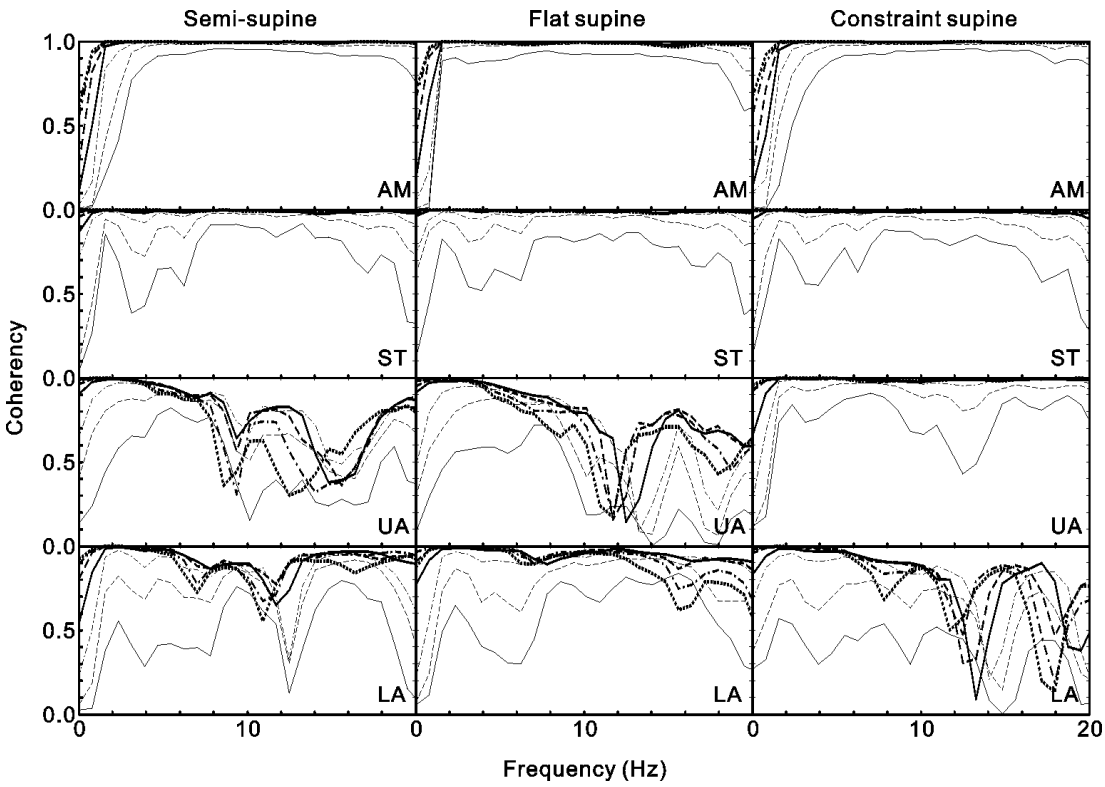

Figure 8.5 Individual (Subject 1, i.e. S1) coherency of the apparent mass (AM) and the transmissibilities to the sternum (ST), upper abdomen (UA) and lower abdomen (LA) with three supine postures (semi-supine; flat supine; constrained semi-supine) at seven vibration magnitudes (——— 0.0313 ms^{-2} r.m.s., — — — 0.0625 ms^{-2} r.m.s., — · — · — 0.125 ms^{-2} r.m.s., ——— 0.25 ms^{-2} r.m.s., ▬ ▬ ▬ 0.5 ms^{-2} r.m.s., ▬ · ▬ · ▬ 0.75 ms^{-2} r.m.s., - - - - - 1.0 ms^{-2} r.m.s.).

8.3.1.1 Effect of vibration magnitude

In all postures, subjects exhibited the typical nonlinearity at vibration magnitudes greater than 0.125 ms^{-2} r.m.s. An example is shown in Figure 8.6.

The effect of vibration magnitude on the modulus and phase of the apparent mass was investigated at the eight selected frequencies. First the Friedman two-way analysis of variance was performed at each frequency over the seven vibration magnitudes. Where this yielded a significant effect of vibration magnitude (i.e. $p < 0.05$), the Wilcoxon matched-pairs signed ranks test was performed between all magnitudes. This statistical procedure was applied to the modulus and phase of the apparent mass. Examples of the procedure for the effect of vibration magnitude on the apparent mass modulus with the semi-supine posture are shown in Table 8.2. The same procedure was used to compare the phases of apparent mass between vibration magnitudes at the same frequencies within each posture. The number of significant differences between pairs (suggesting the degree of nonlinearity) for all postures and transfer functions is summarised in Table 8.4.

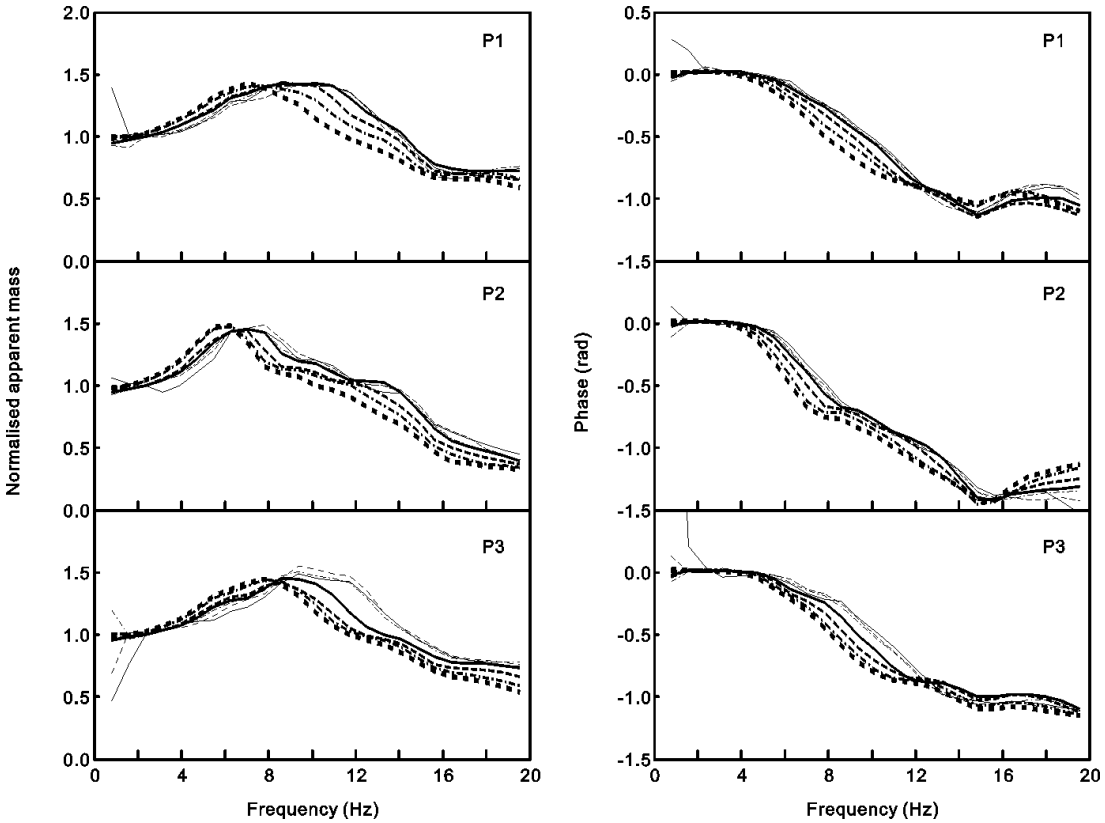

Figure 8.6 Effect of vibration magnitude: normalised apparent mass modulus and phases of one subject (S1) with three supine postures (P1 – semi-supine, P2 – flat supine, P3 – constrained semi-supine) at seven vibration magnitudes (——— 0.0313 ms^{-2} r.m.s., — — — 0.0625 ms^{-2} r.m.s., — · — · — 0.125 ms^{-2} r.m.s., ——— 0.25 ms^{-2} r.m.s., — — — 0.5 ms^{-2} r.m.s., — · — · — 0.75 ms^{-2} r.m.s., - - - - 1.0 ms^{-2} r.m.s.).

With the semi-supine posture, at frequencies lower than 8.59 Hz the apparent mass modulus was significantly greater with higher magnitudes of vibration ($p < 0.05$, Wilcoxon), except between 0.0625 and 0.125 ms^{-2} r.m.s. At frequencies greater than 10.16 Hz, the apparent mass modulus was significantly lower with greater magnitudes of vibration ($p < 0.05$, Wilcoxon), except between 0.0313, 0.0625 and 0.125 ms^{-2} r.m.s. A similar pattern was observed in the other two postures.

In all three postures, the changes in apparent mass were consistent with the resonance frequency decreasing with increasing vibration magnitude, although not consistently so at the lowest magnitudes. Changes in the phase of the apparent mass were consistent with changes in the modulus.

With the semi-supine posture, the median normalised apparent mass resonance frequency decreased from 9.38 to 7.03 Hz as the vibration magnitude increased from 0.0625 to 1.0 ms^{-2} r.m.s., but the resonance frequencies did not differ significantly at magnitudes less than 0.125 ms^{-2} r.m.s. (Figure 8.7 P1).

With the flat supine posture, the median normalised apparent mass resonance frequency decreased from 7.03 to 5.47 Hz as the vibration magnitude increased from 0.0625 to 1.0 ms^{-2} r.m.s., but the resonance frequencies did not differ significantly at magnitudes less than 0.25 ms^{-2} r.m.s. (Figure 8.7 P2).

With the constrained semi-supine posture, the median normalised apparent mass resonance frequency decreased from 10.16 to 7.81 Hz as the vibration magnitude increased from 0.0625 to 1.0 ms^{-2} r.m.s., but the resonance frequencies did not differ significantly at magnitudes less than 0.25 ms^{-2} r.m.s. (Figure 8.7 P3).

Table 8.2 Significance of differences in apparent mass modulus between adjacent vibration magnitudes (1 to 7 for 0.0313 to 1.0 ms^{-2} r.m.s.) at eight frequencies (f_1 to f_8) with posture 1 (semi-supine). At 0.125 ms^{-2} r.m.s. (i.e. magnitude 3), and at greater magnitudes, there are significant differences in apparent mass for 26 of the 32 pairs (see comparisons 3-4, 4-5, 5-6 and 6-7 at all frequencies). At 0.125 ms^{-2} r.m.s., and magnitudes lower than 0.125 ms^{-2} r.m.s., there are significant differences in apparent mass for only 5 of the 16 pairs (see comparisons 1-2 and 2-3).

Posture	f_1 3.91 Hz	f_2 5.47 Hz	f_3 7.03 Hz	f_4 8.59 Hz	f_5 10.16 Hz	f_6 11.72 Hz	f_7 13.28 Hz	f_8 14.84 Hz	Total significant differences
Semi-supine	1-2*	1-2*	1-2*	1-2*	1-2	1-2	1-2	1-2	31/48
	2-3	2-3	2-3	2-3*	2-3	2-3	2-3	2-3	
	3-4*	3-4*	3-4*	3-4*	3-4	3-4*	3-4*	3-4	
	4-5*	4-5*	4-5*	4-5	4-5	4-5*	4-5*	4-5*	
	5-6*	5-6*	5-6*	5-6	5-6*	5-6*	5-6*	5-6*	
	6-7*	6-7*	6-7*	6-7	6-7*	6-7*	6-7*	6-7*	

Vibration magnitudes: 1 – 0.0313 ms^{-2} r.m.s.; 2 – 0.0625 ms^{-2} r.m.s.; 3 – 0.125 ms^{-2} r.m.s.; 4 – 0.25 ms^{-2} r.m.s.; 5 – 0.5 ms^{-2} r.m.s.; 6 – 0.75 ms^{-2} r.m.s.; 7 – 1.0 ms^{-2} r.m.s.

* – significant difference $p<0.05$, Wilcoxon.

Underline – the apparent mass modulus at the lower magnitude was significantly greater than the apparent mass modulus at the higher magnitude ($p<0.05$, Wilcoxon).

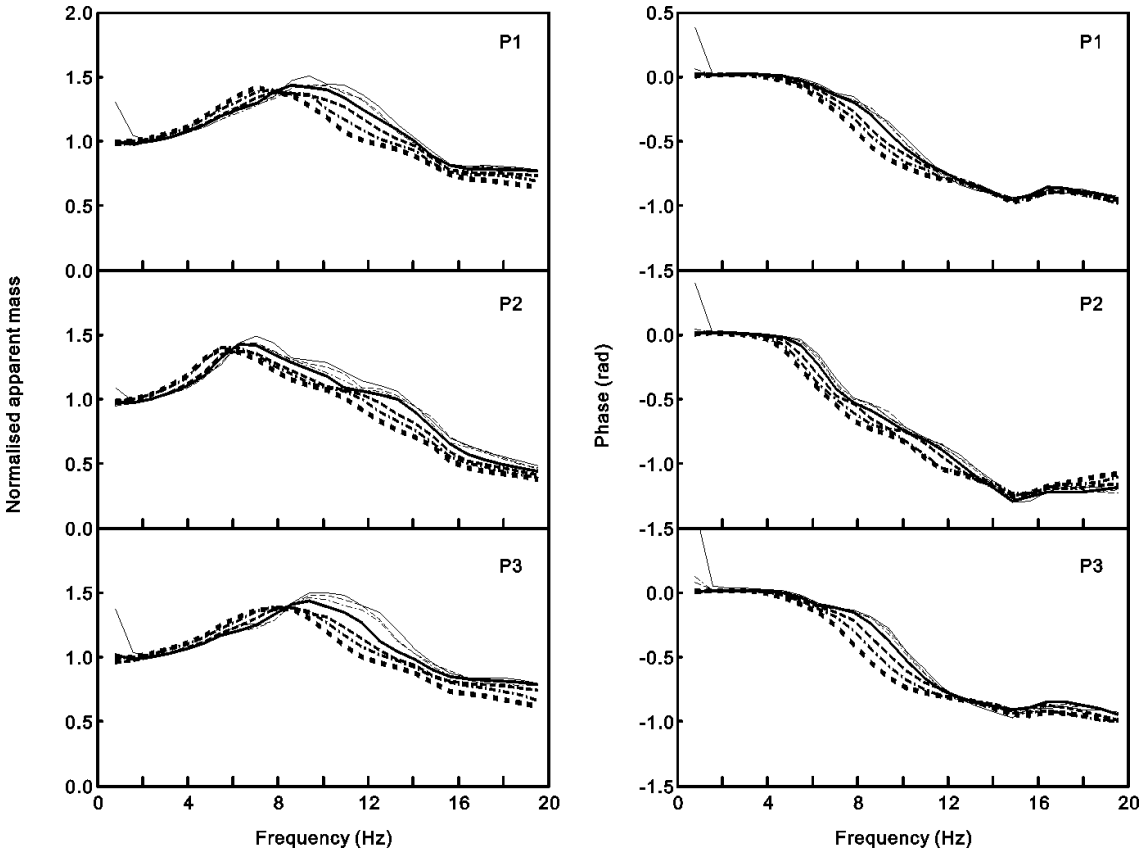

Figure 8.7 Effect of vibration magnitude: median normalised apparent mass modulus and phases of the group of twelve subjects with three supine postures (P1 – semi-supine, P2 – flat supine, P3 – constrained semi-supine) at seven vibration magnitudes (——— 0.0313 ms^{-2} r.m.s., — — — 0.0625 ms^{-2} r.m.s., — · — · — 0.125 ms^{-2} r.m.s., ——— 0.25 ms^{-2} r.m.s., — — — 0.5 ms^{-2} r.m.s., — · — · — 0.75 ms^{-2} r.m.s., - - - - - 1.0 ms^{-2} r.m.s.).

8.3.1.2 Effect of posture

The effect of posture on the modulus and phase of the apparent mass was investigated at the eight selected frequencies and the seven vibration magnitudes using the statistical procedure summarised at the beginning of Section 8.3.1.1. An example is shown in Tables 8.3. At frequencies from 5.47 to 7.03 Hz, the modulus of the apparent mass in the flat supine posture was greater than that in either the semi-supine or the constrained semi-supine posture (p < 0.05, Wilcoxon). Over the frequency range 10.16 to 14.84 Hz, the apparent mass in the flat supine posture was lower than that in either the semi-supine or the constrained semi-supine posture (p < 0.05, Wilcoxon). The apparent masses of the semi-supine and the constrained semi-supine postures were not significantly different over the frequency range 5.47 to 10.16 Hz, where the resonance occurred (p > 0.05, Wilcoxon).

The changes in apparent mass were consistent with the resonance frequency being lower with the flat supine posture than either the semi-supine or the constrained semi-supine posture. These changes also showed that changing from semi-supine

to constrained semi-supine posture caused less change in the apparent mass than changing from semi-supine to flat supine (Table 8.5). Changes in the phase of the apparent mass were consistent with changes in the modulus.

Table 8.3 Significant differences in apparent mass modulus between postures at eight frequencies and seven vibration magnitudes.

Magnitude Number	f_1 3.91 Hz	f_2 5.47 Hz	f_3 7.03 Hz	f_4 8.59 Hz	f_5 10.16 Hz	f_6 11.72 Hz	f_7 13.28 Hz	f_8 14.84 Hz	Total significant differences
1	R-F	R-F	R-F	R-F	R-F	R-F*	R-F*	R-F*	
2	R-F	R-F	R-F	R-F	R-F*	R-F*	R-F*	R-F*	
3	R-F	R-F	R-F	R-F	R-F*	R-F*	R-F*	R-F*	
4	R-F	R-F	R-F	R-F	R-F*	R-F*	R-F*	R-F*	48/56
5	R-F	R-F	R-F	R-F	R-F*	R-F*	R-F*	R-F*	
6	R-F	R-F	R-F	R-F*	R-F*	R-F*	R-F*	R-F*	
7	R-F	R-F	R-F	R-F*	R-F*	R-F	R-F*	R-F*	
1	R-C	R-C	R-C	R-C	R-C	R-C	R-C	R-C	
2	R-C	R-C	R-C	R-C	R-C	R-C	R-C	R-C	
3	R-C	R-C	R-C	R-C	R-C	R-C	R-C	R-C	
4	R-C	R-C	R-C	R-C	R-C	R-C	R-C	R-C	21/56
5	R-C	R-C	R-C	R-C	R-C	R-C	R-C	R-C	
6	R-C	R-C	R-C	R-C	R-C	R-C	R-C	R-C	
7	R-C	R-C	R-C	R-C	R-C	R-C	R-C	R-C	
1	F-C	F-C*	F-C*	F-C*	F-C	F-C	F-C	F-C	
2	F-C	F-C*	F-C*	F-C	F-C	F-C	F-C	F-C	
3	F-C	F-C*	F-C*	F-C	F-C	F-C	F-C	F-C	
4	F-C	F-C*	F-C*	F-C	F-C	F-C	F-C	F-C	45/56
5	F-C	F-C*	F-C*	F-C	F-C	F-C	F-C	F-C	
6	F-C*	F-C*	F-C*	F-C	F-C	F-C	F-C	F-C	
7	F-C*	F-C*	F-C	F-C	F-C	F-C	F-C	F-C	

Postures: R – Semi-supine (as a reference condition); F – Flat supine; C – Constrained semi-supine.

Vibration magnitudes: 1 – 0.0313 ms^{-2} r.m.s.; 2 – 0.0625 ms^{-2} r.m.s.; 3 – 0.125 ms^{-2} r.m.s.; 4 – 0.25 ms^{-2} r.m.s.; 5 – 0.5 ms^{-2} r.m.s.; 6 – 0.75 ms^{-2} r.m.s.; 7 – 1.0 ms^{-2} r.m.s.

*The apparent mass modulus appearing first was significantly greater than the apparent mass modulus appearing second (p<0.05, Wilcoxon).

Grey pairs – insignificant pairs. For example, F-C at a specific frequency 1-3 indicates the apparent mass at 0.0313 ms^{-2} r.m.s. is not significantly different to the apparent mass at 0.0625 ms^{-2} r.m.s. Normal black pairs – significant pairs.

Table 8.4 Number of significant differences in the modulus of the apparent mass (AM) and transmissibilities to the body (ST: sternum; UA: upper-abdomen; LA: lower abdomen) due to vibration magnitude in three supine postures – the total number of significant differences between pairs of adjacent magnitudes over eight frequencies (48 combinations, i.e. 6 adjacent magnitude pairs by 8 frequencies).

	Semi-supine (R)	Flat supine (F)	Constrained semi-supine (C)
AM	31/48	33/48	30/48
ST	13/48	17/48	22/48
UA	17/48	23/48	12/48
LA	15/48	26/48	17/48

Table 8.5 Number of significant differences in the modulus of the apparent mass (AM) and transmissibilities to the body (ST: sternum; UA: upper-abdomen; LA: lower abdomen) due to supine posture at seven vibration magnitudes – the total number of significant differences between the three postures at all seven vibration magnitudes over eight frequencies (56 combinations, i.e. 7 magnitudes by 8 frequencies).

	R-F	R-C	F-C
AM	48/56	21/56	45/56
ST	9/56	8/56	12/56
UA	20/56	31/56	30/56
LA	14/56	1/56	21/56

8.3.2 Transmissibility to the sternum

The inter-subject variability in transmissibility to the sternum tended to be similar at different vibration magnitudes (Figure 8.9).

In all postures, the coherency was in excess of 0.90 at frequencies greater than 1.0 Hz and at vibration magnitudes greater than 0.125 ms^{-2} r.m.s., with no obvious difference between the three supine postures. An example of the coherency for Subject 1 is shown in Figure 8.5 (ST). At the three lowest vibration magnitudes (i.e.

0.0313, 0.0625, 0.125 ms^{-2} r.m.s.), the coherency dropped in two regions: in the range 4 to 6 Hz, and around 18 Hz.

8.3.2.1 Effect of vibration magnitude

In all postures and in all individuals there was evidence of nonlinearity in transmissibility to the sternum, although it was less obvious than in the apparent mass. An example of the nonlinearity for Subject 1 is shown in Figure 8.10 (ST).

The effect of vibration magnitude was examined using the same statistical procedure employed for the apparent mass (see Section 8.3.1.1 and Table 8.2).

With the semi-supine posture, at frequencies less than 8.59 Hz, the modulus of the transmissibility was greater at greater magnitudes of vibration over the range 0.25 to 1.0 ms^{-2} r.m.s. ($p < 0.05$, Wilcoxon). At frequencies greater than 10.16 Hz, the modulus was greater with lower magnitudes of vibration over the range 0.25 to 1.0 ms^{-2} r.m.s. ($p < 0.05$, Wilcoxon). A similar pattern was observed for the other two postures.

In all three postures, the nonlinearity in transmissibility to the sternum was consistent with the primary peak frequency decreasing with increasing vibration magnitude Changes in the phase of the transmissibility were consistent with changes in the modulus.

With the semi-supine posture, the primary peak frequency in the median transmissibility to the sternum reduced from 10.94 to 9.38 Hz as the vibration magnitude increased from 0.0625 to 1.0 ms^{-2} r.m.s. (Figure 8.11 ST). Significant differences between resonance frequencies at adjacent vibration magnitudes were found in the range 0.25 to 1.0 ms^{-2} r.m.s. ($p < 0.05$, Wilcoxon).

With the flat supine posture, the primary peak frequency in the median transmissibility reduced from 10.16 to 7.03 Hz as the vibration magnitude increased from 0.0625 to 1.0 ms^{-2} r.m.s. (Figure 8.11 ST). Significant differences between resonance frequencies at adjacent vibration magnitudes were found in the range 0.25 to 1.0 ms^{-2} r.m.s. ($p < 0.05$, Wilcoxon).

With the constrained semi-supine posture, the primary peak frequency in the median transmissibility reduced from 10.94 to 8.59 Hz as the vibration magnitude increased from 0.0625 to 1.0 ms^{-2} r.m.s. (Figure 8.11 ST). Significant differences between resonance frequencies at adjacent vibration magnitudes were found in the range 0.25 to 1.0 ms^{-2} r.m.s. ($p < 0.05$, Wilcoxon).

The individual transmissibilities (Figure 8.10 ST) and median transmissibilities (Figure 8.11 ST) to the sternum showed nonlinearity in all three postures. Statistical

tests performed at the eight selected frequencies (see Table 8.4) suggested that the nonlinearity was more consistent in the flat supine posture (17 significant pairs) and the constrained semi-supine posture (22 significant pairs) than in the semi-supine posture (13 significant pairs).

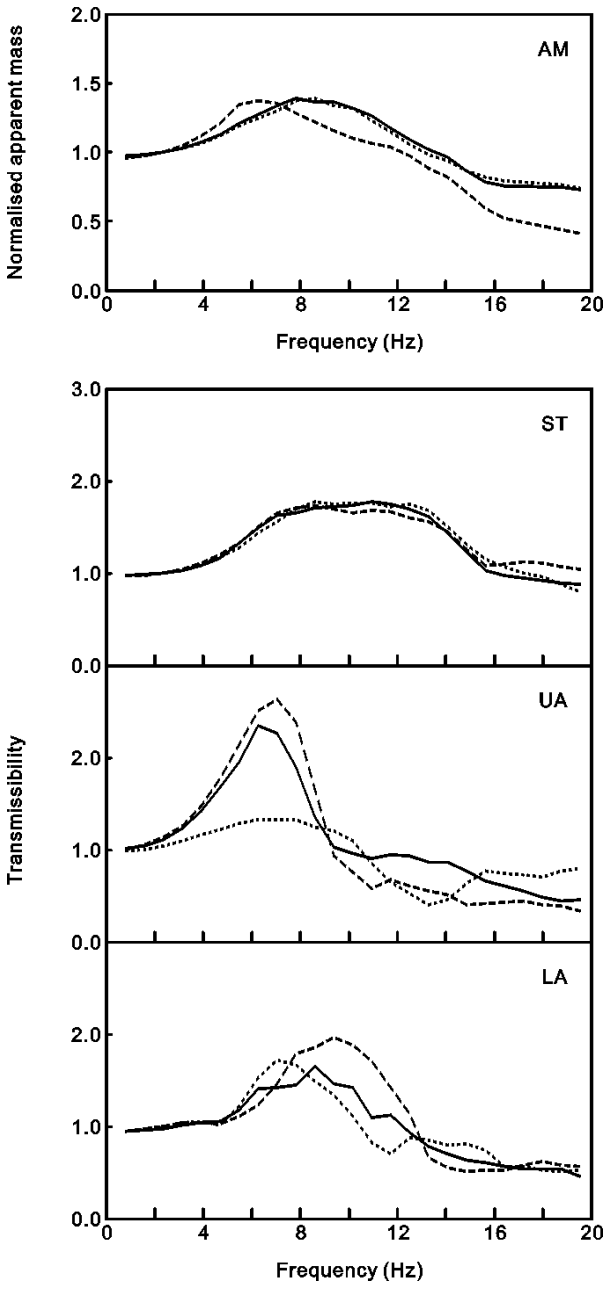

Figure 8.8 Effect of supine posture: median normalised apparent mass (AM) and transmissibilities to the sternum (ST), the upper abdomen (UA) and the lower abdomen (LA) with the three supine postures (——— semi-supine; – – – – flat supine; ..... constrained semi-supine) at the vibration magnitude of 0.5 ms^{-2} r.m.s.

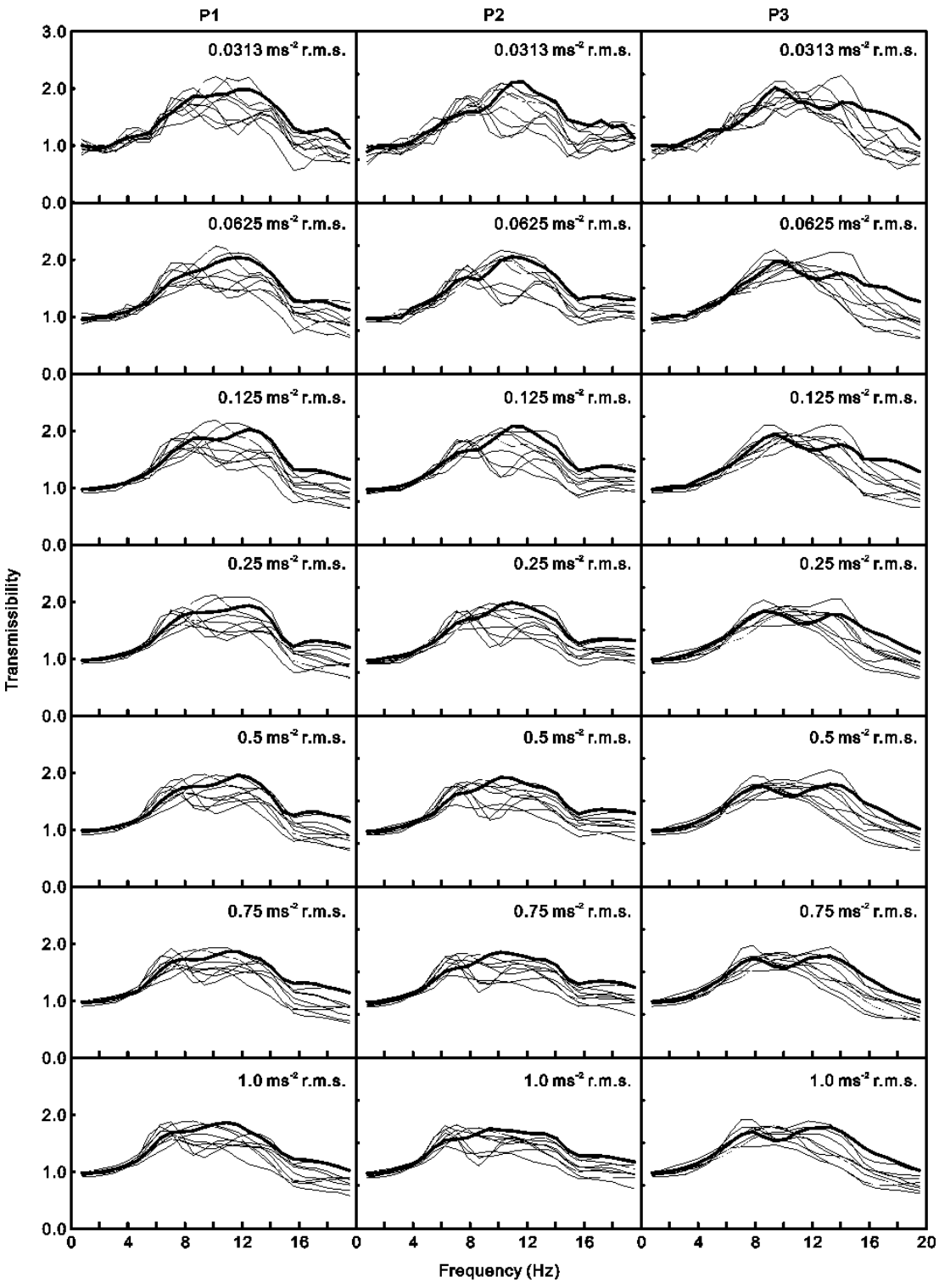

Figure 8.9 Individual sternum transmissibility modulus with three supine postures (P1 – semi-supine, P2 – flat supine, P3 – constrained semi-supine) at seven vibration magnitudes (0.0313, 0.0625, 0.125, 0.25, 0.5, 0.75, 1.0 ms^{-2} r.m.s.) of all twelve subjects. ▬▬ Subject 1; ——— Subject 2 – 12.

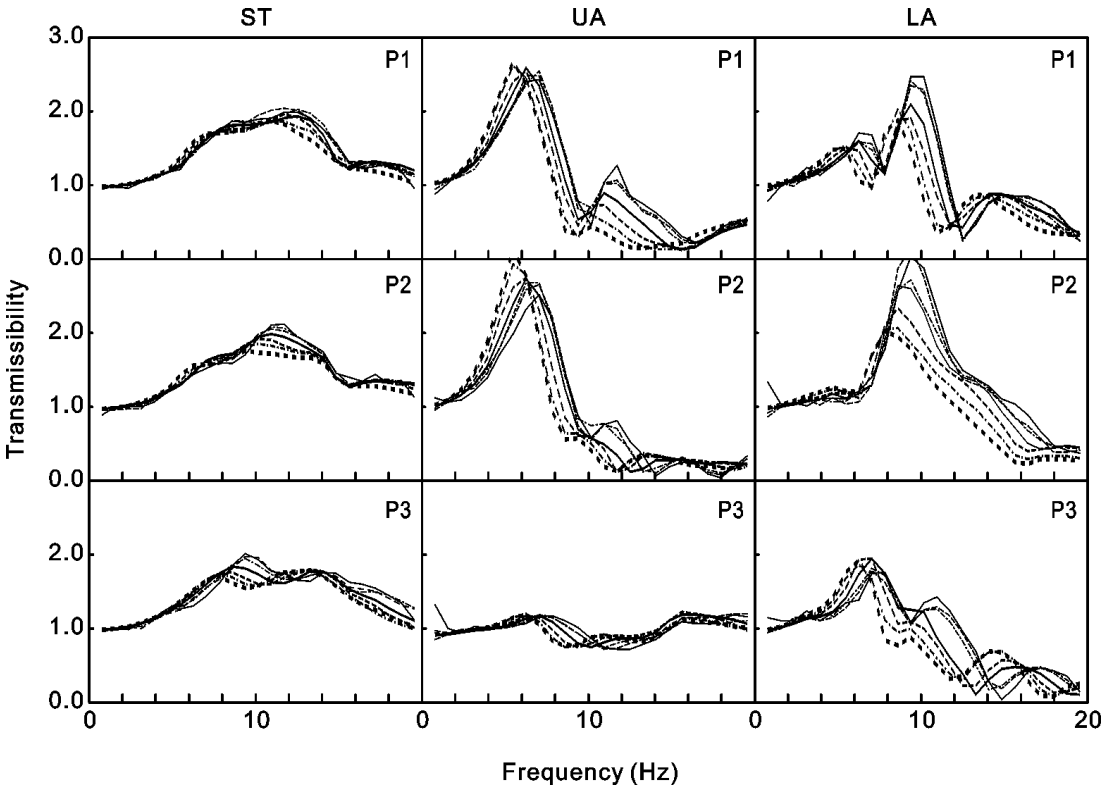

Figure 8.10 Effect of vibration magnitude: transmissibilities to the sternum (ST), the upper abdomen (UA) and the lower abdomen (LA) of one subject (S1) with three supine postures (P1 – semi-supine, P2 – flat supine, P3 – constrained semi-supine) at seven vibration magnitudes (——— 0.0313 ms^{-2} r.m.s., — — — 0.0625 ms^{-2} r.m.s., — · — · — 0.125 ms^{-2} r.m.s., ——— 0.25 ms^{-2} r.m.s., — — — 0.5 ms^{-2} r.m.s., — · — · — 0.75 ms^{-2} r.m.s., - - - - - 1.0 ms^{-2} r.m.s.).

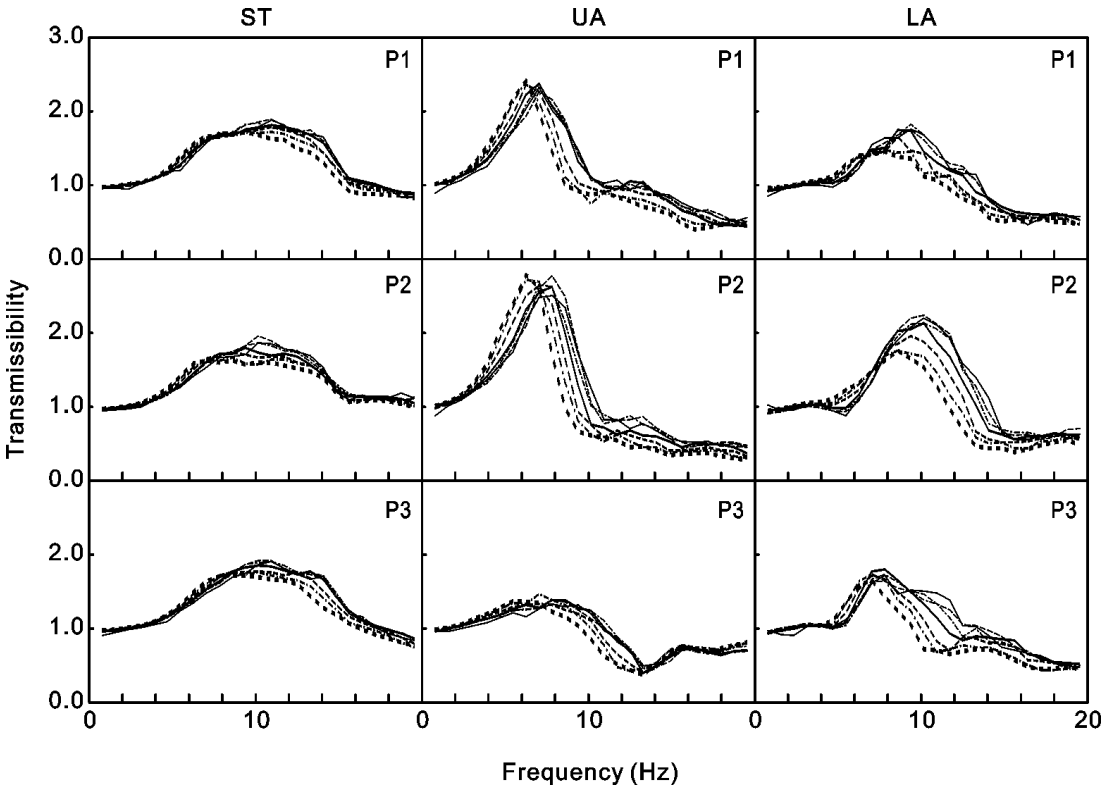

Figure 8.11 Effect of vibration magnitude: median transmissibilities to the sternum (ST), the upper abdomen (UA) and the lower abdomen (LA) of the group of twelve subjects with three supine postures (P1 – semi-supine, P2 – flat supine, P3 – constrained semi-supine) at seven vibration magnitudes (——— 0.0313 ms^{-2} r.m.s., — — — 0.0625 ms^{-2} r.m.s., — · — · — 0.125 ms^{-2} r.m.s., ——— 0.25 ms^{-2} r.m.s., — — — 0.5 ms^{-2} r.m.s., — · — · — 0.75 ms^{-2} r.m.s., - - - - - 1.0 ms^{-2} r.m.s.).

8.3.2.2 Effect of posture

In all three postures, the individual transmissibilities (Figure 8.9) and the median transmissibilities (Figure 8.8 ST) to the sternum were similar at frequencies less than 15 Hz. The effect of posture on the transmissibility was examined using the same procedure employed for the effect of posture on the apparent mass (as described in Section 8.3.1.2 and shown in Table 8.3). Over the frequency range 3.91 to 14.84 Hz, the posture had less effect on transmissibility to the sternum than on apparent mass (Table 8.5).

8.3.3 Transmissibility to the upper abdomen

Inter-subject variability in transmissibility was greater to the upper abdomen than to the sternum (compare Figure 8.12 with Figure 8.9).

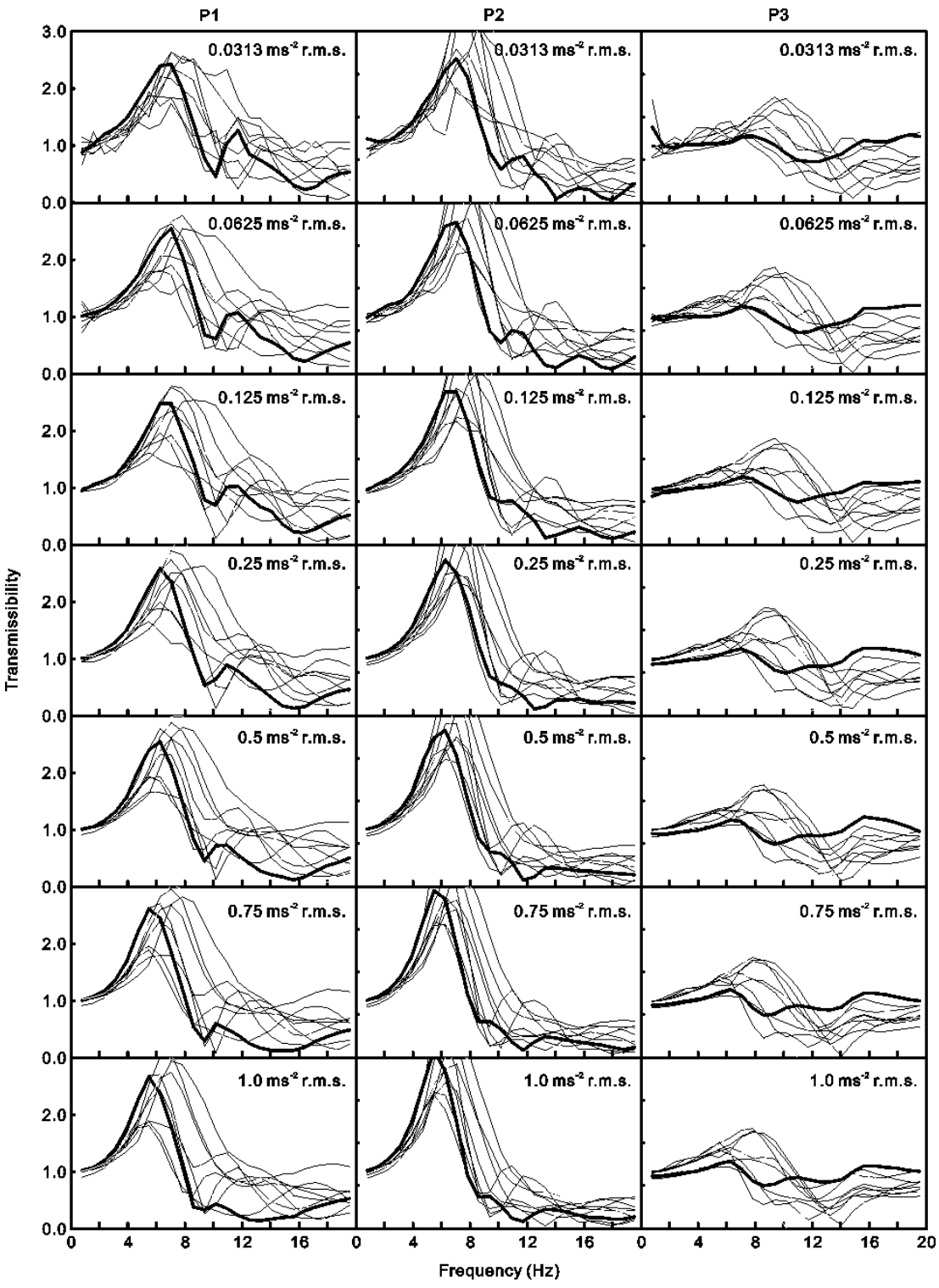

Figure 8.12 Individual upper abdomen transmissibility modulus with three supine postures (P1 – semi-supine, P2 – flat supine, P3 – constrained semi-supine) at seven vibration magnitudes (0.0313, 0.0625, 0.125, 0.25, 0.5, 0.75, 1.0 ms^{-2} r.m.s.) of all twelve subjects. ▬▬ Subject 1; ——— Subject 2 – 12.

An example of coherency is shown for Subject 1 in Figure 8.5 (UA). With the semi-supine posture, a coherency drop occurred over the frequency range 8 to 10 Hz and 12 to 16 Hz. The primary (and secondary) transmissibility peak frequency of this subject with the semi-supine posture was between 5.47 (10.16) and 7.03 (11.72) Hz as vibration magnitude decreased from 1.0 to 0.0313 ms^{-2} r.m.s. With the flat supine posture, the frequency range of the coherency drop was from 10 to 14 and 18 to 20 Hz. The primary (and secondary) transmissibility peak frequency of the same subject with the flat supine posture was between 5.47 (9.38) and 7.03 (11.72) Hz as vibration magnitude decreased from 1.0 to 0.0313 ms^{-2} r.m.s.

The frequency with the lowest coherency in the semi-supine posture and the constrained semi-supine posture tended to be lower with higher magnitudes of vibration (Figure 8.5 (UA)). Although the frequency of the coherency drop varied between subjects, the changes with respect to vibration magnitude were consistent for all subjects.

8.3.3.1 Effect of vibration magnitude

In all postures, individuals exhibited the typical nonlinearity at magnitudes greater than 0.125 ms^{-2} r.m.s. In the constrained semi-supine posture, the resonance peak was eliminated as a result of the constraining harness. In the semi-supine posture and the flat supine posture, individuals showed a primary resonance peak at around 6 to 8 Hz. An example individual response is shown for S1 in Figure 8.10 (UA).

The effect of vibration magnitude was examined using the same statistical procedure described in Section 8.3.1.1 and shown in Table 8.2.

With the semi-supine posture, at frequencies lower than 7.03 Hz the transmissibility was greater with greater magnitudes of vibration over the range 0.25 to 1.0 ms^{-2} r.m.s. ($p < 0.05$, Wilcoxon). At 8.59 Hz and frequencies greater than 8.59 Hz and vibration magnitudes over the range 0.25 to 0.75 ms^{-2} r.m.s., the transmissibility was lower with greater magnitudes of vibration ($p < 0.05$, Wilcoxon). The nonlinearity was more consistent in transmissibility to the upper abdomen than in transmissibility to the sternum, but less consistent than in the apparent mass (Table 8.4). A similar pattern was also observed in the flat supine posture. However, with the constrained semi-supine posture, the transmissibility to the upper abdomen exhibited a less consistent nonlinearity than the transmissibility to the sternum (Table 8.4).

In all postures, the changes in the transmissibility to the upper abdomen were consistent with the primary peak frequency decreasing with increasing vibration magnitude. Changes in the phase of the transmissibility were consistent with changes in the modulus.

With the semi-supine posture, the primary peak frequency of the median transmissibility to the upper abdomen decreased from 7.03 to 6.25 Hz as the vibration magnitude increased from 0.0625 to 1.0 ms^{-2} r.m.s., but the peak frequencies did not differ significantly at magnitudes less than 0.25 ms^{-2} r.m.s. (Figure 8.11 UA).

With the flat supine posture, the primary peak frequency of the median transmissibility to the upper abdomen decreased from 7.81 to 6.25 Hz while the vibration magnitude increased from 0.0625 to 1.0 ms^{-2} r.m.s., but the peak frequencies did not differ significantly at magnitudes less than 0.125 ms^{-2} r.m.s. (Figure 8.11 UA).

With the constrained semi-supine posture, the primary peak frequency of the median transmissibility to the upper abdomen decreased from 7.81 to 5.47 Hz as the vibration magnitude increased from 0.0625 to 1.0 ms^{-2} r.m.s., but the peak frequencies did not differ significantly at magnitudes less than 0.25 ms^{-2} r.m.s. (Figure 8.11 UA).

The individual (Figure 8.10 UA) and median (Figure 8.11 UA) transmissibility to the upper abdomen exhibited the characteristic nonlinearity in all postures, although not consistently so at the lowest vibration magnitudes. The statistical tests performed at the eight selected frequencies showed that in flat supine posture, where nonlinearity was found in the range 0.125 to 1.0 ms^{-2} r.m.s., there was a more consistent nonlinearity than in the semi-supine posture, where the nonlinearity was found from 0.25 to 1.0 ms^{-2} r.m.s. (Table 8.4). The nonlinearity was less consistent in the constrained semi-supine posture than in the semi-supine posture (Table 8.4).

The statistics indicate that the nonlinearity was less consistent in the transmissibility to the upper abdomen than in the apparent mass, and less consistent in the transmissibility to the sternum than in the transmissibility to the upper abdomen (Table 8.4).

8.3.3.2 Effect of posture

The individual (Figure 8.12) and median (Figure 8.8 UA) transmissibility to the upper abdomen showed that the semi-supine posture and the flat supine posture had a similar primary peak frequency around 6 to 8 Hz, with the flat supine having a slightly higher primary peak and a less apparent secondary peak. The constrained semi-supine posture exhibited a highly damped resonance peak at a slightly higher frequency than the other two postures. The effect of posture was examined using the same posture statistical procedure used for the modulus and phase of the apparent mass, as demonstrated in Table 8.3. The statistics indicate that the effect

of posture on transmissibility to the upper abdomen was greater than the effect of posture on transmissibility to the sternum (Table 8.5). Changing from semi-supine to flat supine had less effect on the transmissibility to the upper abdomen than on the apparent mass, whereas changing from semi-supine to constrained semi-supine had a greater effect on transmissibility to the upper abdomen than on the apparent mass.

8.3.4 Transmissibility to the lower abdomen

Similar to transmissibility to the upper abdomen, transmissibility to the lower abdomen showed greater inter-subject variability than transmissibility to the sternum (Figure 8.13).

In all three postures, there were drops in coherency that depended on vibration magnitude similarly to the upper abdomen (Figure 8.5 LA). The coherency drop occurred from 4 to 8 Hz and 10 to 13 Hz in the semi-supine posture, from 14 to 20 Hz in the flat supine posture, and from 12 to 16 and 18 to 20 Hz in the constrained semi-supine posture.

8.3.4.1 Effect of vibration magnitude

In all postures, individuals exhibited the typical nonlinearity at vibration magnitudes greater than 0.125 ms^{-2} r.m.s. In the semi-supine and the flat supine postures, individuals showed a primary resonance peak at around 8 to 10 Hz. A typical individual response is shown for S1 in Figure 8.10 LA.

The effect of vibration magnitude was examined using the same statistical procedures described in Section 8.3.1.1 and shown in Table 8.2.

With the semi-supine posture, at frequencies lower than 7.03 Hz, the transmissibility modulus was greater with greater magnitudes of vibration, but only at magnitudes greater than 0.25 ms^{-2} r.m.s. ($p < 0.05$, Wilcoxon). At frequencies greater than 8.59 Hz and vibration magnitudes greater than 0.125 ms^{-2} r.m.s., the modulus was lower with greater magnitudes of vibration ($p < 0.05$, Wilcoxon). Similar to the upper abdomen transmissibility, the nonlinearity in the transmissibility to the lower abdomen was more consistent than that to the sternum, but less consistent than in the apparent mass (Table 8.4).

In all postures, the changes in the transmissibility to the lower abdomen were consistent with the primary peak frequency decreasing with increasing vibration magnitude. Changes in the phase of the transmissibility were consistent with changes in the modulus.

With the semi-supine posture, the primary peak frequency in the median transmissibility decreased from 9.38 to 7.81 Hz as the vibration magnitude increased from 0.0625 to 1.0 ms^{-2} r.m.s., but the peak frequencies did not differ significantly at magnitudes less than 0.25 ms^{-2} r.m.s. (Figure 8.11 LA).

With the flat supine posture, the primary peak frequency in the median transmissibility decreased from 10.16 to 8.59 Hz as the vibration magnitude increased from 0.0625 to 1.0 ms^{-2} r.m.s., but the peak frequencies did not differ significantly at magnitudes less than 0.125 ms^{-2} r.m.s. (Figure 8.11 LA).

With the constrained semi-supine posture, the primary peak frequency in the median transmissibility changed from 7.81 to 7.03 Hz as the vibration magnitude increased from 0.0625 to 1.0 ms^{-2} r.m.s., but the peak frequencies did not differ significantly at magnitudes less than 0.125 ms^{-2} r.m.s. (Figure 8.11 LA).

The statistical tests at the eight selected frequencies also showed that the nonlinearity in the flat supine posture and the constrained semi-supine posture (where the nonlinearity was found from 0.125 to 1.0 ms^{-2} r.m.s.) was more consistent than in the semi-supine posture (where the nonlinearity was found from 0.25 to 1.0 ms^{-2} r.m.s., Table 8.4).

8.3.4.2 Effect of posture

The individual (Figure 8.13) and median (Figure 8.8 LA) transmissibility to the lower abdomen showed that the semi-supine and the flat supine postures had a similar primary peak frequency around 8 to 10 Hz; the flat supine posture had a slightly higher primary peak and a less apparent secondary peak. The constrained semi-supine posture exhibited a lower resonance peak at a slightly lower frequency (around 6 to 8 Hz) than the other two postures. The effect of posture on the modulus and phase of the transmissibility was investigated using the same statistical procedure described in Table 8.3. Comparing with the semi-supine and the constrained supine posture, the flat supine posture had a greater effect on the transmissibility to the upper abdomen than to the lower abdomen (Table 8.5). Similar to the transmissibility to the upper abdomen, the nonlinearity in transmissibility to the lower abdomen was less consistent than in the apparent mass, but more consistent than that in the transmissibility to the sternum (Table 8.4). Unlike its effect on transmissibility to the upper abdomen, the constrained semi-supine posture had little effect on transmissibility to the lower abdomen.

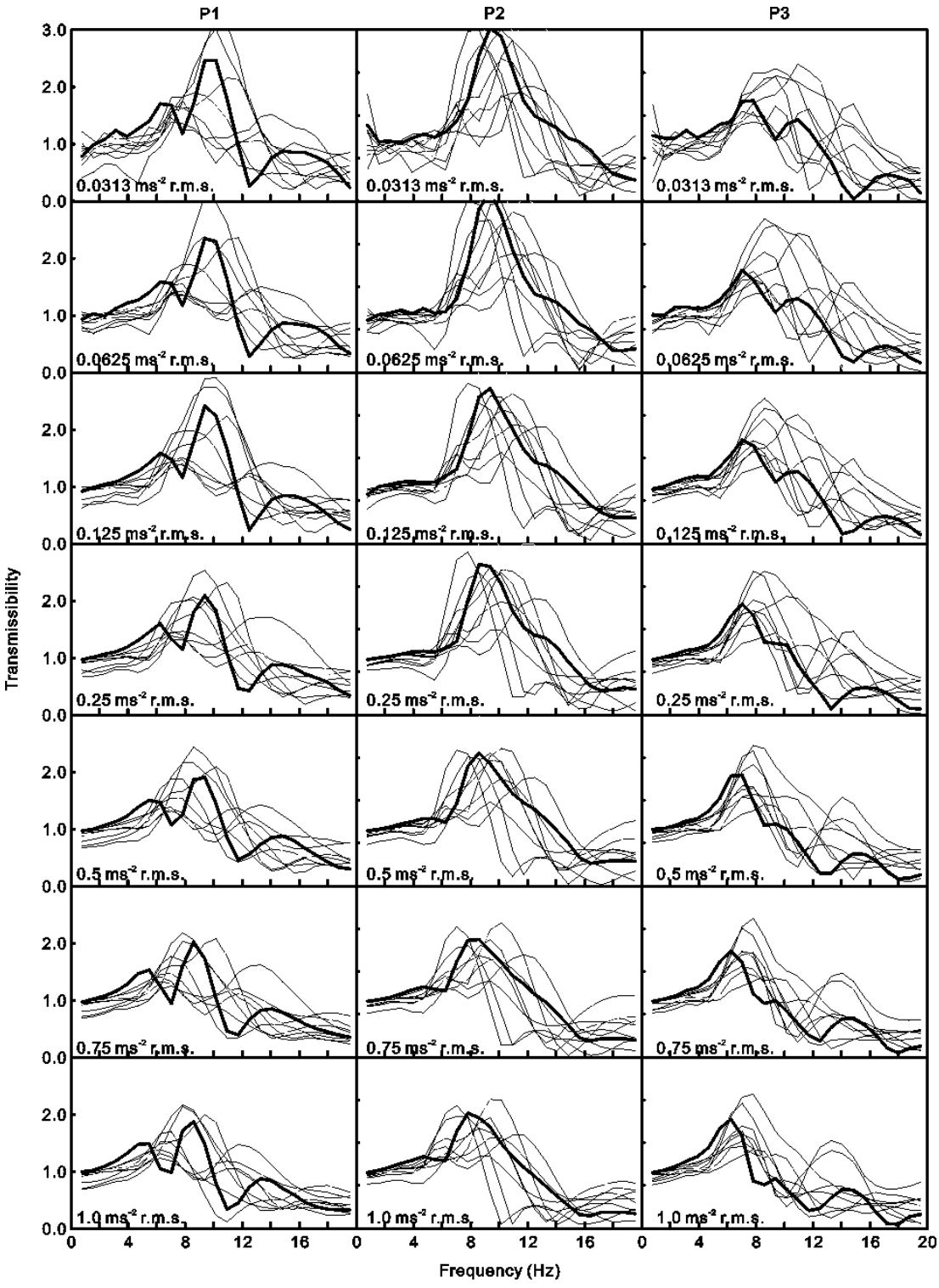

Figure 8.13 Individual lower abdomen transmissibility modulus with three supine postures (P1 – semi-supine, P2 – flat supine, P3 – constrained semi-supine) at seven vibration magnitudes (0.0313, 0.0625, 0.125, 0.25, 0.5, 0.75, 1.0 ms^{-2} r.m.s.) of all twelve subjects. ——— Subject 1; ——— Subject 2 – 12.

8.4 Discussion

8.4.1 Coherency

The coherency associated with the transmissibilities to the upper and lower abdomen varied systematically with frequency, with a clear drop in coherency at a frequency that decreased with increasing vibration magnitude (Figure 8.5). Similar drops in coherency have been seen in the longitudinal (i.e. horizontal, foot-to-head) apparent masses of subjects in the same relaxed semi-supine posture over the frequency range 6 to 20 Hz (Chapter 6). The drop in coherency was attributed to low forces at the back at the frequencies of the coherency drop. Decreases in the coherencies of the transmissibilities to the abdomen in the present study are consistent with either noise or the nonlinearity of soft tissues reducing coherency at frequencies where there is low transmissibility to the abdomen, as seen in the coherencies in Figure 8.5 UA and LA and the transmissibilities in Figure 8.10 UA and LA.

8.4.2 Effect of posture

8.4.2.1 Effect of changes in posture on apparent mass

Changing from the semi-supine posture to the flat supine posture decreased the primary resonance frequency of the apparent mass (Figure 8.8). Although nonlinearity was found in both postures (Figure 8.7), the 'semi-supine' posture with raised lower legs and less soft tissue contact between the body and the vibrating support exhibited slightly less nonlinearity than the 'flat supine' posture (Table 8.4). This is consistent with reduced nonlinearity in seated subjects with reduced thigh contact with a seat when varying footrest-height (Nawayseh and Griffin, 2003).

In the semi-supine subjects, any effect of the constraining harness on the apparent mass was small (Figure 8.8). In seated subjects, an 'elastic belt' to constrain the abdomen had no effect on the apparent mass resonance frequency with a vibration magnitude of 1.0 ms^{-2} r.m.s. and only small effects with 0.2 and 2.0 ms^{-2} r.m.s. (Mansfield and Griffin, 2002). Similar to the present study, the constraining belt did not change the nonlinearity in the apparent mass resonance frequency, possibly because in seated subjects the soft tissues between the body and the vibration source (i.e. buttocks) are unchanged by a belt, and in semi-supine subjects the soft tissues in the body (i.e. viscera and abdomen) were unchanged by the harness.

8.4.2.2 Effect of changes in posture on transmissibilities

Changes to the supine posture had less effect on transmissibility to the sternum than on transmissibility to the abdomen and the apparent mass (Figure 8.11 and

Table 8.5). It seems that changing leg posture and constraints altered the response of soft tissues or the response of joints between the thighs, pelvis, and lower spine, with little change in the transmission to the sternum.

In the semi-supine posture, the constraint provided by the harness increased the nonlinearity in the transmissibility of vibration to the sternum (13 significant differences in 48 comparisons for the unconstrained posture, compared to 22 significant differences in 48 comparisons for the constrained semi-supine posture, Table 8.4 and Figure 8.10). In contrast, the harness reduced the nonlinearity in the transmissibility to the upper abdomen (17 significant differences in 48 comparisons for the unconstrained posture compared with 12 significant differences in 48 comparisons for the constrained posture). In the constrained semi-supine posture, the greater nonlinearity to the sternum might be caused by the harness increasing the coupling of the sternum to soft tissues; the reduced nonlinearity to the abdomen might have been caused by the harness restraining the local movement of some soft tissues.

8.4.3 Effect of vibration magnitude

8.4.3.1 Effect of vibration magnitude on the nonlinearity

Nonlinearities in the apparent mass and transmissibilities were generally statistically significant at vibration magnitudes greater than 0.125 ms^{-2} r.m.s., but not consistently significant at the lower magnitudes (i.e., 0.0313, 0.0625, 0.125 ms^{-2} r.m.s., see Table 8.2, Figure 8.6 and Figure 8.10). Less nonlinearity at the low magnitudes (less than 0.125 ms^{-2} r.m.s. in the present study) may seem inconsistent with greater variation in the apparent mass resonance frequency at low magnitudes (i.e. 0.25 ms^{-2} r.m.s.) when seated subjects make voluntary upper-body movements (Chapter 4). If the nonlinearity is caused by either thixotropy or muscle activity, one or other of these mechanisms should be capable of explaining these findings.

For passive thixotropy to cause the nonlinearity, there must be lower limit to the range of magnitudes over which the structure of body tissues is 'broken down' or 'softened' by movement. In the relaxed semi-supine body it appears the limit is around 0.125 ms^{-2} r.m.s. for the bandwidth of vertical vibration studied here. In an upright sitting posture, more soft tissues (e.g., in the thighs and buttocks) may be involved than when the body is in a semi-supine posture. Furthermore, the seated body appears to amplify low frequency movements more than the supine body (compare Figure 8.7 with Figure 4.4 condition A in Chapter 4). The voluntary periodic bending of the upper-bodies of seated subjects may have increased the

movement within their body sufficiently for vibration at magnitudes less than 0.25 ms^{-2} r.m.s. to reduce the equivalent stiffness of body.

For either voluntary or involuntary muscle activity to cause the observed nonlinearity there must be sufficient variation in muscle activity to influence the effective stiffness of the body over the range of vibration magnitudes where the nonlinearity occurred. In a semi-supine posture, there is no requirement for either voluntary or involuntary muscle activity to maintain posture during vibration and it may be assumed that both are, at least, reduced relative to an upright sitting posture. For any involuntary phasic muscle activity induced by vibration, there will be vibration magnitude below which the muscles are not activated and, perhaps, a variation in the form and extent of the muscle activity as the vibration magnitude increases (Robertson and Griffin, 1989; Blüthner *et al*, 2002). Such changes in muscle activity may seem plausible explanations of the nonlinearity observed in an upright seated posture where a variety of muscles are activated and could influence body motion (e.g., the spinae erector, multifidus, and abdominal muscles). However, in the supine postures studied here, it seems unlikely that there was either sufficient muscle activity, or sufficient variations in muscle activity, to explain the nonlinearity observed.

8.4.3.2 Contribution of soft tissues to the nonlinearity

With seated and standing subjects, nonlinearity has been found in transmissibilities to the pelvis and locations along the spine (e.g. Matsumoto and Griffin, 1998b; Mansfield and Griffin, 2000; Matsumoto and Griffin, 2002a) as well as in the apparent mass. The primary resonance of seated subjects is associated with rocking of the upper-body on the buttocks with bending and rotational motions of the spine in the mid-sagittal plane (e.g. Kitazaki and Griffin, 1998; Matsumoto and Griffin, 1998b).

With supine subjects, there is also nonlinearity in transmissibility and apparent mass, but the nonlinearity in transmissibility to the sternum is less than the nonlinearity in transmissibility to the upper and lower abdomen and also less than the nonlinearity in the apparent mass. The resonance of supine subjects may involve broadly similar mechanisms to those in seated subjects: the entire skeletal structure and internal organs supported on superficial tissues of the back move in the direction of excitation. Transmission of vibration to the spine and pelvis of a seated subject, and to the abdomen of a supine subject, involves more soft tissue (e.g. the buttocks when seated and the viscera and abdomen when supine) than transmission to the sternum of a supine subject. The main transmission path to the sternum of a supine subject is via tissues beneath the recumbent spine, although there may be interaction with soft tissues within the rib cage and the abdomen. Less nonlinearity

at the sternum than at the abdomen would be consistent with soft tissues causing the nonlinearity.

8.4.3.3 Thixotropy hypothesis

The nonlinear softening apparently associated with the soft tissues could be caused by thixotropy. Changes in the apparent mass of the relaxed supine body immediately after exposure to high magnitude and low magnitude vertical vibration are small but apparently characteristic of thixotropy (Chapter 5). The dynamic properties of the body may be assumed to be influenced by the movement of soft tissues that account for most of the body mass and not only by the movement of joints. The movement of joints can be affected by muscular activity, but the movement of soft tissues (including relaxed muscles) is unlikely to be affected by muscle activity in the relaxed supine postures investigated here. Soft tissues will have little influence on the primary transmission path to the sternum but the coupling of the sternum to the soft tissues of the body will allow their nonlinear response to have a small influence on transmission of vibration to the sternum. The varying degrees of nonlinearity found in the apparent mass of the supine body and transmissibilities to the sternum and abdomen seem consistent with the thixotropy of soft tissues being the primary cause of the nonlinear softening of the body apparent with increasing magnitudes of vibration.

8.4.3.4 Muscle activity hypothesis

The supine postures in the present study were designed to minimise the need for voluntary muscular activity. However, it may seem plausible for involuntary muscle activity to have influenced the transmission of vibration, with a greater influence on transmissibility to the abdomen than to the sternum. This might occur if there was phasic muscular activity having a different influence at low and high magnitudes of vibration – the timing of phasic muscular activity may vary with vibration magnitude such that the peak force occurs at different times during high and low magnitudes of vibration, as contemplated in Chapter 4. If muscle activity were a cause of the nonlinearity, it would be expected that the nonlinearity to the sternum would be less since the transmission path to sternum is less influenced by the response of soft tissues (including muscles) than the transmission path to the abdomen.

8.4.3.5 The evidence favours the thixotropy hypothesis

Although involuntary reflex activity of muscles may contribute to nonlinearity, the evidence with seated, standing, and supine subjects is more easily explained by passive thixotropy. The principal resonances in the apparent masses of seated, standing, and supine subjects seem to be associated with movement in the soft

tissues at the subject-excitation interface. A nonlinear response of the soft tissues at the interfaces would be sufficient to cause a nonlinearity that is most apparent at resonance. The nonlinearity has been found in both the vertical and fore-and-aft responses of subjects in various sitting postures during both vertical and fore-and-aft excitation (e.g. Matsumoto and Griffin, 2002b; Nawayseh and Griffin, 2003; Nawayseh and Griffin, 2005a), in the vertical and fore-and-aft responses of subjects standing in various postures during vertical excitation (e.g. Matsumoto and Griffin, 1998a; Subashi *et al*., 2006), and in the vertical and longitudinal responses of subject lying in relaxed semi-supine postures during vertical and longitudinal horizontal excitation (Chapters 5 and 6). In seated subjects, voluntary or involuntary muscular activity along the spine could affect the response of the body and cause a nonlinearity. With various standing conditions, such as with the knees straight and locked, bent, standing on one leg, with an anterior lean or a lordotic posture, the nonlinearity has been consistently found in the apparent mass and transmissibilities to the spinal column, pelvis, and knee (Matsumoto and Griffin, 1998a; Matsumoto and Griffin, 2000; Subashi *et al*, 2006). The results of these studies with standing subjects would be consistent with some nonlinearity in response at the soles of the feet. The soles of the feet are unlikely to have muscular activity sufficient to greatly alter responses to vertical vibration (Matsumoto and Griffin, 1998a). Similarly, in the present study, tissues at the backs of the supine subjects were unlikely to influence the dynamic forces and motions transmitted to the sternum by muscular activity.

A thixotropic characteristic has been reported in a wide range of human tissues, protoplasm, and mucus (e.g. Fung, 1981) and so it seems likely that thixotropy will be present and cause nonlinearity to some degree. The nature of thixotropy is such that it allows perturbations to break down structures but after a period of stillness the structures reform (Tanner, 1985). After Lakie (1986) reported a softening effect of the relaxed human finger with increasing vibratory excitations, thixotropy has been used to describe this dynamic property of human tissues. Thixotropy will cause a softening effect with increasing vibration magnitude and a lowering of resonance frequencies, as observed with a wide range of vibratory excitations of the body. For muscle activity to cause the nonlinearity there must be muscles capable of controlling a significant portion of body mass and body movement, the forces contributed by the muscles must change in an appropriate way with increasing vibration magnitude. For tonic muscle activity to cause the observed nonlinearity, the forces caused by tonic muscular contraction must decrease with increasing vibration magnitude, but this is not evident in those studies that have measured muscle activity during vibration (e.g., Robertson and Griffin, 1989; Blüthner *et al*,

2002). For phasic muscle activity to cause the observed nonlinearity, the contractions must change in magnitude or phase such that they always reduce the overall stiffness of the body with increasing vibration magnitude. Since different muscles would be involved in the different postures and directions of excitation, and phasic muscle activity will depend on the excitation, it seems unlikely that muscle activity would always reduce stiffness and not sometimes increase stiffness with increasing vibration magnitude. Since many more assumptions are required to explain the nonlinearity by muscle activity than by thixotropy, it seems more likely that the principal nonlinearity seen in many biodynamic measurements is primarily caused by thixotropy.

8.5 Conclusions

With a semi-supine posture, a flat supine posture, and constrained semi-supine posture, the apparent mass resonance frequency and the primary peak frequencies in transmissibilities to the upper and lower abdomen decrease with increasing magnitude of vibration from 0.25 to 1.0 ms^{-2} r.m.s. The nonlinearity is less evident at vibration magnitudes less than 0.125 ms^{-2} r.m.s.

The nonlinearity was more apparent in a flat supine posture than a semi-supine posture, suggesting that supporting soft tissues contributed to the nonlinearity.

Although involuntary reflex muscular activity may contribute to nonlinearity in the biodynamic responses of the body, the thixotropy of soft tissues is more likely to be the primary cause of nonlinearity.

Chapter 9

General discussion

Detailed discussion of the findings from each experimental study has been provided in Chapter 4 to Chapter 8. This section commences with a consideration of the methods used to quantify the biodynamic nonlinearity. Then the key findings from the previous and the present studies pertinent to the muscular activity hypothesis and the passive thixotropy hypothesis being the cause of the nonlinearity are compared and contrasted.

9.1 Quantification of the nonlinearity using lumped parameter models

The biodynamic nonlinearity with varying vibration magnitude is evident in a shift in the resonance frequency of frequency response functions of the body (e.g., apparent mass). The limitations of using resonance frequency to quantify the nonlinearity have been discussed in Section 3.5.2. The 0.098-Hz frequency resolution used in all experimental studies described in Chapter 4 to Chapter 8 requires a sampling rate of 200 samples per second and a FFT length of 2048 samples with 36 degrees-of-freedom governed by a sampling duration of 90 seconds. For example, doubling the frequency resolution to 0.049 Hz will require double the FFT length (i.e., 4096 samples) and therefore a sampling duration of 180 seconds for uncompromised confidence level of the spectral density functions (i.e. 36 degrees of freedom). A fine resolution may also introduce variations in transfer functions that are irrelevant to the effect of vibration magnitude, for example, inter-subject variability and intra-subject variability. Fitting simplified but appropriate lumped parameter models to frequency response functions provided an alternative tool for quantifying the resonance frequency.

The two-degree-of-freedom lumped parameter model described in Section 3.5.2 was used as a tool to determine the resonance frequency. With the frequency resolution of the measured apparent mass at 0.098 Hz, the maxima in the modulus of the apparent mass fluctuated considerably within a range of 1 to 2 Hz due to uncertainty (i.e. low confidence level) in the spectral density estimation. The lumped parameter model provided a more consistent resonance frequency by identifying the global modes and was less affected by local fluctuations in the apparent mass modulus. In addition, some model parameters (e.g. m_1, k_1 and c_1) may reflect the dynamic characteristics of the body over the full frequency range rather than only at a single frequency (i.e. the resonance frequency).

Sensitivity analysis is normally performed with biodynamic models to determine which mass-spring-damping system is responsible for the primary resonance of the apparent mass (e.g. Matsumoto, 2001; Nawayseh, 2003; Abdul Jalil, 2005). These tests are often based on medians of the measurements over a group of subjects. In the present studies, both individual and median fittings in Chapter 4, 5 and 6 show that the nonlinear constrained search method is effective in associating the primary resonance in the lower frequency range with m_1, k_1 and c_1, and the minor secondary resonance at the higher frequency range with m_2, k_2 and c_2. Increasing and decreasing by 50% each model parameter (i.e. m_0, m_1, m_2, k_1, k_2, c_1, and c_2) from the optimized values with median results confirmed that m_1, k_1 and c_1 corresponded to the primary resonance (see Figure 9.1).

Despite its advantages, the two-degree-of-freedom lumped parameter model could not represent transmissibilities to the sternum, or the upper and lower abdomen of semi-supine subjects. This limitation arises from the non-mechanistic nature of the model. The model does not represent any physical mechanism of body movement or any anatomical parts of the body. Lumped parameter mechanistic models incorporating a cross-axis response in the mid-sagittal plane with rotational degrees-of-freedom (e.g. Matsumoto and Griffin, 2001; Nawayseh, 2003), and more detailed finite element models of the spinal column (e.g. Kitazaki and Griffin, 1997), have been found to be adequate to represent the movement of different parts of the body (i.e. transmissibility), as well as the dynamic forces at the excitation-subject interface (i.e. apparent mass). However, the models so far developed cannot 'predict' the response of the body. These models rely on fitting the measured apparent mass or transmissibility at each magnitude, so the parameters of the model differ at different magnitudes of vibration. An understanding of the mechanisms describing the nature of the nonlinearity with varying vibration magnitude (e.g., thixotropy) would allow the model to 'predict' the response without optimising the model response to measurements at all magnitudes of vibration.

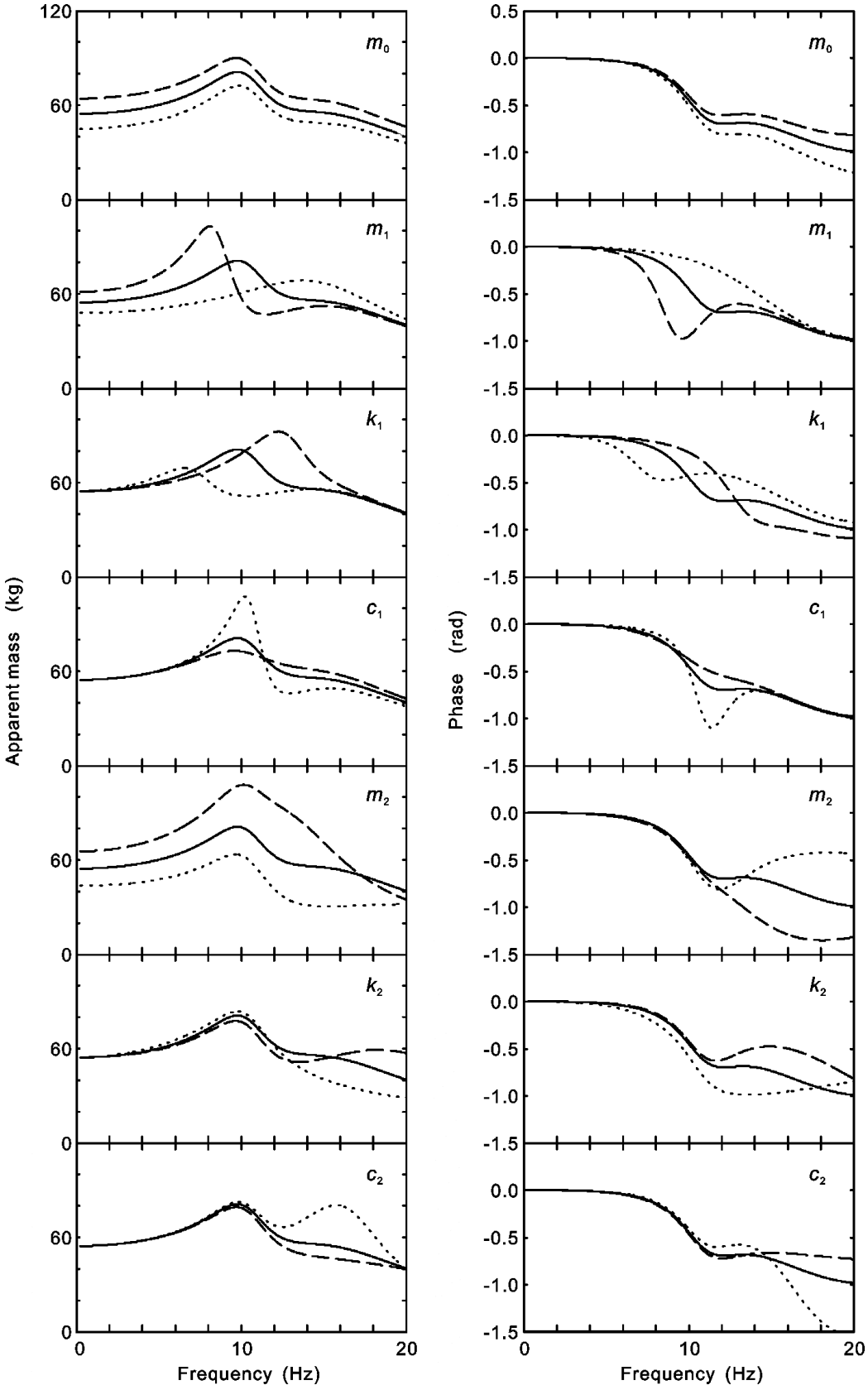

Figure 9.1 Sensitivity analysis of model parameters upon apparent mass modulus and phase. m_0, m_1, k_1, c_1, m_2, k_2, and c_2 are increased by 50% (__ __ __) and decrease by 50% (.....) from the optimized values with median apparent mass (_____) for the relaxed semi-supine subjects exposed to vertical broadband 0.25-20 Hz random vibration at 0.25 ms^{-2} r.m.s. (Data from Chapter 5.)

The effect of vibration magnitude on the apparent mass and transmissibility was insignificant at vibration magnitudes lower than 0.125 ms^{-2} r.m.s. (see Chapter 8). With these low input magnitudes, the effect of noise on the transfer function becomes greater. This decreases the chance of the model and the search method identifying the actual resonance frequency. In order to quantify and compare the nonlinearity in transmissibility and apparent mass at low magnitudes of vibration (i.e., results presented in Chapter 8), the modulus and phase of the frequency response functions at discrete selected frequencies were compared between different vibration magnitudes.

9.2 Active muscular activity and the nonlinearity

Whereas the finding of nonlinearity in the relaxed semi-supine posture reduces the probability that voluntary or involuntary muscular activity is a primary cause of the nonlinearity, muscular activity was not monitored during excitation in the present studies (Chapter 5, 6, 7, and 8). Involuntary phasic muscle reflexes could be responsible for part of the nonlinearity. If phasic muscle activity provides any significant dynamic force, nonlinearity will arise if changes in the magnitude of the acceleration excitation change the lag between muscle activity and the excitation such that the timing of peaks in the muscle force vary relative to the timing of peaks in the acceleration excitation. This could cause the dynamic force at the seat to not increase in proportion to the increase in the magnitude of the acceleration excitation. As a result, there could be a decrease in the dynamic stiffness of the body at higher magnitudes of excitation.

A shorter lag in the EMG activity of back muscles has been reported with lower magnitudes of random excitation (Blüthner *et al*., 2002). Blüthner *et al*. (1997) suggested that a monosynaptic stretch reflex with a latency of about 20 ms was responsible for muscular activity at frequencies lower than 4 Hz (4 Hz being the resonance frequency of the seated subject) and a polysynaptic stretch reflex with a latency of about 65 ms was responsible for muscular activity at frequencies greater than 4 Hz. This may imply that the frequency of the transition between the fast and the slow reflex is associated with the frequency of the resonance. With increased magnitude of excitation, the upper frequency at which the fast reflex dominates the muscular response tends to decrease. A voluntary periodic movement decreased the resonance frequency of the seated body at the lower vibration magnitude of 0.25 ms^{-2} r.m.s. (Chapter 4), possibly because the periodic muscular contraction decreased the frequency range over which the slow reflex dominated the muscle response.

Although, in the study reported in Chapter 4, voluntary muscle activity influenced the change in the resonance frequency with varying vibration magnitude, most previous studies have not found that different degrees of constant muscle tension or variations in sitting postures significantly alter the nonlinearity (e.g. Matsumoto and Griffin, 1998a; Matsumoto and Griffin, 2002b; Mansfield and Griffin, 2002; Mansfield *et al*., 2006). In these studies, changes of muscle tension and posture may have changed the tonic activity of muscles but not their phasic activity. Unless the tonic muscle activity changes with the magnitude of vibration it will not change the stiffness of the body and it will not contribute to nonlinearity. With seated subjects exposed to sinusoidal excitation from 1 to 32 Hz, the tonic activity, represented by the minimal EMG amplitude, tended to be similar with vibration magnitudes increasing from 0.8 to 2.5 ms^{-2} r.m.s. (see Figure 2.69 in Section 2.6.2, and Robertson and Griffin, 1989). In contrast, phasic muscular activity does change with the magnitude of vibration (it varies in both magnitude and timing) and so can affect the stiffness of the body and could contribute to non-linearity during whole-body vibration (see Section 2.6.2). Nevertheless, transfer functions between force at the seat and back muscle EMG activity, and transfer functions between the acceleration at the seat and back muscle EMG activity, suggest 'muscular reaction' is not a primarily cause of the nonlinearity with varying vibration magnitudes at frequencies greater than 1 Hz (see Section 4.2 in Blüthner *et al*., 2002). Any muscular activity that affects the biodynamic response of the body may therefore be at frequencies less than about 1 to 2 Hz.

9.3 Passive thixotropy and the nonlinearity

With relaxed semi-supine subjects exposed to vertical and horizontal intermittent vibration alternately between 1.0 and 0.25 ms^{-2} r.m.s. at an interval of about two seconds, the response of the body was found to be typical of thixotropy (Chapter 5 and 6). The stiffness of the body (indicated by the resonance frequency) with 0.25 ms^{-2} r.m.s. vibration immediately after 1.0 ms^{-2} r.m.s. vibration was lower than the stiffness during 0.25 ms^{-2} r.m.s. continuous vibration; the stiffness with 1.0 ms^{-2} r.m.s. vibration immediately after 0.25 ms^{-2} r.m.s. vibration was higher than the stiffness during 1.0 ms^{-2} r.m.s. continuous vibration. However, the effect was small, even with the reduced interference from muscular activity by using a relaxed supine posture: after 2.56 s of perturbation, the stiffness of the body recovered by about 90%. It was after about 30 s that the stiffness of human fingers subjected to an impulse tap recovered to about 80% (Lakie, 1986). It might be speculated that the difference in recovery time is because the tap of a finger can allow the whole

extensor and flexor muscle to deflect so much so that the breakdown of microstructures in the relaxed muscles and connective tissues is more thorough than that produced by internal movement of tissues involved in whole-body vibration.

A change in the contractile status of muscles could affect their thixotropic behaviour. Muscle tissues consist of about 40% to 50% of the total human soft tissues by weight (Tortora and Grabowski, 2003). A change in the thixotropic behaviour of muscle tissues can affect the nonlinearity of the body. The insignificant changes in nonlinearity reported with a variety of postures and with various constant muscle tension conditions (e.g. Mansfield and Griffin, 2002; Matsumoto and Griffin, 2002b; Blüthner *et al*., 2002; Nawayseh and Griffin, 2003) suggest that, if passive thixotropy is the primary cause of the nonlinearity, the nonlinearity is governed by tissues at the seat-subject interface (i.e., the buttocks of seated subjects), in which muscle tension can hardly be controlled. However, voluntary periodic upper-body movement (involving continuous and periodic contractions of the back and abdominal muscles) changed the nonlinearity (i.e. Chapter 4). Such movements will have caused movement of the tissues (both muscles and other tissues). The phasic muscle activity associated with back-abdomen bending may have accelerated the breakdown of microstructures in muscle tissues, with the contribution of the voluntary muscle activity to the total breakdown being less at the higher magnitudes of vibration. The proportional contribution of voluntary muscle activity to the breakdown would be less at higher magnitudes because the inertia forces from the vibration would cause more breakdown at the higher excitation magnitudes. Also, there must be a limit to the maximum possible structural breakdown to prevent the collapse of the body. Alternatively, the buttocks tissue may have been squeezed periodically by the voluntary back-abdomen bending movement and altered the passive thixotropic behaviour of the soft tissues in the buttocks region that some studies have considered to be involved in both the principal resonance and the nonlinearity of the seated human body (e.g. Kitazaki and Griffin, 1998; Matsumoto and Griffin, 2002a; Nawayseh and Griffin, 2003).

The nonlinearity has been repeatedly found in the inline apparent mass response to vertical excitation (e.g., Mansfield and Griffin, 2000; Nawayseh and Griffin, 2003;) and horizontal excitation (e.g., Mansfield and Lundström, 1999a; Nawayseh and Griffin, 2005a; Abdul Jalil, 2005), and in the cross-axis apparent mass responses in the horizontal directions (fore-and-aft and lateral) during vertical excitation (e.g., Nawayseh and Griffin, 2003, 2004; Mansfield *et al*., 2006; Subashi *et al*., 2006), and in the cross-axis apparent mass responses in the vertical and lateral directions during fore-and-aft excitation (e.g. Nawayseh and Griffin, 2005a, 2005b), and during

multi-axis excitation (e.g. Hinz *et al.*, 2006). The ubiquity of thixotropy in many soft human tissues is consistent with the nonlinearity observed in the large variety of responses. Passive thixotropy offers an explanation for the nonlinearity with fewer assumptions than muscular activity. The nonlinearity found in the vertical and horizontal responses of relaxed semi-supine subjects during vertical excitation, and in the horizontal and vertical responses during horizontal excitation, suggests passive thixotropy is a more likely explanation of the nonlinearity than muscular activity (Chapters 5 and 6). The effect of intermittency (i.e., shear history) on the cross-axis responses during both vertical and horizontal excitation was small compared with that in the inline responses. This may be because there was less movement, and therefore less force to break down the microstructures of body tissues in the cross-axis direction than in the inline direction, especially during vertical excitation of semi-supine subjects.

Distortions in the waveform of the dynamic force have been suggested as being related to the nonlinearity (e.g., Hinz and Seidel, 1987). Studies with seated subjects exposed to sinusoidal excitation show that the harmonic distortion of the force has a peak around the frequency of the resonance and increases with increasing excitation magnitude (e.g., Mansfield, 1995). With the relaxed semi-supine posture, a similar frequency dependence and magnitude dependence of the harmonic force distortion was found with vertical and horizontal sinusoidal excitation (in Chapter 7). These results are consistent with thixotropy being a primary cause of the nonlinearity, and arising from the force during a cycle of sinusoidal oscillation not varying in linear proportion to the excitation acceleration. This may explain reduced resonance frequencies with increased magnitudes of vibration, increased force distortion with increased magnitude of sinusoidal excitation, and reduced coherency at frequencies greater than the resonance frequency previously reported with increased magnitudes of random excitation (in Chapter 6).

With vertical random excitation of subjects in a semi-supine and a flat supine posture, the nonlinearity was more evident in transmissibilities to the lower and upper abdomen than in transmissibility to the sternum; and the nonlinearity was more apparent in the flat supine posture than in the semi-supine posture where there was less soft tissue on the back support (Chapter 8). These results suggest that the nonlinearity arose from the response of soft tissues – any interference from muscular activity in these relaxed supine postures should be small at the abdomen and the back. The transmissibilities to various locations of the body has been found to be similar in seated and standing postures (e.g. Matsumoto and Griffin, 2002a; Matsumoto and Griffin, 1998a). This might be because there is a similar response of key tissues in the motion transmission paths of seated and standing people, such as

the tissues of the buttocks of seated persons and the soles of the feet of standing persons. In supine postures there are independent transmission paths to the sternum and to the abdomen – the path to the abdomen is dominated by soft tissues in the back and the abdomen, while the path to the sternum is dominated by soft tissues in the back and the joints of the skeletal structure. The difference in the nonlinearity of transmission of vibration to the sternum and the abdomen might have been because there is more soft tissue involved the transmission to the abdomen and less damping at the abdomen. However, the appreciable nonlinearity in the transmissibility to the sternum suggests that soft tissues at the excitation-subject interface also makes a significant contribution to the nonlinearity.

With the supine subjects exposed to vertical random vibration, the nonlinearity in apparent mass was insignificant at magnitudes less than 0.125 ms^{-2} r.m.s. (Chapter 8). If thixotropy was the primary cause of the nonlinearity, it must have a lower limit to the range of magnitudes over which the microstructure of body tissues is broken down. Similarly, with high magnitudes of vibration, there must be an upper limit at which the body ceases to decrease its stiffness, so as to maintain its integrity and to avoid collapse. The bands of different thixotropic behaviour are shown schematically in Figure 9.2. The 'degree of breakdown' (Figure 9.2a) in the microstructure of soft tissues indicates that: (1) at extremely low magnitudes (i.e., less than a_1) there is negligible thixotropic effect and the 'effective stiffness of tissues' (Figure 9.2b) is not dependent on the excitation magnitude – this is a 'linear' band; (2) at intermediate magnitudes between a_1 and a_2, the tissues exhibit typical thixotropic behaviour in which the breakdown accelerates and the effective stiffness decreases with increasing magnitude of excitation – this is 'Thixotropy A' band; (3) at high magnitudes (i.e., higher than a_2), the thixotropic breakdown is retarded and the effective stiffness becomes less dependent on the excitation magnitude – this is 'Thixotropy B' band. The effective stiffness s_1 at a_1 and s_2 at a_2 are reflected in corresponding resonance frequencies. Currently there is no clear method to define and quantify the degree of breakdown b_1 at a_1 and b_2 at a_2. However, it is proposed that, in order to quantify and to model the degree of the thixotropic breakdown, two factors need to be considered: (i) the instantaneous reduction in the proportional change of resultant force when increasing or decreasing the magnitude of excitation, and (ii) the recovery time constant associated with the change in body stiffness when altering the excitation magnitude.

With relaxed supine subjects exposed to vertical broadband random vibration, a_1 could be around 0.125 ms^{-2} r.m.s. Previous and present results showing a significant nonlinearity reflect 'Thixotropy A' band behaviour. With seated subjects exposed to vertical random vibration, some studies show that the nonlinear change

in resonance frequency due to vibration magnitude is greater at lower magnitudes of vibration (e.g. Matsumoto and Griffin, 2002a; see Figure 2.16). Some other studies report insignificant differences between the absolute change in the resonance frequency between two lower magnitudes and between two higher magnitudes of vibration (e.g. Mansfield and Griffin, 2000; Matsumoto and Griffin, 2002b; Nawayseh and Griffin 2003; Nawayseh and Griffin 2004; see Figure 2.16). With relaxed semi-supine subjects exposed to both vertical and horizontal random vibration, the change in the apparent mass resonance frequency is slightly greater at lower magnitudes of vibration (see Figure 9.3). The inconsistency may be caused by inter-subject variability with seated subjects (see Figure 2.15) and semi-supine subjects in the present study (see Figure 9.4). These results suggest that, even within the band 'Thixotropy A', the change in the breakdown, or the effective stiffness, is not proportional to a change in the excitation magnitude, as indicated in Figure 9.2.

In summary, the present studies provide experimental evidence for passive thixotropy, rather than voluntary or involuntary muscular activity, being a primary cause of the nonlinearity seen in the frequency response functions of the human body during whole-body vibration. The studies suggest that the nonlinearity is likely to be caused, at least in part, by the response of soft tissues close to the excitation-subject interface. Whereas previous studies in which changes of muscle tension when seated resulted in little change in the nonlinearity, a study reported in this thesis found that suitable voluntary periodic movement while seated could significantly change the nonlinearity. This confirmed that the main cause of the nonlinearity was either muscular activity or passive thixotropy, or both. Intermittent vertical and horizontal vibration of relaxed semi-supine subjects showed that the dynamic response of the body was dependent on the shear history, typical of thixotropy behaviour. Harmonic distortions in the dynamic force of the semi-supine subjects exposed to sinusoidal acceleration had a similar dependence on the frequency and magnitude of excitation as previously reported with seated subjects, again suggesting thixotropy as a primary cause of the nonlinearity, due to the force during a cycle of sinusoidal oscillation not varying in proportion to the excitation acceleration. A substantial nonlinearity found in transmissibilities to both the sternum and abdomen of supine subjects, and previously reported in the transmissibilities of seated and standing subjects, implies that soft tissues at the excitation-subject interface contribute to the nonlinearity.

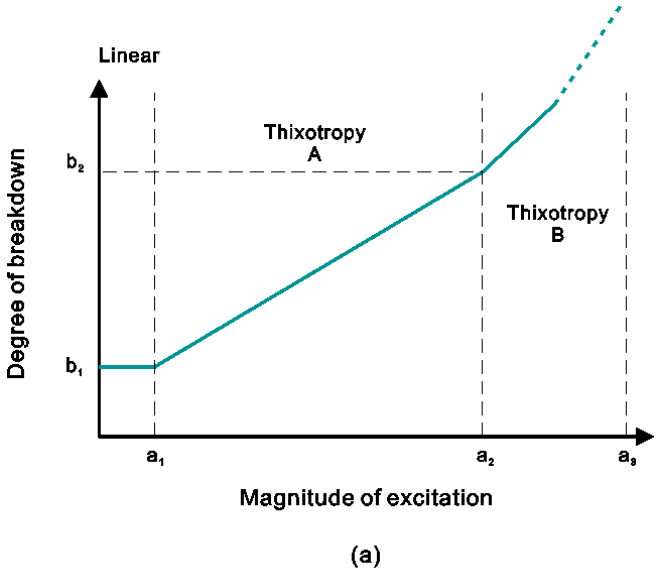

(a)

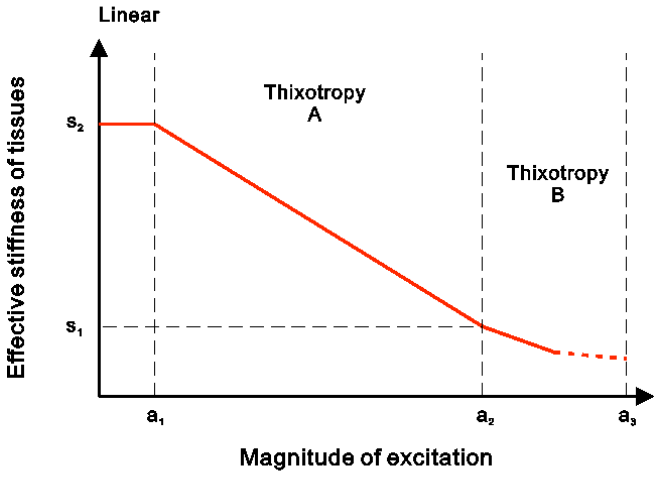

(b)

Figure 9.2 Schematic of the thixotropy bands. The vibration magnitude a_1 is the lower limit of the excitation magnitude for thixotropy to occur (i.e. the lower measurable limit for the nonlinearity); a_2 is the upper limit above which the thixotropic behaviour becomes less apparent; a_3 is the ultimate limit for the body tissue to collapse. b_1 and b_2 represent the degree of breakdown at a_1 and a_2 respectively; s_1 and s_2 represent the effective stiffness of tissues at a_1 and a_2 respectively.

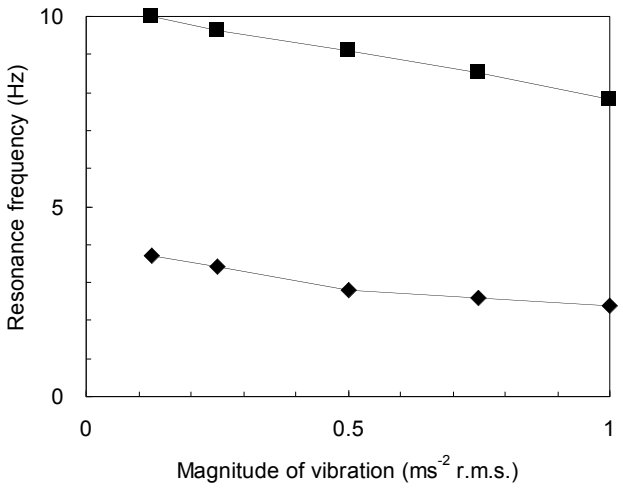

Figure 9.3 The effect of vibration magnitude on the median apparent mass resonance frequency of semi-supine subjects exposed to broadband random vertical (■) and longitudinal horizontal (♦) vibration in comparison with Figure 2.16.

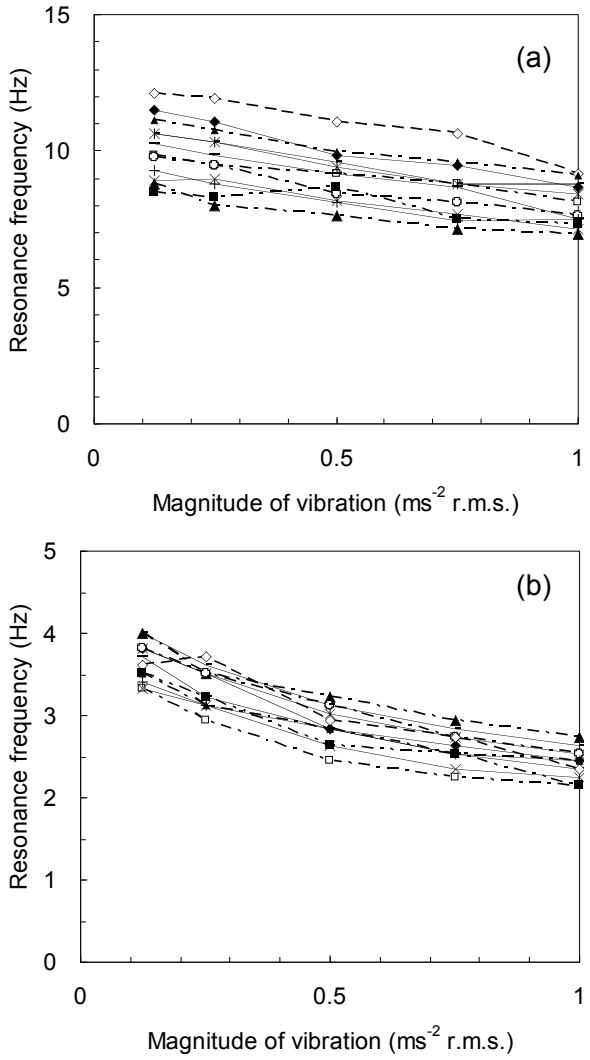

Figure 9.4 Inter-subject variability: the effect of vibration magnitude on the apparent mass resonance frequency of the same group of 12 semi-supine subjects exposed to broadband random vertical (a, in Chapter 5) and longitudinal horizontal (b, in Chapter 6) vibration.

Chapter 10

General conclusions and recommendations

10.1 General conclusions

Suitable voluntary periodic muscular activity can significantly change the nonlinearity in apparent mass resonance frequency during static sitting, in which subjects maintain a constant posture. Voluntary periodic muscle activity alters the equivalent stiffness of the body more at low magnitudes of excitation (e.g. 0.25 ms^{-2} r.m.s.) than at high magnitudes (e.g. 2.0 ms^{-2} r.m.s.). Muscular activity, or, some passive thixotropy property, of muscles, or other soft tissues involved during the periodic voluntary movement of the back and the upper body, significantly influence the biodynamic responses of the body to vibration.

With minimal voluntary and involuntary muscular activity, the relaxed semi-supine body showed a consistent nonlinear biodynamic response, in the vertical (*x*-axis) direction and the horizontal (z-axis) cross-axis direction during vertical excitation, and in the horizontal (z-axis) direction and the vertical (*x*-axis) cross-axis direction during horizontal (z-axis) excitation. The responses of the semi-supine body during intermittent random vibration have a typical thixotropic characteristic at both low magnitudes of vibration (e.g., 0.25 ms^{-2} r.m.s.) and high magnitudes of vibration (e.g., 1.0 ms^{-2} r.m.s.). The dynamic stiffness of the body with 0.25 ms^{-2} r.m.s. vibration immediately after 1.0 ms^{-2} r.m.s. vibration was lower than the stiffness with 0.25 ms^{-2} r.m.s. continuous vibration; the stiffness with 1.0 ms^{-2} r.m.s. vibration immediately after 0.25 ms^{-2} r.m.s. vibration was higher than the stiffness during 1.0 ms^{-2} r.m.s. continuous vibration. These findings lead to the conclusion that a passive thixotropic property of the body, rather than any active muscular activity, is the primary cause of the nonlinearity seen in measures of the apparent mass and transmissibility of the human body.

Harmonic distortions in dynamic force during sinusoidal excitation of semi-supine subjects showed a similar dependence on the frequency and magnitude of excitation as seated subjects. Passive thixotropy, a primary cause of the nonlinearity, could result in the force during a cycle of sinusoidal oscillation not varying proportionally with the excitation acceleration.

It is concluded from the substantial nonlinearity found in the transmissibilities to both the sternum and the abdomen of the supine subjects, and the similar nonlinearities previously reported for the transmissibilities of seated and standing subjects, that the soft tissues close to the excitation-subject interface contribute to the nonlinearity.

10.2 Recommendations

In the present studies, any voluntary or involuntary muscle activity was not monitored during exposure to whole-body vibration in the relaxed semi-supine posture. The EMG activity measured on the backs of seated subjects during sinusoidal vertical or horizontal excitation shows that the magnitude of phasic muscular activity is dependent on both the frequency and the magnitude of vibration (e.g., Robertson and Griffin, 1989). With random vibration, the time lag in the EMG activity at the back has also been found to change with both the frequency and magnitude of vibration (e.g. Blüthner *et al*., 2002). It is recommended that EMG activity in major postural-control skeletal muscles (at the abdomen and the back) are measured in a totally relaxed posture, such as the semi-supine posture, to help to identify the contribution of any voluntary or involuntary muscle activity to the biodynamic responses (i.e., apparent mass and transmissibility). The transfer functions between the input acceleration and the EMG activity, and between the dynamic force at the excitation-subject interface and the EMG activity, will quantify the magnitude and the frequency-dependence of any muscle activity caused by the vibration.

The development of mechanistic models of thixotropy will require data on the dynamic behaviour of different body parts and the interactions between them. This means that, for example, the boundaries of the thixotropic bands described in Figure 9.2 and the breakdown-excitation magnitude relationships within each band need to be determined experimentally. Previous biodynamic studies of seated and standing subjects suggest that the properties of soft tissues at the excitation-subject interface (e.g., the buttocks), and the interactions between internal soft tissues and organs (e.g., the viscera) and the spinal column are key to understanding the resonances and nonlinearity of the human body (e.g., Kitazaki, 1994; Matsumoto, 1999; Nawayseh, 2003). Due to the complexity of the anatomical arrangement of the human body, excitation in a single axis results in a multi-axis response of the body. It can be expected that increasing the number of axes of excitation will increase the motion transmitted to each body part – roughly equivalent to increasing the excitation magnitude in a single axis. The first step in improving understanding of the biodynamic nonlinearity is not to investigate the response of the body during multi-axis excitation but to understand the dynamic behaviour of individual body parts and develop a mechanistic model of thixotropy with single axis excitation.

Appendix A

SUBJECT INSTRUCTION

(Chapter 4)

The objective of this experiment is to investigate effects of muscle activity on the dynamic response of the human body during vertical whole-body vibration. The experiment consists of one session of 30 to 45 minutes with seven sitting conditions and vertical random vibration at two magnitudes: 0.25 and 2.0 ms^{-2}r.m.s. During the test session there will be 14 motions with each lasting for 90 seconds.

Experimental conditions

The seven sitting conditions – two stationary and five with periodic movements – are all based on condition A (Table 1) with an upright posture and minimum thigh contact.

Condition A (Upright posture and minimum thigh contact): straight back, hands on your laps, hold your head as if looking straight ahead, minimum thigh contact with lower legs vertical.

Condition B (Upper-body tighten-up): with the upright posture and minimum thigh contact (condition A), tense all parts of your body above the seat surface, from buttocks to the head and arms. Hold your breath but exhale-inhale every 15 seconds.

Conditions C to G (five periodic movement conditions): with the upright posture and minimum thigh contact (condition A), these five conditions will be achieved by periodic movement of specific body parts with smooth and continuous movements (Table 1). Make movements with one complete cycle every 3 seconds.

The experimenter will demonstrate the seven conditions and you will practise them before starting the experiment.

Experimental procedures

1. Before getting on the platform:

- After scrutinizing the instructions, you will have an opportunity to ask any questions about the experiment.
- You will be asked to provide informed consent for your participation.

- You will complete a questionnaire, and some anthropometric measurements will be made.
- You will practice the seven sitting conditions (two stationary sitting and five periodic movement conditions) in Table 1.

2. On the platform without movement:

- You will wear a loose safety belt.
- You should hold an emergency stop button that may be used to stop the platform at any time.
- Maintain the upright sitting posture (condition A in Table 1), with your hands on your lap, and hold your head as if looking straight ahead during the test.

3. On the platform rising to mid-travel position:

- You will be asked to adopt sitting conditions A to G in Table 1, which will be present in front of you. The motion will start after 5 seconds.

4. On the platform with vibration:

- 90 seconds of vertical random vibration either at 0.25 or 2.0 ms^{-2} r.m.s will present on the platform.
- After the first motion, please advise the experimenter if you are happy with the sitting condition or if you would like to repeat the motion in case you failed to maintain the sitting condition.
- After the first motion, rest on the platform at the mid-travel position for about 1 to 2 minutes before the next motion starts.

Table 1 Seven sitting conditions

Condition number	Diagram	Description
A	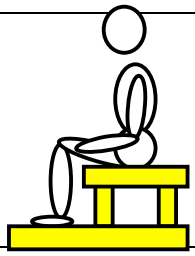	Upright minimum thigh contact [Reference]
B	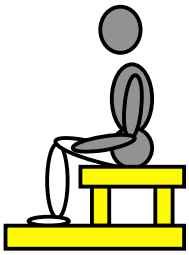	Upper-body tighten-up
C	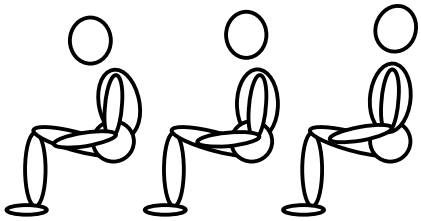	Back-abdomen bending
D	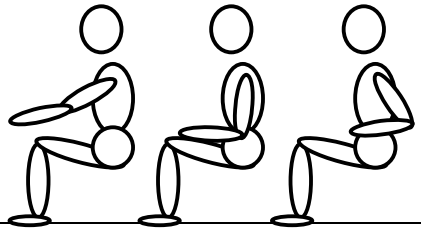	Folding-stretching arms from back to far front
E	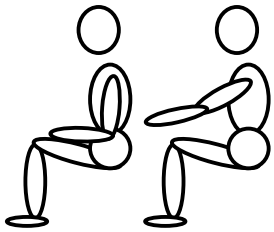	Stretching arms from rest to far front
F	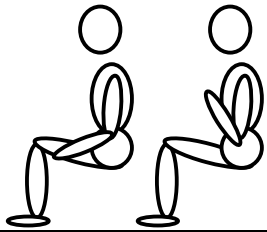	Folding arms from elbow
G	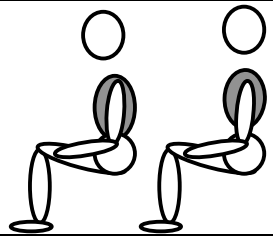	Deep breath

Appendix B

SUBJECT INSTRUCTION

(Chapters 5, 6 and 7)

The objective of this experiment is to investigate the biodynamic response of the human body under a supine position (like a space shuttle posture) during vertical and horizontal whole-body vibration.

The experiment consists of two sessions in two separate days, one on the 1 metre stroke vertical vibrator and another on the 1 metre stroke horizontal vibration. Each session will last approximately 100 minutes. There will be about 30 test motions with each lasting 2 to 3 minutes.

The procedures within a single session are:

1. You will be asked to sign a consent form for this experiment.
2. You will wear a safety belt (on the 1 metre vertical vibrator) or a safety harness (on the 1 metre horizontal vibrator).
3. Mount yourself on to the supporting surfaces of the vibrator as shown:

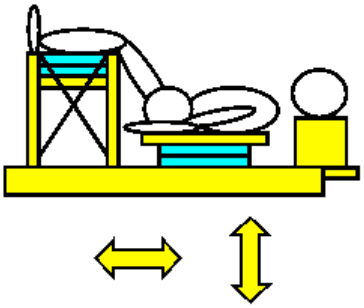

4. You will be holding an emergency stop button during the experiment.
5. Now please **RELAX** as if you are sleeping with your eyes closed and test motions will start.
6. Please inform the experimenter verbally if you need a break.

Appendix C

SUBJECT INSTRUCTION

(Chapter 8)

The objective of this experiment is to investigate the biodynamic response of the human body under a supine position (like a space shuttle posture) during vertical whole-body vibration.

The procedures within a single session are:

- You will be asked to sign a consent form for this experiment.
- You will be asked to adopt three supine postures with each posture you will be exposed to seven testing motions (0.0315, 0.0625, 0.125, 0.25, 0.5, 0.75 and 1.0 ms^{-2} r.m.s.) each lasting for 90 seconds.
- Before mounting yourself on to the vibrator you will be asked to wear three accelerometers attached to three elastic belts across your upper-body.
- Mount yourself on to the supporting surfaces of the vibrator as shown in Figure 1.

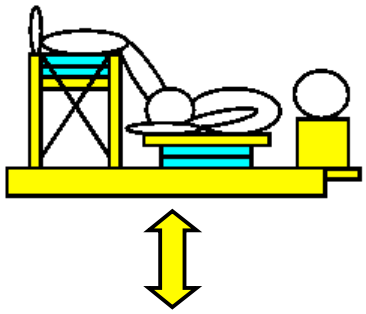

Figure 1 Supine position

- You will be holding an emergency stop button during the experiment.
- Now please **RELAX** as if you are sleeping (eyes closed) and test motions will start.
- Please inform the experimenter verbally if you need a break.

References

Abdul Jalil NA (2005). Transmission of vibration through backrests and apparent mass of the back during whole-body fore-and-aft vibration. Ph.D. thesis, University of Southampton, England.

Belytschko T and Privitzer E (1978). Refinement and validation of a three-dimensional head-spine model. Report no. AMRL-TR-78-7, Aerospace Medical Research Laboratory, Wright-Patterson Air Force Base, OH.

Blüthner R, Seidel H and Hinz B (1997). Can reflex-mechanism explain the timing of back muscles during sinusoidal whole-body vibration and transients? The 33rd United Kingdom Group Meeting on Human Responses to Vibration, 61 – 72, 17th – 19th September 1997, Southampton, England.

Blüthner R, Seidel H, and Hinz B (2001). Examination of the myoelectric activity of back muscles during random vibration – methodical approach and first results. Clinical Biomechanics 16, Supplement No. 1, S25 – S30.

Blüthner R, Seidel H, and Hinz B (2002). Myoelectric response of back muscles to vertical random whole-body vibration with different magnitudes at different postures. Journal of Sound and Vibration 253(1) 37 – 56.

Boileau P-É and Rakheja S (1998). Whole-body vertical biodynamic response characteristics of the seated vehicle driver – Measurement and model development. International Journal of Industrial Ergonomics 22, 449 – 472.

British Standards Institution (1987). Measurement and evaluation of human exposure to whole-body mechanical vibration and repeated shock. BS 6841.

Fairley TE (1986). Predicting the dynamic performance of seats. PhD thesis, University of Southampton, England.

Fairley TE and Griffin MJ (1989). The apparent mass of the seated human body: vertical vibration, Journal of Biomechanics 22(2), 81 – 94.

Fairley TE and Griffin MJ (1990). The apparent mass of the seated human body in the fore-and-aft and lateral directions. Journal of Sound and Vibration 139(2), 299 – 306.

Fritz M (2000). Description of the relation between the forces acting in the lumbar spine and whole-body vibrations by means of transfer functions. Clinical Biomechanics 15, 234 – 240.

Fung YC (1981). Biomechanics – mechanical properties of living tissues. Springer-Verlag New York.

Gail PDe, Lance JW and Neilson PD (1966). Differential effects on tonic and phasic reflex mechanisms produced by vibration of muscles in man. Journal of Neurology, Neurosurgery and Psychiatry 29, 1 – 11.

Granata KP, Slota GP and Bennett BC (2004). Paraspinal muscle reflex dynamics. Journal of Biomechanics 37, 241 – 247.

Griffin MJ (1990). Handbook of human vibration. Academic Press, London.

Griffin MJ (2001). The validation of biodynamic models. Clinical Biomechanics 16, Supplement No.1, S81 – S92.

Griffin MJ and Lewis CH (1978). A review of the effects of vibration on visual acuity and continuous manual control, Part 1: Visual acuity. Journal of Sound and Vibration 56(3), 383 – 413.

Hagbarth KE, Hagglund JV, Nordin M and Wallin EU (1985). Thixotropic behaviour of human finger flexor muscles with accompanying changes in spindle and reflex responses to stretch. Journal of Physiology, London, 368, 323 – 342.

Hagena F-W, Wirth CJ, Piehler J, Plitz W, Hofmann GO and Zwingers Th (1985). In-vivo experiments on the response of the human spine to sinusoidal Gz-vibration. AGARD Conference Proceedings 378, 1 – 12.

Herterich J and Schnauber H (1992). The effect of vertical mechanical vibration on standing man. Journal of Low Frequency Noise and Vibration 11, 52 – 61.

Hill DK (1968). Tension due to interaction between the sliding filaments in resting striated muscle. The effect of stimulation. Journal of Physiology (London) 199, 637 – 684.

Hinz B, Blüthner R, Menzel G, Rützel S, Seidel H and Wölfel HP (2006). Apparent mass of seated men – Determination with single- and multi-axis excitations at different magnitudes. Journal of Sound and Vibration 298, 788 – 809.

Hinz B and Seidel H (1987). The nonlinearity of the human body's dynamic response during sinusoidal whole body vibration. Industrial Health 25 (1987), 169 – 181.

Hinz B, Seidel H, Bräuer D, Menzel G, Blüthner R and Erdmann U (1988). Bidimensional accelerations of lumbar vertebrae and estimation of internal spinal load during sinusoidal vertical whole-body vibration: a pilot study. *Clinical Biomechanics* 3 (1988), 241 – 248.

Holmlund P and Lundström R (1998). Mechanical impedance of the human body in the horizontal direction. Journal of Sound and Vibration 215(4), 801 – 812.

Holmlund P and Lundström R (2001). Mechanical impedance of the sitting human body in single-axis compared to multi-axis whole-body vibration exposure, Clinical Biomechanics 16, Supplement No. 1, S101 – S110.

Homma I and Hagbarth KE (2000). Thixotropy of rib cage respiratory muscles in normal subjects. Journal of Applied Physiology 89, 1753 – 1758.

Hopkins GR (1971). Non-linear lump parameter mathematical model of dynamic response of the human body. Symposium on Biodynamic Modes and their Application, Daytona, Ohio, 26 – 28 October, Paper 25, 649 – 669, Technical report no. 71-29. Aerospace Medical Research Laboratories.

Human Experimentation Safety and Ethics Committee (1996). Guide to experimentation involving human subjects. ISVR Technical Memorandum No 808, October 1996. University of Southampton.

International Organization for Standardization (1981). Vibration and shock – mechanical driving point impedance of the human body. ISO 5982.

International Organization for Standardization (2001). Vibration and shock – Range of idealized values to characterize seated-body biodynamic response under vertical vibration. ISO 5982.

International Organization for Standardization (1997). Vibration and shock – evaluation of human exposure to whole-body vibration. ISO 2631.

Kitazaki S (1994). Modelling mechanical responses to human whole-body vibration. PhD thesis, University of Southampton, England.

Kitazaki S (1997). The apparent mass of the foot and prediction of floor carpet transfer function. The 33rd United Kingdom Group Meeting on Human Responses to Vibration, 17 – 19 September 1997, Southampton, England.

Kitazaki S and Griffin MJ (1995). A data correction method for surface measurement of vibration on the human body. Journal of Biomechanics 28(7), 885 – 890.

Kitazaki S and Griffin MJ (1997). A modal analysis of whole-body vertical vibration using a finite element model of the human body. Journal of Sound and Vibration 200(1), 83 – 103.

Kitazaki S and Griffin NJ (1998). Resonance behaviour of the seated human body and effects of posture. Journal of Biomechanics 31, 143 – 149.

Labeit and Kolmerer (1995). Titins: giant proteins in charge of muscle ultrastructure and elasticity. Science 270, 293 – 296.

Lakie M (1986). Vibration causes stiffness changes (thixotropic behaviour) in relaxed human muscle. United Kingdom Group Informal Meeting on Human Response to Vibration, Loughborough University of Technology, 22 – 23 September.

Lakie M, Walsh EG and Wright GW (1979). Passive wrist movements – a large thixotropic effect. Journal of Physiology 300, 36 – 37.

Lewis CH (2001). An adaptive electro-mechanical model for simulating the driving point force response of the human body with different input motions. The 36th United Kingdom Group Meeting on Human Responses to Vibration, 12 – 14 September, QinetiQ, Farnborough, England.

Lewis CH and Griffin MJ (1978). A review of the effects of vibration on visual acuity and continuous manual control, Part 2: Continuous manual control. Journal of Sound and Vibration 56(3), 415 – 457.

Linke WA, Ivemeyer M, Olivieri N, Kolmerer B, Rüegg JC and Labeit S (1996). Towards a molecular understanding of the elasticity of titin. Journal of Molecular Biology 261, 62 – 71.

Liu JZ, Kubo M, Aoki H, and Terauchi F (1996). The transfer function of human body on vertical sinusoidal vibration. The Japanese Journal of Ergonomics 32(1), 29 – 38.

Lundström R and Holmlund P (1998). Absorption of energy during whole-body vibration exposure. Journal of Sound and Vibration 215(4), 789 – 799.

Lundström R and Lindberg L (1983). Whole-body vibrations in road construction vehicles. The Swedish National Board of Occupational Safety and Health 18, 1983.

Mansfield NJ (1995). Distortion of the dynamic response of the pelvis when exposed to whole-body sinusoidal vibration. The 31st United Kingdom Group Meeting on Human Responses to Vibration, 61 – 72, 18th – 20th September 1995, Silsoe, England.

Mansfield NJ (1997). A consideration of alternative non-linear lumped parameter models of the apparent mass of a seated person. The 33rd United Kingdom Group Meeting on Human Responses to Vibration, 17th – 19th September 1997, ISVR, University of Southampton, Southampton, England.

Mansfield NJ (1998). Non-linear biodynamic response of the seated person to whole-body vibration. PhD thesis, University of Southampton, England.

Mansfield NJ (2005). Impedance methods (apparent mass, driving point mechanical impedance and absorbed power) for assessment of the biomechanical response of the seated person to whole-body vibration. Industrial Health 43, 378 – 389.

Mansfield NJ and Griffin MJ (1998). Effect of magnitude of vertical whole-body vibration on absorbed power for the seated human body. Journal of Sound and Vibration 215(4), 813 – 825.

Mansfield NJ and Griffin MJ (2000). Non-linearities in apparent mass and transmissibility during exposure to whole-body vertical vibration, Journal of Biomechanics 33, 933 – 941.

Mansfield NJ and Griffin MJ (2002). Effects of posture and vibration magnitude on apparent mass and pelvis rotation during exposure to whole-body vertical vibration, Journal of Sound and Vibration 253(1), 93 – 107.

Mansfield NJ, Holmlund P and Lundström R (2001). Apparent mass and absorbed power during exposure to whole-body vibration and repeated shocks. Journal of Sound and Vibration 248(3), 427 – 440.

Mansfield NJ, Holmlund P, Lundström R, Lenzuni P and Nataletti P (2006). Effect of vibration magnitude, vibration spectrum and muscle tension on apparent mass and cross axis transfer functions during whole-body vibration exposure. Journal of Biomechanics 39 (16), 3062 – 3070.

Mansfield NJ and Lundström R (1999a). The apparent mass of the human body exposed to non-orthogonal horizontal vibration. Journal of Biomechanics 32, 1269 – 1278.

Mansfield NJ and Lundström R (1999b). Models of the apparent mass of the seated human body exposed to horizontal whole-body vibration. Aviation Space and Environmental Medicine 70(12), 1166 – 1172.

Mansfield NJ and Maeda S (2005). Effect of backrest and torso twist on the apparent mass of the seated body exposed to vertical vibration. Industrial Health 43, 413 – 420.

Markolf KL and Steidel RF (1970). The dynamic characteristics of the human intervertebral joint. ASME paper No. 70-WA/BHF-6.

Matsumoto Y (1999). Dynamic response of standing and seated persons to whole-body vibration: principal resonance of the body. PhD thesis, University of Southampton, England.

Matsumoto Y and Griffin MJ (1998a). Dynamic response of the standing human body exposed to vertical vibration: influence of posture and vibration magnitude, Journal of Sound and Vibration 212(1), 85 – 107.

Matsumoto Y and Griffin MJ (1998b). Movement of the upper-body of seated subjects exposed to vertical whole-body vibration at the principal resonance frequency, Journal of Sound and Vibration 215, 743 – 762.

Matsumoto Y and Griffin MJ (2001). Modelling the dynamic mechanisms associated with the principal resonance of the seated human body. Clinical Biomechanics 16, Supplement No.1, S31 – S44.

Matsumoto Y and Griffin MJ (2002a). Non-linear characteristics in the dynamic responses of seated subjects exposed to vertical whole-body vibration, Journal of Biomechanical Engineering 124, 527 – 532.

Matsumoto Y and Griffin MJ (2002b). Effect of muscle tension on non-linearities in the apparent mass of seated subjects exposed to vertical whole-body vibration, Journal of Sound and Vibration 253(1), 77 – 92.

Matsumoto Y and Griffin MJ (2003). Mathematical models for the apparent masses of standing subjects exposed to vertical whole-body vibration. Journal of Sound and Vibration 260, 431 – 451.

Mertens H (1978). Nonlinear behaviour of sitting humans under increasing gravity. Aviation, Space, and Environmental Medicine 49(1), 287 – 298.

Mertens H and Vogt LH (1978). The response of a realistic computer model for sitting humans to different types of shocks. AGARD Conference Proceedings CP-253, A26-1-17: Models and Analogues for the Evaluation of Human Biodynamic Response, Performance and Protection, Paris, 6 – 10 November, (von Gierke HE ed.), Paper 26, Advisory Group of Aerospace Research and Development.

Moorhouse KM and Granata KP (2006). Role of reflex dynamics in spinal stability: intrinsic muscle stiffness alone is insufficient for stability. Journal of Biomechanics, in press.

Muksian R and Nash CD (1974). A model for the response of seated humans to sinusoidal displacements of the seat. Journal of Biomechanics 7, 209 – 215.

Muksian R and Nash CD (1976). On frequency-dependent damping coefficients in lumped-parameter models of human beings. Journal of Biomechanics 9, 339 – 342.

National Aeronautics and Space Administration (1978). Anthropometric source book, Vol. 1, anthropometry for designers. NASA Reference Publication 1024.

Nawayseh N (2003). Cross-axis movements of the seated human body in response to whole-body vertical and fore-and-aft vibration. PhD thesis, University of Southampton, England.

Nawayseh N and Griffin MJ (2003). Non-linear dual-axis biodynamic response to vertical whole-body vibration, Journal of Sound and Vibration 268, 503 – 523.

Nawayseh N and Griffin MJ (2004). Tri-axial forces at the seat and backrest during whole-body vertical vibration, Journal of Sound and Vibration 277, 309 – 326.

Nawayseh N and Griffin MJ (2005a). Non-linear dual-axis biodynamic response to fore-and-aft whole-body vibration, Journal of Sound and Vibration 282, 831-862.

Nawayseh N and Griffin MJ (2005b). Tri-axial forces at the seat and backrest during whole-body fore-and-aft vibration, Journal of Sound and Vibration 281, 921 – 942.

Paddan GS and Griffin MJ (1988). The transmission of translational seat vibration to the head. I. Vertical seat vibration. Journal of Biomechanics 21, 191 – 197.

Paddan GS and Griffin MJ (1988). The transmission of translational seat vibration to the head. II. Horizontal seat vibration. Journal of Biomechanics 21, 199 – 206.

Paddan GS and Griffin MJ (1993). The transmission of translational floor vibration to the heads of standing subjects. Journal of Sound and Vibration 160, 503 – 521.

Pankoke S, Buck B and Woelfel HP (1998). FE model of sitting man adjustable to body height, body mass and posture used for calculating internal forces in the lumbar vertebral disks. Journal of Sound and Vibration 215, 827 – 30.

Pope MH, Svensson M, Broman H and Andersson GBJ (1986). Mounting of the transducers in measurement of segmental motion of the spine. Journal of Biomechanics 19, 675 – 677.

Pope MH, Broman H and Hansson T (1989). Impact response of the standing subject – a feasibility study. Clinical Biomechanics 4, 195 – 200.

Robertson CD and Griffin MJ (1989). Laboratory studies of the electromyographic response to whole-body vibration. ISVR Technical Report 184, University of Southampton.

Rakheja S, Haru I, and Boileau PE (2002). Seated occupant apparent mass characteristics under automotive postures and vertical vibration. Journal of Sound and Vibration 253, 57 – 75.

Sandover (1978). Modelling human responses to vibration. Aviation Space and Environmental Medicine 49(1), 335 – 339.

Seidel H and Heide R (1986). Long term effects of whole-body vibration: a critical survey of the literature. International Archives of Occupational and Environmental Health 58, 1 – 26.

Seidel H, Blüthner R and Hinz B (2001). Application of finite-element models to predict forces acting on the lumbar spine during whole-body vibration. Clinical Biomechanics 16, Supplement No.1, S81 – S92.

Seidel H and Griffin MJ (2001). Modelling the response of the spinal system to whole-body vibration and repeated shock. Clinical Biomechanics 16, Supplement No.1, S3 – S7.

Siegel S and Castellan NJ (1988). Nonparametric statistics for the behavioral sciences. New York: McGraw-Hill, Inc.

Smith SD (1994). Non-linear resonance behaviour in the human exposed to whole-body vibration. Shock and Vibration, Vol. 1, No. 5, 439 – 450.

Smith SD (2000). Modeling differences in the vibration response characteristics of the human body. Journal of Biomechanics 33, 1513 – 1516. Supplementary material: Human vibration data collection, analysis, and modeling (http://www.elsevier.nl:80/inca/publications/store/3/2/1).

Subashi GHMJ, Matsumoto Y and Griffin MJ (2006). Apparent mass and cross-axis apparent mass of standing subjects during exposure to vertical whole-body vibration. Journal of Sound and Vibration 293(1-2), 78 – 95.

Suggs CW, Abrams CF and Stikeleather LF (1969). Application of a damped spring-mass human vibration simulator in vibration testing of vehicle seats. Ergonomics 12(1), 79 – 90.

Tanner RI (1985). Engineering Rheology. Oxford engineering science series 14. Clarendon press, Oxford.

Tortora GJ and Grabowski SR (2003). Principles of anatomy and physiology, tenth edition. John Wiley & Sons, Inc.

Toward MGR (2002). Apparent mass of the human body in the vertical direction: effect of input spectra. The 37th United Kingdom Group Meeting on Human Responses to Vibration, 18th – 20th September 2002, Department of Human Sciences, Loughborough University, Loughborough, England.

Toward MGR (2003). Apparent mass of the human body in the vertical direction: effect of seat backrest. The 38th United Kingdom Group Meeting on Human Responses to Vibration, 17th – 19th September 2003, Naval Medicine, Alverstoke, Gosport, England.

Valencia FP and Munro RR (1985). An electromyographic study of the lumbar multifidus in man. Electromyography and Clinical Neurophysiology, 25, 205 – 221.

Vogt LH, Krause HE, Hohlweck H and May E (1973). Mechanical impedance of supine humans under sustained acceleration. Aerospace Medicine 44(2), 123 – 128.

Vogt LH, Mertens H and Krause HE (1978). Model of the supine human body and its reactions to external forces. Aviation, Space, and Environmental Medicine 49(1), 270 – 278.

Vykukal HC (1968). Dynamic response of the human body to vibration when combined with various magnitudes of linear acceleration. Aerospace Medicine 39, 1163 – 1166.

Wei L (2000). Predicting transmissibility of car seats from the seat impedance and the apparent mass of the human body. PhD thesis, University of Southampton, England.

Wei L and Griffin MJ (1998a). Mathematical models for the apparent mass of the seated human body exposed to vertical vibration. Journal of Sound and Vibration 212(5), 855 – 874.

Wei L and Griffin MJ (1998b). The prediction of seat transmissibility from measures of seat impedance. Journal of Sound and Vibration 214(1), 121 – 137.

Wittmann TJ and Phillips NS (1969). Human body nonlinearity and mechanical impedance analysis. Journal of Biomechanics, Vol. 2, 281 – 288.

Wolfgang A. Linke, Marc Ivemeyer, Nicoletta Olivieri, Bernhard Kolmerer, Caspar J. Rüegg, Siegfried Labeit (1996). Towards a molecular understanding of the elasticity of titin. Journal of Molecular Biology, Vol. 261, Issue 1, 62-71.